

厚生労働科学研究費補助金
難治性疾患等政策研究事業

マイクロアレイ染色体検査で見つかる
染色体微細構造異常症候群の
診療ガイドラインの確立

平成27-29年度 総合研究報告書

研究代表者 倉橋 浩樹

平成30（2018）年 3月

目 次

I. 総合研究報告	
マイクロアレイ染色体検査で見つかる染色体微細構造異常症候群の 診療ガイドラインの確立	----- 1
研究代表者・倉橋浩樹（藤田保健衛生大学・総合医科学研究所 ・分子遺伝学研究部門・教授）	
（資料1）対象疾患のリスト	
（資料2）定量的エクソームXHMMのデータとマイクロアレイの比較	
II. 分担研究報告	----- 25
III. 研究成果の刊行に関する一覧表	----- 29
IV. 研究成果の刊行物・別刷	----- 35

厚生労働科学研究費補助金（難治性疾患等政策研究事業）
総合研究報告書

マイクロアレイ染色体検査でみつかると染色体微細構造異常症候群の
診療ガイドラインの確立
研究代表者 倉橋 浩樹
藤田保健衛生大学・総合医科学研究所・分子遺伝学研究部門・教授

研究要旨

本研究では、マイクロアレイ染色体検査により診断される、多発奇形・発達遅滞を主症状とする染色体微細構造異常症候群の診療ガイドラインの確立を目的として、国内の多施設共同研究により、代表的な 30 疾患に関して、全国調査による国内患者の把握や、臨床診断基準、重症度判定基準の策定を実施する。昨年度に引き続き、実臨床の中での新規患者の掘り起こしに向けたマイクロアレイ染色体検査、ならびに診療情報の収集、整理などを行った。一方で、未診断症例に関しては、第一段階のスクリーニング検査としてのエクソーム解析も平行しておこない、その有用性の検討を行った。その結果、複数の遺伝子が欠失・重複する染色体微細構造異常症候群の場合、XHMM アルゴリズム（エクソーム隠れマルコフモデル法）による定量は検出感度が十分に高く、その有用性が確認された。ただ、確認のための二次検査が必要であり、マイクロアレイ染色体検査は定量性の精度が高く、二次検査として有用であることが確認された。

研究分担者

大橋博文 埼玉県立小児医療センター遺伝科・部長
黒澤健司 地方独立行政法人神奈川県立病院機構神奈川県立こども医療センター・遺伝科・部長
山本俊至 東京女子医科大学・遺伝子医療センター・ゲノム診療科・教授
涌井敬子 信州大学医学部遺伝医学・予防医学教室 講師

査の普及により、CNV の検出感度が飛躍的に向上した。欧米では、多発奇形・発達遅滞の原因の精査としては従来の染色体検査にかわる第 1 選択の診断ツールとされてきた。多発奇形・発達遅滞の患者で G 分染法では 3% であった異常検出率が、マイクロアレイ染色体検査の導入により、15-20% の患者で責任変異を同定できるとされ、数多くの新規疾患も定義された。日本でも、すでに 5000 以上の患者データが蓄積されている。しかし、網羅的検査に特有の意義不明の CNV の解釈（variation of unknown significance: VUS）、偶発的所見（incidental findings: IF）や二次的所見（secondary findings: SF）への対応などの問題点が未解決であり、一般臨床検査としての提供体制が整っているとはいえない。近年、マイクロアレイ染色体検査が診断に必須な疾患が小児慢性特定疾患や指定難病に追加されるなど、臨床的有用性は高いものの、高コストの問題があり、自費診療の中で一部の患者がその恩恵を被るにとどまる。

A. 研究目的

染色体の欠失や重複のような微細構造異常によるコピー数の変化（copy number variation: CNV）は、器官発生に関わる転写因子や、ヒストン修飾因子、クロマチン因子などの転写調節因子が遺伝子の量的効果の影響を受けやすいため、先天性疾患の原因となることが多い。従来は G 分染法による染色体検査や FISH 法での診断が行われてきたが、マイクロアレイ染色体検

一方で、近年は、多発奇形・発達遅滞の患者の原因の精査としては、次世代シーケンサーによるエクソーム解析の台頭もあり、現場での検査適応のための指針が必要である。

研究代表者を含む本研究班員はこれまで、厚労省難治性疾患克服研究事業の支援も受け、多発奇形・発達遅滞の患者の原因の精査としてのマイクロアレイ染色体検査を診療の中でおこなってきた。本研究ではそれを継続する形で、3年間を通じて、患者サンプルの収集とマイクロアレイ染色体検査を行う。各施設で合計年間500例ほどの解析を目標とする。そして、3年目には、代表的な30疾患（1年目に見直し、2疾患を加え、合計32疾患）に関して、新たな臨床診断基準の作成、そして、個々の構造異常の発生メカニズムの解析を行うことを目標とする。これまでにリストの30疾患の多くには診療ガイドラインはなく、本研究は極めて有用な成果を創出する。

また、近年は、多発奇形・発達遅滞の患者の原因へのアプローチとしては、次世代シーケンサーによるエクソーム解析の有用性が確立した。このエクソーム解析はリード数を定量することでCNVを同定することが可能であり、マイクロアレイ染色体検査と同等のデータを創出することができる可能性があるため、多発奇形・発達遅滞の責任変異のスクリーニングにおいて第一選択となりうる。本研究では、多発奇形・発達遅滞の責任変異のスクリーニング法としてのマイクロアレイ染色体検査とエクソームの定量の感度や精度を比較し、その有用性を検討する。

B. 研究方法

日本全国の主な診療施設の小児科もしくは遺伝診療科に連絡を取り、染色体微細構造異常が疑われるような多発奇形・発達遅滞の患者のサーベイランス、患者登録を行う。とくに、リストの32疾患（資料1）に関しては診断未確定患者の発掘のために、診断につなが

る臨床情報を公開する。この調査は、日本小児遺伝学会（小崎健次郎理事長、本研究の研究協力者）との連携のもとに行う。集まった患者情報に基づいて、詳細な臨床情報と末梢血サンプルの収集を行う。末梢血サンプルに対しては、研究代表者を含む各研究分担者が個々の施設でマイクロアレイ染色体検査、必要に応じてFISH解析を行う。各施設の合計として年間500例ほどの解析を目標とする。

研究代表者を含む各研究分担者の研究施設には、すでにマイクロアレイ染色体検査を行う設備が整っており、これまでに臨床検査として行ってきた十分な実績がある。その際、ダウン症候群などの染色体異数性による疾患のような、従来のG分染法が有用である疾患や、22q11欠失症候群などのように疾患特異的FISH解析が第1選択になるような疾患を、表現型で除外できるように、染色体微細構造異常の診断のためのマイクロアレイ染色体検査の適応を決めるガイドラインを確立する。

多発奇形・発達遅滞の患者の原因の精査として従来はマイクロアレイ染色体検査による診断を進め、疾患責任CNVが確定しない場合にはエクソーム解析へと進めていた。一方で、近年のエクソーム解析の普及と低価格化に伴い、エクソーム解析を先行させ、その定量により疾患責任CNVの候補を推定し、二次検査としてマイクロアレイ染色体検査で確定させるという考えもある。本研究ではスクリーニング検査としてエクソーム解析を先行させ、検出されたCNVをマイクロアレイ染色体検査、MLPA法、qPCR法により確認した。エクソームのデータはターゲットエクソーム解析、全エクソーム解析ともに、Log2変換法や隠れマルコフモデル（exome hidden Markov model:XHMM）によるアルゴリズムなどを用いて観察研究として比較検討を行った。

（倫理面への配慮）

本研究は、ヒトゲノム・遺伝子解析研究に関

する倫理指針、人を対象とする医学系研究に関する倫理指針を遵守して行った。解析試料の取得は書面でのインフォームドコンセントの上でおこない、研究対象者に対するプライバシーの保護など、人権擁護上の問題については十分に配慮したうえで行った。各関連施設から送付される試料は、試料提供機関において連結可能匿名化が行われ、研究代表者や研究分担者の所属機関には匿名化された試料と、予めチェックリストとして作成した臨床データのみが送付されることとした。試料は研究代表者や研究分担者の所属機関にて保管し、研究期間終了後に同意書に基づき破棄を行う予定である。データは研究代表者や研究分担者の所属機関内の鍵のかかるキャビネットに研究期間内、保管する。報告又は発表に際しては、被験者のプライバシー保護に十分配慮する。偶発的所見を含めた、発生しうる諸問題には、各施設の遺伝カウンセリング部門が対応する。マイクロアレイ染色体検査に関する研究は、すでに研究代表者や研究分担者の所属機関のヒトゲノム・遺伝子解析研究倫理審査委員会の承認を得ている（「染色体コピー数異常症に関する研究」藤田保健衛生大学・ヒトゲノム・遺伝子解析研究倫理審査委員会、平成22年3月12日承認、5年後再承認、10年後再承認、HG13-003。）。

C. 研究結果

(1) マイクロアレイ染色体検査について

研究代表者を含め各班員が、所属施設における実臨床の中での新規患者の発見に向けたマイクロアレイ染色体検査、ならびに診療情報のチェックを行った。本研究の対象疾患である、染色体微細構造異常症 30 疾患の掘り起こしを行った。

(2) 染色体微細構造異常症 30 疾患について

昨年度の第 1 回「マイクロアレイ染色体検査でみつける染色体微細構造異常症候群の診

療ガイドラインの確立研究班」班会議で対象疾患の見直しを行い、当初の 30 疾患に 9q34 欠失症候群と 1q 重複症候群の 2 疾患の追加を行い、対象疾患を 32 疾患に拡大した（資料 1）。昨年度までに 7 つの疾患（1p36 欠失症候群、4p16 欠失症候群、5p サブテロメア欠失症候群、11p12-p14 欠失症候群、11/22 混合トリソミー、1q 重複症候群、9q34 欠失症候群）に関しては診断基準、重症度判定基準の作成へと進めることができている。

一方、残りの 25 疾患に関して、順次臨床診断基準の作成をおこなうことに関しては、十分な検討を行った。その結果、疾患によっては難病指定を目指すべき疾患と小児慢性特定疾患を目指すべき疾患があり、それらはすでに「先天異常症候群」や「常染色体異常症」という形で認定されている枠組みに紐付けすることを目指す。個々の疾患の特性は、疾患によって大きく異なるので、診断基準策定は個別に対応する必要があることが確認された。

(3) エクソーム解析との関連性

未診断の多発奇形・発達遅滞患者 88 例に対して、エクソーム・ファーストでアプローチし、Log2 変換法や XHMM によるアルゴリズムなどの定量的エクソーム解析と、マイクロアレイ染色体検査の比較検討を行った。その結果、36 例（41%）に責任変異としての SNV/indel が同定された。一方、構造異常としての CNV は 4 例（5%）に同定された。欠失が 2 例、重複が 2 例であった。既知の疾患責任遺伝子を含んでいたり、*de novo* であったりすることにより、患者の症状の責任変異であると確定した。マイクロアレイ染色体検査は確定検査として有用であった。一方で、エクソームデータの定量で見つからなかった症例にマイクロアレイ染色体検査を行い、新たな CNV が同定された症例はなかった。以上により、未診断の多発奇形・発達遅滞患者の診断には、エクソーム・ファーストでアプ

ローチし、定量的エクソーム解析で同定された CNV に対しマイクロアレイ染色体検査でヴァリデーションすることが妥当であると思われた。

D. 考察

近年のエクソームの急速な普及と低価格化とが相俟って、定量的エクソーム解析と、マイクロアレイ染色体検査の位置づけを検討する必要性を認識し、比較検討を開始した。本年度の研究成果により、定量的エクソームを第一段階のスクリーニング検査として使用した場合に、複数の遺伝子が欠失・重複しているような CNV の検出に関しては、XHMM の有用性が確認された。一方で、定量的エクソームのデータには確認作業が必要であり、確定的検査としての二次検査として、マイクロアレイ染色体検査が必要であることを確認した。エクソーム解析により、塩基レベルの遺伝子変化と、複数の遺伝子が欠失・重複しているような CNV の検出とが同時に可能である点で、スクリーニング検査としてのパフォーマンスは、マイクロアレイ染色体検査を完全に凌駕している。今後、次世代シーケンスのさらなる低コスト化が進むと、未診断患者のスクリーニング検査は、エクソーム・ファーストという位置づけとなる可能性が高い。

診断基準、重症度判定基準の作成の作業は実質的には小休止となった。「先天異常症候群」や「常染色体異常症」という大きな枠組みの中でのガイドラインの策定なども考慮されたが、個々の疾患の特性は、疾患によって大きく異なるので、最終的には、診断基準策定は個別に対応する必要があることが確認された。「国際標準に立脚した奇形症候群領域の診療指針に関する学際的・網羅的検討研究班（小崎班）」とも連携をとりながら、個別の疾患単位で進める必要がある。診療ガイドラインなどの研究成果は、ウェブ上で公開してゆく。また、指定難病認定に向けての

準備、その後、これらの疾患の診断に必要な遺伝学的検査としてのエクソーム解析やマイクロアレイ染色体検査の保険収載などを視野に入れ、研究を進めていく。本研究の成果は、これらの疾患の患者や家族に対する支援、稀少難病の医療や福祉の向上に貢献することが期待される。

E. 結論

本研究では、マイクロアレイ染色体検査により診断される、多発奇形・発達遅滞を主症状とする染色体微細構造異常症候群の診療ガイドラインの確立を目的として、国内の多施設共同研究により、代表的な 32 疾患に関して、全国調査による国内患者の把握や、臨床診断基準、重症度判定基準の策定を開始し、7つの疾患に関しては診断基準、重症度判定基準の作成を行うことができたが、定量的エクソーム解析とマイクロアレイ染色体検査の比較研究というタスクができてしまったため、残りの対象疾患に関しては積み残しとなってしまった。今後、新たな研究班を組織し、残りの対象疾患に関して、研究代表者を含めた各班員が実臨床の中での新規患者の掘り起こしに向けたマイクロアレイ染色体検査、ならびに診療情報の収集、チェックなどを行い、同様の検討を進めてゆく。一方で、エクソーム解析の定量とマイクロアレイ染色体検査との比較検討に関しては、スクリーニング検査としてのエクソーム解析の定量の有用性が明らかとなったが、エクソーム解析の定量の二次検査としてマイクロアレイ染色体検査の重要性も再確認された。

F. 健康危険情報

特になし。

G. 研究発表

1. 論文発表

(1) [Kurahashi H](#), Kato T, Miyazaki J, Nishizawa H,

- Nishio E, Furukawa H, Miyamura H, Ito M, Endo T, Ouchi Y, Inagaki H, Fujii T. Preimplantation genetic diagnosis/screening by comprehensive molecular testing. **Reprod Med Biol** 15(1), 13-19, 2015.
- (2) Yokoi S, Ishihara N, Miya F, Tsutsumi M, Yanagihara I, Fujita N, Yamamoto H, Kato M, Okamoto N, Tsunoda T, Yamasaki M, Kanemura Y, Kosaki K, Kojima S, Saitoh S, Kurahashi H, Natsume J. TUBA1A mutation can cause a hydranencephaly-like severe form of cortical dysgenesis. **Sci Rep** 5, 15165, 2015.
- (3) Miyazaki J, Ito M, Nishizawa H, Kato T, Minami Y, Inagaki H, Ohye T, Miyata M, Boda H, Kiriyama Y, Kuroda M, Sekiya T, Kurahashi H, Fujii T. Intragenic duplication in the PKHD1 gene in autosomal recessive polycystic kidney disease. **BMC Med Genet** 16(1), 98, 2015.
- (4) Morine M, Kohmoto T, Masuda K, Inagaki H, Watanabe M, Naruto T, Kurahashi H, Maeda K, Imoto I. A unique TBX5 microdeletion with microinsertion detected in patient with Holt-Oram syndrome. **Am J Med Genet A** 167(12), 3192-3196, 2015.
- (5) Nakagawa T, Taniguchi-Ikeda M, Murakami Y, Nakamura S, Motooka D, Emoto T, Satake W, Nishiyama M, Toyoshima D, Morisada N, Takada S, Tairaku S, Okamoto N, Morioka I, Kurahashi H, Toda T, Kinoshita T, Iijima K. A novel PIGN mutation and prenatal diagnosis of inherited glycosylphosphatidylinositol deficiency. **Am J Med Genet A** 170(1), 183-188, 2016.
- (6) Yagasaki H, Shichino H, Shimizu N, Ohye T, Kurahashi H, Yoshikawa T, Takahashi S. Nine-year follow-up in a child with chromosomal integration of human herpesvirus 6 transmitted from an unrelated donor through the Japan Marrow Donor Program. **Transpl Infect Dis** 17(1), 160-1, 2015.
- (7) Miura H, Kawamura Y, Kudo K, Ihira M, Ohye T, Kurahashi H, Kawashima N, Miyamura K, Yoshida N, Kato K, Takahashi Y, Kojima S, Yoshikawa T. Virological analysis of inherited chromosomally integrated human herpesvirus-6 in three hematopoietic stem cell transplant patients. **Transpl Infect Dis** 17(5), 728-31, 2015.
- (8) Tacharoenuang R, Komoto S, Guntapong R, Ide T, Haga K, Katayama K, Kato T, Ouchi Y, Kurahashi H, Tsuji T, Sangkitporn S, Taniguchi K. Whole genomic analysis of an unusual human G6P[14] rotavirus strain isolated from a child with diarrhea in Thailand: evidence for bovine-to-human interspecies transmission and reassortment events. **PLoS One** 10(9), e0139381, 2015.
- (9) Komoto S, Tacharoenuang R, Guntapong R, Ide T, Haga K, Katayama K, Kato T, Ouchi Y, Kurahashi H, Tsuji T, Sangkitporn S, Taniguchi K. Emergence and characterization of unusual DS-1-like G1P[8] rotavirus strains in children with diarrhea in Thailand. **PLoS One** 10(11), e0141739, 2015.
- (10) Nakamura Y, Kikugawa S, Seki S, Takahata M, Iwasaki N, Terai H, Matsubara M, Fujioka F, Inagaki H, Kobayashi T, Kimura T, Kurahashi H, Kato H. PCSK5 mutation in a patient with the VACTERL association. **BMC Res Notes** 8, 228, 2015.
- (11) Tsuge I, Morishita M, Kato T, Tsutsumi M, Inagaki H, Mori Y, Yamawaki K, Inuo C, Ieda K, Ohye T, Hayakawa A, Kurahashi H. Novel FATP4 mutations responsible for ichthyosis prematurity syndrome in a Japanese patient. **Hum Genome Var** 2, 15003, 2015.
- (12) Tairaku S, Taniguchi-Ikeda M, Okazaki Y, Noguchi Y, Nakamachi Y, Mori T, Kubokawa I, Hayakawa A, Shibata A, Emoto T, Kurahashi H, Toda T, Kawano S, Yamada H, Morioka I, Iijima K. Prenatal genetic testing for familial severe congenital protein C deficiency. **Hum Genome Var** 2, 15017, 2015.

- (13) Inagaki H, Kato T, Tsutsumi M, Ouchi Y, Ohye T, Kurahashi H. Palindrome-mediated translocations in humans: a new mechanistic model for gross chromosomal rearrangements. **Front Genet** 7, 125, 2016.
- (14) Tsutsumi M, Yokoi S, Miya F, Miyata M, Kato M, Okamoto N, Tsunoda T, Yamasaki M, Kanemura Y, Kosaki K, Saitoh S, Kurahashi H. Novel compound heterozygous variants in PLK4 identified in a patient with autosomal recessive microcephaly and chorioretinopathy. **Eur J Hum Genet** 24(12), 1702-1706, 2016.
- (15) Boda H, Uchida H, Takaiso N, Ouchi Y, Fujita N, Kuno A, Hata T, Nagatani A, Funamoto Y, Miyata M, Yoshikawa T, Kurahashi H, Inagaki H. A PDE3A mutation in familial hypertension and brachydactyly syndrome. **J Hum Genet** 61(8), 701-3, 2016.
- (16) Taniguchi-Ikeda M, Takeshima Y, Lee T, Nishiyama M, Awano H, Yagi M, Unzaki A, Nozu K, Nishio H, Matsuo M, Kurahashi H, Toda T, Morioka I, Iijima K. Next-generation sequencing discloses a nonsense mutation in the dystrophin gene from long preserved dried umbilical cord and low-level somatic mosaicism in the proband mother. **J Hum Genet** 61(4), 351-5, 2016.
- (17) Markoff A, Kurahashi H, Grandone E, Bogdanova N. Annexin A5 haplotype M2 is not a risk factor for recurrent miscarriages in Northern Europe, is there sufficient evidence? **Reprod Biomed Online** 32(5), 469-73, 2016.
- (18) Markoff A, Kurahashi H, Grandone E, Bogdanova N. Authors' response to the letter of Nagirnaja et al., "Response to annexin A5 haplotype M2 is not a risk factor for recurrent miscarriages in Northern Europe, is there sufficient evidence?" **Reprod Biomed Online** 33(1), 116-7, 2016.
- (19) Ohye T, Kawamura Y, Inagaki H, Yoshikawa A, Ihira M, Yoshikawa T, Kurahashi H. A simple cytogenetic method to detect chromosomally integrated human herpesvirus-6. **J Virol Methods** 228, 74-8, 2016.
- (20) Suzuki E, Shima H, Toki M, Hanew K, Matsubara K, Kurahashi H, Narumi S, Ogata T, Kamimaki T, Fukami M. Complex X-Chromosomal Rearrangements in Two Women with Ovarian Dysfunction: Implications of Chromothripsis/Chromoanaysynthesis-Dependent and -Independent Origins of Complex Genomic Alterations. **Cytogenet Genome Res** 150(2), 86-92, 2016.
- (21) Miyazaki J, Nishizawa H, Kambayashi A, Ito M, Noda Y, Terasawa S, Kato T, Miyamura H, Shioyama K, Sekiya T, Kurahashi H, Fujii T. Increased levels of soluble corin in pre-eclampsia and fetal growth restriction. **Placenta** 48, 20-25, 2016.
- (22) Yasui T, Suzuki T, Hara F, Watanabe S, Uga N, Naoe A, Yoshikawa T, Ito T, Nakajima Y, Miura H, Sugioka A, Kato Y, Tokoro T, Tanahashi Y, Kasahara M, Fukuda A, Kurahashi H. Successful living donor liver transplantation for classical maple syrup urine disease. **Pediatr Transplant** 20(5), 707-710, 2016.
- (23) Takaiso N, Nishizawa H, Nishiyama S, Sawada T, Hosoba E, Ohye T, Sato T, Inagaki H, Kurahashi H. Mutation analysis of the JUNO gene in female infertility of unknown etiology. **Fujita Med J** 2(3), 59-61, 2016.
- (24) Rinaldi VD, Bolcun-Filas E, Kogo H, Kurahashi H, Schimenti JC. The DNA damage checkpoint eliminates mouse oocytes with chromosome synapsis failure. **Mol Cell** 67, 1026-1036.e2, 2017.
- (25) Nakae S, Kato T, Murayama K, Sasaki H, Abe M, Kumon M, Kumai T, Yamashiro K, Inamasu J, Hasegawa M, Kurahashi H, Hirose Y. Remote intracranial recurrence of IDH mutant gliomas is associated with TP53 mutations and an 8q gain.

Oncotarget 8, 84729-84742, 2017.

(26) Azuma Y, Töpf A, Evangelista T, Lorenzoni PJ, Roos A, Viana P, Inagaki H, Kurahashi H, Lochmüller H. Intragenic DOK7 deletion detected by whole-genome sequencing in congenital myasthenic syndromes. **Neurol Genet** 3, e152, 2017.

(27) Nagasaka M, Taniguchi-Ikeda M, Inagaki H, Ouchi Y, Kurokawa D, Yamana K, Harada R, Nozu K, Sakai Y, Mishra SK, Yamaguchi Y, Morikoka I, Toda T, Kurahashi H, Iijima K. Novel missense mutation in DLL4 in a Japanese sporadic case of Adams-Oliver syndrome. **J Hum Genet** 62, 869, 2017.

(28) Kawamura Y, Ohye T, Miura H, Ihira M, Kato Y, Kurahashi H, Yoshikawa T. Analysis of the origin of inherited chromosomally integrated human herpesvirus 6 in the Japanese population. **J Gen Virol** 98, 1823-1830, 2017.

(29) Kato T, Ouchi Y, Inagaki H, Makita Y, Mizuno S, Kajita M, Ikeda T, Takeuchi K, Kurahashi H. Genomic characterization of chromosomal insertions: Implication for mechanism leading to the chromothripsis. **Cytogenet Genome Res** 153, 1-9, 2017.

(30) Kohmoto T, Okamoto N, Naruto T, Murata C, Ouchi Y, Fujita N, Inagaki H, Satomura S, Okamoto N, Saito M, Masuda K, Kurahashi H, Imoto I. A case with concurrent duplication, triplication, and uniparental isodisomy at 1q42.12-qter supporting microhomology-mediated break-induced replication model for replicative rearrangements. **Mol Cytogenet** 10, 15, 2017.

(31) Kato M, Kato T, Hosoba E, Ohashi M, Fujisaki M, Ozaki M, Yamaguchi M, Sameshima H, Kurahashi H. PCS/MVA syndrome caused by an Alu insertion in the BUB1B gene. **Hum Genome Var** 4, 17021, 2017.

(32) Inoue Y, Sakamoto Y, Sugimoto M, Inagaki H, Boda H, Miyata M, Kato H, Kurahashi H,

Okumoto T. A family with craniofrontonasal syndrome: the first report of familial cases of craniofrontonasal syndrome with bilateral cleft lip and palate. **Cleft Palate Craniofac J**, 15347, 2018.

(33) Taniguchi-Ikeda M, Morisada N, Inagaki H, Ouchi Y, Takami Y, Tachikawa M, Satake W, Kobayashi K, Tsuneishi S, Takada S, Yamaguchi H, Nagase H, Nozu K, Okamoto N, Nishio H, Toda T, Morioka I, Wada H, Kurahashi H, Iijima K. Two patients with PNKP mutations presenting with microcephaly, seizure, and oculomotor apraxia. **Clin Genet** 93(4), 931-933, 2018.

(34) Ohwaki A, Nishizawa H, Aida N, Kato T, Kambayashi A, Miyazaki J, Ito M, Urano M, Kiriya Y, Kuroda M, Nakayama M, Sonta SI, Suzumori K, Sekiya T, Kurahashi H, Fujii T. Twin pregnancy with chromosomal abnormalities mimicking a gestational trophoblastic disorder and coexistent foetus on ultrasound. **J Obstet Gynaecol**. 2018 Mar 9:1-3.

(35) Terasawa S, Kato A, Nishizawa H, Kato T, Yoshizawa H, Noda Y, Miyazaki J, Ito M, Sekiya T, Fujii T, Kurahashi H. Multiplex PCR in noninvasive prenatal diagnosis for FGFR3-related disorders. **Congenit Anom (Kyoto)**. 2018 Mar 14.

(36) Kibe M, Ibara S, Inagaki H, Kato T, Kurahashi H, Ikeda T. Lethal persistent pulmonary hypertension of the newborn in Bohring-Opitz syndrome. **Am J Med Genet A**. 2018 May;176(5):1245-1248. Prenatal diagnosis of premature chromatid separation/mosaic variegated aneuploidy (PCS/MVA) syndrome.

(37) Yamaguchi T, Yamaguchi M, Akeno K, Fujisaki M, Sumiyoshi K, Ohashi M, Sameshima H, Ozaki M, Kato M, Kato T, Hosoba E, Kurahashi H. **J Obstet Gynaecol Res**. 2018 Apr 19.

(38) Fukami M, Kurahashi H. Clinical consequences of chromothripsis and other catastrophic cellular events. **Methods Mol Biol**. 2018;1769:21-33.

- (39) Yokoi K, Nakajima Y, Ohye T, Inagaki H, Wada Y, Fukuda T, Sugie H, Yuasa I, Ito T, Kurahashi H. Disruption of the responsible Gene in a phosphoglucomutase 1 deficiency patient by homozygous chromosomal inversion. **JIMD Rep**. 2018 May 12.
- (40) Tsutsumi M, Fujita N, Suzuki F, Mishima T, Fujieda S, Watari M, Takahashi N, Tonoki H, Moriwaka O, Endo T, Kurahashi H. Constitutional jumping translocation involving the Y and acrocentric chromosomes. **Asian J Androl**, in press.
- (41) Sharma R, Gardner A, Homan C, Douglas E, Mefford H, Wiczorek D, Stark Z, Nowak C, Douglas J, Parsons G, Mark P, Loidi L, Mosher TM, Herman G, Gillespie M, Brady L, Madrigal I, Domenech Salgado L, Rabionet R, Ishihara N, Inagaki H, Kurahashi H, Palmer E, Field M, Gecz J. Clinical and functional assessment of novel variation in THOC2, an essential component of nuclear mRNA export machinery. **Hum Mutat**, in press.
- (42) 加藤武馬、稲垣秀人、堤真紀子、倉橋浩樹. 染色体異常の発生メカニズム、小児内科、47(10)、1813-5、2015.
- (43) 倉橋浩樹. 遺伝カウンセリングって何?、難病と在宅ケア、22(1)、57-59、2016.
- (44) 宮崎純、西澤春紀、倉橋浩樹. 染色体異常発生のメカニズム、産科と婦人科、84(1)、49-54、2017.
- (45) 倉橋浩樹. ゲノム医療の現状と遺伝カウンセリング、日本血栓止血学会誌、28(1)、9-15、2017.
- (46) 加藤武馬、西澤春紀、倉橋浩樹. 出生前診断におけるマイクロアレイ検査とNGS、産婦人科の実際、66(4)、497-502、2017.
- (47) 加藤麻希、倉橋浩樹. 造血器腫瘍のクリニカルシーケンスにおける遺伝診療体制の構築、日本小児血液・がん学会雑誌、印刷中
- (48) 加藤武馬、倉橋浩樹. 周産期のゲノムシーケンスの現状、遺伝子医学 MOOK 34 号、印刷中
2. 学会発表
[2015 年度]
- (1) Kurahashi H, Mishra D, Kato T, Inagaki H, Kosho T, Wakui K, Kido Y, Sakazume S, Taniiguchi-Ikeda M, Morisada N, Iijima K, Fukushima Y, Emanuel BS. Breakpoint analysis of the recurrent constitutional t(8;22)(q24.13;q11.21) translocation. European Human Genetics Conference 2015, Glasgow, UK, June 6-9, 2015.
- (2) Inagaki H, Miyamura H, Tsutsumi M, Kato T, Nishizawa H, Kurahashi H. Massive parallel sequencing revealed the conformational dynamics of the non-B form DNA at the promoter. 65th annual meeting of American Society of Human Genetics. Baltimore, MA, USA, October 6-10, 2015.
- (3) Inagaki H, Ota S, Nishizawa H, Miyamura H, Nakahira M, Suzuki M, Tsutsumi M, Kato T, Nishiyama S, Yanagihara I, Kurahashi H. Deep sequencing of sodium bisulfite-treated genomic DNA revealed in vivo G-quadruplex structure affecting the gene expression of ANXA5 that causes obstetric complications. The 11th International Workshop on Advanced Genomics, Tokyo, May 20-22, 2015.
- (4) Kurahashi H, Kato T, Inagaki H, Mishra D, Ouchi Y, Tsutsumi M, Ohye T. Palindrome-mediated chromosomal translocations in humans. International Symposium on Genome Science 2015, Tokyo, January 20-21, 2015.
- (5) Kurahashi H. Age-related increase of aneuploidy in human oocytes. IFFS/JSRM International Meeting 2015, Yokohama, April 26-29, 2015.
- (6) 倉橋浩樹. 網羅的手法による着床前診断. 第 67 回日本産科婦人科学会学術集会、横浜、April, 10-12, 2015.

- (7) 倉橋浩樹. ヒト卵母細胞における染色体分離異常の加齢依存性増加機構、日本人類遺伝学会第 60 回大会、東京、October, 14-17, 2015.
- (8) 倉橋浩樹. ヒト卵母細胞における加齢依存性染色体分離異常の発生メカニズム、第 1 回産科婦人科遺伝診療学会、長崎、December, 18-19, 2015.
- (9) 倉橋浩樹. 細胞遺伝学の基本. 第 25 回遺伝医学セミナー、千葉、September, 10-12, 2009.
- (10) 倉橋浩樹. 網羅的手法による着床前診断. 北海道出生前診断研究会、札幌、November, 7, 2015.
- (11) 倉橋浩樹、染色体の遺伝学、第 7 回遺伝医学セミナー入門コース、千葉、February, 6-7, 2015.
- (12) 西澤春紀、宮村浩徳、加藤武馬、稲垣秀人、柳原格、倉橋浩樹. 習慣流産における ANXA5 遺伝子プロモーター多型の検討、第 1 回アネキシン研究会、東京、October, 11, 2015.
- (13) 稲垣秀人、宮村浩徳、大江瑞恵、堤真紀子、加藤武馬、西澤春紀、倉橋浩樹. 次世代シーケンサー解析によるプロモータ部位の DNA 高次構造変化の解析、日本人類遺伝学会第 60 回大会、東京、October, 14-17, 2015.
- (14) 加藤武馬、大内雄矢、稲垣秀人、蒔田芳男、水野誠司、倉橋浩樹. 染色体挿入の発生機序. 日本人類遺伝学会第 60 回大会、東京、October, 14-17, 2015.
- (15) 大江瑞恵、水野誠司、村松友佳子、大橋博文、柘植郁哉、岡本伸彦、倉橋浩樹. 小型過剰マーカー染色体の発生メカニズム解明へのアプローチ. 日本人類遺伝学会第 60 回大会、東京、October, 14-17, 2015.
- (16) 堤真紀子、加藤武馬、稲垣秀人、大江瑞恵、倉橋浩樹. 均衡型相互転座保因者モデルマウスにおける減数分裂期の性染色体不活化異常の発生機構の解明. 日本人類遺伝学会第 60 回大会、東京、October, 14-17, 2015.
- (17) 伊藤真友子、宮崎純、寺澤すみれ、野田佳照、宮村浩徳、西澤春紀、藤井多久磨、倉橋浩樹. 羊水を用いた遺伝子解析による常染色体劣性多発性嚢胞腎の出生前診断. 第 67 回日本産科婦人科学会学術集会、横浜、April, 10-12, 2015.
- (18) 池田敏郎、倉橋浩樹、時任ゆり、桑波田知樹、中江光博. 羊水染色体検査で発見された過剰マーカー染色体の遺伝カウンセリング. 第 67 回日本産科婦人科学会学術集会、横浜、April, 10-12, 2015.
- (19) 宮崎純、加藤武馬、西澤春紀、宮村浩徳、西尾永司、大内雄矢、稲垣秀人、越知正憲、竹内一浩、遠藤俊明、藤井多久磨、倉橋浩樹. 着床前診断における次世代シーケンサーの有用性に関する基礎的検討. 第 67 回日本産科婦人科学会学術集会、横浜、April, 10-12, 2015.
- (20) 寺澤すみれ、西澤春紀、伊藤真友子、加藤武馬、大内雄矢、関谷隆夫、藤井多久磨、倉橋浩樹. タナトフォリック骨異形成症に対して胎児 3D-CT と母体血による無侵襲的出生前遺伝子検査による出生前診断を施行した 1 例、第 1 回産科婦人科遺伝診療学会、長崎、December, 18-19, 2015.
- (21) 野田佳照、西澤春紀、加藤武馬、本多真澄、寺澤すみれ、大脇晶子、宮崎純、坂部慶子、伊藤真友子、上林あす香、倉橋浩樹、藤井多久磨. 母体血を用いた無侵襲的出生前遺伝学的検査 (NIPT) による胎児の性別判定、第 1 回産科婦人科遺伝診療学会、長崎、December, 18-19, 2015.
- (22) 斎藤伸道、宇津宮隆史、大津英子、野見山真理、田中温、伊熊慎一郎、加藤武馬、大内雄矢、稲垣秀人、倉橋浩樹. 複雑な染色体組換を有するカップルのマイクロアレイによる着床前診断の検討. 第 1 回産科婦人科遺伝診療学会、長崎、December, 18-19, 2015.
- (23) 池田敏郎、折田有史、新谷光央、加藤武馬、加藤麻希、稲垣秀人、倉橋浩樹、堂地勉. NT 肥厚、Potter sequence を呈した Fryns 症候群の 1 症例. 第 1 回産科婦人科遺伝診療学会、長崎、December, 18-19, 2015.

- (24) 伊熊慎一郎、竹本洋一、田中威づみ、山口貴史、御木多美登、永吉基、田中温、小川昌宣、齋藤伸道、竹田省、倉橋浩樹. 単一遺伝子疾患の着床前診断(PGD)を外部検査機関に委託するまでの過程. 第1回産科婦人科遺伝診療学会、長崎、December, 18-19, 2015.
- (25) 大東由佳、大江瑞恵、西澤春紀、倉橋浩樹、佐藤労. NIPTにおける夫婦の意識調査による遺伝カウンセリングの重要性. 第39回遺伝カウンセリング学会、千葉、June, 25-28, 2015.
- (26) 河合美紀、佐藤労、大江瑞恵、倉橋浩樹. 色素失調症の支援への遺伝カウンセリングの役割. 第39回遺伝カウンセリング学会、千葉、June, 25-28, 2015.
- (27) 大江瑞恵、稲垣秀人、池田敏郎、尾崎守、西澤春紀、宮崎純、伊藤真友子、守屋光彦、倉橋浩樹. 羊水染色体検査の追加検査としてのマイクロアレイの重要性. 第39回遺伝カウンセリング学会、千葉、June, 25-28, 2015.
- (28) 森川真紀、大江瑞恵、倉橋浩樹、佐藤労. 神経線維腫症1型の未成年患者に対する病気の説明と保護者支援の在り方. 第39回遺伝カウンセリング学会、千葉、June, 25-28, 2015.
- (29) 高磯伸枝、大江瑞恵、倉橋浩樹、佐藤労. 「キャリアカウンセリング」理論を活用した遺伝カウンセリングの検討 -若年がん患者の心理・社会的支援にむけて-. 第39回遺伝カウンセリング学会、千葉、June, 25-28, 2015.
- (30) 岡村春江、村田透、大瀬戸久美子、藤井正宏、不破嘉崇、西前香寿、大江瑞恵、倉橋浩樹、佐藤労. 乳がん遺伝カウンセリング開設2年の経験と今後の課題. 第39回遺伝カウンセリング学会、千葉、June, 25-28, 2015.
- (31) 伊藤美月、大江瑞恵、倉橋浩樹、佐藤労. リンチ症候群における日常診療から遺伝カウンセリングまでのボトルネック調査. 第39回遺伝カウンセリング学会、千葉、June, 25-28, 2015.
- (32) 堤真紀子、倉橋浩樹. ヒト卵母細胞におけるコヒーシンの加齢に伴う減少. 第38回日本分子生物学会年会、千葉、December, 1-4, 2015.
- (33) 稲垣秀人、宮村浩徳、大江瑞恵、堤真紀子、加藤武馬、西澤春紀、倉橋浩樹. NGSによるプロモータ部位のDNA高次構造変化の解析. 第38回日本分子生物学会年会、千葉、December, 1-4, 2015.
- (34) 加藤武馬、大内雄矢、稲垣秀人、蒔田芳男、水野誠司、倉橋浩樹. 染色体挿入の発生機序. 第38回日本分子生物学会年会、千葉、December, 1-4, 2015.
- (35) 小原尚美、船戸悠介、大脇さよこ、岡本薫、平井雅之、川口博史、山田緑、舟本有里、倉橋浩樹. 家族性腎性低尿酸血症を認めた運動後急性腎不全の1例. 第51回中部日本小児科学会、名古屋、August, 23, 2015.
- (36) 石原尚子、三宅未紗、中島葉子、松本祐嗣、山本康人、加藤武馬、稲垣秀人、諸岡正史、伊藤哲哉、西野一三、倉橋浩樹、吉川哲史. 筋病理でCollagen VIが陽性であったUllrich病の1例. 第43回日本小児神経学会東海地方会、名古屋、August, 1, 2015.

[2016年度]

- (1) Kurahashi H, Mechanism for Structural Variation. APAC RGH Symposium, Singapore, Oct 4, 2016.
- (2) Kurahashi H. Palindrome-mediated recurrent translocations in humans. ICHG2016, Kyoto, Japan, Apr 3-7, 2016.
- (3) Kato T, Ouchi Y, Inagaki H, Makita Y, Mizuno S, Kurahashi H. Mechanisms of interchromosomal insertional translocation. ICHG2016, Kyoto, Japan, Apr 3-7, 2016.
- (4) Inagaki H, Boda H, Uchida H, Takaiso N, Ouchi Y, Fujita N, Kuno A, Hata T, Nagatani A, Funamoto Y, Miyata M, Yoshikawa T, Kurahashi H. *APDE3A* mutation in familial hypertension and brachydactyly syndrome. ICHG2016, Kyoto, Japan, Apr 3-7, 2016.

- (5) Tsutsumi M, Kato T, Inagaki H, Ohye T, Kurahashi H. Spermatogenic failure by impaired meiotic sex chromosome inactivation in a mouse with reciprocal translocation. ICHG2016, Kyoto, Japan, Apr 3-7, 2016.
- (6) Sugimoto M, Inagaki H, Tsutsumi M, Inoue Y, Taguchi Y, Boda H, Miyata M, Okumoto T, Yoshikawa T, Kurahashi H. Cell culture model for X-linked disorder: craniofrontonasal dysplasia and severe phenotype in female. ICHG2016, Kyoto, Japan, Apr 3-7, 2016.
- (7) Ishihara N, Inagaki H, Miyake M, Ouchi Y, Ohye T, Tsutsumi M, Yoshikawa T, Kurahashi H. A child presenting distinct phenotype in severe alternating hemiplegia with a novel ATP1A3 mutation. ICHG2016, Kyoto, Japan, Apr 3-7, 2016.
- (8) Noda Y, Nishizawa H, Kato T, Kambayashi A, Terasawa S, Miyazaki J, Ito M, Kurahashi H, Fujii T. Sex determination of the fetus by noninvasive prenatal testing (NIPT) with maternal blood. ICHG2016, Kyoto, Japan, Apr 3-7, 2016.
- (9) Miyazaki J, Nishizawa H, Kambayashi A, Ito M, Noda Y, Terasawa S, Kato T, Miyamura H, Sekiya T, Kurahashi H, Fujii T. Increased levels of soluble corin in patients with pre-eclampsia and fetal growth restriction. ICHG2016, Kyoto, Japan, Apr 3-7, 2016.
- (10) Unzaki A, Taniguchi-Ikeda M, Takeshima Y, Lee T, Awano H, Yagi M, Kurahashi H, Morioka I, Toda T, Matsuo M, Iijima K. Advantage of next generation sequencing in molecular diagnosis in DMD -mutation screening with long preserved dried umbilical cord and detection of mosaicism-. ICHG2016, Kyoto, Japan, Apr 3-7, 2016.
- (11) Ohashi M, Yamaguchi M, Ishii M, Yamaguchi T, Akeno K, Fijisaki M, Sumiyoshi C, Sameshima H, Ozaki M, Kato T, Inagaki H, Kurahashi H. Prenatal diagnosis of the Premature chromosome separation/ mosaic variegated aneuploidy (PCS/MVA) syndrome in fetus with microcephalus. ICHG2016, Kyoto, Japan, Apr 3-7, 2016.
- (12) Kurahashi H, Kato T, Suzuki M, Tsutsumi M, Ohye T, Inagaki H. De novo translocation frequency of the recurrent constitutional t(11;22)(q23;q11.2) in normal somatic tissues. ESHG2016, Barcelona, Spain, May 21-24, 2016.
- (13) Tsutsumi M, Yokoi S, Miya F, Miyata M, Kato M, Okamoto N, Tsunoda T, Yamasaki M, Kanemura Y, Kosaki K, Saitoh S, Kurahashi H. Missense mutations in the *PLK4* gene identified in a patient with autosomal recessive microcephaly and chorioretinopathy. ASHG2016, Vancouver, Canada, Oct 18-22, 2016.
- (14) Kato T, Ouchi Y, Inagaki H, Makita Y, Mizuno S, Kurahashi H. Mechanistic analysis and prediction of interchromosomal insertional translocation. ASHG2016, Vancouver, Canada, Oct 18-22, 2016.
- (15) Hattori T, Togawa T, Togawa Y, Kawabe H, Kato T, Kurahashi H, Saitoh S, Kouwaki M, Koyama N. 13q22.2q34 tetrasomy mosaicism due to an inverted duplication with a neocentromere. ASHG2016, Vancouver, Canada, Oct 18-22, 2016.
- (16) Ishihara N, Sasaki H, Kato T, Inagaki H, Tsutsumi M, Shiroki R, Kurahashi H. Relationship between various clinical features in a genotyped population investigated for tuberous sclerosis complex. ASHG2016, Vancouver, Canada, Oct 18-22, 2016.
- (17) Hattori S, Hagihara H, Kameyama T, Ouchi Y, Inagaki H, Kurahashi H, Huang FL, Huang KP, Miyakawa T. Gene expression analysis reveals molecular phenotypes related to schizophrenia in Neurogranin knockout mice. Neuroscience 2016, San Diego, USA, Nov 12-16, 2016.
- (18) 倉橋浩樹、造血器腫瘍のクリニカルシーケンスにおける遺伝カウンセリング体制の構築、AMED・臨床ゲノム情報統合データベース整備事業 がん領域における臨床ゲノムデータストレージの整備に関する研究（堀部班）

第1回班会議、名古屋、Sep 1, 2016.

(19) 倉橋浩樹、造血器腫瘍のクリニカルシーケンスにおける遺伝カウンセリング体制の構築、AMED・臨床ゲノム情報統合データベース整備事業 がん領域における臨床ゲノムデータストレージの整備に関する研究(堀部班) 第2回班会議、名古屋、Mar 31, 2017.

(20) 倉橋浩樹、不育症のゲノム医療を目指して、第1回 AMED 不育症班会議(齋藤班)、東京、Jan 9, 2017.

(21) 倉橋浩樹、不育症のゲノム医療を目指して、第2回 AMED 不育症班会議(齋藤班)、東京、May 29, 2016.

(22) 倉橋浩樹、染色体構造異常の発生メカニズム、AMED(難治性疾患実用化研究事業)「小児科・産科領域疾患の大規模遺伝子解析ネットワークとエピゲノム解析拠点整備」第1回班会議(松原班)、東京、Dec 20, 2016.

(23) 倉橋浩樹、ゲノム医療の現状と遺伝カウンセリング、奈良県立医科大学セミナー、奈良、Apr 15, 2016.

(24) 倉橋浩樹、ゲノム医療の現状と遺伝カウンセリング、名古屋第一赤十字病院セミナー、名古屋、Apr 25, 2016.

(25) 倉橋浩樹、網羅的手法による次世代型着床前診断、第23回セントルカ・セミナー、大分、Jun 12, 2016.

(26) 倉橋浩樹、遺伝性乳がん卵巣がんの分子遺伝学概論、第13回日本乳癌学会中部地方会、名古屋、Sep 10, 2016.

(27) 倉橋浩樹、Palindrome-mediated chromosomal translocations in humans. 日本放射線影響学会第59回大会、広島、Oct 28, 2016.

(28) 倉橋浩樹、網羅的手法による次世代型着床前診断、第25回勝川ART研究会、名古屋、Oct 29, 2016.

(29) 倉橋浩樹、結節性硬化症における遺伝学的検査、TSC Round Table Meeting in Aichi、名古屋、Oct 31, 2016.

(30) 倉橋浩樹、重症妊娠高血圧腎症における

アネキシン A5 遺伝子多型の解析、第2回アネキシン研究会、札幌、Nov 5, 2016.

(31) 倉橋浩樹、網羅的手法による次世代型着床前診断、第2回エンブリオロジストのためのPGS/PGDを学ぶ会、高崎、Nov 19, 2016.

(32) 倉橋浩樹、小児における染色体疾患の解析—NGSでの新知見、第1回 eurofins 学術セミナー、東京、Dec 10, 2016.

(33) 倉橋浩樹、受ける? 受けない? 遺伝子検査、藤田保健衛生大学医学部公開講座、豊明、Dec 15, 2016.

(34) 倉橋浩樹、細胞遺伝学的検査と染色体異常の発生機序について、第8回遺伝カウンセリングアドバンスセミナー、東京、Jan 28 2017.

(35) 倉橋浩樹、染色体の遺伝学、第8回遺伝医学セミナー入門コース、大阪、Feb 5, 2016.

(36) 倉橋浩樹、次世代シーケンサーを用いた着床前診断(PGD)と出生前診断の最先端、第17回関西出生前診療研究会、第47回臨床細胞分子遺伝研究会、西宮、Mar 4, 2017.

(37) 河合美紀、佐藤労、大江瑞恵、倉橋浩樹、色素失調症患者の着床前診断・出生前診断への関心と遺伝カウンセリングの重要性. 第40回遺伝カウンセリング学会、京都、Apr, 3-6, 2016.

(38) 加藤麻希、西澤春紀、西尾永司、大江瑞恵、倉橋浩樹、佐藤労、性差による考え方の違いが配偶子提供による妊娠および養子縁組の選択へ及ぼす影響. 第40回遺伝カウンセリング学会、京都、Apr, 3-6, 2016.

(39) 森山育実、倉橋浩樹、大江瑞恵、佐藤労、Marfan 症候群女性が妊娠出産を決断するための要因の検討. 第40回遺伝カウンセリング学会、京都、Apr, 3-6, 2016.

(40) 完山和生、大江瑞恵、倉橋浩樹、佐藤労、一般市民および認定遺伝カウンセラーに対する Incidental Findings に関する意識調査. 第40回遺伝カウンセリング学会、京都、Apr, 3-6, 2016.

- (41) 堤真紀子、横井摂理、宮冬樹、宮田昌史、加藤光広、岡本伸彦、角田達彦、山崎麻美、金村米博、小崎健次郎、齋藤伸治、倉橋浩樹、小頭症患者で同定された *PLK4* 遺伝子の新規ミスセンス変異が中心小体複製に与える影響. 第 39 回日本小児遺伝学会学術集会、東京、Dec 9-10. 2016.
- (42) 加藤麻希、加藤武馬、大橋昌尚、藤崎碧、山口昌俊、鮫島浩、堤真紀子、稲垣秀人、大江瑞恵、佐藤労、倉橋浩樹、PCS/MVA 症候群で同定された *Alu* 配列挿入による *BUB1B* 変異. 第 39 回日本小児遺伝学会学術集会、東京、Dec 9-10. 2016.
- (43) 鈴木江莉奈、島彦仁、土岐真智子、羽二生邦彦、松原圭子、倉橋浩樹、鳴海覚志、緒方勤、上牧務、深見真紀、卵巣機能不全患者 2 例における複雑 X 染色体再構成の同定. 第 39 回日本小児遺伝学会学術集会、東京、Dec 9-10. 2016.
- (44) 長坂美和子、池田真理子、稲垣秀人、大内雄矢、西山将宏、栗野宏之、永瀬裕朗、森岡一朗、戸田達史、倉橋浩樹、飯島一誠、症候性てんかんと新生児期に重篤な心機能障害を認めた兄弟例. 第 39 回日本小児遺伝学会学術集会、東京、Dec 9-10. 2016.
- (45) 宮崎純、西澤春紀、関谷隆夫、倉橋浩樹、藤井多久磨. 妊娠高血圧腎症および胎児発育不全における *corin* 発現に関する検討. 第 68 回日本産科婦人科学会学術講演会、東京、2016 年 4 月.
- (46) 野田佳照、西澤春紀、上林あす香、加藤武馬、大脇晶子、宮崎純、坂部慶子、伊藤真友子、藤井多久磨、倉橋浩樹. 母体血を用いた無侵襲的出生前遺伝学的検査による胎児の性別判定と次世代シーケンサーによる SNP 解析. 第 48 回藤田学園医学会、愛知、2016 年 10 月.
- (47) 寺澤すみれ、西澤春紀、上林あす香、宮崎純、伊藤真友子、野田佳照、坂部慶子、大脇晶子、吉澤ひかり、加藤武馬、大内雄矢、関谷隆夫、倉橋浩樹、藤井多久磨. *FGFR3* 遺伝子異常症に対する母体血による出生前遺伝子検査の検討. 第 2 回日本産科婦人科遺伝診療学会、京都、2016 年 12 月.
- (48) 野田佳照、西澤春紀、上林あす香、加藤武馬、大内雄矢、吉澤ひかり、大脇晶子、坂部慶子、寺澤すみれ、伊藤真友子、宮崎純、倉橋浩樹、藤井多久磨. NIPT による胎児の性別判定と X 連鎖劣性遺伝性疾患への臨床応用. 第 2 回日本産科婦人科遺伝診療学会、京都、2016 年 12 月.
- (49) 吉澤ひかり、西澤春紀、加藤武馬、上林あす香、吉貝香里、澤田富夫、西山幸江、大脇晶子、宮崎純、野田佳照、坂部慶子、伊藤真友子、宮村浩徳、倉橋浩樹、藤井多久磨. 分割停止胚に対する次世代シーケンサーによる染色体解析. 第 2 回日本産科婦人科遺伝診療学会学術講演会、京都、2016 年 12 月.
- (50) 森山育実、西澤春紀、稲垣秀人、大江瑞恵、佐藤労、倉橋浩樹. 早発乳児てんかん性脳症 (EIEE) の出生前診断. 第 20 回中部出生前医療研究会、名古屋、2017 年 3 月.
- (51) 加藤麻希、加藤武馬、大江瑞恵、佐藤労、倉橋浩樹、遺伝カウンセリング外来を受診しムコ多糖症 II 型の保因者診断を実施した 1 例. 第 20 回中部出生前医療研究会、名古屋、2017 年 3 月.
- (52) 加藤麻希、加藤武馬、大橋昌尚、藤崎碧、山口昌俊、鮫島浩、堤真紀子、稲垣秀人、大江瑞恵、佐藤労、倉橋浩樹、PCS/MVA 症候群で同定された *Alu* 配列挿入による *BUB1B* 変異. 第 10 回東海小児遺伝カンファレンス、名古屋、Sep 16, 2016.
- (53) 稲葉美枝、河合美紀、村松友佳子、谷合弘子、水野誠司、倉橋浩樹、Cohen 症候群の一男児例. 第 10 回東海小児遺伝カンファレンス、名古屋、Sep 16, 2016.
- (54) 内田英利、眞鍋正彦、川井有里、長谷有紗、帽田仁子、宮田昌史、畑忠善、完山和生、加藤武馬、稲垣秀人、倉橋浩樹、動脈管開存症で紹介された *Cantu* 症候群の 1 例. 第 10 回東

海小児遺伝カンファレンス, 名古屋, Sep 16, 2016.

(55) 森山育実、倉橋浩樹、大江瑞恵、佐藤芳、Marfan 症候群女性が妊娠・出産を選択する際に影響する要因. 日本遺伝看護学会第 15 回学術大会、新潟、Sep 24-25, 2016.

(56) 林孝彰、片桐聡、月花環、稲垣秀人、倉橋浩樹、常岡寛、家族歴聴取を契機に診断された S 錐体 1 色覚の 1 家系第 64 回日本臨床視覚電気生理学会、伊勢、Sep 30-Oct 1, 2016.

(57) 垣田彩子、四馬田恵、高柳武志、牧野真樹、倉橋浩樹、道上敏美、鈴木敦詞、CLCN7 ミスセンス変異による大理石骨病の一家系第 26 回臨床内分泌代謝 Update、大宮、Nov 18-19, 2016.

[2017 年度]

(1) Kurahashi H. Screening for Genetic Disease within the Asian context. ASPIRE 3rd Masterclass, Preimplantation Genetic Testing: Screening and Diagnosis, Beijing, China, Oct 12, 2017.

(2) Kurahashi H., Kato T, Kato M, Ouchi Y, Tsutsumi M, Inagaki H. Towards optimization of PGD for recurrent t(11;22) carrier. ESHG2017, Copenhagen, Denmark, May 27-30, 2017.

(3) Inagaki H, Kanyama K, Kato T, Ouchi Y, Yamamoto T, Kurahashi H. Breakpoint analysis of chromosomes having inverted duplication with terminal deletion by NGS. ASHG2017, Orlando, USA, Oct 17-21, 2017.

(4) Ishihara N, Inagaki H, Kawai M, Inuo C, Kurahashi H. Intellectual disability with severe self-injury behavior caused by THOC2 splice site variant. ASHG2017, Orlando, USA, Oct 17-21, 2017.

(5) Taniguchi-Ikeda M, Morisada N, Inagaki H, Okamoto N, Toda T, Morioka I, Kurahashi H. Kazumoto I. Two patients with PNKP mutations presenting microcephaly, seizure, and oculomotor apraxia. ASHG2017, Orlando, USA, Oct 17-21,

2017.

(6) Kato T, Nishiyama S, Nishiyama Y, Yoshikai K, Matsuda Y, Sawada T, Yoshizawa H, Furukawa H, Nishizawa H, Kato M, Kanbayashi A, Kurahashi H. Comprehensive chromosomal analysis of blastomeres with developmental arrest. ISPD2017, SanDiego, USA, Jul 9-12, 2017.

(7) Inagaki H, Kanyama K, Kato T, Ouchi Y, Yamamoto T, Kurahashi H. Breakpoint analysis of chromosomes having inverted duplication with terminal deletion by NGS. 12th International Workshop on Advanced Genomics, Tokyo, Japan, Jun 27-29, 2017.

(8) Ito T, Nakajima Y, Maeda Y, Sakai Y, Gotoh K, Suzuki T, Kurahashi H, Yoshikawa T. Severity and variety of management in 5 patients with methylmalonyl-CoA mutase deficiency. ICIEM2017, Rio de Janeiro, Brazil, Sep 5-8, 2017.

(9) Ishihara N, Inagaki H, Miyake M, Kawamura Y, Yoshikawa T, Kurahashi H. A case of catastrophic early life epilepsy with a novel ATP1A3 mutation. 6th Symposium on ATP1A3 in Disease, Tokyo, Japan, Sep 21-22, 2017.

(10) Ishimaru S, Ishihara N, Mori Y, Miyake M, Hibino H, Kawai M, Inuo C, Tsuge I, Hayakawa M, Kurahashi H. A case of oculoectodermal syndrome with acute transverse myelopathy caused by spinal dural arteriovenous fistula. AOCCN2017, Fukuoka, May 11-14, 2017.

(11) Hattori S, Hagihara H, Takayama Y, Kameyama T, Ouchi Y, Inagaki H, Kurahashi H. Huang FL, Huang KP, Miyakawa T. Neurogranin deficiency causes behavioral and molecular phenotypes related to schizophrenia. Neuroscience 2017, Washington DC, USA, Nov 11-15, 2017.

(12) 倉橋浩樹、造血器腫瘍のクリニカルシーケンスにおける遺伝カウンセリング体制の構築、AMED・臨床ゲノム情報統合データベース整備事業 がん領域における臨床ゲノムデータストレージの整備に関する研究 (堀部班)

- 平成 29 年度第 1 回班会議、名古屋、Dec 22, 2017.
- (13) 倉橋浩樹、不育症のゲノム医療を目指して、第 1 回 AMED 不育症班会議 (齋藤班)、東京、Jul 2, 2017.
- (14) 倉橋浩樹、不育症のゲノム医療を目指して、第 2 回 AMED 不育症班会議 (齋藤班)、東京、Jan 14, 2017.
- (15) 倉橋浩樹、網羅的手法による次世代型 PGD ~PGD の実際とこれから、JISART シンポジウム、名古屋、Jun 11, 2017.
- (16) 倉橋浩樹、網羅的手法による次世代型着床前診断、広島生殖医療研究会、広島、Jun 17, 2017.
- (17) 倉橋浩樹、次世代型 PGD/PGS の現状と問題点、第 24 回セントルカ・セミナー、大分、Jun 18, 2017.
- (18) 倉橋浩樹、網羅的手法による遺伝子染色体診断 ~次世代型 PGD の台頭~ 大阪大学 IRUD 講演会、大阪、Jul 11, 2017.
- (19) 倉橋浩樹、網羅的手法による次世代型 PGD、神和メディカル株式会社創立 15 周年記念学術講演会、神戸、Aug 6, 2017.
- (20) 倉橋浩樹、網羅的手法による次世代型着床前診断、第 18 回東北 ART 研究会、仙台、Aug 20, 2017.
- (21) 倉橋浩樹、染色体異常の発生メカニズム -男と女-、第 2 回発生遺伝研究会、徳島、Sep 9, 2017.
- (22) 倉橋浩樹、家族性腫瘍における遺伝子検査と遺伝カウンセリングの実際 Scientific Exchange Meeting (SEM) 、名古屋、Oct 7, 2017.
- (23) 倉橋浩樹、遺伝って何だろう? 第 2 1 回 FabryNEXT 交流会 in 名古屋、名古屋、Nov 4, 2017.
- (24) 倉橋浩樹、着床前診断の現状と今後の展望、第 1 9 回日本イアンドナルド超音波講座、広島、Nov 5, 2017.
- (25) 倉橋浩樹、造血器腫瘍のクリニカルシーケンスにおける遺伝診療体制の構築、第 5 9 回日本小児血液がん学会学術集会、松山、Nov 9, 2017.
- (26) 倉橋浩樹、次世代型 PGD/PGS の現状と問題点、第 6 2 回日本生殖医学会学術講演会、下関、Nov 16, 2017.
- (27) 倉橋浩樹、Recent advance in our understanding of the molecular nature of chromosomal abnormalities. 日本人類遺伝学会第 6 2 回大会、神戸、Nov 17, 2017.
- (28) 倉橋浩樹、がんと遺伝子検査、藤田保健衛生大学医学部公開講座、豊明、Dec 13, 2017.
- (29) 倉橋浩樹、網羅的手法による着床前診断の現状と問題点、大阪大学医学部全国教授の会 第 5 回総会、Dec 23, 2017.
- (30) 倉橋浩樹、染色体の遺伝学、第 9 回遺伝医学セミナー入門コース、名古屋、Feb 17-18, 2018.
- (31) 倉橋浩樹、PGD/PGS の現状と問題点、日本生殖発生医学会第 1 3 回学術集会、東京、Mar 18, 2018.
- (32) 倉橋浩樹、網羅的手法による PGD/PGS 入門、日本 A-PART 学術講演会 2018、東京、Mar 25, 2018.
- (33) 稲垣秀人、加藤武馬、完山和生、大内雄矢、山本俊至、倉橋浩樹、逆位重複・端部欠失の全ゲノムシーケンスによる切断点解析、日本人類遺伝学会第 6 2 回大会、神戸、Nov 17, 2017.
- (34) 加藤武馬、加藤麻希、吉貝香里、松田有希野、新井千登勢、浅井菜緒美、中野英子、澤田富夫、倉橋浩樹、初期胚に発生する染色体異常は栄養外胚葉に蓄積する、日本人類遺伝学会第 6 2 回大会、神戸、Nov 17, 2017.
- (35) 堤真紀子、藤田尚子、三島隆、藤枝聡子、外木秀文、森若治、遠藤俊明、倉橋浩樹、Y 染色体転座保因者の子に認められた別の染色体への Y の再転座、日本人類遺伝学会第 6 2 回大会、神戸、Nov 17, 2017.
- (36) 加藤麻希、西澤春紀、森山育実、市原慶和、佐藤芳、倉橋浩樹、着床前診断における家系

内発端者の遺伝学的情報の重要性、日本人類遺伝学会第62回大会、神戸、Nov 17, 2017.

(37) 河合美紀、杉本篤哉、平野聡子、石原靖紀、堤真紀子、倉橋浩樹、色素失調症の低頻度モザイク変異解析、日本人類遺伝学会第62回大会、神戸、Nov 17, 2017.

(38) 藤盛伸美、柘植郁哉、市原慶和、稲垣秀人、堤真紀子、佐藤芳、大江瑞恵、倉橋浩樹、デュシェンヌ型筋ジストロフィー双生児の卵性診断、日本人類遺伝学会第62回大会、神戸、Nov 17, 2017.

(39) 浅井喜美子、倉橋浩樹、大江瑞恵、佐藤芳、看護職者が受けた遺伝教育の現状と臨床で求められる遺伝看護実践、日本人類遺伝学会第62回大会、神戸、Nov 17, 2017.

(40) 障害のある子どもを持つ家族への遺伝カウンセラーとしての支援の在り方、久野千恵子、倉橋浩樹、稲垣秀人、杉本賢政、堤真紀子、大江瑞恵、佐藤芳、日本人類遺伝学会第62回大会、神戸、Nov 17, 2017.

(41) 稲垣秀人、堤真紀子、井上義一、田口佳広、帽田仁子、宮田昌史、奥本隆行、吉川哲史、倉橋浩樹、細胞培養モデルが明らかにした X連鎖の疾患での女性重症化、第40回日本分子生物学会年会、神戸、Dec 6-9, 2017.

(42) 加藤武馬、稲垣秀人、新海保子、堤真紀子、藤田尚子、山本俊至、倉橋浩樹、メイトペアシーケンスによる染色体構造異常の発生メカニズムの解析、第40回日本分子生物学会年会、神戸、Dec 6-9, 2017.

(43) 堤真紀子、加藤武馬、稲垣秀人、倉橋浩樹、均衡型相互転座モデルマウスの精子形成における性染色体不活化異常の発生機構、第40回日本分子生物学会年会、神戸、Dec 6-9, 2017.

(44) 加藤武馬、稲垣秀人、藤田尚子、新海保子、蒔田芳男、水野誠司、梶田光晴、池田敏郎、竹内一浩、柘植郁哉、倉橋浩樹、染色体挿入の発生機序、第40回日本小児遺伝学会学術集会、東京、Jan 12-13, 2018.

(45) 河合美紀、堤真紀子、鮫島希代子、道和

百合、稲垣秀人、倉橋浩樹、失が修復された健全な母親に起因する Jacobsen 症候群の同胞例、第40回日本小児遺伝学会学術集会、第40回日本小児遺伝学会学術集会、東京、Jan 12-13, 2018.

(46) 堤真紀子、加藤武馬、稲垣秀人、倉橋浩樹、均衡型相互転座保因者モデルマウスにおける精母細胞の性染色体不活化異常、第49回藤田学園医学会、豊明、Oct 12-13, 2017.

(47) 河合美紀、大江瑞恵、佐藤芳、倉橋浩樹「色素失調症患者と家族の集い」開催からの考察、第49回藤田学園医学会、豊明、Oct 12-13, 2017.

(48) 加藤麻希、西澤春紀、大江瑞恵、倉橋浩樹、佐藤芳、配偶子提供による妊娠および養子縁組に関する意識調査、第41回遺伝カウンセリング学会、大阪、Jun, 22-25, 2017.

(49) 河合美紀、大江瑞恵、佐藤芳、倉橋浩樹、「色素失調症患者と家族の集い」開催からの考察、第41回遺伝カウンセリング学会、大阪、Jun, 22-25, 2017.

(50) 加藤麻希、加藤武馬、大江瑞恵、市原慶和、佐藤芳、倉橋浩樹、25年前のへその緒で出生前診断を回避できたムコ多糖症Ⅱ型の遺伝カウンセリング、第20回中部出生前医療研究会、Mar 4, 2018.

(50) 吉貝香里、加藤武馬、松田有希野、新井千登勢、浅井菜緒美、中野英子、澤田富夫、倉橋浩樹、NGS を用いた TE・ICM 間における核型一致率の比較、第58回日本乱視学会学術集会、沖縄、Jun 2-3, 2017.

(51) 松田有希野、加藤武馬、吉貝香里、新井千登勢、中野英子、澤田富夫、倉橋浩樹、5日目、6日目の胚盤胞凍結時の細胞のサイズと染色体解析、第58回日本乱視学会学術集会、沖縄、Jun 2-3, 2017.

(52) 稲葉美枝、村松友佳子、谷合弘子、野々部典枝、倉橋浩樹、水野誠司、エクソームシーケンスで診断し得た VPS13 遺伝子のエクソン欠失とナンセンス変異を認めた Cohen 症候群

の一男児例. 第 59 回小児神経学会、大阪、Jun 15-17, 2017.

(53) 日尾野宏美, 石原尚子, 川口将宏, 後藤研誠, 西村直子, 尾崎隆男, 倉橋浩樹、頭部打撲をきっかけとする反復性脳症の 1 家系における遺伝学的検討. 第 59 回小児神経学会、大阪、Jun 15-17, 2017.

(54) 横井摂理, 堤真紀子, 宮冬樹, 宮田昌史, 加藤光広, 岡本伸彦, 角田達彦, 山崎麻美, 金村米博, 小崎健次郎, 齋藤伸治, 倉橋浩樹、Novel compound heterozygous variants in *PLK4* cause microcephaly and chorioretinopathy. 第 59 回小児神経学会、大阪、Jun 15-17, 2017.

(55) Ishihara N, Sasaki H, Shima S, Miyake M, Hibino H, Kato T, Shiroki R, Kurahashi H、Correlation between neurological deficits and genotype in patients with tuberous sclerosis complex. 第 59 回小児神経学会、大阪、Jun 15-17, 2017.

(56) 松本祐嗣、池住洋平、宮田昌史、近藤朋実、長谷有紗、川井有里、内田英利、中島葉子、帽田仁子、伊藤哲哉、臨床経過より疑い遺伝子検査により Renal tubular dysgenesis と診断した乳児腎不全例、第 52 回小児腎臓病学会、東京、Jun 1-3, 2017.

(57) 亀井宏一、倉橋浩樹、稲垣秀人、藤丸拓也、蘇原映誠、宍戸清一郎、小椋雅夫、佐藤舞、義岡孝子、緒方謙太郎、石倉健司、ARPKD と同様の臨床像を呈し遺伝子解析で *PKD1* の複合ヘテロ変異が疑われた男児例. 第 39 回日本小児腎不全学会、淡路、Sep 21-22, 2017.

(58) 松本祐嗣、池住洋平、近藤朋実、横井克幸、中島葉子、伊藤哲哉、吉川哲史、倉橋浩樹、ネフローゼ症候群を契機に発症し補体 I 因子変異を認めた aHUS の一乳児例、第 47 回日本腎臓学会西部学術大会、岡山、Oct 13-14, 2017.

(59) 河合美紀、堤真紀子、鮫島希代子、道和百合、稲垣秀人、倉橋浩樹、Jacobsen 症候群の同胞例 — 親の解析で見つかった痕跡 —、第 12 回東海小児遺伝カンファレンス、名古屋、

Sep 15, 2017.

(60) 河合美紀、堤真紀子、稲垣秀人、倉橋浩樹、色素失調症 20 家系の遺伝子解析 — 低頻度モザイク変異検出への手がかり —、第 13 回東海小児遺伝カンファレンス、名古屋、Feb 24, 2018.

(61) 大江瑞恵、村松友佳子、水野誠司、秋山秀彦、倉橋浩樹。マイクロアレイ染色体検査によるマーカー染色体の由来検索、第 18 回日本検査血液学会学術集会、札幌、Jul 22-23, 2017.

(62) 加藤麻希、新海保子、加藤武馬、池住洋平、中島葉子、松本祐嗣、稲垣秀人、堤真紀子、倉橋浩樹。Bartter 症候群を例に相同性の高い塩基配列を持つ責任遺伝子における変異解析手法の検討。第 5 回 NGS 現場の会、仙台、May 22-24, 2017.

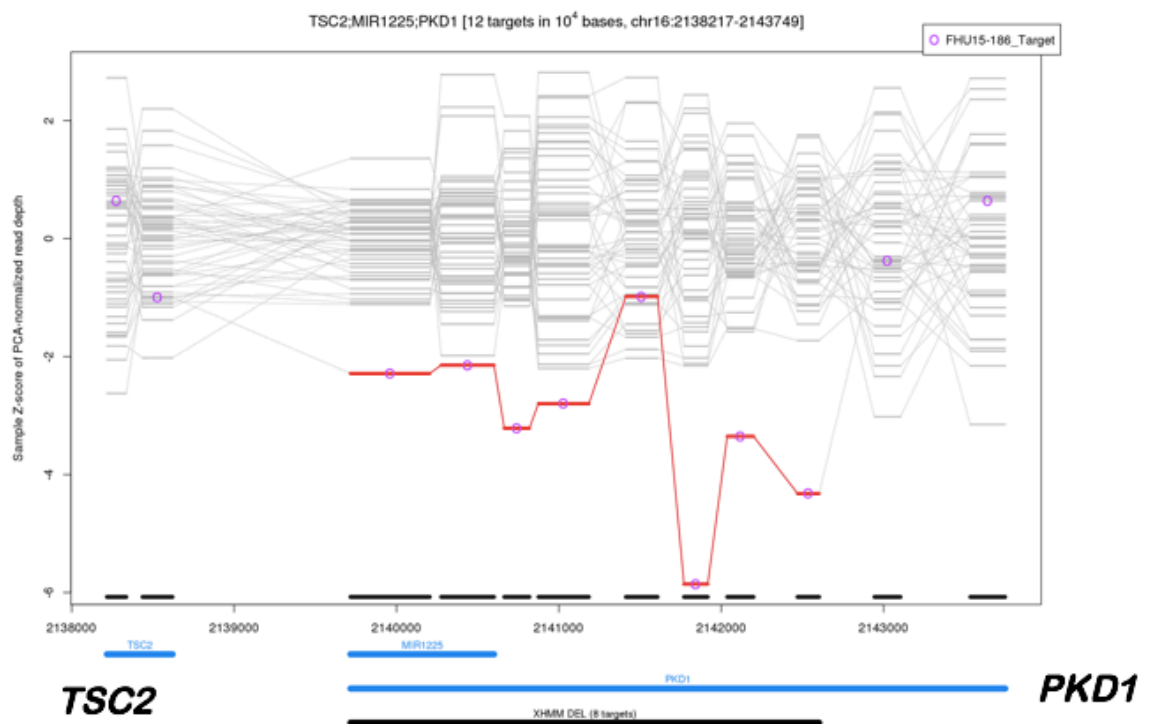
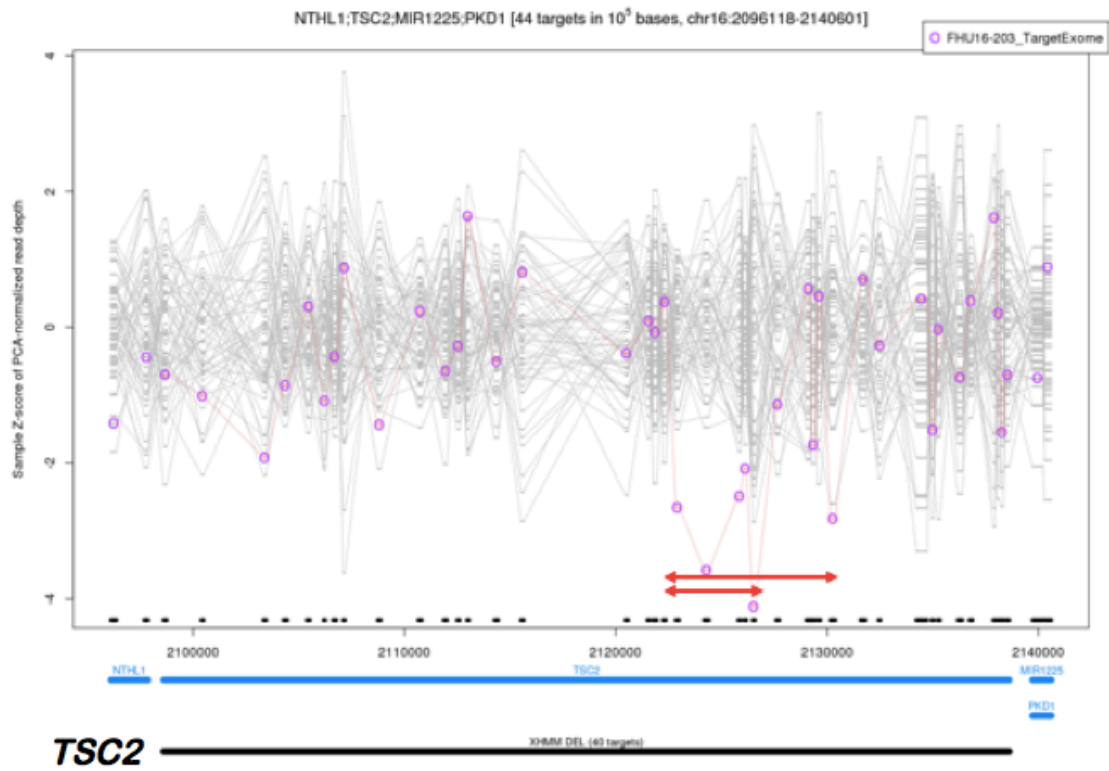
H. 知的財産権の出願・登録状況
特になし。

(資料1)

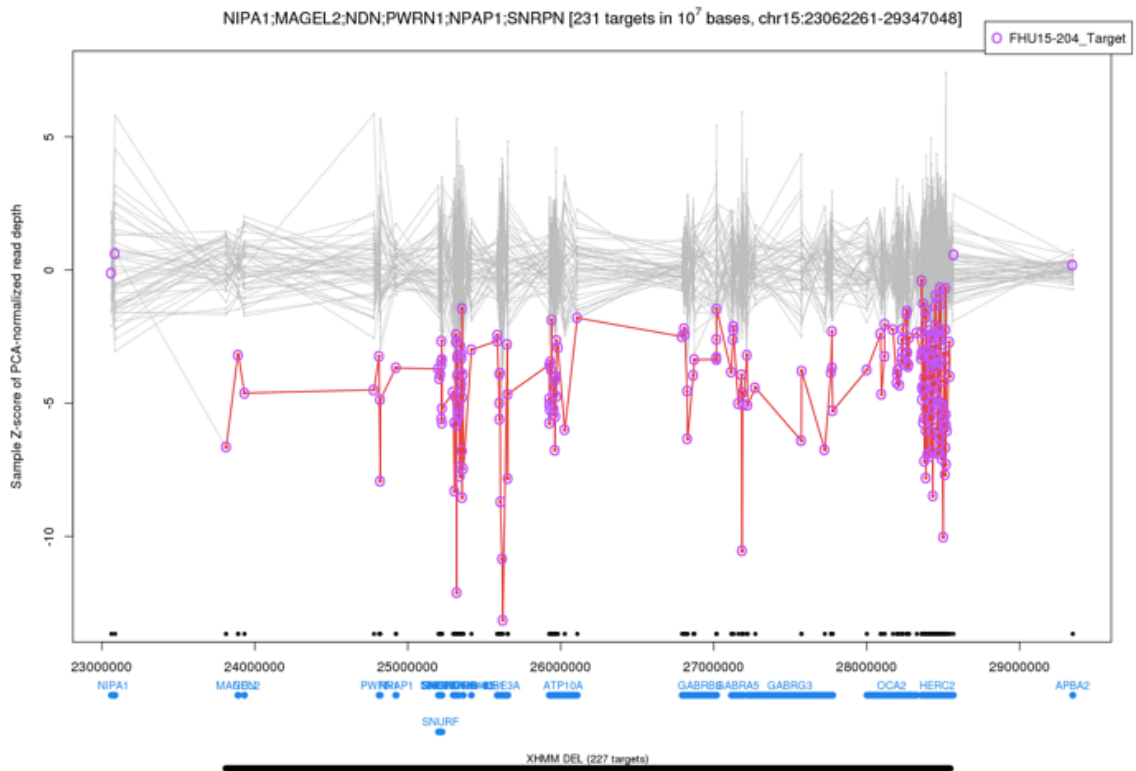
マイクロアレイ染色体検査でみつける染色体微細構造異常症候群の診療ガイドラインの確立

	対象疾患リスト	担当
1	1p36欠失症候群	山本俊至
2	1q44欠失症候群	大橋博文
3	2p15-p16.1欠失症候群	大橋博文
4	Feingold症候群(2p24.3欠失)	涌井敬子
5	2q23.1欠失症候群(<i>MBD5</i>)	涌井敬子
6	2q24.2-q24.3欠失/重複症候群(<i>SCN1A</i>)	山本俊至
7	2q32.1-q33.3欠失/重複症候群(<i>SATB2</i>)	黒澤健司
8	2q37欠失症候群	大橋博文
9	3p21.31欠失症候群	大橋博文
10	4p16欠失(Wolf-Hirschhorn症候群)	涌井敬子
11	Cri-du-chat症候群(5pサブテロメア欠失)	涌井敬子
12	5q14.3欠失症候群(<i>MEF2C</i>)	山本俊至
13	5q31欠失症候群	山本俊至
14	8pサブテロメア欠失	黒澤健司
15	Langer-Giedion症候群(8q24.11欠失)	倉橋浩樹
16	11p12-p14欠失症候群	山本俊至
17	Jacobsen症候群(11qサブテロメア欠失)	倉橋浩樹
18	16p11.2欠失/重複症候群	山本俊至
19	Miller-Dieker症候群(17pサブテロメア欠失)	黒澤健司
20	17p13.1欠失症候群(<i>GABARAP</i>)	黒澤健司
21	Smith-Magenis症候群(17p11.2欠失)	黒澤健司
22	Potocki-Lupski症候群(17p11.2重複)	涌井敬子
23	21qサブテロメア欠失症候群	黒澤健司
24	Emanuel症候群(11/22混合トリソミー)	倉橋浩樹
25	22q11.2重複症候群	倉橋浩樹
26	Cat eye症候群(22q11テトラソミー)	倉橋浩樹
27	Phelan-McDermid症候群(22q13欠失)	大橋博文
28	Xp11.3-p11.4欠失(<i>MAOA, MAOB, CASK</i>)	涌井敬子
29	Xq11.1欠失症候群(<i>ARHGEF9</i>)	山本俊至
30	MECP2重複症候群(Xq28重複)	倉橋浩樹
31	9q34欠失症候群	黒澤健司
32	1q重複症候群	涌井敬子

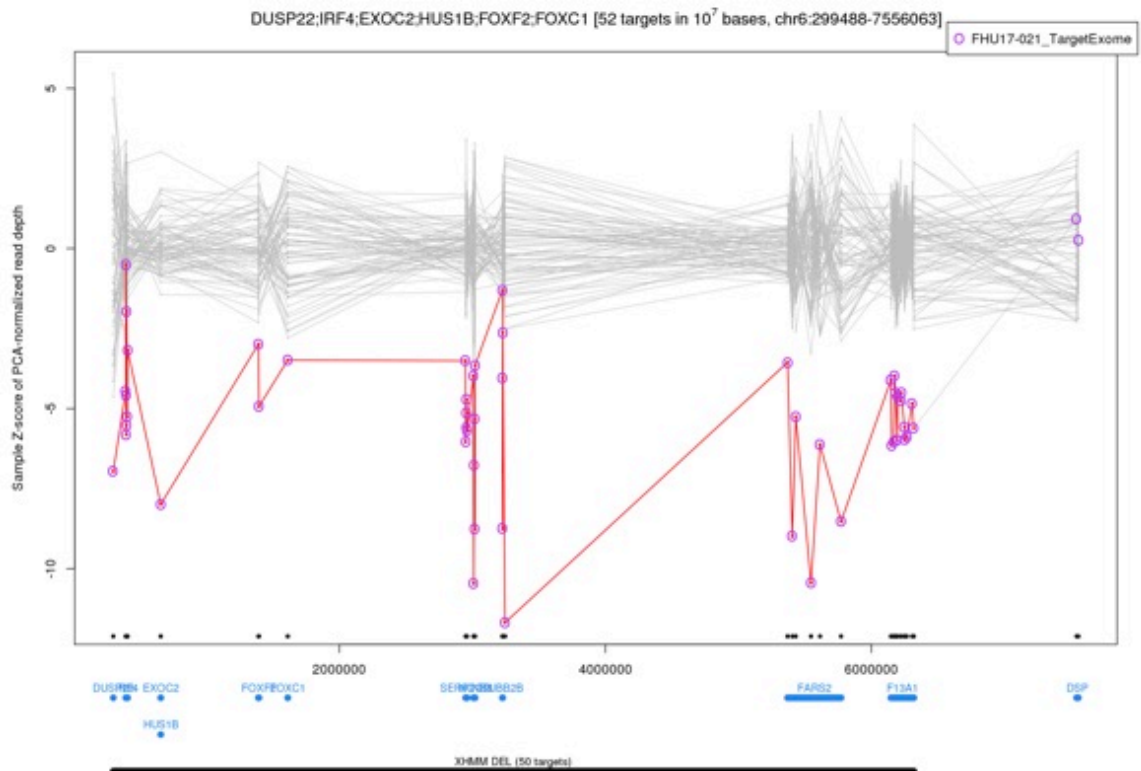
(資料 2)



エクソン単位の欠失・重複



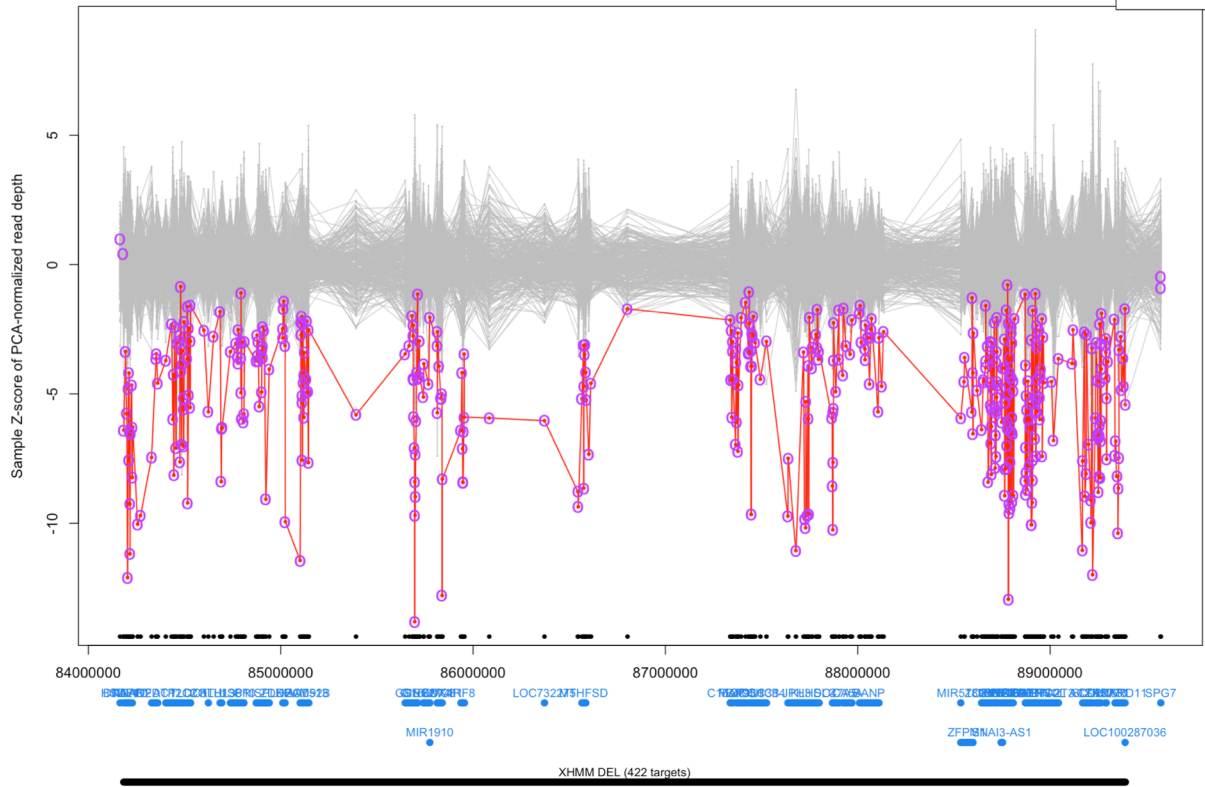
UBE3A



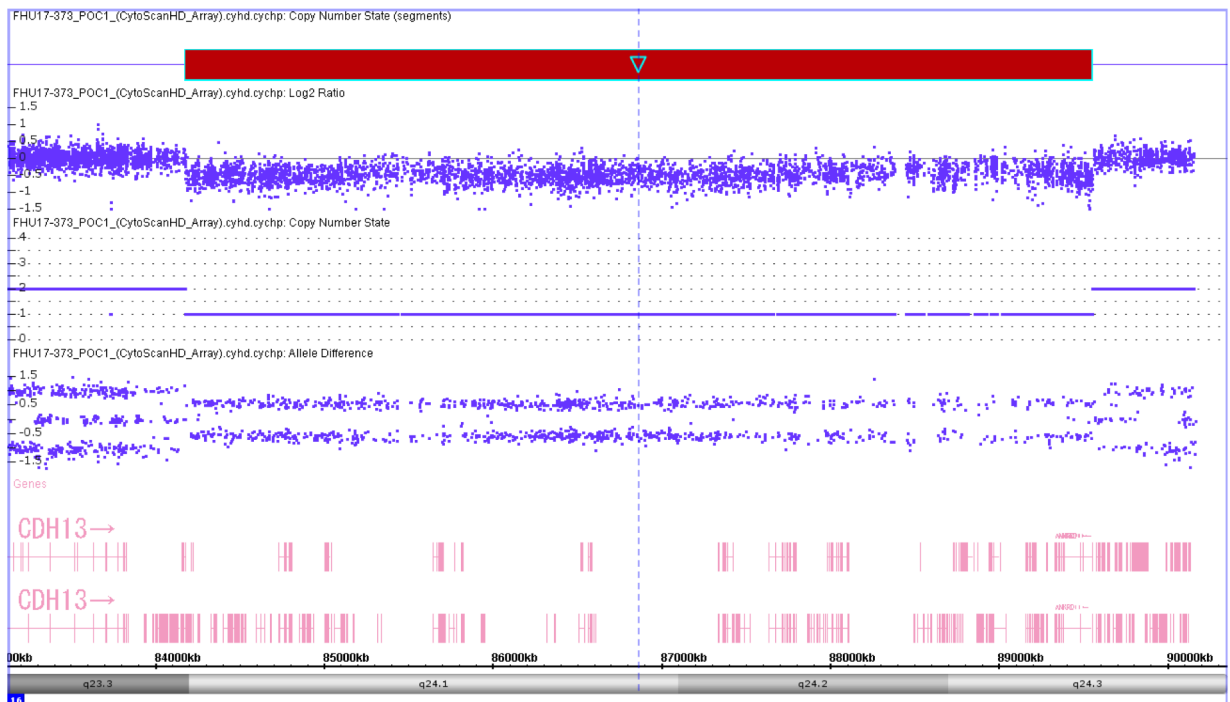
FOXC1

HSDL1;DNAAF1;TAF1C;ADAD2;WFDC1;ATP2C2 [426 targets in 10⁷ bases, chr16:84164556-89575581]

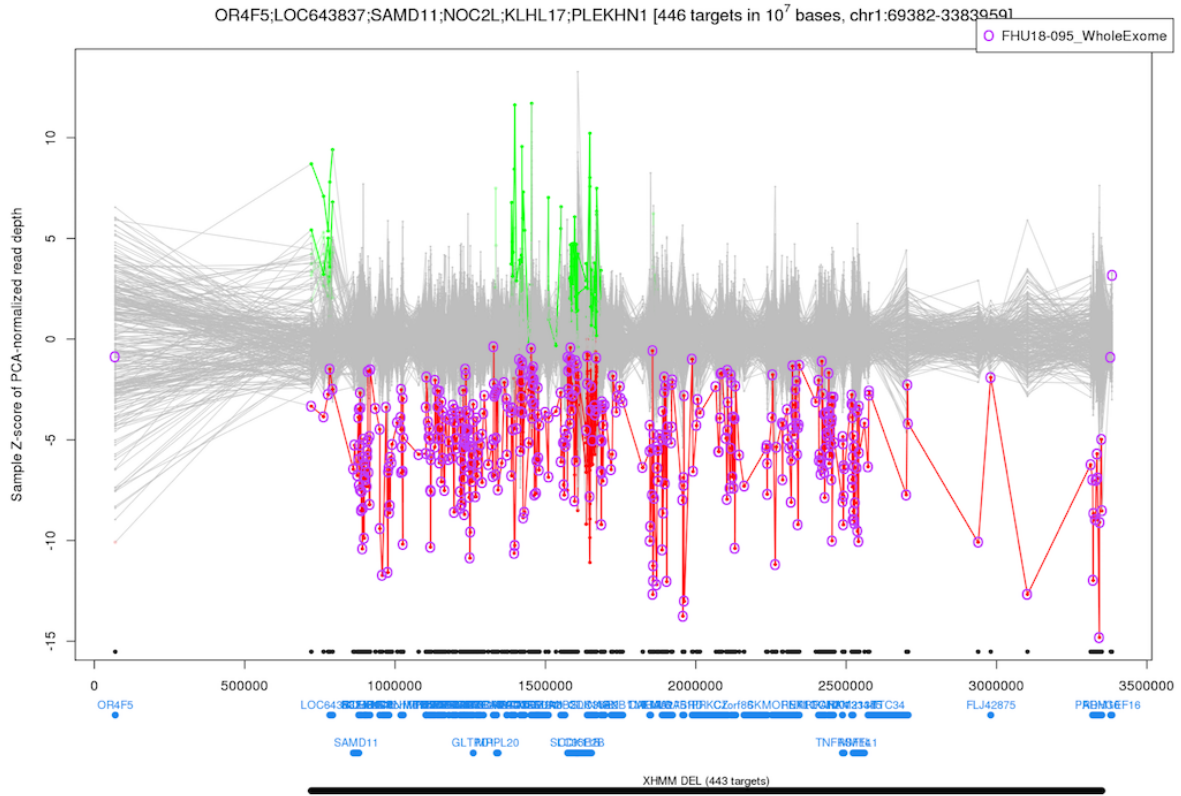
○ FHU17-373



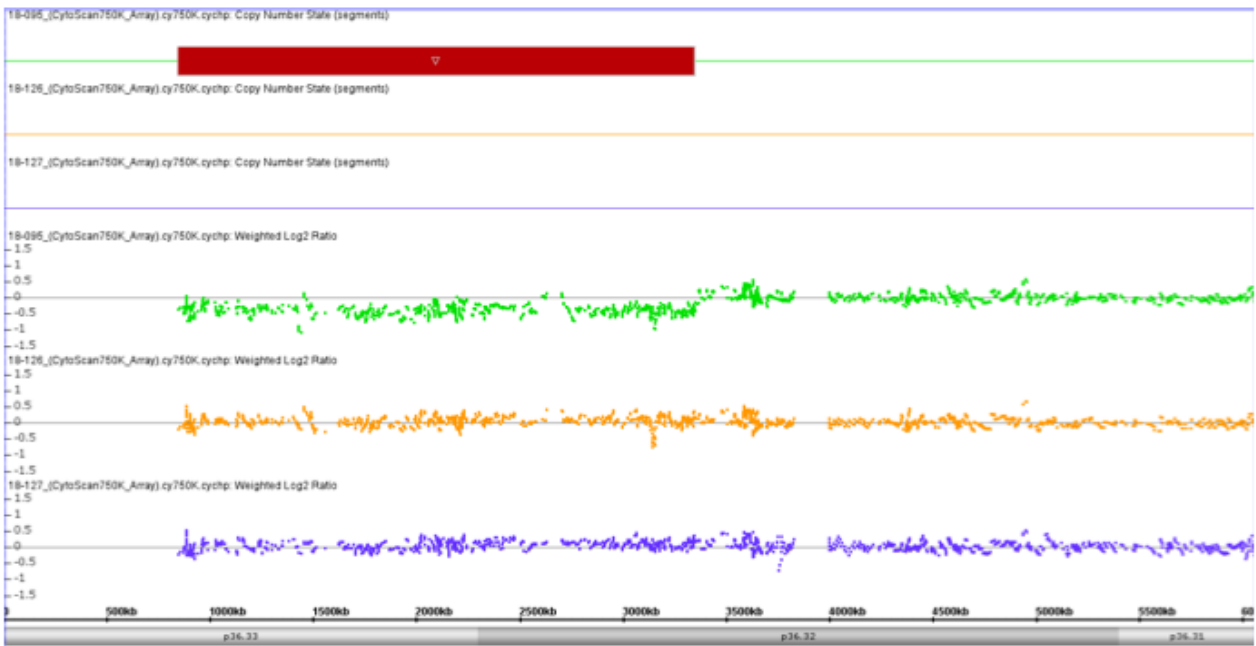
XHMMによる欠失の同定



マイクロアレイによる欠失の確認



XHMMによる欠失の同定



マイクロアレイによるde novo欠失の確認

マイクロアレイ染色体検査を用いた診療体制の確立

研究分担者 黒澤健司

地方独立行政法人神奈川県立病院機構神奈川県立こども医療センター 遺伝科部長

研究要旨

先天異常は、一般集団の約 2-3%に及ぶ遺伝的異質性の高い疾患で、医療においてその正確な診断は不可欠である。この集団に対してマイクロアレイ染色体検査で検出できる疾患は 12%程度とされている。診断未確定症例約 1000 例に対してマイクロアレイ染色体検査によるスクリーニングを行い、約 14%で変異を検出することができた。この中には、**recognizable syndrome** も含まれるが、多くの例は記載あるものの実際には **unrecognizable** な疾患に分類された。一方で比較的頻度が高いとされる **SATB2** 異常症は含まれず、発生頻度が低い多くの症候群は、専門医療機関でも遭遇する頻度は極めて低いことが分かった。医療としてマイクロアレイ染色体を行う際の指針をまとめた。

A. 研究目的

先天異常は、一般集団の約 2-3%に及ぶ遺伝的異質性の高い疾患で、その発生頻度からも病因解析研究は常に医学の大きな課題である。医療においてその正確な診断は不可欠である。しかし、遺伝的異質性が高いが故に、原因解明は膨大な労力を要する。一般に中等度以上の精神遅滞の病因における遺伝的背景の占める割合は、染色体検査で検出可能な疾患は 3%、マイクロアレイ染色体検査で検出できる疾患は 12%程度とされている。本研究では、次世代シーケンス技術やマイクロアレイ染色体検査を用いて、正確な診断を行い、診療ガイドラインを確立することを目的とする。

B. 研究方法

施設内スクリーニングの対象は、神奈川県立こども医療センター受診歴のある診断

未確定症例約 1000 例で、染色体検査などなど一般的遺伝学的検査がなされて染色体異常症は臨床的に否定されている。マイクロアレイ CGH は、Agilent 社製マイクロアレイシステムを用い、アレイは SurePrint G3 Human CGH Microarray kit 8x60K を用いた。解析手順は、Agilent 社による標準プロトコールに準じて進めた。得られたデータの解析は Agilent Genomic Workbench ソフトウェアを用いた。データは DLR spread 値 < 0.30 を採用した。比較対照 DNA は、Promega 社製 Female および Male genomic DNA を用いた。解析したゲノム DNA は、QIAamp DNA Blood Mini kit を用いて自動抽出機で末梢血液から抽出した。アレイ CGH で検出されたゲノムコピー数異常は、ISCN2009 に準じて記載した。参照ゲノムマップとして UCSC Genome Browser on Human Feb. 2009 (hg19)

Assembly を用いた。

検出された CNV を原因とする染色体微細構造異常量の医療管理および疾患概要は文献的考察を中心にまとめた。先天異常症候群を含む遺伝病の疾患概要ならびに遺伝カウンセリング、診療ガイドラインとして GeneReviews

(<https://www.ncbi.nlm.nih.gov/>) や OMIM (<https://www.ncbi.nlm.nih.gov/omim>) や個別症例報告も参照した。

(倫理面への配慮)

マイクロアレイ CGH による解析は、こども医療センター倫理審査において、研究課題「原因不明多発奇形精神遅滞症候群のゲノムワイドな病因解析」として平成 22 年 7 月 22 日に承認を得たものである。検査前に十分な説明を行い、文書により同意のもとで解析を行った。解析にあたっては、全ての個人情報情報を潜在化した。

C、D. 研究結果と考察

施設内診断未確定 1000 症例中には、CNV による SATB2 異常症は検出されなかった。一般に発生頻度は、診断未確定精神遅滞症例の 0.25-0.3% と推定されている。実際には、さらに頻度は低い可能性がある。

マイクロアレイ染色体検査を診療として用いる場合の指針を総説としてまとめ、使用頻度が高い小児科医を対象として総説にまとめた (マイクロアレイ染色体検査 小児臨床検査のポイント 2017 小児内科 2017;49 (増刊号):687-690)。

時代は次世代シーケンスによる網羅的解析に移りつつあることから、次世代氏一県シングからマイクロアレイまで幅広く対応

できる臨床検査としての網羅的解析の中にマイクロアレイを組み入れ、説明文書を立案した。

E. 結論

マイクロアレイも含めた網羅的ゲノム解析検査を前提とした取り組みが今後の課題と考えられた。

F. 研究発表

1. 論文発表

Ono H, Kurosawa K, Wakamatsu N, Masuda S. Hearing impairment in a female infant with interstitial deletion of 2q24.1q24.3. *Congenit Anom (Kyoto)*. 2016 Dec 30. doi: 10.1111/cga.12207. [Epub ahead of print]

Hossain MA, Yanagisawa H, Miyajima T, Wu C, Takamura A, Akiyama K, Itagaki R, Eto K, Iwamoto T, Yokoi T, Kurosawa K, Numabe H, Eto Y. The severe clinical phenotype for a heterozygous Fabry female patient correlates to the methylation of non-mutated allele associated with chromosome 10q26 deletion syndrome. *Mol Genet Metab*. 2017 Mar;120(3):173-179. doi: 10.1016/j.ymgme.2017.01.002.

Shimbo H, Oyoshi T, Kurosawa K. A contiguous gene deletion neighboring TWIST1 identified in a patient with Saethre-Chotzen syndrome associated with neurodevelopmental delay: possible contribution of HDAC9.

Congenit Anom (Kyoto). 2017 Feb 21.
doi: 10.1111/cga.12216. [Epub ahead of
print]

Shimbo H, Yokoi T, Aida N, Mizuno S,
Suzumura H, Nagai J, Ida K,
Enomoto Y, Hatano C, Kurosawa K.
Haploinsufficiency of BCL11A
associated with cerebellar
abnormalities in 2p15p16.1 deletion
syndrome. *Molecular Genetics &
Genomic Medicine* 2017;5(4):429-
437.

Hori I, Kawamura R, Nakabayashi K,
Watanabe H, Higashimoto K,
Tomikawa J, Ieda D, Ohashi K,
Negishi Y, Hattori A, Sugio Y, Wakui
K, Hata K, Soejima H, Kurosawa K,
Saitoh S. CTCF deletion syndrome:
clinical features and epigenetic
delineation. *J Med Genet.* 2017 Aug
28. pii: jmedgenet-2017-104854. doi:
10.1136/jmedgenet-2017-104854.
[Epub ahead of print]

黒澤健司 マイクロアレイ染色体検査 小
児臨床検査のポイント 2017 小児内
科 2017;49 (増刊号) :687-690.

2. 学会発表

Hatano C, Yokoi T, Enomoto Y, Tsurusaki
Y, Saito T, Nagai J, Kurosawa K.
Dosage Changes of *NIPBL* cause
various types of neurodevelopmental
disability. The 13th International
Congress of Human Genetics
2016.4.3-7 Kyoto

Enomoto Y, Yokoi T, Hatano C, Ohashi I,

Kuroda Y, Tsurusaki Y, Ida K, Naruto
T, Kurosawa K. The comprehensive
genetic analysis of Rubinstein-Taybi
syndrome(RSTS). The 13th
International Congress of Human
Genetics 2016.4.3-7 Kyoto

Shimbo H, Yokoi T, Mizuno S, Suzumura
H, Aida N, Nagai J, Ida K, Enomoto Y,
Hatano C, Kurosawa K. Structural
brain abnormalities associated with
deletion at chromosome 2p16.1. The
13th International Congress of Human
Genetics 2016.4.3-7 Kyoto

湊川真理、羽田野ちひろ、横井貴之、大橋
育子、黒田友紀子、黒澤健司 Pitt-
Hopkins 症候群 3 例に対する診断アプ
ローチ 第 119 回日本小児科学会学術
集会 2016.5.13-15 札幌

榎本友美、黒澤健司 CNV 検出手法
XHMM と log2ratio 変換法の比較—実
際の解析例について— 第 169 回染色
体研究会 2017.4.8. 東京慈恵医大

Kurosawa K, Minatogawa M, Yokoi T,
Enomoto Y, Ida K, Harada N, Nagai J,
Tsurusaki Y. Microdeletion of
17q21.31 causes a novel
malformation syndrome. *American
Society of Human Genetics* 2017,
2017.10.17-21. Orlando.

G. 知的財産権の出願・登録状況

なし

別紙4

研究成果の刊行に関する一覧表レイアウト

書籍

著者氏名	論文タイトル名	書籍全体の編集者名	書籍名	出版社名	出版地	出版年	ページ
Fukami M, Kurahashi H	Clinical consequences of chromothripsis and other catastrophic cellular events	Franck Pellenstor	Methods Mol Biol.	Springer	UK	2017	21-34

雑誌

発表者氏名	論文タイトル名	発表誌名	巻号	ページ	出版年
Kurahashi H, Kato T, Miyazaki J, Nishizawa H, Nishio E, Furukawa H, Miyamura H, Ito M, Endo T, Ouchi Y, Inagaki H, Fujii T	Preimplantation genetic diagnosis/screening by comprehensive molecular testing.	Reprod Med Biol	15(1)	13-19	2015
Yokoi S, Ishihara N, Miyai F, Tsutsumi M, Yanagihara I, Fujita N, Yamamoto H, Kato M, Okamoto N, Tsunoda T, Yamasaki M, Kanemura Y, Kosaki K, Kojima S, Saitoh S, Kurahashi H, Natsume J.	TUBA1A mutation can cause a hydranencephaly-like severe form of cortical dysgenesis.	Sci Rep	5	15165	2015
Miyazaki J, Ito M, Nishizawa H, Kato T, Minami Y, Inagaki H, Ohya T, Miyata M, Boda H, Kiriya Y, Kuroda M, Sekiya T, Kurahashi H, Fujii T	Intragenic duplication in the PKHD1 gene in autosomal recessive polycystic kidney disease.	BMC Med Genet	16(1)	98	2015
Morine M, Kohmoto T, Masuda K, Inagaki H, Watanabe M, Naruto T, Kurahashi H, Maeda K, Imoto I	A unique TBX5 microdeletion with microinsertion detected in patient with Holt-Oram syndrome.	Am J Med Genet A	167(12)	3192-3196	2015
Nakagawa T, Taniguchi-Ikeda M, Murakami Y, Nakamura S, Motooka D, Emoto T, Satake W, Nishiyama M, Toyoshima D, Morisada N, Takada S, Tairaku S, Okamoto N, Morioka I, Kurahashi H, Toda T, Kinoshita T, Iijima K	A novel PIGN mutation and prenatal diagnosis of inherited glycosylphosphatidylinositol deficiency.	Am J Med Genet A	170(1)	183-188	2016

Yagasaki H, Shichino H, Shimizu N, Ohye T, <u>Kurahashi H</u> , Yoshikawa T, Takahashi S.	Nine-year follow-up in a child with chromosomal integration of human herpesvirus 6 transmitted from an unrelated donor through the Japan Marrow Donor Program.	Transpl Infect Dis	17(1)	160-1	2015
Miura H, Kawamura Y, Kudo K, Ihira M, Ohye T, <u>Kurahashi H</u> , Kawashima N, Miyamura K, Yoshida N, Kato K, Takahashi Y, Kojima S, Yoshikawa T	Virological analysis of inherited chromosomally integrated human herpesvirus-6 in three hematopoietic stem cell transplant patients.	Transpl Infect Dis	17(5)	728-31	2015
Tacharoenmuang R, Komoto S, Guntapong R, Ide T, Haga K, Katayama K, Kato T, Ouchi Y, <u>Kurahashi H</u> , Tsujitani T, Sangkitporn S, Taniguchi K	Whole genomic analysis of an unusual human G6P[14] rotavirus strain isolated from a child with diarrhea in Thailand: evidence for bovine-to-human interspecies transmission and reassortment events.	PLoS One	10(9)	e0139381	2015
Komoto S, Tacharoenmuang R, Guntapong R, Ide T, Haga K, Katayama K, Kato T, Ouchi Y, <u>Kurahashi H</u> , Tsujitani T, Sangkitporn S, Taniguchi K	Emergence and characterization of unusual DS-1-like G1P[8] rotavirus strains in children with diarrhea in Thailand.	PLoS One	10(11)	e0141739	2015
Nakamura Y, Kikugawa S, Seki S, Takahata M, Iwasaki N, Terai H, Matsubara M, Fujioka F, Inagaki H, Kobayashi T, Kimura T, <u>Kurahashi H</u> , Kato H	PCSK5 mutation in a patient with the VACTERL association.	BMC Res Notes	8	228	2015
Tsuge I, Morishita M, Kato T, Tsutsumi M, Inagaki H, Mori Y, Yamawaki K, Inuo C, Ieda K, Ohye T, Hayakawa A, <u>Kurahashi H</u> .	Novel FATP4 mutations responsible for ichthyosis prematurity syndrome in a Japanese patient.	Hum Genome Var	2	15003	2015
Tairaku S, Taniguchi-Ikeda M, Okazaki Y, Noguchi Y, Nakamachi Y, Mori T, Kubokawa I, Hayakawa A, Shibata A, Emoto T, <u>Kurahashi H</u> , Toda T, Kawano S, Yamada H, Morioka I, Iijima K	Prenatal genetic testing for familial severe congenital protein C deficiency.	Hum Genome Var	2	15017	2015
Inagaki H, Kato T, Tsutsumi M, Ouchi Y, Ohye T, <u>Kurahashi H</u> .	Palindrome-mediated translocations in humans: a new mechanistic model for gross chromosomal rearrangements.	Front Genet	7	125	2016

Tsutsumi M, Yokoi S, Miya F, Miyata M, Kato M, Okamoto N, Tsunoda T, Yamasaki M, Kanemura Y, Kosaki K, Saitoh S, <u>Kurahashi H</u> .	Novel compound heterozygous variants in PLK4 identified in a patient with autosomal recessive microcephaly and chorioretinopathy.	Eur J Hum Genet	24(12)	1702-1706	2016
Boda H, Uchida H, Takaiso N, Ouchi Y, Fujita N, Kuno A, Hata T, Nagatani A, Funamoto Y, Miyata M, Yoshikawa T, <u>Kurahashi H</u> , Inagaki H.	A PDE3A mutation in familial hypertension and brachydactyly syndrome.	J Hum Genet	61(8)	701-3	2016
Taniguchi-Ikeda M, Takeshima Y, Lee T, Nishiyama M, Awano H, Yagi M, Unzaki A, Nozuka K, Nishio H, Matsuo M, <u>Kurahashi H</u> , Toda T, Morioka I, Iijima K.	Next-generation sequencing discloses a nonsense mutation in the dystrophin gene from long preserved dried umbilical cord and low-level somatic mosaicism in the proband mother.	J Hum Genet	61(4)	351-5	2016
Markoff A, <u>Kurahashi H</u> , Grandone E, Bogdanova N.	Annexin A5 haplotype M2 is not a risk factor for recurrent miscarriages in Northern Europe, is there sufficient evidence?	Reprod Biomed Online	32(5)	469-73	2016
Markoff A, <u>Kurahashi H</u> , Grandone E, Bogdanova N.	Authors' response to the letter of Nagirnaja et al. "Response to annexin A5 haplotype M2 is not a risk factor for recurrent miscarriages in Northern Europe, is there sufficient evidence?"	Reprod Biomed Online	33(1)	116-7	2016
Ohye T, Kawamura Y, Inagaki H, Yoshikawa A, Ihira M, Yoshikawa T, <u>Kurahashi H</u> .	A simple cytogenetic method to detect chromosomally integrated human herpesvirus-6.	J Virol Methods	228	74-8	2016
Suzuki E, Shima H, Toki M, Hanew K, Matsubara K, <u>Kurahashi H</u> , Narumi S, Ogata T, Kamimaki T, Fukami M.	Complex X-Chromosomal Rearrangements in Two Women with Ovarian Dysfunction: Implications of Chromothripsis/Chromosynthesis-Dependent and -Independent Origins of Complex Genomic Alterations.	Cytogenet Genome Res	150(2)	86-92	2016
Miyazaki J, Nishizawa H, Kambayashi A, Ito M, Noda Y, Terasawa S, Kato T, Miyamura H, Shiogama K, Sekiya T, <u>Kurahashi H</u> , Fujii T.	Increased levels of soluble corin in pre-eclampsia and fetal growth restriction.	Placenta	48	20-25	2016

Yasui T, Suzuki T, Harada F, Watanabe S, Uga N, Naoe A, Yoshikawa T, Ito T, Nakajima Y, Miura H, Sugioka A, Kato Y, Tokoro T, Tanahashi Y, Kasahara M, Fukuda A, <u>Kurahashi H</u> .	Successful living donor liver transplantation for classical maple syrup urine disease.	Pediatr Transplant	20(5)	707-710	2016
Takaiso N, Nishizawa H, Nishiyama S, Sawada T, Hosoba E, Ohye T, Sato T, Inagaki H, <u>Kurahashi H</u> .	Mutation analysis of the JUNO gene in female infertility of unknown etiology.	Fujita Med J	2(3)	59-61	2016
Rinaldi VD, Bolcun-Filas E, Kogo H, <u>Kurahashi H</u> , Schimenti JC.	The DNA damage checkpoint eliminates mouse oocytes with chromosome synapsis failure.	Mol Cell	67	1026-1036.e2	2017
Nakae S, Kato T, Murayama K, Sasaki H, Abernethy M, Kumon M, Kumai T, Yamashiro K, Inamasu J, Hasegawa M, <u>Kurahashi H</u> , Hirose Y.	Remote intracranial recurrence of IDH mutant gliomas is associated with TP53 mutations and an 8q gain.	Oncotarget	8	84729-84742	2017
Azuma Y, Töpf A, Evangelista T, Lorenzoni P, Roos A, Viana P, Inagaki H, <u>Kurahashi H</u> , Lochmüller H.	Intragenic DOK7 deletion detected by whole-genome sequencing in congenital myasthenic syndromes.	Neurol Genet	3	e152	2017
Nagasaka M, Taniguchi-Ikeda M, Inagaki H, Ouchi Y, Kurokawa D, Yamana K, Harada R, Nozu K, Sakai Y, Mishra SK, Yamaguchi Y, Morikoka I, Toda T, <u>Kurahashi H</u> , Iijima K.	Novel missense mutation in DLL4 in a Japanese sporadic case of Adams-Oliver syndrome.	J Hum Genet	62	869	2017
Kawamura Y, Ohye T, Miura H, Ihira M, Kato Y, <u>Kurahashi H</u> , Yoshikawa T.	Analysis of the origin of inherited chromosomally integrated human herpesvirus 6 in the Japanese population.	J Gen Virol	98	1823-1830	2017
Kato T, Ouchi Y, Inagaki H, Makita Y, Mizuno S, Kajita M, Ikeda T, Takeuchi K, <u>Kurahashi H</u> .	Genomic characterization of chromosomal insertions: Implication for mechanism leading to the chromothripsis.	Cytogenet Genome Res	153	1-9	2017
Kohmoto T, Okamoto N, Naruto T, Murata C, Ouchi Y, Fujita N, Inagaki H, Satomura S, Okamoto N, Saito M, Magasuda K, <u>Kurahashi H</u> , Inamoto I.	A case with concurrent duplication, triplication, and uniparental isodisomy at 1q42.12-qter supporting microhomology-mediated break-induced replication model for replicative rearrangements.	Mol Cytogenet	10	15	2017

Kato M, Kato T, Hosoba E, Ohashi M, Fujisaki M, Ozaki M, Yamaguchi M, Sameshima H, Kurahashi H.	PCS/MVA syndrome caused by an Alu insertion in the BUB1B gene.	Hum Genome Var	4	17021	2017
Inoue Y, Sakamoto Y, Sugimoto M, Inagaki H, Boda H, Miyata M, Kato H, Kurahashi H, Okamoto T.	A family with craniofrontonasal syndrome: the first report of familial cases of craniofrontonasal syndrome with bilateral cleft lip and palate.	Cleft Palate Craniofac J	1	15347	2018
Taniguchi-Ikeda M, Morisada N, Inagaki H, Ouchi Y, Takami Y, Tachikawa M, Satake W, Kobayashi K, Tsuneishi S, Takada S, Yamaguchi H, Nagase H, Nozu K, Okamoto N, Nishio H, Toda T, Morioka I, Wada H, Kurahashi H, Iijima K.	Two patients with PNKP mutations presenting with microcephaly, seizure, and oculomotor apraxia.	Clin Genet	93(4)	931-933	2018
Ohwaki A, Nishizawa H, Aida N, Kato T, Kambayashi A, Miyazaki J, Ito M, Urano M, Kiriyama Y, Kuroda M, Nakayama M, Sonta SI, Suzumori K, Sekiya T, Kurahashi H, Fujii T..	Twin pregnancy with chromosomal abnormalities mimicking a gestational trophoblastic disorder and coexistent fetus on ultrasound.	J Obstet Gynaecol.	In press	In press	2018
Terasawa S, Kato A, Nishizawa H, Kato T, Yoshizawa H, Noda Y, Miyazaki J, Ito M, Sekiya T, Fujii T, Kurahashi H.	Multiplex PCR in noninvasive prenatal diagnosis for FGFR3-related disorders.	Congenit Anom (Kyoto)	In press	In press	2018
Kibe M, Ibara S, Inagaki H, Kato T, Kurahashi H, Ikeda T.	Lethal persistent pulmonary hypertension of the newborn in Bohring-Opitz syndrome.	Am J Med Genet A	176(5)	1245-1248	2018
Yamaguchi T, Yamaguchi M, Akeno K, Fujisaki M, Sumiyoshi K, Ohashi M, Sameshima H, Ozaki M, Kato M, Katano T, Hosoba E, Kurahashi H.	Prenatal diagnosis of premature chromatid separation/mosaic variegated aneuploidy (PCS/MVA) syndrome.	J Obstet Gynaecol Res	In press	In press	2018

Yokoi K, Nakajima Y, Ohye T, Inagaki H, Wada Y, Fukuda T, Sugie H, Yuasa I, Ito T, <u>Kurahashi H.</u>	Disruption of the responsible Gene in a phosphoglucomutase 1 deficiency patient by homozygous chromosomal inversion.	JIMD Rep	In press.	In press.	2018
Tsutsumi M, Fujita N, Suzuki F, Mishima T, Fujieda S, Watari M, Takahashi N, Tonoki H, Moriwaka O, Endo T, <u>Kurahashi H.</u>	Constitutional jumping translocation involving the Y and acrocentric chromosomes.	Asian J Androl	In press.	In press.	2018
Sharma R, Gardner A, Homan C, Douglas E, Mefford H, Wiczorek D, Stark Z, Nowak C, Douglas J, Parsons G,	Clinical and functional assessment of novel variation in THOC2, an essential component of nuclear mRNA export machine	Hum Mutat	In press.	In press.	2018

Preimplantation genetic diagnosis/screening by comprehensive molecular testing

Hiroki Kurahashi^{1,2} · Takema Kato¹ · Jun Miyazaki^{1,3} · Haruki Nishizawa³ · Eiji Nishio³ · Hiroshi Furukawa⁴ · Hironori Miyamura³ · Mayuko Ito³ · Toshiaki Endo⁵ · Yuya Ouchi² · Hidehito Inagaki^{1,2} · Takuma Fujii³

Received: 26 May 2015 / Accepted: 1 July 2015
© Japan Society for Reproductive Medicine 2015

Abstract Although embryo screening by preimplantation genetic diagnosis (PGD) has become the standard technique for the treatment of recurrent pregnancy loss in couples with a balanced gross chromosomal rearrangement, the implantation and pregnancy rates of PGD using conventional fluorescence in situ hybridization (FISH) remain suboptimal. Comprehensive molecular testing, such as array comparative genomic hybridization and next-generation sequencing, can improve these rates, but amplification bias in the whole genome amplification method remains an obstacle to accurate diagnosis. Recent advances in amplification procedures combined with improvements in the microarray platform and analytical method have overcome the amplification bias, and the data accuracy of the comprehensive PGD method has reached the level of clinical laboratory testing. Currently, comprehensive PGD is also applied to recurrent pregnancy loss due to recurrent fetal aneuploidy or infertility with recurrent implantation failure, known as preimplantation genetic

screening. However, there are still numerous problems to be solved, including misdiagnosis due to somatic mosaicism, cell cycle-related background noise, and difficulty in diagnosis of polyploidy. The technology for comprehensive PGD also requires further improvement.

Keywords Microarray · Next-generation sequencing · Preimplantation genetic diagnosis · Recurrent pregnancy loss · Translocation

Introduction

Recurrent pregnancy loss (RPL) is a common clinical condition affecting approximately 5 % of couples trying to conceive [1]. A significant proportion of RPL is associated with chromosomal etiologies. For example, in 3.5 % of couples with RPL, one of the partners is a carrier of a balanced gross chromosomal rearrangement such as translocation or inversion. These particular cases could be treated by preimplantation genetic diagnosis (PGD). PGD involves chromosomal analysis of the fertilized egg using fluorescence in situ hybridization (FISH). Human fertilized eggs undergo cell division about every 24 h, and single blastomere biopsy of the 8-cell stage embryo at day 3 followed by FISH is the conventional approach for PGD. Three-color FISH can theoretically distinguish a cell with balanced chromosomal content from that with an unbalanced chromosome that will result in pregnancy loss.

Nonetheless, the implantation and pregnancy rates of PGD using the conventional FISH method remain suboptimal, partly due to the technical uncertainty of FISH, mostly due to errors caused by overlapping or split signals. Another problem is chromosomal mosaicism among blastomeres, as discussed in detail below. A large series of

✉ Hiroki Kurahashi
kura@fujita-hu.ac.jp

¹ Division of Molecular Genetics, Institute for Comprehensive Medical Science, Fujita Health University, 1-98 Dengakugakubo, Kutsukake-cho, Toyoake, Aichi 470-1192, Japan

² Genome and Transcriptome Analysis Center, Fujita Health University, Toyoake, Aichi 470-1192, Japan

³ Department of Obstetrics and Gynecology, Fujita Health University School of Medicine, Toyoake, Aichi 470-1192, Japan

⁴ Department of Laboratory Medicine, Fujita Health University Hospital, Toyoake, Aichi 470-1192, Japan

⁵ Department of Obstetrics and Gynecology, Sapporo Medical University, Sapporo, Hokkaido 060-8543, Japan

studies show a diagnostic error rate of approximately 10 % [2]. To improve accuracy, FISH using two blastomeres was attempted since it was believed that one or two blastomeres could be taken without damaging the biopsied embryos [3]. However, some studies have indicated that 2-cell biopsy is harmful to the embryo [4]. Another idea is blastocyst biopsy at day 5 to take more trophectodermal cells [5]. However, after the embryo has reached the 8-cell stage, the cells start to compact and the cell size becomes smaller than at the blastomere stage, which might adversely affect the accuracy of the diagnosis [6]. Development of a more secure diagnostic method that can overcome the uncertainty of the conventional FISH method is required.

Comprehensive PGD

Another issue that can affect the pregnancy rate in PGD is the effect of chromosomal aneuploidy. At least 40 % of conceptuses are aneuploid, and most aneuploid conceptuses lead to pregnancy loss [7]. Intrinsically, oocytes undergo errors in chromosome segregation much more frequently than sperm or somatic cells. The origin of the extra chromosome in trisomic fetuses or conceptuses is predominantly maternal [8]. This is because the pachytene checkpoint in the prophase of meiosis I that prevents aneuploidy during gametogenesis is less stringent in oogenesis than spermatogenesis [9, 10]. It also seems likely that the loss of spindle assembly checkpoint occurs during oogenesis when the single egg cell becomes very large [11].

In addition, maternal age considerably affects the rate of chromosomal aneuploidy in conceptuses [8, 12]. The magnitude of the effect is extraordinary: among women under the age of 25 years, ~2 % of all pregnancies are trisomic, but, among women over 40 years, this rate increases to 35 %. Age-dependent loss of meiotic cohesion is suggested to be responsible for the age-dependent increase in oocyte aneuploidy [13, 14]. Moreover, translocation affects the segregation error of non-translocated chromosomes via non-homologous synapsis in meiosis, which is called the interchromosomal effect [15]. This proposed mechanism is based on anecdotal observation, but might increase the aneuploidy of the preimplantation embryos, increasing the rate of pregnancy loss. However, the influence of this effect is so low as to be negligible [16].

Thus, in PGD for a couple with a chromosomal translocation carrier, even if the chromosomal content affected by the translocation, balanced or unbalanced, is accurately diagnosed by FISH, the effect of the aneuploidy is too large for the pregnancy rate to be sufficiently improved. To screen more chromosomes, an increased

number of probes has been tried [2]. The application of two or even three rounds of FISH could provide information on 24 chromosomes. However, as far as FISH is concerned, the more probes applied, the greater the chances of diagnostic errors.

Microarray is a useful tool for overcoming these difficulties. The microarray, a tool for comprehensive quantitative analysis of genes, was originally developed for genome-wide expression profiling, in particular, for comparative study between two cell populations. Later, the microarray was used for cytogenetics, and it is now an indispensable tool in molecular cytogenetics to detect submicroscopic deletions and duplications. This technique is a product of a revolutionary idea. In a standard FISH, chromosomes of the samples are placed on a glass slide and labeled probes are hybridized on the slide. In the cytogenetic microarray, numerous probes are placed on the slide, and the genomic DNA of the test samples is labeled and hybridized on the slide. In the earlier studies, two types of platforms were used and compared: microarrays equipped with either oligonucleotide probes or bacterial artificial chromosomes (BAC) clones that have an insert of 200 kb long. The sensitivity of the oligonucleotide microarray was subsequently found to be better [17]. Thus, oligonucleotide microarray is currently the standard technique for the molecular diagnosis of patients with mental retardation or multiple congenital anomalies in clinical settings.

In PGD, only one blastomere or ~5 trophectodermal cells can be used for genetic testing. Whole genome amplification (WGA) is required to obtain sufficient genomic DNA for microarray analysis. However, WGA always involves a degree of amplification bias. This bias affects the results of the cytogenetic microarray to varying degrees (Fig. 1). The amplification bias might present as

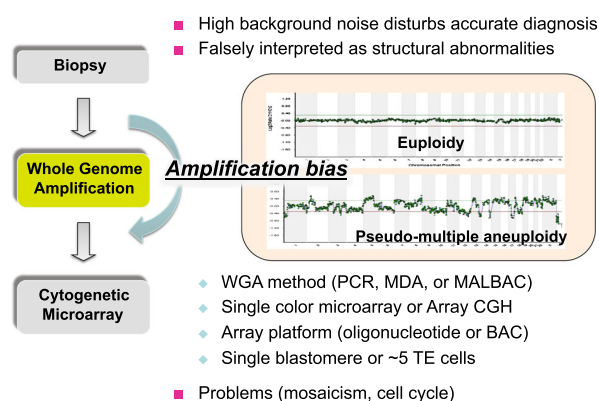


Fig. 1 Problems associated with WGA in cPGD/PGS. Examples for cPGD are shown. *Upper panel* indicates a standard result for euploid sample, whereas *lower panel* indicates the pseudo-multiple aneuploidy with high background noise produced by the amplification bias or the effect of DNA replication

background noise that is too high to accurately quantify copy numbers or might be falsely interpreted as structural abnormalities [18]. These concerns considerably affect the interpretation of comprehensive PGD (cPGD) results.

Overcoming the amplification bias

Improvements in the cPGD technique have resulted from advances in reducing amplification bias. In earlier studies, cPGD was performed using genomic DNA prepared by a PCR-based amplification method [19]. However, the PCR-based method is always accompanied by an intrinsic amplification bias. Because PCR is based on DNA synthesis, short DNA fragments are preferentially amplified. Another problem is sequence-dependent bias. Amplification of GC-rich regions is difficult because they are more resistant to denaturation and more likely to form secondary structures. Later, a multiple displacement amplification (MDA) method using a phi29 DNA polymerase with strand displacement activity was introduced. Because this polymerase can theoretically resolve secondary structures in template DNA, sequence-dependent WGA bias can be somewhat reduced [20, 21]. However, the bias is still an obstacle for the analysis of a single cell or a small number of cells.

Array comparative genomic hybridization (CGH) is one solution for the amplification bias problem. The sequence-specific amplification bias should be similar among human samples because >99 % of nucleotide sequences are identical. In array CGH, test and reference samples are prepared, labeled with different fluorescent dyes, and simultaneously hybridized to one microarray. When the data are interpreted as a ratio of the two samples, any sequence-specific bias would be offset. Initial CGH analysis was performed on metaphase chromosome specimens, but now on DNA probes spotted or synthesized on the microarray platform [19, 22–24].

Another improvement involves the selection of the microarray probes. The standard oligonucleotide microarray, which shows good performance in clinical pediatrics, is considerably influenced by WGA bias. For WGA-amplified samples, BAC arrays were found to work better because the large size of the probes can dilute the effect of the amplification bias at individual sites [25]. Recently, new WGA technology that can significantly reduce the amplification bias has led to a breakthrough in this field. The method is based on MDA, but the DNA fragments synthesized in the initial amplification cycles form a loop that prevents further amplification, which is called multiple annealing and looping-based amplification cycles (MAL-BAC) [26, 27]. The combination of this amplification

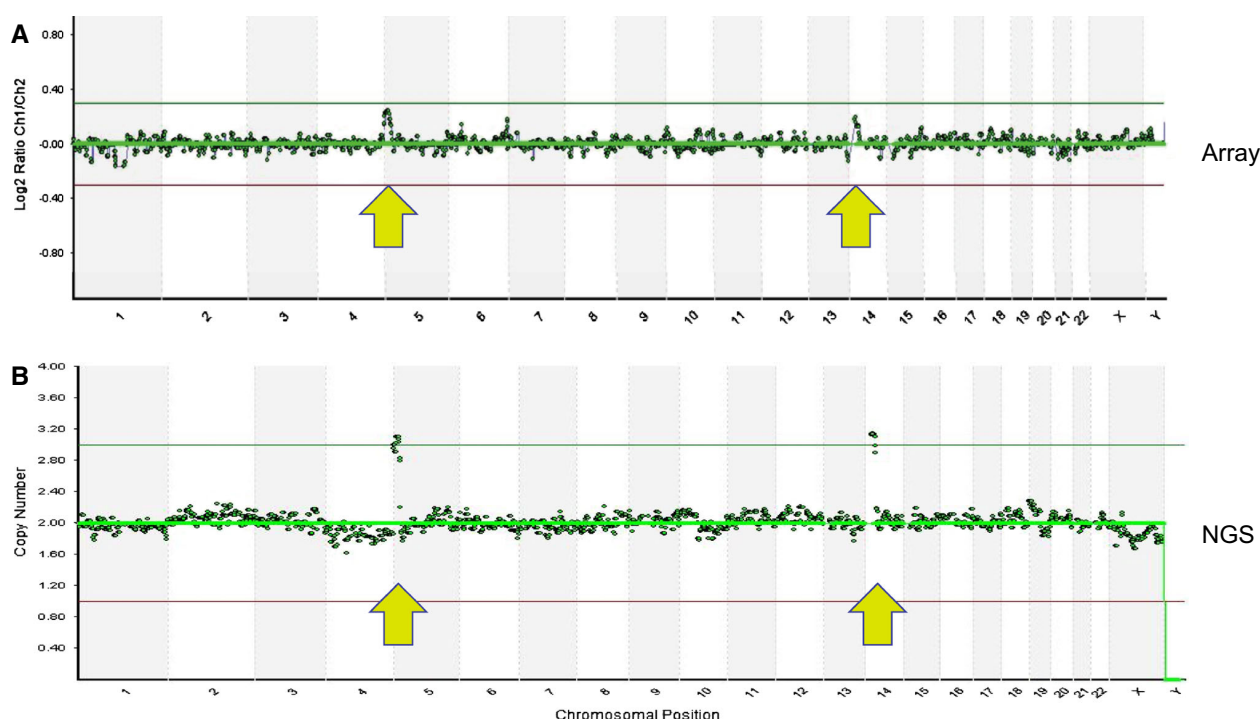


Fig. 2 Comparison of cPGD by BAC array and NGS. Single cell from EBV-transformed lymphoblastoid cell line with 47,XX,+der(14)t(5;14)(p14.3;p13.2) was subjected to WGA followed by analyses with array CGH using BAC array (a) or NGS (b). This

cell line carries 20.9 Mb partial trisomy at 5p and 13.2 Mb partial trisomy at 14p. In this case, sensitivity appears better in NGS than BAC array

method and the array CGH on the BAC array has yielded good performance in PGD [28]. Currently, the BAC array-based protocol (3000 probes per haploid genome) is becoming the standard technique in cPGD for translocation carriers (Fig. 2a).

On the other hand, in the case of the oligonucleotide microarray, dilution of the effect of the amplification bias could be achieved by altering the setup of the window when the raw data are being analyzed. The processed data obtained by averaging the signal intensities of the probes within the window appear to be reasonably accurate. More recently, an array platform specific for PGD was also designed by the selection of probes that are not subject to an amplification bias [29]. These efforts have improved the quality of the cPGD data from the molecular biology research level to that of the clinical laboratory test.

Problems remaining

One of the problems still affecting the interpretation of the results is mosaicism. Blastomeres in cleavage stage embryos show a high rate of mosaicism for aneuploidy, as well as structural abnormalities [30]. In general, chromosome segregation is strictly regulated by the spindle assembly checkpoint. However, in the oocyte or blastomere, where the protein components are diluted in a large cell volume, the function of the spindle assembly checkpoint is transiently deficient, leading to a high rate of mosaicism in this period [11]. This phenomenon raises a fundamental question of whether data obtained from a single blastomere can represent the data of the embryo. Thus, sampling of 3–5 cells by trophectoderm biopsy is now becoming a mainstream approach in cPGD.

Aneuploidy mosaicism in the blastomere stage leads to another aspect that complicates the interpretation of the PGD results: self-correction. A considerable number of embryos showing aneuploidy in the blastomere biopsy undergo self-correction and become euploid embryos during further culture [31, 32]. This means that a low rate of mosaicism might be insignificant. Experimental data using a mixture of DNA from euploid cells and aneuploid cells show that samples with mosaic rates of more than 25 % can be detected by cytogenetic array [33]. This detection rate might be reasonable for missing the low rate of mosaicism of aneuploids intentionally.

Next, cell cycle-related problems also affect the results. In humans, DNA replication starts at more than 10,000 sites throughout the genome. During S phase, the DNA copy number status is like a patchwork. The genomic regions where the DNA replication has already finished have two copies and the remaining regions still have only one copy. This is also a serious problem because these copy

number differences might be falsely interpreted as structural abnormalities or might present as high background noise [34, 35]. To avoid this phenomenon, it might be possible to perform sampling just after the cell division under continuous observation using a live imaging system. If the number of cells for the test sample can be increased by trophectoderm biopsy in the blastocyst stage, the effects of different DNA replication timing in each cell might be reduced.

Further, the detection of polyploidism by cytogenetic microarray is generally difficult. Because triploidy is one of the most frequently observed chromosomal aberrations in the aborted fetus, a failure to detect triploidy might affect the birth rate. Using both 46,XX and 46,XY samples as references, the ratio of sex chromosome signals in the test sample relative to references can give some information regarding the polyploidy, but the results are still ambiguous. Microarrays equipped with probes for genotyping of single nucleotide polymorphisms (SNPs) can be used for the detection of polyploidy, but current SNP arrays are not optimized for WGA [36]. Hopefully, SNP array platforms that can show quantitative signals after WGA will be developed.

Preimplantation screening

As mentioned above, a significant proportion of RPL is associated with chromosomal etiologies. Although one of the partners in 3.5 % of couples with RPL is a carrier of a balanced gross chromosomal rearrangement, some couples have normal karyotypes but undergo RPL due to recurrent fetal aneuploidy. These couples undergo the loss of multiple pregnancies due to trisomy of different chromosomes, called heterotrissomy [37, 38]. Recent studies indicate that greater than 60–90 % of all first trimester miscarriages may be the result of aneuploidy [39]. However, these RPL couples are likely to carry susceptibility for aneuploidy in gametes [40, 41]. Such couples with RPL can be theoretically treated by the screening of 24 chromosomes in PGD, referred to as preimplantation genetic screening (PGS).

A similar situation also arises due to an advanced maternal age [8]. For women above 40 years of age, the miscarriage rate is as high as 45 % [42]. Because most pregnancy losses in this context are due to chromosomal aneuploidy, it is reasonable to imagine that PGS might benefit these couples. In addition, some couples with recurrent implantation failure might be candidates for PGS because a subset of these failures might be due to recurrent chromosomal aneuploidy in their zygotes [43].

Initial PGS attempts involved screening by multicolor and multicycle FISH, but optimal results were not obtained because the number of examined chromosomes was limited

and the resolution of the signal was low [44]. Next, establishment of 24-chromosome screening was achieved by technical improvements in cytogenetic microarrays. PGS is much easier than cPGD because the patients need only the copy number information of the entire chromosome, which is much larger than the unbalanced region of the reciprocal translocations. The European Society of Human Reproduction and Embryology PGD Consortium has reported four times more oocyte retrievals for PGS than for PGD in couples with cytogenetic abnormalities [45]. In Japan, the Japanese Society of Obstetrics and Gynecology will start a 3-year randomized clinical trial to investigate the effectiveness of PGS for couples with RPL or recurrent implantation failure.

However, these patient groups consist of couples with RPL or infertility with heterogeneous etiologies. It is important to identify the couples who can potentially benefit from PGS prior to the procedure. Clinical research combined with genetic analyses should be used to identify susceptibility genes for chromosomal aneuploidy in gametes. Hopefully, personalized medicine for RPL or recurrent implantation failure will one day be established.

Emergence of next-generation sequencing

Since the emergence of next-generation sequencing (NGS), genetic analysis has undergone a dramatic paradigm shift. NGS is a powerful tool that can allow both qualitative and quantitative analyses to be simultaneously performed. Exome analysis is the best example. Previously, patients with possible Mendelian disease were screened by the Sanger sequence for genetic alterations at the nucleotide resolution, whereas multi-exon deletions/duplications were screened by cytogenetic microarray or a different technology, multiplex ligation-dependent probe amplification. In contrast, exome analysis enables genome-wide mutation screening and, at the same time, quantitative analysis of the exome data provides information on multi-exon deletions/duplications [46]. In this sense, NGS might replace the cytogenetic microarray in the near future.

In these days, NGS is commonly used for chromosomal copy number analysis, particularly in the non-invasive prenatal test for trisomy detection. Fetal DNA can be found in maternal plasma as cell-free fetal DNA, but only as a minor fraction (~10 %). Massive parallel sequencing by NGS followed by quantitative determination according to chromosomal assignment enables the prediction of fetal aneuploidy [47, 48].

In cPGD/PGS, the copy numbers of 24 chromosomes are estimated in a similar way [49]. Indeed, WGA-amplified genomic DNA is sequenced using an NGS-based protocol. Approximately three million sequence reads are

mapped and divided into ~1 Mb windows (2500 windows per haploid genome), and then reads in each window are quantified. NGS-based cPGD/PGS appears to be more versatile than microarrays (Fig. 2b). In general, only 0.02 times coverage of the whole genome is enough to identify not only the copy number abnormalities of whole chromosomes, but also those derived from unbalanced translocations. If the sensitivity needs to be increased to detect smaller unbalanced regions, sequence reads can be increased accordingly. The size or position of the window can also be modified for specific cases.

Some ethicists and sociologists have ethical concerns about whole genome embryo sequencing. If people know the nucleotide sequences of all of the genes of their offspring, they would want to know not only the genetic information regarding disease susceptibility, but also that of learning ability or athletic performance. Finally, people might want to change the genetic code of the embryos, leading to “designer babies”. For cPGD/PGS, sequence information obtained by the current protocol is equivalent to only 0.02 times coverage of the whole genome. However, it is technically easy to obtain the sequence data of the entire genome. In Japan, the Japanese Society of Obstetrics and Gynecology has not yet permitted PGS in clinical practice. Because the permission of an academic society might lower the hurdle, this issue requires careful handling.

Conclusions

By overcoming the WGA bias, cPGD/PGS has recently become the standard technique in the clinical setting. For couples with a balanced translocation, the sensitivity of the detection of small unbalanced translocations needs to be tested. The procedure needs to be optimized on an individual basis and tailor-made protocols are required. Although it still has some problems, including incidental findings, cPGD/PGS is likely to benefit some couples with RPL or infertility. However, it would be better to determine who can benefit by using a blood test for any susceptibility gene before cPGD/PGS. Of course, it is also important to support the right of refusal when it comes to cPGD/PGS.

Acknowledgments The authors thank Drs. M. Tsutsumi and T. Ohye for helpful discussions. These studies were supported by a grant-in-aid for Scientific Research from the Ministry of Education, Culture, Sports, Science, and Technology of Japan, and grants for Research on Intractable Diseases from the Ministry of Health, Labour and Welfare of Japan.

Compliance with ethical standard

Conflict of interest Hiroki Kurahashi, Takema Kato, Jun Miyazaki, Haruki Nishizawa, Eiji Nishio, Hiroshi Furukawa, Hironori

Miyamura, Mayuko Ito, Toshiaki Endo, Yuya Ouchi, Hidehito Inagaki, and Takuma Fujii declare that they have no conflict of interest.

Human rights statements and informed consent Human rights statements and informed consent: All procedures followed were in accordance with the ethical standards of the responsible committee on human experimentation (institutional and national) and with the Helsinki Declaration of 1964 and its later amendments. Informed consent was obtained from all patients for being included in the study.

Human/animal studies This article does not contain any studies with human or animal subjects performed by any of the authors.

References

- Sierra S, Stephenson M. Genetics of recurrent pregnancy loss. *Semin Reprod Med*. 2006;24(1):17–24 (review).
- Sermon K, Van Steirteghem A, Liebaers I. Preimplantation genetic diagnosis. *Lancet*. 2004;363(9421):1633–41 (review).
- Van de Velde H, De Vos A, Sermon K, Staessen C, De Rycke M, Van Assche E, Lissens W, Vandervorst M, Van Ranst H, Liebaers I, Van Steirteghem A. Embryo implantation after biopsy of one or two cells from cleavage-stage embryos with a view to preimplantation genetic diagnosis. *Prenat Diagn*. 2000;20(13):1030–7.
- Cohen J, Munné S. Two-cell biopsy and PGD pregnancy outcome. *Hum Reprod*. 2005;20(8):2363–4 (author reply 2364–5. **No abstract available**).
- Ruangvutitert P, Delhanty JD, Serhal P, Simopoulou M, Rodeck CH, Harper JC. FISH analysis on day 5 post-insemination of human arrested and blastocyst stage embryos. *Prenat Diagn*. 2000;20(7):552–60.
- Sermon K. Current concepts in preimplantation genetic diagnosis (PGD): a molecular biologist's view. *Hum Reprod Update*. 2002;8(1):11–20.
- Nagaoka SI, Hassold TJ, Hunt PA. Human aneuploidy: mechanisms and new insights into an age-old problem. *Nat Rev Genet*. 2012;13(7):493–504. doi:10.1038/nrg3245 (review).
- Hassold T, Hunt P. To err (meiotically) is human: the genesis of human aneuploidy. *Nat Rev Genet*. 2001;2(4):280–91 (review).
- Kurahashi H, Bolor H, Kato T, Kogo H, Tsutsumi M, Inagaki H, Ohye T. Recent advance in our understanding of the molecular nature of chromosomal abnormalities. *J Hum Genet*. 2009;54(5):253–60. doi:10.1038/jhg.2009.35 (epub 2009 Apr 17. review).
- Kurahashi H, Bolor H, Kato T, Kogo H, Tsutsumi M, Inagaki H, Ohye T. Failure of homologous synapsis and sex-specific reproduction problems. *Front Genet*. 2012;3:112. doi:10.3389/fgene.2012.00112 (eCollection 2012).
- Shao H, Li R, Ma C, Chen E, Liu XJ. Xenopus oocyte meiosis lacks spindle assembly checkpoint control. *J Cell Biol*. 2013;201(2):191–200. doi:10.1083/jcb.201211041 (Epub 2013 Apr 8).
- Munné S, Chen S, Colls P, Garrisi J, Zheng X, Cekleniak N, Lenzi M, Hughes P, Fischer J, Garrisi M, Tomkin G, Cohen J. Maternal age, morphology, development and chromosome abnormalities in over 6000 cleavage-stage embryos. *Reprod Biomed Online*. 2007;14(5):628–34.
- Hodges CA, Revenkova E, Jessberger R, Hassold TJ, Hunt PA. SMC1beta-deficient female mice provide evidence that cohesins are a missing link in age-related nondisjunction. *Nat Genet*. 2005;37(12):1351–5 (epub 2005 Oct 30).
- Tsutsumi M, Fujiwara R, Nishizawa H, Ito M, Kogo H, Inagaki H, Ohye T, Kato T, Fujii T, Kurahashi H. Age-related decrease of meiotic cohesins in human oocytes. *PLoS ONE*. 2014;9(5):e96710. doi:10.1371/journal.pone.0096710 (eCollection 2014).
- Blanco J, Egozcue J, Vidal F. Interchromosomal effects for chromosome 21 in carriers of structural chromosome reorganizations determined by fluorescence in situ hybridization on sperm nuclei. *Hum Genet*. 2000;106(5):500–5.
- Munné S, Escudero T, Fischer J, Chen S, Hill J, Stelling JR, Estop A. Negligible interchromosomal effect in embryos of Robertsonian translocation carriers. *Reprod Biomed Online*. 2005;10(3):363–9.
- Ou Z, Kang SH, Shaw CA, Carmack CE, White LD, Patel A, Beaudet AL, Cheung SW, Chinault AC. Bacterial artificial chromosome-emulation oligonucleotide arrays for targeted clinical array-comparative genomic hybridization analyses. *Genet Med*. 2008;10(4):278–89. doi:10.1097/GIM.0b013e31816b4420.
- Vanneste E, Voet T, Le Caignec C, Ampe M, Konings P, Melotte C, Debrock S, Amyere M, Vikkula M, Schuit F, Fryns JP, Verbeke G, D'Hooghe T, Moreau Y, Vermeesch JR. Chromosome instability is common in human cleavage-stage embryos. *Nat Med*. 2009;15(5):577–83. doi:10.1038/nm.1924 (Epub 2009 Apr 26).
- Wells D, Sherlock JK, Handyside AH, Delhanty JD. Detailed chromosomal and molecular genetic analysis of single cells by whole genome amplification and comparative genomic hybridization. *Nucleic Acids Res*. 1999;27(4):1214–8.
- Handyside AH, Robinson MD, Simpson RJ, Omar MB, Shaw MA, Grudzinskas JG, Rutherford A. Isothermal whole genome amplification from single and small numbers of cells: a new era for preimplantation genetic diagnosis of inherited disease. *Mol Hum Reprod*. 2004;10(10):767–72 (Epub 2004 Aug 20).
- Hellani A, Coskun S, Benkhalifa M, Tbakhi A, Sakati N, Al-Odaib A, Ozand P. Multiple displacement amplification on single cell and possible PGD applications. *Mol Hum Reprod*. 2004;10(11):847–52 (Epub 2004 Oct 1).
- Hu DG, Webb G, Hussey N. Aneuploidy detection in single cells using DNA array-based comparative genomic hybridization. *Mol Hum Reprod*. 2004;10(4):283–9 (Epub 2004 Jan 29).
- Le Caignec C, Spits C, Sermon K, De Rycke M, Thienpont B, Debrock S, Staessen C, Moreau Y, Fryns JP, Van Steirteghem A, Liebaers I, Vermeesch JR. Single-cell chromosomal imbalances detection by array CGH. *Nucleic Acids Res*. 2006;34(9):e68.
- Fiegler H, Geigl JB, Langer S, Rigler D, Porter K, Unger K, Carter NP, Speicher MR. High resolution array-CGH analysis of single cells. *Nucleic Acids Res*. 2007;35(3):e15 (epub 2006 Dec 18).
- Wells D, Alfarawati S, Fragouli E. Use of comprehensive chromosomal screening for embryo assessment: microarrays and CGH. *Mol Hum Reprod*. 2008;14(12):703–10. doi:10.1093/molehr/gan062 (Epub 2008 Oct 28).
- Zong C, Lu S, Chapman AR, Xie XS. Genome-wide detection of single-nucleotide and copy-number variations of a single human cell. *Science*. 2012;338(6114):1622–6. doi:10.1126/science.1229164.
- Hou Y, Fan W, Yan L, Li R, Lian Y, Huang J, Li J, Xu L, Tang F, Xie XS, Qiao J. Genome analyses of single human oocytes. *Cell*. 2013;155(7):1492–506. doi:10.1016/j.cell.2013.11.040.
- Fiorentino F, Spizzichino L, Bono S, Biricik A, Kokkali G, Rienzi L, Ubaldi FM, Iammarrone E, Gordon A, Pantos K. PGD for reciprocal and Robertsonian translocations using array comparative genomic hybridization. *Hum Reprod*. 2011;26(7):1925–35. doi:10.1093/humrep/der082 (Epub 2011 Apr 12).
- Konstantinidis M, Alfarawati S, Hurd D, Paolucci M, Shovelton J, Fragouli E, Wells D. Simultaneous assessment of aneuploidy, polymorphisms, and mitochondrial DNA content in human polar

- bodies and embryos with the use of a novel microarray platform. *Fertil Steril*. 2014;102(5):1385–92. doi:10.1016/j.fertnstert.2014.07.1233 **Epub 2014 Sep 11**.
30. Mertzaniidou A, Wilton L, Cheng J, Spits C, Vanneste E, Moreau Y, Vermeesch JR, Sermon K. Microarray analysis reveals abnormal chromosomal complements in over 70% of 14 normally developing human embryos. *Hum Reprod*. 2013;28(1):256–64. doi:10.1093/humrep/des362 **Epub 2012 Oct 9**.
 31. Munné S, Velilla E, Colls P, Garcia Bermudez M, Vemuri MC, Steuerwald N, Garrisi J, Cohen J. Self-correction of chromosomally abnormal embryos in culture and implications for stem cell production. *Fertil Steril*. 2005;84(5):1328–34.
 32. Barbash-Hazan S, Frumkin T, Malcov M, Yaron Y, Cohen T, Azem F, Amit A, Ben-Yosef D. Preimplantation aneuploid embryos undergo self-correction in correlation with their developmental potential. *Fertil Steril*. 2009;92(3):890–6. doi:10.1016/j.fertnstert.2008.07.1761 **Epub 2008 Sep 30**.
 33. Novik V, Moulton EB, Sisson ME, Shrestha SL, Tran KD, Stern HJ, Mariani BD, Stanley WS. The accuracy of chromosomal microarray testing for identification of embryonic mosaicism in human blastocysts. *Mol Cytogenet*. 2014;7(1):18. doi:10.1186/1755-8166-7-18.
 34. Van der Aa N, Cheng J, Mateiu L, Zamani Esteki M, Kumar P, Dimitriadou E, Vanneste E, Moreau Y, Vermeesch JR, Voet T. Genome-wide copy number profiling of single cells in S-phase reveals DNA-replication domains. *Nucleic Acids Res*. 2013;41(6):e66. doi:10.1093/nar/gks1352 (**epub 2013 Jan 7**).
 35. Dimitriadou E, Van der Aa N, Cheng J, Voet T, Vermeesch JR. Single cell segmental aneuploidy detection is compromised by S phase. *Mol Cytogenet*. 2014;7:46. doi:10.1186/1755-8166-7-46 (**eCollection 2014**).
 36. Northrop LE, Treff NR, Levy B, Scott RT Jr. SNP microarray-based 24 chromosome aneuploidy screening demonstrates that cleavage-stage FISH poorly predicts aneuploidy in embryos that develop to morphologically normal blastocysts. *Mol Hum Reprod*. 2010;16(8):590–600. doi:10.1093/molehr/gaq037 (**epub 2010 May 17**).
 37. Warburton D, Dallaire L, Thangavelu M, Ross L, Levin B, Kline J. Trisomy recurrence: a reconsideration based on North American data. *Am J Hum Genet*. 2004;75(3):376–85 **Epub 2004 Jul 8**.
 38. Rai R, Regan L. Recurrent miscarriage. *Lancet*. 2006;368(9535):601–11 (**review**).
 39. Brezina PR, Brezina DS, Kearns WG. Preimplantation genetic testing. *BMJ*. 2012;18(345):e5908. doi:10.1136/bmj.e5908 (**review. No abstract available**).
 40. Bolor H, Mori T, Nishiyama S, Ito Y, Hosoba E, Inagaki H, Kogo H, Ohye T, Tsutsumi M, Kato T, Tong M, Nishizawa H, Pryor-Koishi K, Kitaoka E, Sawada T, Nishiyama Y, Udagawa Y, Kurahashi H. Mutations of the SYCP3 gene in women with recurrent pregnancy loss. *Am J Hum Genet*. 2009;84(1):14–20. doi:10.1016/j.ajhg.2008.12.002 **Epub 2008 Dec 24**.
 41. McCoy RC, Demko Z, Ryan A, Banjevic M, Hill M, Sigurjonsson S, Rabinowitz M, Fraser HB, Petrov DA. Common variants spanning PLK4 are associated with mitotic-origin aneuploidy in human embryos. *Science*. 2015;348(6231):235–8. doi:10.1126/science.aaa3337.
 42. Stephenson M, Kutteh W. Evaluation and management of recurrent early pregnancy loss. *Clin Obstet Gynecol*. 2007;50(1):132–45 (**review**).
 43. Voullaire L, Wilton L, McBain J, Callaghan T, Williamson R. Chromosome abnormalities identified by comparative genomic hybridization in embryos from women with repeated implantation failure. *Mol Hum Reprod*. 2002;8(11):1035–41.
 44. Mastenbroek S, Twisk M, van Echten-Arends J, Sikkema-Radtz B, Korevaar JC, Verhoeve HR, Vogel NE, Arts EG, de Vries JW, Bossuyt PM, Buys CH, Heineman MJ, Repping S, van der Veen F. In vitro fertilization with preimplantation genetic screening. *N Engl J Med*. 2007;357(1):9–17 **epub 2007 Jul 4**.
 45. Moutou C, Goossens V, Coonen E, De Rycke M, Kokkali G, Renwick P, SenGupta SB, Vesela K, Traeger-Synodinos J. ESHRE PGD Consortium data collection XII: cycles from January to December 2009 with pregnancy follow-up to October 2010. *Hum Reprod*. 2014;29(5):880–903. doi:10.1093/humrep/deu012 **Epub 2014 Mar 11**.
 46. Piazza R, Magistrini V, Pirola A, Redaelli S, Spinelli R, Redaelli S, Galbiati M, Valletta S, Giudici G, Cazzaniga G, Gambacorti-Passerini C. CEQer: a graphical tool for copy number and allelic imbalance detection from whole-exome sequencing data. *PLoS ONE*. 2013;8(10):e74825. doi:10.1371/journal.pone.0074825 (**eCollection 2013**).
 47. Fan HC, Blumenfeld YJ, Chitkara U, Hudgins L, Quake SR. Noninvasive diagnosis of fetal aneuploidy by shotgun sequencing DNA from maternal blood. *Proc Natl Acad Sci USA*. 2008;105(42):16266–71. doi:10.1073/pnas.0808319105 **Epub 2008 Oct 6**.
 48. Chiu RW, Chan KC, Gao Y, Lau VY, Zheng W, Leung TY, Foo CH, Xie B, Tsui NB, Lun FM, Zee BC, Lau TK, Cantor CR, Lo YM. Noninvasive prenatal diagnosis of fetal chromosomal aneuploidy by massively parallel genomic sequencing of DNA in maternal plasma. *Proc Natl Acad Sci USA*. 2008;105(51):20458–63. doi:10.1073/pnas.0810641105 **Epub 2008 Dec 10**.
 49. Fiorentino F, Biricik A, Bono S, Spizzichino L, Cotroneo E, Cottone G, Kokocinski F, Michel CE. Development and validation of a next-generation sequencing-based protocol for 24-chromosome aneuploidy screening of embryos. *Fertil Steril*. 2014;101(5):1375–82. doi:10.1016/j.fertnstert.2014.01.051 **Epub 2014 Mar 6**.

A Unique *TBX5* Microdeletion with Microinsertion Detected in Patient with Holt–Oram Syndrome

Mikio Morine,¹ Tomohiro Kohmoto,^{2,3} Kiyoshi Masuda,² Hidehito Inagaki,⁴ Miki Watanabe,^{2,3} Takuya Naruto,⁵ Hiroki Kurahashi,⁴ Kazuhisa Maeda,¹ and Issei Imoto^{2*}

¹General Perinatal Medical Center, Shikoku Medical Center for Children and Adults, Zentsuji, Japan

²Department of Human Genetics, Institute of Biomedical Sciences, Tokushima University Graduate School, Tokushima, Japan

³Student Lab, Tokushima University Faculty of Medicine, Tokushima, Japan

⁴Division of Molecular Genetics, Institute for Comprehensive Medical Science, Fujita Health University, Toyoake, Japan

⁵Department of Stress Science, Institute of Biomedical Sciences, Tokushima University Graduate School, Tokushima, Japan

Manuscript Received: 18 June 2015; Manuscript Accepted: 24 August 2015

Holt–Oram syndrome (HOS) is an autosomal dominant condition characterized by upper limb and congenital heart defects and caused by numerous germline mutations of *TBX5* producing preterminal stop codons. Here, we report on a novel and unusual heterozygous *TBX5* microdeletion with microinsertion (microindel) mutation (c.627delinsGTGACTCAGGAAACGCTTTCCTGA), which is predicted to synthesize a truncated *TBX5* protein, detected in a sporadic patient with clinical features of HOS prenatally diagnosed by ultrasonography. This uncommon and relatively large inserted sequence contains sequences derived from nearby but not adjacent templates on both sense and antisense strands, suggesting two possible models, which require no repeat sequences, causing this complex microindel through the bypass of large DNA adducts via an error-prone DNA polymerase-mediated translesion synthesis.

© 2015 Wiley Periodicals, Inc.

Key words: microindel; *TBX5*; Holt–Oram syndrome; error-prone DNA polymerase

INTRODUCTION

Holt–Oram syndrome (HOS; MIM# 142900) is a rare autosomal dominant disorder characterized by bilateral upper limb defects involving mainly the pre-axial radial ray and variable congenital heart defects (CHD), most commonly ostium secundum atrial septal defect (ASD) and ventricular septal defect (VSD) [Holt and Oram, 1960; Basson et al., 1994; Huang, 2002]. Although HOS is a highly penetrant disorder, inter- and intra-familial variability is frequently described [Basson et al., 1994; Newbury-Ecob et al., 1996; Brassington et al., 2003]. Mutations in the *TBX5* gene (MIM# *601620) encoding a member of the T-box family of transcription factors cause HOS [Basson et al., 1997; Li et al., 1997]. More than 70% of individuals who meet strict diagnostic criteria for HOS had *TBX5* mutations spread throughout coding exons [Heinritz et al., 2005; McDermott et al., 2005]. Most *TBX5* mutations cause

How to Cite this Article:

Morine M, Kohmoto T, Masuda K, Inagaki H, Watanabe M, Naruto T, Kurahashi H, Maeda K, Imoto I. 2015. A unique *TBX5* microdeletion with microinsertion detected in patient with Holt–Oram syndrome.

Am J Med Genet Part A 167A:3192–3196.

premature truncation of the primary transcript, leading to haploinsufficiency.

Among the various types of germline and somatic mutations causing human genetic diseases, deletions with insertions (indels) are a special and uncommon mutation class, defined as a colocalized insertion and deletion of nucleotides resulting in a net change in the total number of nucleotides, where the two changes are near each other on the DNA [Scaringe et al., 2008]. A microindel (microdeletion with microinsertion) is defined as an indel that results in a net change of one to 50 nucleotides [Gonzalez et al., 2007]. Although a deletion followed by an insertion, or vice-versa, has been suggested to occur by simple combinations of the same mechanisms that cause pure microinsertions and pure microdeletions in microindelogenesis [Chuzhanova et al., 2003],

Mikio Morine and Tomohiro Kohmoto contributed equally to this study.

Conflict of Interest: None.

Grant sponsor: JSPS KAKENHI; Grant number: 26293304.

*Correspondence to:

Issei Imoto, M.D., Ph.D., Department of Human Genetics, Institute of Biomedical Sciences, Tokushima University Graduate School, 3-18-15 Kuramoto-cho, Tokushima, Tokushima 770-8503, Japan.

E-mail: issehgen@tokushima-u.ac.jp

Article first published online in Wiley Online Library (wileyonlinelibrary.com): 4 September 2015

DOI 10.1002/ajmg.a.37359

Scaringe et al. [2008] proposed that microindels are not caused predominantly by combinations of the mutational mechanisms of insertion and deletion but occur during error-prone repair of DNA adducts by translesional polymerase in a one-step manner.

Here, we describe a prenatally diagnosed girl with sporadic HOS in whom we found a novel and unusual microindel of the *TBX5* gene having a 1-nucleotide deletion and a 24-nucleotide insertion with a net gain of 23 nucleotides, resulting in the production of a truncated protein. The inserted sequence with its nearby sequence and a deletion observed in the present case supports the hypothesis that microindels are caused via the activity of a highly error-prone translesional polymerase to bypass a bulky DNA adduct formed by various causes, e.g., genotoxic chemicals and oxidative stress, in the germline, and seems to be consistent with two models, the “Tarzan model” [Scaringe et al., 2008] and the “template switching model” [Sale, 2012].

CLINICAL REPORT

A 29-year-old Japanese woman, gravida 2, para 1, with an uneventful spontaneous vaginal delivery two years previously was referred to our tertiary medical centre at 30 + 3 weeks of gestation for further evaluation of fetal bilateral upper limb abnormalities and CHD. She had no relevant past medical history and there was no history of consanguinity, structural anomalies, or genetic disorders on either side of the family. Prenatal three-dimensional (3-D) ultrasonography (Voluson E8 Expert; GE Healthcare, Waukesha, WI) showed absence of thumb in the right hand and absence of thumb and index finger in the left hand with bilateral radial deviation of the wrist (Fig. 1A and B). Echocardiography revealed multiple muscular and perimembranous ASD and VSD and a persistent left superior vena cava with sinus bradycardia (Fig. 1C and D). No sign of cardiac failure or hydropic findings were present. Biparietal diameter, abdominal circumference and length of the femur, tibiae, fibulae, and humerus were normal for the gestational age, and all the other organs appeared normal. Normal fetal growth, amniotic fluid volume and blood flow velocity waveforms in the umbilical and middle cerebral arteries were recorded. Because the parents opted for fetal karyotyping after counselling, an amniocentesis was performed at 33 + 2 weeks of gestation and the karyotype analysis revealed a normal female karyotype of 46,XX in all examined metaphases. According to the clinical findings, a prenatal diagnosis of HOS was suspected.

At 41 + 1 weeks of gestation, a 2,922 g female with Apgar scores of eight and nine at 1 and 5 min, respectively, was delivered vaginally. On examination, the right upper limb had a radially bowed forearm, radial deviation of the wrist associated with flexion deformity at the elbow and wrist joint caused by absence of the radius and absence of thumb (Fig. 1E). The left upper limb had a shortened middle segment, stiff fingers, and absence of thumb and index finger (Fig. 1F). Radiological examination showed bilateral radial dysplasia with complete absence of the right radius and thumb, the absence of the left radius, thumb and index finger, and hypoplasia of the left humerus (Fig. 1G). Echocardiography confirmed muscular and perimembranous VSD, large secundum ASD, and persistent left superior vena cava draining into a dilated coronary sinus with sinus bradycardia. In addition, there was a right folded ear and abdominal ultrasonography revealed a large

bladder. Brain ultrasonography and radiography of the spine were normal. On the basis of the established criteria for clinical diagnosis, the patient was diagnosed with HOS [McDermott et al., 2005].

MATERIALS AND METHODS

This study was approved by the ethical committees of Shikoku Medical Center for Children and Adults and Tokushima University. Molecular diagnosis was performed using genomic DNA extracted from the patient’s whole blood after informed consent was obtained from her parents. Each coding exon of *TBX5* including exon–intron boundaries was amplified by polymerase chain reaction (PCR) using PrimeSTAR[®] GXL DNA Polymerase (TAKARA Bio, Shiga, Japan) and specific primer sets [Basson et al., 1997; Gruenauer-Kloevekorn and Froster, 2003], and bidirectional sequencing of PCR products was performed using the BigDye[®] Terminator v. 3.1 Cycle Sequencing kit (Applied Biosystems, Foster City, CA) in an ABI 3130 Genetic Analyzer Sequencer (Applied Biosystems).

RESULTS

Genetic Analysis

Molecular analysis of the proband identified a novel heterozygous microindel mutation in exon 6 of the *TBX5* gene, NM_000192.3(*TBX5_v001*):c.627delinsGTGACTCAGGAAACGCTTTCCTGA (Fig. 2AA), which introduces a stop codon at position 210 (NM_00192.3(*TBX5_i001*):p. (Ala210*)) and creates a truncated *TBX5* protein of 209 amino acids lacking part of the T-box domain sequences involved in DNA binding [Bruneau et al., 2001]. Given that most previously reported *TBX5* mutations cause premature truncation of the primary *TBX5* transcript, resulting in haploinsufficiency, this microindel is a likely pathogenic mutation for HOS in this patient. Indeed, the mutation is not present in the NHLBI GO Exome Sequencing Project (ESP6500) Variant Server (<http://evs.gs.washington.edu/EVS/>), the 1,000 Genomes Project database (<http://www.1000genomes.org/>) or the Human Genetic Variation Database (HGVD, <http://www.genome.med.kyoto-u.ac.jp/SnpDB/>), although it has never been reported in the Human Gene Mutation Database professional 2015.2 (HGMD, <http://www.hgmd.org/>) or ClinVar (<http://www.ncbi.nlm.nih.gov/clinvar/>). Because parental DNA was not available, the mutation was not confirmed as de novo.

DISCUSSION

Both germline and somatic indels are uncommon and tend to shorten the nucleotide sequence, with the majority resulting in a net deletion that also shifts the reading frame [Chuzhanova et al., 2003; Scaringe et al., 2008; Stenson et al., 2014]. In mutation databases including HGMD and ClinVar, only one case of a *TBX5* microindel, which had a one-nucleotide deletion and a two-nucleotide insertion, was reported [Basson et al., 1999]. In addition, only one case with an insertion of more than three bases, which contained a 6-base duplication, has been reported in *TBX5* [Debeer et al., 2007]. Thus, the one-base deletion and 24-base insertion with a net 23-base gain detected in our HOS case is the first microindel with an unusually long insertion in the *TBX5* gene.

The 24-base inserted sequence contains 8-base sense and anti-sense (reverse complementary) sequences, which are likely to derive from the same nearby but not adjacent template, with three nucleotides of separation and an additional five nucleotides (Fig. 2A). This finding is mostly consistent with the characteristics of microindels reported by Scaringe et al. [2008] from their analysis of somatic microindels. In microindels, the inserted sequences derive from nearby but not adjacent template sequences on the

sense or antisense strand, in contrast to the slippage that characterises the great majority of pure microinsertions. It was also shown that the mechanisms of microindels, at least those with larger insertions, are highly error-prone overall, with an estimated error rate of 13% per base pair, consistent with the error rates of certain Y-family translesion polymerases [Scaringe et al., 2008]. Thus, the mutation detected in our case seems to be a microindel with a relatively large and complex insertion that arises from the error-

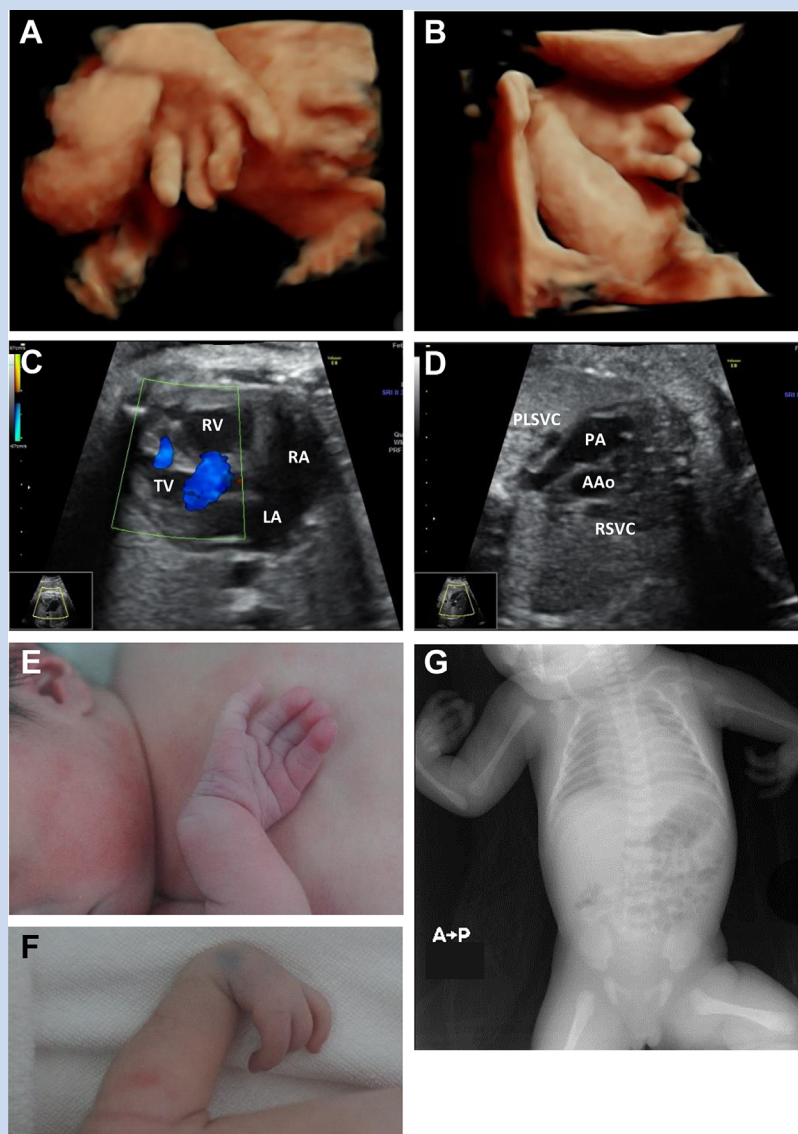


FIG. 1. Clinical photographs of an HOS patient. (A and B) 3-D ultrasonographic images of the fetal upper limbs. The right hand (A) showed absence of thumb, with radial deviation of the wrist, whereas the left hand (B) showed stiff fingers, and absence of thumb and index finger with radial deviation of the wrist. (C and D) Echocardiographic images of the fetus. A four-chamber view (C) showed large perimembranous and muscular VSD, and a three-vessel view (D) showed supernumerary fourth vessels [persistent left superior vena cava, PLSVC] to the left of the pulmonary artery [PA], LV, left ventricle; LA, left atrium; RV, right ventricle; RA, right atrium; AA, ascending aorta; RSVC, right superior vena cava. (E and F) Postnatal appearance of bilateral upper limbs. The right upper limb (E) had a radially bowed forearm, radial deviation of the wrist associated with flexion deformity at the elbow and wrist joint and absence of thumb, whereas the left upper limb (F) had a shortened middle segment, stiff fingers and absence of thumb, and index finger. (G) X-rays of the infant showing the absence of the radius and thumb in the right upper limb and absence of radius, thumb and index finger with hypoplastic humerus in the left upper limb. [Color figure can be seen in the online version of this article, available at <http://wileyonlinelibrary.com/journal/ajmga>].

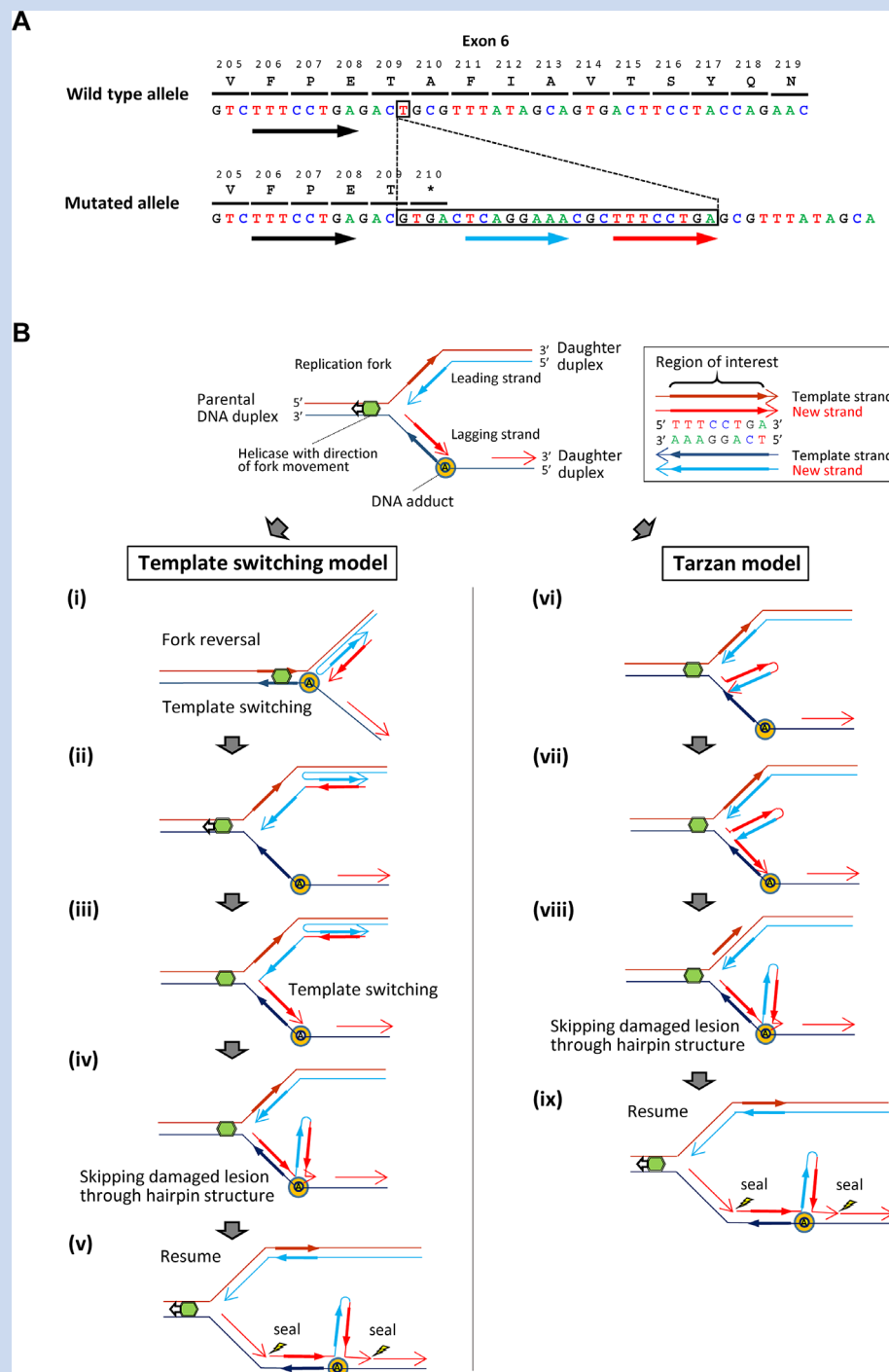


FIG. 2. Characterization of the *TBX5* microindel detected in an HOS patient. **A:** Schematic representation of wild-type (top) and mutated (bottom) sequences observed in *TBX5* exon 6 in the HOS patient. Boxes indicate a 1-nucleotide deletion (top) and a 24-nucleotide insertion (bottom). Red and blue arrows indicate a match and reverse complement to the putative template (black arrows), respectively, observed in the inserted sequence. **B:** Schematic representation of two alternative models causing the *TBX5* microindel in this case. Replication by normal DNA polymerase is blocked by a DNA adduct (orange circle) located around the deletion on the template DNA (upper). For lagging strand synthesis to progress in the presence of a DNA adduct, a sequential nucleotide synthesis from the template strand (ii and iii) occurs after the association of the two nascent DNA strands [i; “template switching model,” lower left] or the nucleotide synthesis from nascent and template strands [vi and vii] after the dissociation of the nascent strand from the template [vi; “Tarzan model” [Scaringe et al., 2008], lower right] with some errors using an error-prone translesion polymerase. In both models, the translesion polymerase is able to swing across a DNA adduct (iv and viii), resulting in skipping of one nucleotide on the template and the normal polymerase can proceed with replication. [Color figure can be seen in the online version of this article, available at <http://wileyonlinelibrary.com/journal/ajmga>.]

prone translesion polymerase-mediated post-replication repair to bypass a DNA adduct, blocking the replication of lagging-strand synthesis (Fig. 2B, upper). On the basis of the inserted sequence containing both sense and antisense sequences derived from the nearby template observed in our case, two alternative models for indelogenesis may be presented. To save a cell with a DNA adduct that blocks replication by normal polymerase, an error-prone translesion polymerase complex may be recruited for the progression of lagging-strand synthesis [Scaringe et al., 2008; Sale, 2012]. In the “template switching model” (Fig. 2B; lower left, i–v), the association of the two nascent DNA strands is followed by additional synthesis on the nascent strand while constituting the inserted sequence from two templates sequentially when switching templates [Sale, 2012]. In the “Tarzan model” previously proposed by Scaringe et al. [2008] (Fig. 2B; lower right, iv–ix), the helicase unwinds the nearby nucleotides of the nascent strand from the template so that the translesion polymerase can loop back on itself and back up on the template strand. In both models, the association of sense and antisense sequences synthesized on the nascent strand from the nearby template form a hairpin structure with some additional length acting like a vine that the translesion polymerase uses to swing across the adduct [Scaringe et al., 2008]. In addition, existence of sequences whose template is undetermined in the insertion, other than sense, and antisense sequences derived from the nearby template, supports the involvement of error-prone translesion polymerase. Because of the lack of repeat sequences around the microindel in our case, serial replication of slippage models, a possible alternative mechanism for microindels with large insertion sizes [Chen et al., 2005], may not be involved in the indelogenesis of the microindel in the present case. Although non-homologous end joining after DNA double-strand breaks is unable to be completely excluded as another possible mechanism for microindel generation, the inserted sequence containing both sense and antisense sequences derived from the nearby template is difficult to be explained by this mechanism.

ACKNOWLEDGMENTS

We thank the family members of the patient for their participation in this study. This work was partly performed in the Cooperative Research Project Program of the Medical Institute of Bioregulation, Kyushu University, and supported by JSPS KAKENHI Grant Numbers 26293304 (I.I.) from the Ministry of Education, Culture, Sports, Science and Technology, Japan.

REFERENCES

- Basson CT, Cowley GS, Solomon SD, Weissman B, Poznanski AK, Traill TA, Seidman JG, Seidman CE. 1994. The clinical and genetic spectrum of the Holt–Oram syndrome (heart hand syndrome). *N Engl J Med* 330:885–891.
- Basson CT, Bachinsky DR, Lin RC, Levi T, Elkins JA, Soultis J, Grayzel D, Kroumpouzou E, Traill TA, Leblanc-Straceski J, Renault B, Kucherlapati R, Seidman JG, Seidman CE. 1997. Mutations in human TBX5 cause limb and cardiac malformation in Holt–Oram syndrome. *Nat Genet* 15:30–35.
- Basson CT, Huang T, Lin RC, Bachinsky DR, Weremowicz S, Vaglio A, Bruzzone R, Quadrelli R, Lerone M, Romeo G, Silengo M, Pereira A, Krieger J, Mesquita SF, Kamisago M, Morton CC, Pierpont ME, Müller CW, Seidman JG, Seidman CE. 1999. Different TBX5 interactions in heart and limb defined by Holt–Oram syndrome mutations. *Proc Natl Acad Sci USA* 96:2919–2924.
- Brassington AME, Sung SS, Toydemir RM, Le T, Roeder AD, Rutherford AE, Whitby FG, Jorde LB, Bamshad MJ. 2003. Expressivity of Holt–Oram syndrome is not predicted by TBX5 genotype. *Am J Hum Genet* 73:74–85.
- Bruneau BG, Nemer G, Schmitt JP. 2001. A murine model of Holt–Oram syndrome defines roles of the T-box transcription factor Tbx5 in cardiogenesis and disease. *Cell* 106:709–721.
- Chen JM, Chuzhanova N, Stenson PD, Ferec C, Cooper DN. 2005. Complex gene rearrangements caused by serial replication slippage. *Hum Mutat* 26:125–134.
- Chuzhanova NA, Anassis EJ, Ball EV, Krawczak M, Cooper DN. 2003. Meta-analysis of indels causing human genetic disease: Mechanisms of mutagenesis and the role of local DNA sequence complexity. *Hum Mutat* 21:28–44.
- Debeer P, Race V, Gewillig M, Devriendt K, Frijns JP. 2007. Novel TBX5 mutations in patients with Holt–Oram syndrome. *Clin Orthop Relat Res* 462:20–26.
- Gonzalez KD, Hill KA, Li K, Li W, Scaringe WA, Wang JC, Gu D, Sommer SS. 2007. Somatic microindels: Analysis in mouse soma and comparison with the human germline. *Hum Mutat* 28:69–80.
- Gruenauer-Kloevekorn C, Froster UG. 2003. Holt–Oram syndrome: A new mutation in the TBX5 gene in two unrelated families. *Ann Genet* 46:19–23.
- Heinritz W, Shou L, Moschik A, Froster UG. 2005. The human TBX5 gene mutation database. *Hum Mutat* 26:397.
- Holt M, Oram S. 1960. Familial heart disease with skeletal malformations. *Br Heart J* 22:236–242.
- Huang T. 2002. Current advances in Holt–Oram syndrome. *Curr Opin Pediatr* 14:691–695.
- Li QY, Newbury-Ecob RA, Terrett JA, Wilson DI, Curtis AR, Yi CH, Gebuhr T, Bullen PJ, Robson SC, Strachan T, Bonnet D, Lyonnet S, Young ID, Raeburn JA, Buckler AJ, Law DJ, Brook JD. 1997. Holt–Oram syndrome is caused by mutations in TBX5, a member of the Brachy-ury (T) gene family. *Nat Genet* 15:21–29.
- McDermott DA, Bressan MC, He J, Lee JS, Aftimos S, Brueckner M, Gilbert F, Graham GE, Hannibal MC, Innis JW, Pierpont ME, Raas-Rothschild A, Shanske AL, Smith WE, Spencer RH, St John-Sutton MG, van Maldergem L, Waggoner DJ, Weber M, Basson CT. 2005. TBX5 genetic testing validates strict clinical criteria for Holt–Oram syndrome. *Pediatr Res* 58:981–986.
- Newbury-Ecob RA, Leanage R, Raeburn JA, Young ID. 1996. Holt–Oram syndrome. *Am J Med Genet* 65:128–132.
- Sale JE. 2012. Competition, collaboration and coordination – determining how cells bypass DNA damage. *J Cell Sci* 125:1633–1643.
- Scaringe WA, Li K, Gu D, Gonzalez KD, Chen Z, Hill KA, Sommer SS. 2008. Somatic microindels in human cancer: The insertions are highly error-prone and derive from nearby but not adjacent sense and antisense templates. *Hum Mol Genet* 17:2910–2918.
- Stenson PD, Mort M, Ball EV, Shaw K, Phillips A, Cooper DN. 2014. The Human Gene Mutation Database: Building a comprehensive mutation repository for clinical and molecular genetics, diagnostic testing and personalized genomic medicine. *Hum Genet* 133:1–9.



Palindrome-Mediated Translocations in Humans: A New Mechanistic Model for Gross Chromosomal Rearrangements

Hidehito Inagaki^{1,2}, Takema Kato¹, Makiko Tsutsumi¹, Yuya Ouchi², Tamae Ohye³ and Hiroki Kurahashi^{1,2*}

¹ Division of Molecular Genetics, Institute for Comprehensive Medical Science, Fujita Health University, Toyoake, Japan,

² Genome and Transcriptome Analysis Center, Fujita Health University, Toyoake, Japan, ³ Department of Molecular Laboratory Medicine, Faculty of Medical Technology, School of Health Science, Fujita Health University, Toyoake, Japan

OPEN ACCESS

Edited by:

Karen M. Vasquez,
The University of Texas at Austin, USA

Reviewed by:

Ruslan Sadreyev,
Howard Hughes Medical Institute,
USA
Albino Bacolla,
The University of Texas MD Anderson
Cancer Center, USA

*Correspondence:

Hiroki Kurahashi
kura@fujita-hu.ac.jp

Specialty section:

This article was submitted to
Bioinformatics and Computational
Biology,
a section of the journal
Frontiers in Genetics

Received: 06 May 2016

Accepted: 28 June 2016

Published: 12 July 2016

Citation:

Inagaki H, Kato T, Tsutsumi M,
Ouchi Y, Ohye T and Kurahashi H
(2016) Palindrome-Mediated
Translocations in Humans: A New
Mechanistic Model for Gross
Chromosomal Rearrangements.
Front. Genet. 7:125.
doi: 10.3389/fgene.2016.00125

Palindromic DNA sequences, which can form secondary structures, are widely distributed in the human genome. Although the nature of the secondary structure—single-stranded “hairpin” or double-stranded “cruciform”—has been extensively investigated *in vitro*, the existence of such unusual non-B DNA *in vivo* remains controversial. Here, we review palindrome-mediated gross chromosomal rearrangements possibly induced by non-B DNA in humans. Recent advances in next-generation sequencing have not yet overcome the difficulty of palindromic sequence analysis. However, a dozen palindromic AT-rich repeat (PATRR) sequences have been identified at the breakpoints of recurrent or non-recurrent chromosomal translocations in humans. The breakages always occur at the center of the palindrome. Analyses of polymorphisms within the palindromes indicate that the symmetry and length of the palindrome affect the frequency of the *de novo* occurrence of these palindrome-mediated translocations, suggesting the involvement of non-B DNA. Indeed, experiments using a plasmid-based model system showed that the formation of non-B DNA is likely the key to palindrome-mediated genomic rearrangements. Some evidence implies a new mechanism that cruciform DNAs may come close together first in nucleus and illegitimately joined. Analysis of PATRR-mediated translocations in humans will provide further understanding of gross chromosomal rearrangements in many organisms.

Keywords: palindrome, inverted repeat, cruciform, chromosomal translocation, gross chromosomal rearrangement

INTRODUCTION

DNA palindromes consist of two units of identical sequences connected in an inverted position with respect to each other. In palindromes, the sequences on the complementary strands read the same in either direction. In other words, the complementary sequence appears in the same strand in an inverted orientation. Palindromic DNA can consequently form specific tertiary structures,

Abbreviations: PATRR, palindromic AT-rich repeat.

namely, single-stranded “hairpin” or double-stranded “cruciform” DNA. Such unusual DNA tertiary structures are called non-B DNA structures (Sinden, 1994; Wang and Vasquez, 2014). These non-B DNA structures are presumed to be generated in a cell under specific situations, although their *in vivo* existence is still a controversial subject.

Hairpin structures can be formed when the double helix DNA is dissociated into single-stranded DNA molecules at the palindrome. Such single-stranded DNA might occur during DNA or RNA synthesis during replication or transcription. On the other hand, cruciform formation starts from unwinding of the center of the double-stranded palindromic DNA, followed by extrusion at the center of the palindrome to form an intra-strand base-pairing of each strand. As the DNA unwinds, the cruciform gets bigger. Cruciform formation requires an under-twisted state, that is, negative superhelicity, of the DNA. Such unusual DNA structure itself could have an impact on DNA replication, repair, transcription, or other important biological pathways (Inagaki and Kurahashi, 2013). The DNA regions that potentially form non-B DNA structures often manifest genomic instability that induces gross chromosomal rearrangements (Pearson et al., 2005; Tanaka et al., 2005; Maizels, 2006; Raghavan and Lieber, 2006; Mirkin, 2007; McMurray, 2010).

PALINDROME-MEDIATED CHROMOSOMAL TRANSLOCATIONS IN HUMAN SPERM

The best-studied palindromic sequences are the breakpoint sequences of the constitutional t(11;22)(q23;q11.2) translocation, a well-known recurrent non-Robertsonian translocation in humans. Balanced carriers are healthy but often have reproductive problems such as infertility, recurrent pregnancy loss, and offspring with Emanuel syndrome (Carter et al., 2009; Ohye et al., 2014; Emanuel et al., 2015). Breakpoint analysis of 11q23 and 22q11 revealed that these regions contain a large palindrome of hundreds of base pairs that is extremely AT-rich (Kurahashi et al., 2000a, 2007; Edlmann et al., 2001; Kurahashi and Emanuel, 2001a; Tapia-Páez et al., 2001). These so-called palindromic AT-rich repeats (PATRRs) have been identified at both breakpoints on chromosomes 11 and 22 and are named PATRR11 and PATRR22, respectively. These PATRRs have several features in common. Both are several hundred base pairs in length and have greater than 90% AT content. They manifest nearly perfect palindromes without spacer regions but share little homology between the two chromosomes.

The most prominent feature of the t(11;22) translocation is that *de novo* translocations frequently arise at a similar breakpoint location. Translocation-specific PCR with primers flanking the breakpoints on chromosomes 11 and 22 can detect all of the t(11;22) junction sequence in the translocation carriers (Kurahashi et al., 2000b). We performed PCR at the single-molecule detection level using sperm DNA from normal healthy men with the 46, XY karyotype as template. Some DNA aliquots tested positive for t(11;22)-specific PCR products

while others were negative, suggesting that the PCR detected *de novo* t(11;22) translocations (Kurahashi and Emanuel, 2001b). The frequency was about one in 10,000. However, when the DNA of blood cells or cheek swab cells from the same men was analyzed, no translocation could be found. Furthermore, all of the lymphoblastoid cell lines or cultured fibroblasts examined also tested negative in PCR analysis. These results imply that the t(11;22) translocation arises in a sperm-specific fashion. There is no evidence for the occurrence of the t(11;22) translocation during female gametogenesis because of the limited availability of human oocytes for testing. However, in *de novo* t(11;22) families, analysis of the parental origin of the translocation chromosomes using the polymorphic feature of PATRR11 and PATRR22 revealed that all of the *de novo* t(11;22) translocations were of paternal origin, supporting a hypothesized sperm-specific mechanism of t(11;22) translocation formation (Ohye et al., 2010).

DNA SECONDARY STRUCTURE IN THE PALINDROME: HAIRPIN OR CRUCIFORM

What is behind the sperm-specific occurrence of the PATRR-mediated translocation? It is not unreasonable to discuss the mechanism leading to the t(11;22) translocation in the context of DNA secondary structure. The DNA secondary structure at the PATRR is potentially evidenced by the fact that a polymorphism within the PATRR affects the *de novo* t(11;22) translocation frequency (Kato et al., 2006; Tong et al., 2010). PATRR11 and PATRR22 have size polymorphisms in the general population due to deletion within the palindromic region. Carriers with long symmetric alleles preferably produce *de novo* t(11;22) translocations more frequently than carriers with PATRR asymmetric arms. These data indirectly but strongly implicate the presence of DNA secondary structure during translocation formation.

One hypothesis to explain the sperm specificity of the t(11;22) translocation is that it develops during DNA replication. Sperm production involves many cell divisions, each requiring DNA replication. During DNA replication, single-stranded DNA is generated in the template DNA for the synthesis of not only the lagging strand DNA, but also the leading strand (Azeroglu et al., 2014). When the replication fork comes to the palindromic region, a long single-stranded DNA is formed, inducing the formation of a single-stranded hairpin structure. The stalling of the replication fork produces DNA breakage at the palindromic region that can potentially induce translocations.

Because the germ stem cells in men replicate about 23 times per year, mature sperm from older men have undergone a greater number of replication cycles. The frequency of *de novo* point mutations in sperm cells increases according to the age of the sample donor (Crow, 2000; O’Roak et al., 2012). If the t(11;22) translocation is mediated by replication, the frequency of the *de novo* t(11;22) translocation should be higher in sperm from older men than in younger men for a similar reason. A previous analysis of the t(11;22) translocation

suggested, however, that there is no tendency for an increase in t(11;22) translocation frequency in the sperm of older men (Kato et al., 2007).

To determine the involvement of DNA replication in translocation formation, we established a model system for the t(11;22) translocation in cultured cells by using plasmids harboring PATRR11 or PATRR22 (Inagaki et al., 2009). Both plasmids were transfected into the HEK293 human cell line and we monitored the fusion of the different plasmids at each PATRR using GFP expression or translocation-specific PCR (Figure 1A). The results indicated that a translocation-like reaction took place. In this reaction, both PATRRs were cleaved at the center of the palindrome and joined via non-homologous end-joining in a similar manner to the human t(11;22) translocation. Crucially, the plasmids had no replication origin for human cells, which means that the translocation took place without DNA replication.

POST-MEIOSIS HYPOTHESIS FOR PATRR-MEDIATED TRANSLOCATIONS

On the other hand, it is possible that the translocation is mediated by another secondary structure, the DNA cruciform. In our model system, the plasmids were purified from *Escherichia coli* using a standard alkaline lysis method. Plasmid DNA isolated from *E. coli* has a strong negative superhelicity. If the plasmid has a palindromic region, the negative superhelicity facilitates cruciform extrusion (Kurahashi et al., 2004). Under an alkaline condition that induces denaturation of the plasmid DNA during purification, most of the PATRR-harboring plasmids extrude cruciform structures. Via the use of a non-denaturing condition and subsequent topoisomerase treatment, such superhelicity was relieved before cruciform extrusion. In this way, we can prepare different topoisomers of the same plasmid, both cruciform-extruded DNA and not extruded DNA. We tested the effect

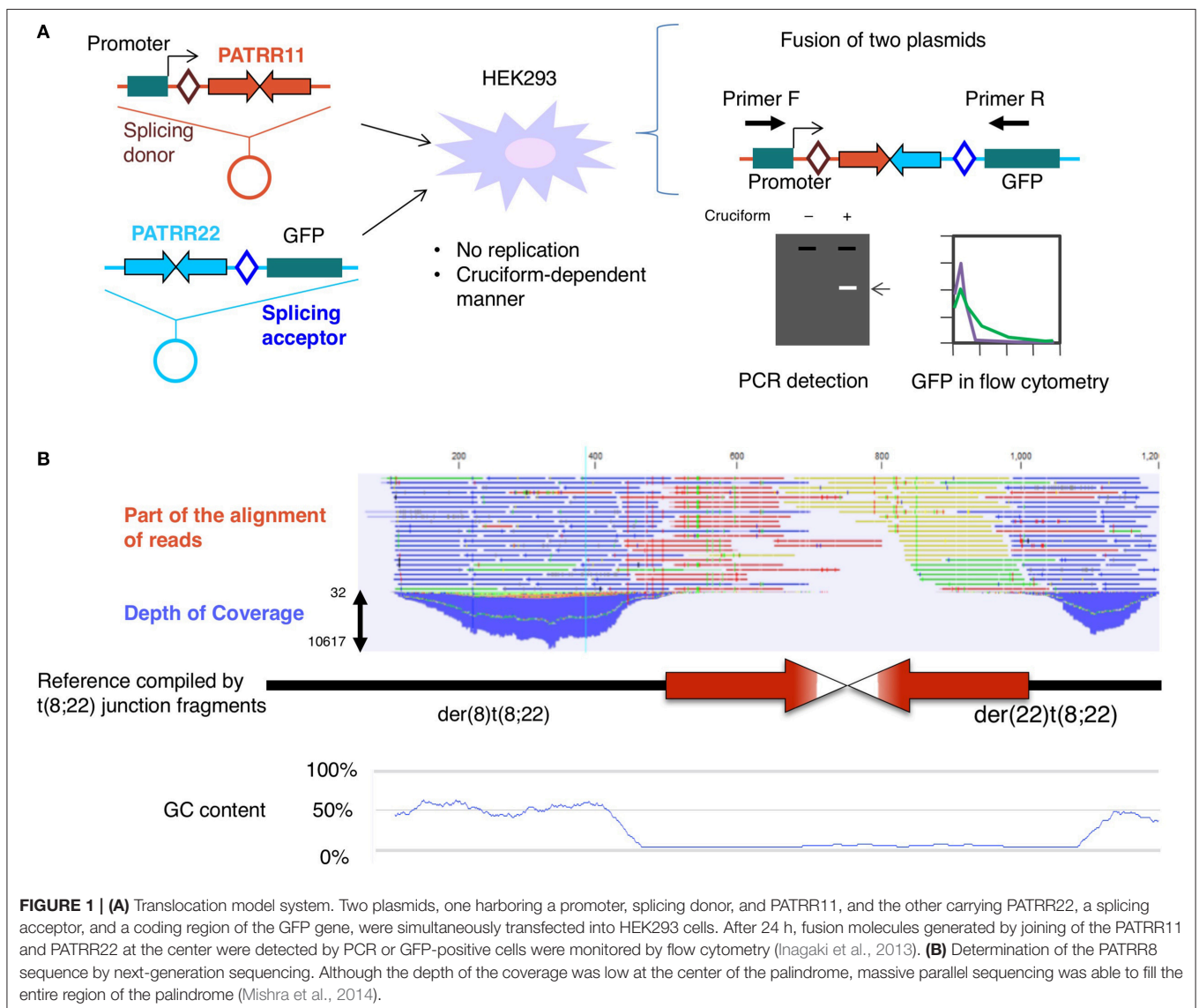


FIGURE 1 | (A) Translocation model system. Two plasmids, one harboring a promoter, splicing donor, and PATRR11, and the other carrying PATRR22, a splicing acceptor, and a coding region of the GFP gene, were simultaneously transfected into HEK293 cells. After 24 h, fusion molecules generated by joining of the PATRR11 and PATRR22 at the center were detected by PCR or GFP-positive cells were monitored by flow cytometry (Inagaki et al., 2013). **(B)** Determination of the PATRR8 sequence by next-generation sequencing. Although the depth of the coverage was low at the center of the palindrome, massive parallel sequencing was able to fill the entire region of the palindrome (Mishra et al., 2014).

of the cruciform on the translocation-like reaction in the cell using a mixture of cruciform and non-cruciform plasmids. The frequency of the translocation-like reaction was found to depend on the proportion of the cruciform-extruded plasmid DNA (**Figure 1A**; Inagaki et al., 2009). These results suggest that cruciform extrusion at the palindromic region induces PATRR-mediated translocation.

Notably however, in living cells the conversion of a DNA structure from that of standard B DNA to cruciform DNA is unlikely to occur under normal physiological conditions from a point of view of thermodynamics. Cruciform extrusion at the palindromic region occurs only when the DNA has strong free negative superhelicity. Theoretically, such superhelicity would potentially occur only at the post-meiosis stage in late spermatogenesis. At this developmental stage, histones are replaced by protamines to reduce the cell size (Gaucher et al., 2010). During histone removal, DNA has a transient excess of negative supercoiling, which might induce cruciform extrusion at the palindromic DNA that leads to translocation formation (Boissonneault, 2002). It is highly possible that PATRR-mediated translocations occur at this developmental stage of spermatogenesis (Kurahashi et al., 2010).

Although the post-meiosis hypothesis is captivating, there is some evidence contradicting this hypothesis. One example is the presence of somatic mosaicism of the t(11;22) translocation and normal cells in humans (Kurahashi et al., 2000b). This indicates that the t(11;22) translocation in this case was generated during the mitotic cell cycles after fertilization. Another example is the existence of *de novo* cases of Emanuel syndrome (Kurahashi et al., 2000b). Emanuel syndrome generally occurs via 3:1 segregation of the translocation chromosomes during meiosis I in a t(11;22) balanced carrier. However, a *de novo* Emanuel syndrome case would have arisen via 3:1 segregation of the t(11;22) chromosomes during the pre-meiotic somatic cell cycles of gametogenesis.

ANALYSIS OF THE PATRR BY NEXT-GENERATION SEQUENCING

In addition to PATRR11 and PATRR22, a dozen PATRRs have been found at other translocation breakpoints. A recurrent t(17;22)(q11.2;q11.2) translocation was found in neurofibromatosis type 1 patients (Kehrer-Sawatzki et al., 2002; Kurahashi et al., 2003). Identification of another recurrent translocation between 8q24.1 and 22q11.2 led to the definition of a new malformation syndrome (Sheridan et al., 2010). Other PATRRs at 4q35.1, 1p21.2, 3p14, and 9p21 were identified at the breakpoints of non-recurrent constitutional translocations (Nimmakayalu et al., 2003; Gotter et al., 2004; Tan et al., 2013; Kato et al., 2014). These PATRRs share little homology but have features of AT-richness and symmetric palindromic structure in common. Intriguingly, all of the palindrome-mediated translocations occur between one PATRR and another PATRR.

We attempted to perform genome-wide screening of *de novo* PATRR-mediated translocations to identify unknown PATRRs using next-generation sequencing. We used the PATRR22

sequence as bait for the detection of any unknown sequences next to the PATRR22 due to *de novo* translocation. However, several difficulties were encountered. We could not confirm the presence of the translocation because most of the PATRR-mediated non-recurrent translocations occurred at a frequency below the detection levels of PCR using sperm from normal healthy donors. Furthermore, we could not analyze the novel translocation junction because the partner sequence could not be mapped to the human reference sequence. None of the translocation-related PATRR sequences identified to date appear in the human genome assembly.

Although the genome projects for many organisms including humans determined their complete nucleotide sequences, difficult-to-sequence regions remain as “gaps.” Recent novel sequencing technologies have made it possible to access some of the gaps and provide more precise genomic data (Chaisson et al., 2015). The PATRR sequences do not appear even in such human reference databases. Palindrome sequences are one such type of a difficult-to-sequence region due to a “triple whammy” of factors affecting sequence analysis: the palindromic sequences are generally refractory to cloning to vectors, PCR amplification, and Sanger sequencing (Inagaki et al., 2005; Lewis et al., 2005). These features are due to the nature of the palindromic sequence itself. The longer the palindrome, the more difficult its analysis.

DEEP SEQUENCING OF THE PATRR REGION HAS GENERATED A NOVEL HYPOTHESIS

We applied next-generation sequencing technology to determine the complete sequence of the PATRR on 8q24, which was found at the breakpoint of t(8;22)(q24;q11) (Mishra et al., 2014). Sequencing of a random sheared library of PCR products and reconstruction of the original DNA via the computer-aided alignment of thousands of DNA molecules allowed us to successfully determine the entire PATRR8 (**Figure 1B**). The next-generation sequencing method does not require cloning and can directly analyze numerous DNA molecules at the same time. Although this strategy still requires PCR to amplify the single molecules and improve signal detection, the random digestion of the palindrome increases the chance of generating asymmetric cleavages of the palindromic center, which improves the PCR efficiency.

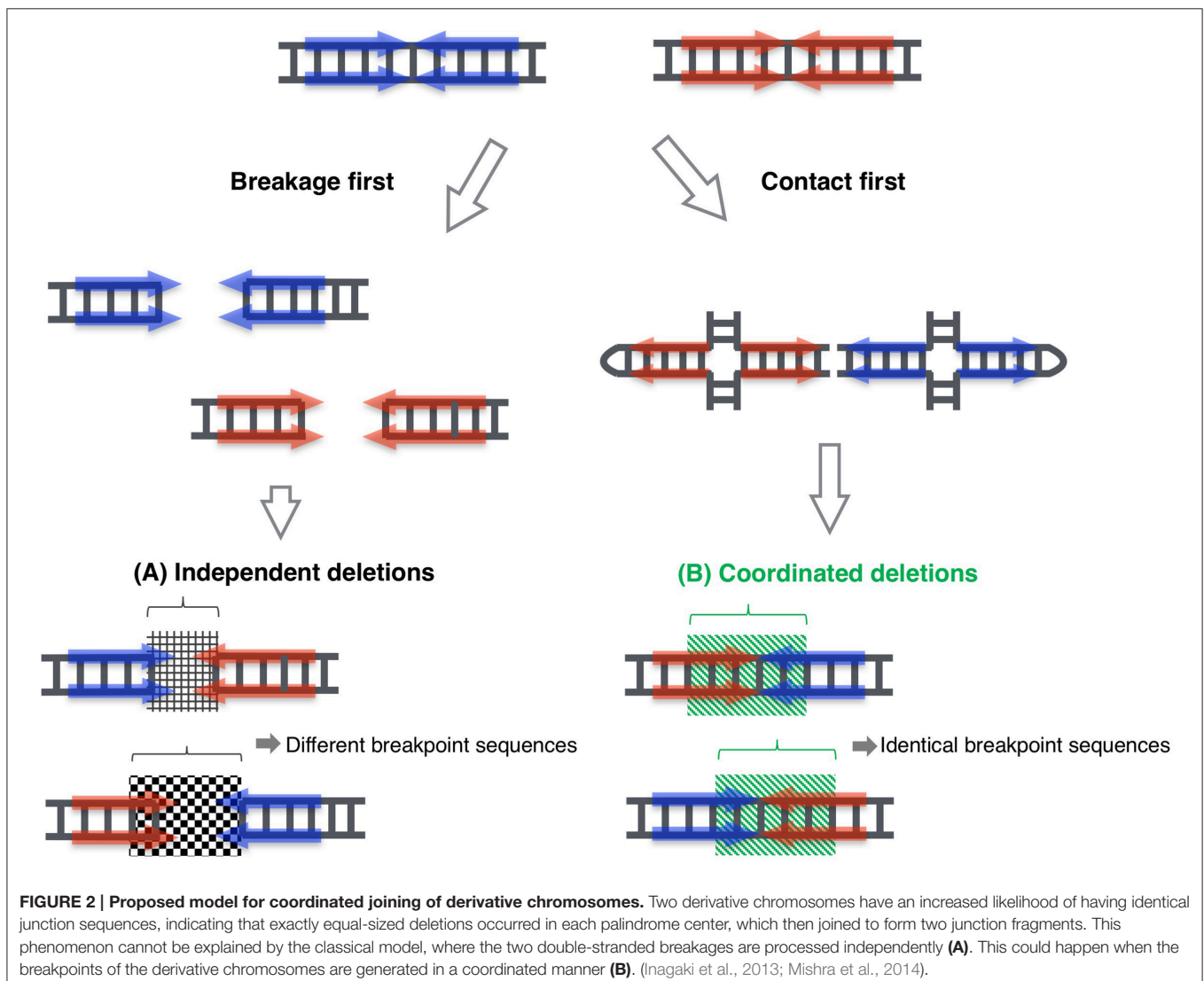
By means of this system, we determined the entire PATRR8 sequence, even at the center of the symmetry. This PATRR8 sequence allowed us to develop t(8;22)-specific PCR primers to analyze the junction fragments. The breakage always occurred at the center of the PATRR8 and PATRR22. The fusion was accompanied by the deletion of small nucleotides at the breakpoint regions. Interestingly, the nucleotide sequences around the junctions are identical between the der(8) and der(22) (Mishra et al., 2014). This cannot happen if the two breakages at the PATRR8 and PATRR22 occur independently and are followed by random nucleotide deletion at the breakage ends. This implies coordinated processing of PATRR8 and

PATRR22. Similar features of identical junctions in the two derivative chromosomes were also found in t(11;22) and t(17;22) (Kurahashi and Emanuel, 2001a; Kurahashi et al., 2003).

The standard models for gross chromosomal rearrangement include the breakage-first model and the contact-first model (Misteli and Soutoglou, 2009). In the breakage-first model, two DNA breaks located far from each other in the nucleus seek each other out to form a fusion chromosome. The artificial translocation model for the observation of the spatiotemporal chromosomal location in living cells revealed the dynamic movement of chromosomes after their breakage (Roukos et al., 2013). On the other hand, according to the contact-first model, translocation takes place between two closely located sites in the nucleus. Our previous data suggested that PATRR11 and PATRR22 are closer than other control chromosomal regions, indicating that this shorter distance might partly contribute to the recurrent nature of the t(11;22) translocation (Ashley et al., 2006). However, these

two models do not explain specific translocations between two PATRRs.

Again, the identical sequences of the two derivative chromosomes imply that the two DNA breakage sites are unlikely to have been processed independently. The two derivative chromosomes were likely to be generated in a coordinated manner. Taken together, in the case of a PATRR-mediated translocation, PATRR appears to extrude cruciform structures at some stage during spermatogenesis. The two cruciform DNA molecules seek each other out and finally join together (Figure 2). In our translocation model system in cultured cells described above, the data suggested that two cleavage processes—cleaved diagonal cleavage of the cruciform structure and cleavage of the tip of the hairpin structure—are involved in translocation development (Inagaki et al., 2013). Our data also suggest that the pathway involves the participation of Artemis and ligase IV, which are components of the V(D)J recombination system that act by bringing two chromosomal sites close together



and connecting them. In V(D)J recombination, RAG1 and RAG2 proteins bind the two cleavage sites to hold the resulting ends, both of which are specific for the V(D)J recombination machinery in lymphocytes. Similar mechanism is known in a DNA repair system of non-homologous end joining, in which Ku70/80 holds the two broken end until the subsequent repair machinery associate to process and join the ends (Deriano and Roth, 2013). Artemis and ligase IV as well as DNA-PK and other factors also participate in the joining reactions. It is possible that a part of such systems, or other novel factors might be involved in the contact between the two extruded cruciform structures and in keeping them in position during processing until the two derivative chromosomes are generated. We are now investigating how two cruciform DNA molecules come close together to elucidate the third mechanistic model that leads to recurrent chromosomal translocations in humans. Such investigation of dynamics of the cruciforms in nuclei will shed light on the role of non-B DNAs in gross chromosomal rearrangements in other eukaryotes.

REFERENCES

- Ashley, T., Gaeth, A. P., Inagaki, H., Seftel, A., Cohen, M. M., Anderson, L. K., et al. (2006). Meiotic recombination and spatial proximity in the etiology of the recurrent t(11;22). *Am. J. Hum. Genet.* 79, 524–538. doi: 10.1086/507652
- Azeroglu, B., Lincker, F., White, M. A., Jain, D., and Leach, D. R. (2014). A perfect palindrome in the *Escherichia coli* chromosome forms DNA hairpins on both leading- and lagging-strands. *Nucleic Acids Res.* 42, 13206–13213. doi: 10.1093/nar/gku1136
- Boissonneault, G. (2002). Chromatin remodeling during spermiogenesis: a possible role for the transition proteins in DNA strand break repair. *FEBS Lett.* 514, 111–114. doi: 10.1016/S0014-5793(02)02380-3
- Carter, M. T., St Pierre, S. A., Zackai, E. H., Emanuel, B. S., and Boycott, K. M. (2009). Phenotypic delineation of Emanuel syndrome (supernumerary derivative 22 syndrome): clinical features of 63 individuals. *Am. J. Med. Genet. A.* 149, 1712–1721. doi: 10.1002/ajmg.a.32957
- Chaisson, M. J., Huddleston, J., Dennis, M. Y., Sudmant, P. H., Malig, M., Hormozdiari, F., et al. (2015). Resolving the complexity of the human genome using single-molecule sequencing. *Nature* 517, 608–611. doi: 10.1038/nature13907
- Crow, J. F. (2000). The origins, patterns and implications of human spontaneous mutation. *Nat. Rev. Genet.* 1, 40–47. doi: 10.1038/35049558
- Deriano, L., and Roth, D. B. (2013). Modernizing the nonhomologous end-joining repertoire: alternative and classical NHEJ share the stage. *Annu. Rev. Genet.* 47, 433–455. doi: 10.1146/annurev-genet-110711-155540
- Edelmann, L., Spiteri, E., Koren, K., Pulijal, V., Bialer, M. G., Shanske, A., et al. (2001). AT-rich palindromes mediate the constitutional t(11;22) translocation. *Am. J. Hum. Genet.* 68, 1–13. doi: 10.1086/316952
- Emanuel, B. S., Zackai, E. H., and Medne, L. (2015). “Emanuel syndrome,” in *GeneReviews*, eds R. A. Pagon, M. P. Adam, H. H. Ardinger, S. E. Wallace, A. Amemiya, L. J. H. Bean, T. D. Bird, C. T. Fong, H. C. Mefford, R. J. H. Smith, and K. Stephens (Seattle, DC: University of Washington).
- Gaucher, J., Reynoird, N., Montellier, E., Bousouar, F., Rousseaux, S., and Khochbin, S. (2010). From meiosis to postmeiotic events: the secrets of histone disappearance. *FEBS J.* 277, 599–604. doi: 10.1111/j.1742-4658.2009.07504.x
- Gotter, A. L., Shaikh, T. H., Budarf, M. L., Rhodes, C. H., and Emanuel, B. S. (2004). A palindrome-mediated mechanism distinguishes translocations involving LCR-B of chromosome 22q11.2. *Hum. Mol. Genet.* 13, 103–115. doi: 10.1093/hmg/ddh004
- Inagaki, H., and Kurahashi, H. (2013). “Cruciform DNA,” in *Brenner’s Encyclopedia of Genetics, 2nd Edn.*, eds S. Maloy and K. Hughes (London, UK: Elsevier), 241–243.
- ## AUTHOR CONTRIBUTIONS
- HI and HK wrote the initial manuscript. All authors discussed the text and commented on the manuscript.
- ## FUNDING
- This study was supported by Grants-in-Aid for Scientific Research (HI, HK) and the MEXT-Supported Program for the Strategic Research Foundation at Private Universities (HK) from the Ministry of Education, Culture, Sports, Science, and Technology of Japan, and a Health and Labour Sciences Research Grant (HK) from the ministry of Health, Labour and Welfare of Japan.
- ## ACKNOWLEDGMENTS
- We thank Dr. Beverly S. Emanuel and the members of our laboratory for discussion and advice on this manuscript.
- Inagaki, H., Ohye, T., Kogo, H., Kato, T., Bolor, H., Taniguchi, M., et al. (2009). Chromosomal instability mediated by non-B DNA: cruciform conformation and not DNA sequence is responsible for recurrent translocation in humans. *Genome Res.* 19, 191–198. doi: 10.1101/gr.079244.108
- Inagaki, H., Ohye, T., Kogo, H., Tsutsumi, M., Kato, T., Tong, M., et al. (2013). Two sequential cleavage reactions on cruciform DNA structures cause palindrome-mediated chromosomal translocations. *Nat. Commun.* 4:1592. doi: 10.1038/ncomms2595
- Inagaki, H., Ohye, T., Kogo, H., Yamada, K., Kowa, H., Shaikh, T. H., et al. (2005). Palindromic AT-rich repeat in the NF1 gene is hypervariable in humans and evolutionarily conserved in primates. *Hum. Mutat.* 26, 332–342. doi: 10.1002/humu.20228
- Kato, T., Franconi, C. P., Sheridan, M. B., Hacker, A. M., Inagaki, H., Glover, T. W., et al. (2014). Analysis of the t(3;8) of hereditary renal cell carcinoma: a palindrome-mediated translocation. *Cancer Genet.* 207, 133–140. doi: 10.1016/j.cancergen.2014.03.004
- Kato, T., Inagaki, H., Yamada, K., Kogo, H., Ohye, T., Kowa, H., et al. (2006). Genetic variation affects *de novo* translocation frequency. *Science* 311, 971. doi: 10.1126/science.1121452
- Kato, T., Yamada, K., Inagaki, H., Kogo, H., Ohye, T., Emanuel, B. S., et al. (2007). Age has no effect on *de novo* constitutional t(11;22) translocation frequency in sperm. *Fertil. Steril.* 88, 1446–1448. doi: 10.1016/j.fertnstert.2007.01.019
- Kehrre-Sawatzki, H., Assum, G., and Hameister, H. (2002). Molecular characterisation of t(17;22)(q11.2;q11.2) is not consistent with NF1 gene duplication. *Hum. Genet.* 111, 465–467. doi: 10.1007/s00439-002-0794-3
- Kurahashi, H., and Emanuel, B. S. (2001a). Long AT-rich palindromes and the constitutional t(11;22) breakpoint. *Hum. Mol. Genet.* 10, 2605–2617. doi: 10.1093/hmg/10.23.2605
- Kurahashi, H., and Emanuel, B. S. (2001b). Unexpectedly high rate of *de novo* constitutional t(11;22) translocations in sperm from normal males. *Nat. Genet.* 29, 139–140. doi: 10.1038/ng1001-139
- Kurahashi, H., Inagaki, H., Hosoba, E., Kato, T., Ohye, T., Kogo, H., et al. (2007). Molecular cloning of a translocation breakpoint hotspot in 22q11. *Genome Res.* 17, 461–469. doi: 10.1101/gr.5769507
- Kurahashi, H., Inagaki, H., Ohye, T., Kogo, H., Tsutsumi, M., Kato, T., et al. (2010). The constitutional t(11;22): implications for a novel mechanism responsible for gross chromosomal rearrangements. *Clin. Genet.* 78, 299–309. doi: 10.1111/j.1399-0004.2010.01445.x
- Kurahashi, H., Inagaki, H., Yamada, K., Ohye, T., Taniguchi, M., Emanuel, B. S., et al. (2004). Cruciform DNA structure underlies the etiology for palindrome-mediated human chromosomal translocations. *J. Biol. Chem.* 279, 35377–35383. doi: 10.1074/jbc.M400354200

- Kurahashi, H., Shaikh, T. H., Hu, P., Roe, B. A., Emanuel, B. S., and Budarf, M. L. (2000a). Regions of genomic instability on 22q11 and 11q23 as the etiology for the recurrent constitutional t(11;22). *Hum. Mol. Genet.* 9, 1665–1670. doi: 10.1093/hmg/9.11.1665
- Kurahashi, H., Shaikh, T. H., Zackai, E. H., Celle, L., Driscoll, D. A., Budarf, M. L., et al. (2000b). Tightly clustered 11q23 and 22q11 breakpoints permit PCR-based detection of the recurrent constitutional t(11;22). *Am. J. Hum. Genet.* 67, 763–768. doi: 10.1086/303054
- Kurahashi, H., Shaikh, T., Takata, M., Toda, T., and Emanuel, B. S. (2003). The constitutional t(17;22): another translocation mediated by palindromic AT-rich repeats. *Am. J. Hum. Genet.* 72, 733–738. doi: 10.1086/368062
- Lewis, S. M., Chen, S., Strathern, J. N., and Rattray, A. J. (2005). New approaches to the analysis of palindromic sequences from the human genome: evolution and polymorphism of an intronic site at the NF1 locus. *Nucleic Acids Res.* 33, e186. doi: 10.1093/nar/gni189
- Maizels, N. (2006). Dynamic roles for G4 DNA in the biology of eukaryotic cells. *Nat. Struct. Mol. Biol.* 13, 1055–1059. doi: 10.1038/nsmb1171
- McMurray, C. T. (2010). Mechanisms of trinucleotide repeat instability during human development. *Nat. Rev. Genet.* 11, 786–799. doi: 10.1038/nrg2828
- Mirkin, S. M. (2007). Expandable DNA repeats and human disease. *Nature* 447, 932–940. doi: 10.1038/nature05977
- Mishra, D., Kato, T., Inagaki, H., Kosho, T., Wakui, K., Kido, Y., et al. (2014). Breakpoint analysis of the recurrent constitutional t(8;22)(q24.13;q11.21) translocation. *Mol. Cytogenet.* 7:55. doi: 10.1186/s13039-014-0055-x
- Misteli, T., and Soutoglou, E. (2009). The emerging role of nuclear architecture in DNA repair and genome maintenance. *Nat. Rev. Mol. Cell Biol.* 10, 243–254. doi: 10.1038/nrm2651
- Nimmakayalu, M. A., Gotter, A. L., Shaikh, T. H., and Emanuel, B. S. (2003). A novel sequence-based approach to localize translocation breakpoints identifies the molecular basis of a t(4;22). *Hum. Mol. Genet.* 12, 2817–2825. doi: 10.1093/hmg/ddg301
- Ohye, T., Inagaki, H., Kato, T., Tsutsumi, M., and Kurahashi, H. (2014). Prevalence of Emanuel syndrome: theoretical frequency and surveillance result. *Pediatr. Int.* 56, 462–466. doi: 10.1111/ped.12437
- Ohye, T., Inagaki, H., Kogo, H., Tsutsumi, M., Kato, T., Tong, M., et al. (2010). Paternal origin of the *de novo* constitutional t(11;22)(q23;q11). *Eur. J. Hum. Genet.* 18, 783–787. doi: 10.1038/ejhg.2010.20
- O’Roak, B. J., Vives, L., Girirajan, S., Karakoc, E., Krumm, N., Coe, B. P., et al. (2012). Sporadic autism exomes reveal a highly interconnected protein network of *de novo* mutations. *Nature* 485, 246–250. doi: 10.1038/nature10989
- Pearson, C. E., Edamura, K. N., and Cleary, J. D. (2005). Repeat instability: mechanisms of dynamic mutations. *Nat. Rev. Genet.* 6, 729–742. doi: 10.1038/nrg1689
- Raghavan, S. C., and Lieber, M. R. (2006). DNA structures at chromosomal translocation sites. *Bioessays* 28, 480–494. doi: 10.1002/bies.20353
- Roukos, V., Voss, T. C., Schmidt, C. K., Lee, S., Wangsa, D., and Misteli, T. (2013). Spatial dynamics of chromosome translocations in living cells. *Science* 341, 660–664. doi: 10.1126/science.1237150
- Sheridan, M. B., Kato, T., Haldeman-Englert, C., Jalali, G. R., Milunsky, J. M., Zou, Y., et al. (2010). A palindrome-mediated recurrent translocation with 3:1 meiotic nondisjunction: the t(8;22)(q24.13;q11.21). *Am. J. Hum. Genet.* 87, 209–218. doi: 10.1016/j.ajhg.2010.07.002
- Sinden, R. R. (1994). *DNA Structure and Function*. San Diego, CA: Academic Press.
- Tan, X., Anzick, S. L., Khan, S. G., Ueda, T., Stone, G., Digiovanna, J. J., et al. (2013). Chimeric negative regulation of p14ARF and TBX1 by a t(9;22) translocation associated with melanoma, deafness, and DNA repair deficiency. *Hum. Mutat.* 34, 1250–1259. doi: 10.1002/humu.22354
- Tanaka, H., Bergstrom, D. A., Yao, M. C., and Tapscott, S. J. (2005). Widespread and nonrandom distribution of DNA palindromes in cancer cells provides a structural platform for subsequent gene amplification. *Nat. Genet.* 37, 320–327. doi: 10.1038/ng1515
- Tapia-Páez, I., Kost-Alimova, M., Hu, P., Roe, B. A., Blennow, E., Fedorova, L., et al. (2001). The position of t(11;22)(q23;q11) constitutional translocation breakpoint is conserved among its carriers. *Hum. Genet.* 109, 167–177. doi: 10.1007/s004390100560
- Tong, M., Kato, T., Yamada, K., Inagaki, H., Kogo, H., Ohye, T., et al. (2010). Polymorphisms of the 22q11.2 breakpoint region influence the frequency of *de novo* constitutional t(11;22)s in sperm. *Hum. Mol. Genet.* 19, 2630–2637. doi: 10.1093/hmg/ddq150
- Wang, G., and Vasquez, K. M. (2014). Impact of alternative DNA structures on DNA damage, DNA repair, and genetic instability. *DNA Repair.* 19, 143–151. doi: 10.1016/j.dnarep.2014.03.017

Conflict of Interest Statement: The authors declare that the research was conducted in the absence of any commercial or financial relationships that could be construed as a potential conflict of interest.

Copyright © 2016 Inagaki, Kato, Tsutsumi, Ouchi, Ohye and Kurahashi. This is an open-access article distributed under the terms of the Creative Commons Attribution License (CC BY). The use, distribution or reproduction in other forums is permitted, provided the original author(s) or licensor are credited and that the original publication in this journal is cited, in accordance with accepted academic practice. No use, distribution or reproduction is permitted which does not comply with these terms.

ARTICLE

Novel compound heterozygous variants in *PLK4* identified in a patient with autosomal recessive microcephaly and chorioretinopathy

Makiko Tsutsumi^{1,13}, Setsuri Yokoi^{1,2,13}, Fuyuki Miya^{3,4}, Masafumi Miyata⁵, Mitsuhiro Kato^{6,14}, Nobuhiko Okamoto⁷, Tatsuhiko Tsunoda^{3,4}, Mami Yamasaki⁸, Yonehiro Kanemura^{9,10}, Kenjiro Kosaki¹¹, Shinji Saitoh¹² and Hiroki Kurahashi^{*1}

It has been well documented that variants in genes encoding centrosomal proteins cause primary autosomal recessive microcephaly, although the association between centrosomal defects and the etiology of microcephaly syndromes is not fully understood. Polo-like kinase 4 (*PLK4*) is one of the centrosomal proteins required for centriole duplication. We here describe a patient with microcephaly and chorioretinopathy that harbors compound heterozygous missense variants, c.[442A>G]; [2336G>A], in the *PLK4* gene. One of these variants, c.442A>G (p.(M148V)), resides in the kinase domain, and the other, c.2336G>A (p.(C779Y)), in the polo-box domain. Aberrant spindle formation was observed in a LCL derived from this patient. Overexpression experiments of the variant *PLK4* proteins demonstrated that the p.(C779Y) but not the p.(M148V) had lost centriole overduplication ability. The altered mobility pattern of both variant proteins on a western blot further suggested alterations in post-translation modification. Our data lend support to the hypothesis that impaired centriole duplication caused by *PLK4* variants may be involved in the etiology of microcephaly disorder.

European Journal of Human Genetics (2016) 00, 1–5. doi:10.1038/ejhg.2016.119

INTRODUCTION

Autosomal recessive microcephaly and chorioretinopathy (MCCRP) is a developmental disorder characterized by primary microcephaly, delayed psychomotor development, growth retardation with dwarfism and visual impairment. Recently, variants in the *PLK4* gene, one of the key regulators of centriole duplication, were identified in patients with microcephaly, growth failure and retinopathy^{1,2} (MCCRP2 [MIM616171]).

In our current study, we describe a female MCCRP patient with missense variants in *PLK4*. She was affected by autosomal recessive microcephaly and developmental eye disease that were consistent with the MCCRP phenotype. Cell biological analyses using a lymphoblastoid cell line (LCL) derived from this patient and functional analyses of the variant *PLK4* proteins were performed to examine the impacts on centriole biosynthesis.

MATERIALS AND METHODS

Patient

The genetic testing used in this study was approved by the ethical committees of Fujita Health University in accordance with the principles of the Declaration of Helsinki, and the Ethical Guidelines for Human Genome/Gene Analysis Research by the Ministry of Education, Culture, Science, and Technology,

the Ministry of Health, Labor, and Welfare, and the Ministry of Economy, Trade, and Industry of Japan. Blood samples from the affected individual and her parents were obtained with informed consent in accordance with local institutional review board guidelines.

Whole-exome sequencing and validation

Genomic DNA extraction from the peripheral blood of the patient and parents and whole-exome sequencing and validation were performed as previously described.³ The identified *PLK4* variants were submitted to the LOVD database at <http://www.LOVD.nl/PLK4> (individual ID: 00072170).

Cell culture

An Epstein–Barr virus transformed LCL line was established from peripheral blood mononuclear cells and cultured in RPMI 1640 containing 10% FBS established from a healthy control also. Asynchronous growing cells were fixed with ice-cold methanol to analyze the number of centrosomes and mitotic spindle formation by immunofluorescence.

Transfection experiments

The cDNA encoding wild-type (WT) human *PLK4* was chemically synthesized and cloned into the pEGFP-C1 vector. Mutations were generated by PCR using the WT construct as a template. All constructs were verified by DNA

¹Division of Molecular Genetics, Institute for Comprehensive Medical Science, Fujita Health University, Toyoake, Japan; ²Department of Pediatrics, Nagoya University Graduate School of Medicine, Nagoya, Japan; ³Department of Medical Science Mathematics, Medical Research Institute, Tokyo Medical and Dental University, Tokyo, Japan; ⁴Laboratory for Medical Science Mathematics, RIKEN Center for Integrative Medical Sciences, Yokohama, Japan; ⁵Department of Pediatrics, Fujita Health University School of Medicine, Toyoake, Japan; ⁶Department of Pediatrics, Yamagata University Faculty of Medicine, Yamagata, Japan; ⁷Department of Medical Genetics, Osaka Medical Center and Research Institute for Maternal and Child Health, Osaka, Japan; ⁸Department of Pediatric Neurosurgery, Takatsuki General Hospital, Osaka, Japan; ⁹Division of Regenerative Medicine, Institute for Clinical Research, Osaka National Hospital, National Hospital Organization, Osaka, Japan; ¹⁰Department of Neurosurgery, Osaka National Hospital, National Hospital Organization, Osaka, Japan; ¹¹Center for Medical Genetics, Keio University School of Medicine, Tokyo, Japan; ¹²Department of Pediatrics and Neonatology, Nagoya City University Graduate School of Medical Sciences, Nagoya, Japan

*Correspondence: Professor H Kurahashi, Division of Molecular Genetics, Institute for Comprehensive Medical Science, Fujita Health University, 1-98 Dengakugakubo, Kutsukake-cho, Toyoake, Aichi 470-1192, Japan. Tel: +81 562 939391; Fax: +81 562 93 8831; E-mail: kura@fujita-hu.ac.jp

¹³These authors contributed equally to this work.

¹⁴Current address: Department of Pediatrics, Showa University School of Medicine, Tokyo, Japan.

Received 4 March 2016; revised 29 June 2016; accepted 5 August 2016

sequencing and transfected into HeLa cells. At 24 h posttransfection, cell lysates were prepared for western blot analysis, or the cells were fixed with ice-cold methanol for immunofluorescence analysis.

Western blotting

Whole-cell lysate of the asynchronously growing LCL and recombinant proteins expressed in HeLa cells were analyzed by western blot followed by image analysis performed as described previously.⁴ Rabbit anti-PLK4 (1:500; Proteintech, Rosemont, IL, USA), mouse anti-ACTB (AC-15) (1:500000; Sigma, St Louis, MO, USA) or rabbit anti-GFP (1:500; MBL, Nagoya, Japan) was used as the primary antibody. HRP-conjugated anti-rabbit IgG or anti-mouse IgG (Thermo Scientific, Rockford, IL) was used as the secondary antibody.

Immunofluorescence

The fixed LCL or HeLa cells were stained with primary antibodies at the following dilutions: rabbit anti-GFP (1:500), mouse anti- α -tubulin (1:250; Santa Cruz Biotechnology, Santa Cruz, CA, USA), mouse anti- γ -tubulin (1:1000; Sigma), rabbit polyclonal anti-phospho Histone H3 (pH3) (Ser10) antibody (1:100; Merck Millipore, Darmstadt, Germany). The secondary antibodies used were donkey anti-rabbit IgG Alexa Fluor 488, donkey anti-rabbit IgG Alexa Fluor 594, donkey anti-mouse IgG Alexa Fluor 488 and donkey anti-mouse IgG Alexa Fluor 594 (Life Technologies, Carlsbad, CA, USA) at a 1:1000 dilution. Image acquisition was performed as previously described.³ For centrosome scoring, we counted the γ -tubulin signals of the LCL and HeLa mitotic cells. Spindle formation of the mitotic LCL was classified into four types in the similar way of the previous study.¹ Bipolar spindles were normal, monopolar cells had only one spindle pole, multipolar cells had excess spindle poles and disorganized cells failed to establish a spindle pole.

RESULTS

Patient characteristics

The study patient was a female born at a gestational age of 37 weeks. Her parents were healthy and non-consanguineous. Her birth weight

was 1322 g (-3.9 SD), head circumference was 20.6 cm (-7.3 SD), and body length was 38.0 cm (-5.1 SD). She had microcephaly, bilateral microphthalmos and persistent hyperplastic primary vitreous of her left eye. Brain MRI revealed trigonocephaly, microcephaly with simplified gyri, colpocephaly and bilateral asymmetric periventricular nodular heterotopia (Figure 1A). Her karyotype was normal (46,XX).

Her developmental quotient at 2 years of age, measured using the Tsumori-Inage Developmental Questionnaire, was 21. Her development was considered to be severely delayed. At the age of 32 months, her weight was 6440 g (-4.2 SD), head circumference was 34.7 cm (-8.9 SD), and body length was 67.6 cm (-6.8 SD).

Identification of variants in PLK4

We performed whole-exome sequencing analysis of this patient and identified novel compound heterozygous variants, c.[442A>G]; [2336G>A], in the *PLK4* gene (NG_041821.1; NM_014264.4; Figure 1B and C and Supplementary Table S1). Subsequent Sanger sequencing confirmed these variants (Figure 1C). The c.442A>G (p.(M148V)) variant was inherited from the healthy mother, and the c.2336G>A (p.(C779Y)) variant from the healthy father. Both variants were predicted to be damaging by Polyphen-2 and SIFT (Supplementary Table S1). No variants related to microcephaly were identified in any other genes in the patient (Supplementary Table S1). M148 and C779 residues are highly conserved amino acids in the *PLK4* protein across species. The M148 residue is located in the kinase domain, whereas the C779 residue is located in the second of the three polo-box domains, PB2. The C779 residue is defined as a homodimer interface by the NCBI Conserved Domain Database (accession number cd13115; <http://www.ncbi.nlm.nih.gov/Structure/cdd/cdd.shtml>⁵).

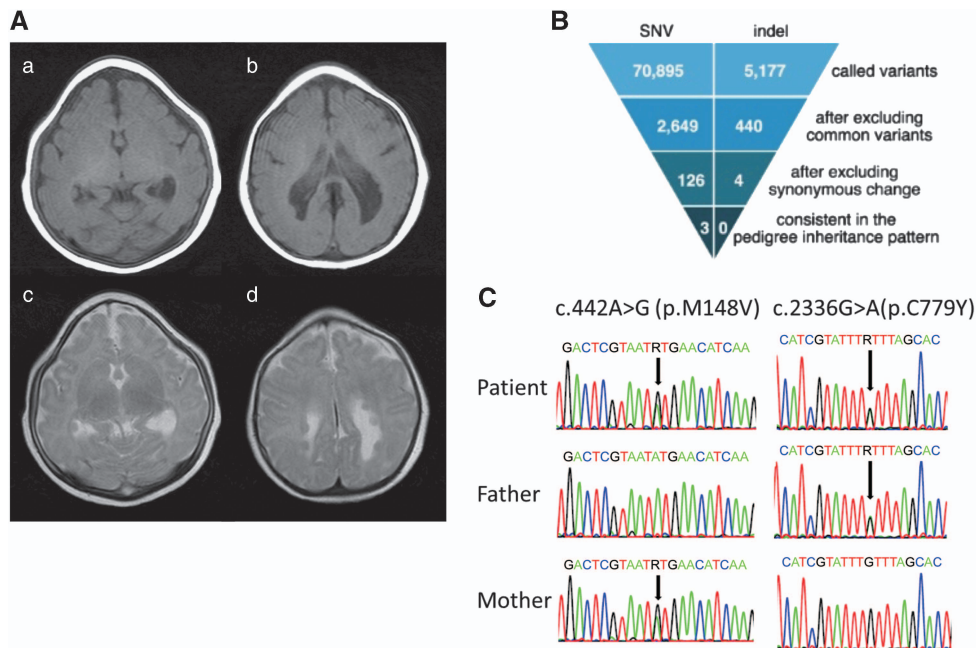


Figure 1 (A) Brain MRI of the patient at the age of 6 months. **a** and **b**: T1-weighted images. **c** and **d**: T2-weighted images. (B) Filtering steps for determining candidate variants in the databases, except for those that are also known as variants affecting function. The second row shows the number of variants remaining after filtering out known variants in the databases, except for those that are also known as variants affecting function. The third row indicates the number of variants remaining after excluding synonymous change variants. The bottom row indicates the number of variants consistent with the phenotype in the pedigree (ie, the total number of autosomal recessive, X-linked recessive, *de novo* and compound heterozygous variants). (C) Validation of the *PLK4* variants by Sanger sequencing.

Abnormal centrosome number and impaired mitotic spindle formation in the study patient

PLK4 protein level of an LCL derived from the patient was found to be comparable to that of control by western blot (Figure 2a). To examine whether centriole biosynthesis was impaired in our patient, the LCL was used to analyze the centrosome number. Asynchronously growing cells were fixed and stained with anti- γ -tubulin antibodies (Figure 2b). In mitotic cells, the normal centrosome number is theoretically 2. However, 16.7% of the cells from our patient had 1 or ≥ 3 centrosomes (Figure 2c). This rate was slightly higher than that of the control cells (14.7%, Figure 2c).

We also analyzed spindle polarity of the mitotic cells because the centrosome plays a role in the formation of bipolar mitotic spindles. α -tubulin labeling of the LCL from our patient revealed that 25% of the mitotic cells had an aberrant spindle morphology, whereas $>90\%$ of the control mitotic cells were bipolar (Figure 2d and e). Of note, cells with a monopolar spindle were increased in our patient. Other morphological defects, such as excess spindle poles or a disorganized spindle, were more frequent in our patient than in the control cells (Figure 2e). These results suggest that spindle formation was impaired in our patient because of a centriole duplication abnormality.

Centriole amplification abilities of the variant PLK4 proteins

We next examined the properties of PLK4 proteins harboring the p.(M148V) and p.(C779Y) variants. It is known that the overexpression of PLK4 induces centriole amplification.^{6,7} EGFP-tagged variant proteins were overexpressed in HeLa cells and analyzed by immunofluorescence (Figure 3). When WT PLK4 was overexpressed in HeLa cells, centriole amplification was observed and $>70\%$ of the cells had excess centrosomes (Figure 3a and b). In contrast, overexpression of the p.(C779Y) variant had no effect on centriole amplification, suggesting a loss of function in centriole duplication. On the other hand, overexpression of the p.(M148V) proteins could amplify the centrioles and produce excess centrosomes to the same extent as WT PLK4 (Figure 3a and b). Intense immunofluorescent signals corresponding to both EGFP-tagged WT and the p.(M148V) variant PLK4 were detected at the centrioles in the centrosomes, whereas the p.(C779Y) PLK4 signals were weak in the centrosomes and found to be predominantly diffused within the cytoplasm (Figure 3a). These results suggest that the p.(C779Y) variant within the PB2 domain of PLK4 prevented its localization to the centrioles leading to a dysfunction in centriole duplication.

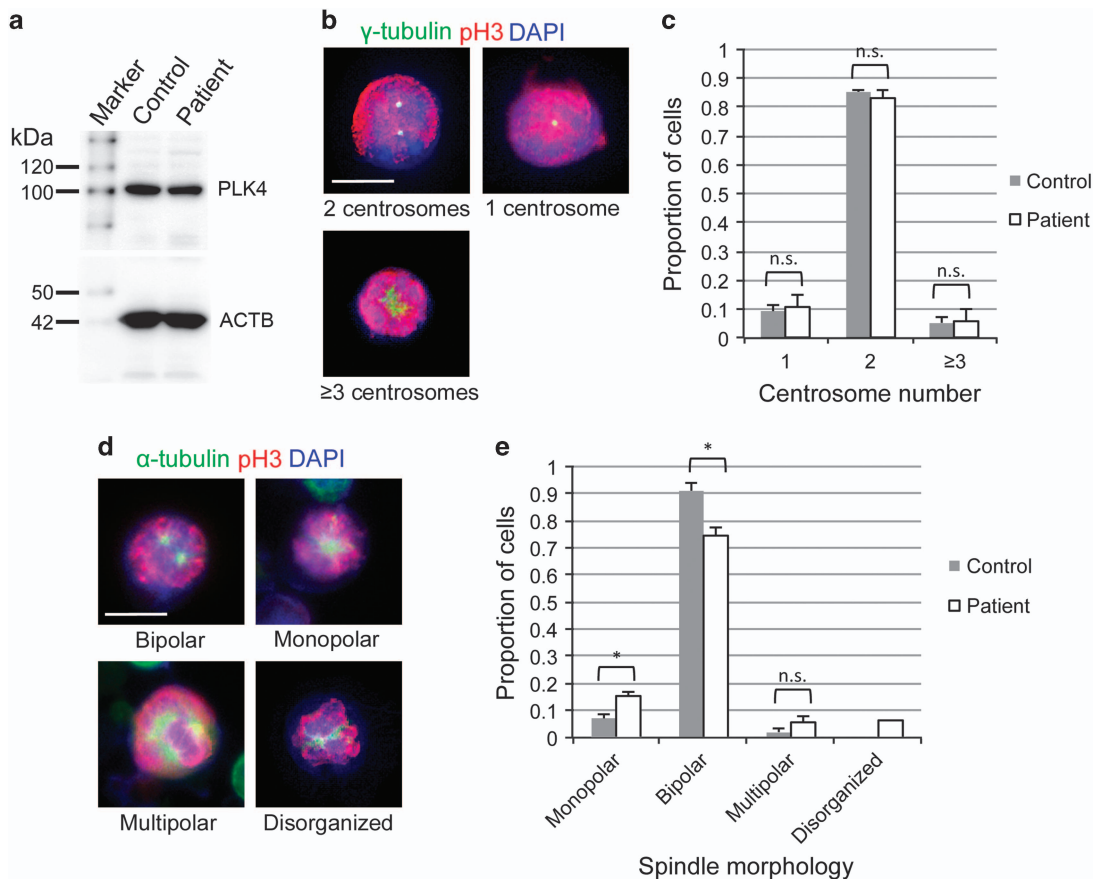


Figure 2 PLK4 expression, centrosome number and spindle formation in LCL. (a) Western blot analysis of PLK4 protein in LCL derived from a control and the patient. (b) Representative immunofluorescent microscopic images of the mitotic LCL derived from the patient. γ -tubulin (green) is a centrosome marker. Phospho-histone H3 (red) was used as a mitotic marker. The centrosome number is indicated in each image. Scale bar, 10 μ m. (c) Proportion of cells with the indicated centrosome number. (d) Representative immunofluorescent microscopic images of the mitotic LCL derived from the patient. α -tubulin (green) is a spindle marker. Spindle morphology is indicated in each image. (e) Proportion of cells with the indicated spindle morphology ($*P < 0.05$, two-tailed Student's *t*-test). The results in c and e were obtained from three independent experiments shown in b and d, respectively. $n = 50$ cells in each experiment. Data are the average value \pm SEM.

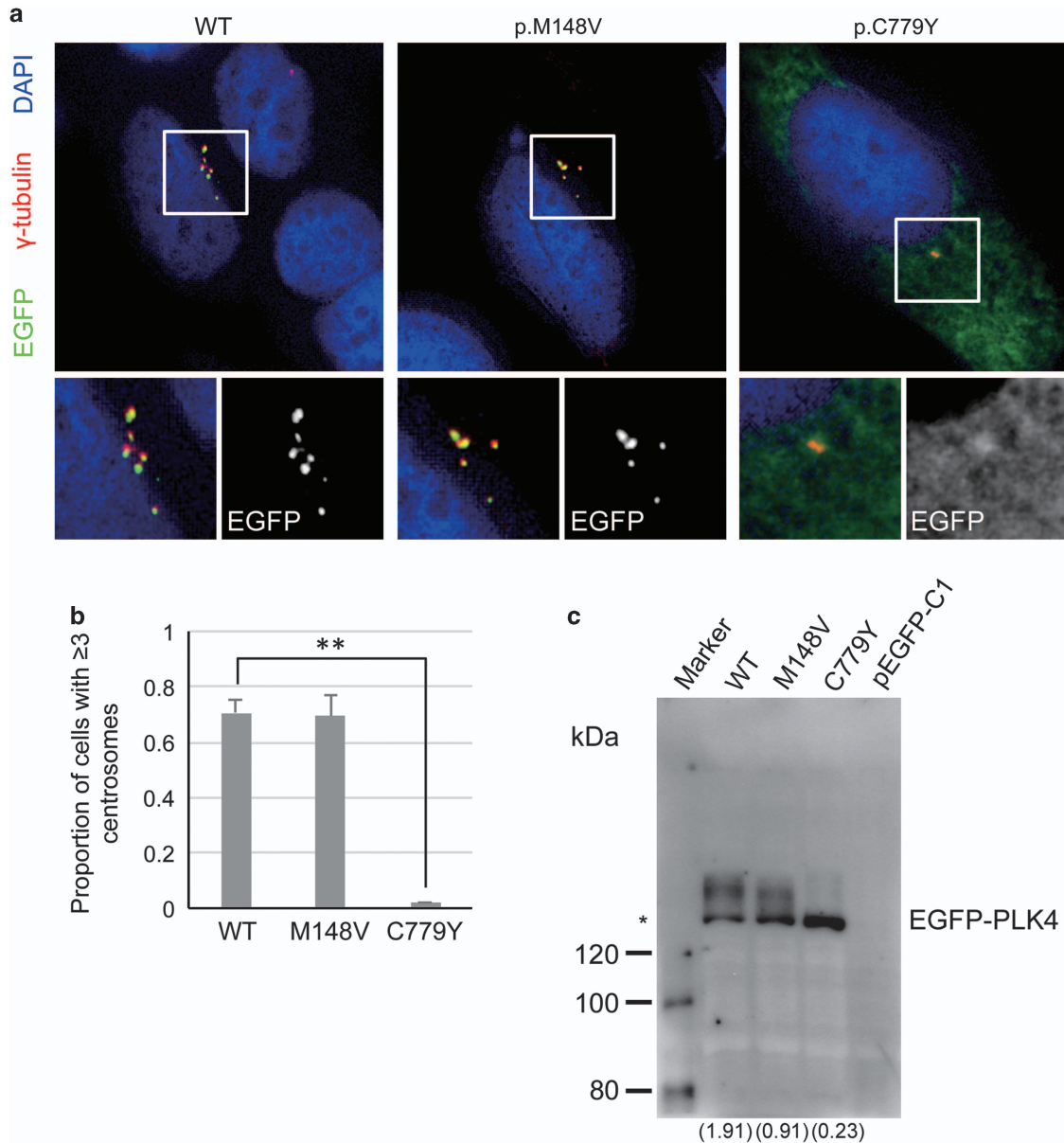


Figure 3 Overexpression analysis of the PLK4 variants. (a) Representative immunofluorescent microscopic images of HeLa cells transfected with the indicated EGFP-tagged PLK4 expression plasmids. γ -tubulin (centrosome) and EGFP (centriole) are shown in red and green, respectively. Centrosomes in the boxes are magnified. Scale bar, 10 μ m. (b) Proportion of cells with more than two centrosomes were examined from the experiments shown in (a). The results of three independent experiments are shown. $n=50$ cells in each experiment. Data are average values \pm SEM (** $P<0.01$, two-tailed Student's t -test). (c) Western blot analysis using an anti-GFP antibody. Asterisk indicates the normal band size estimated from a molecular weight calculation of EGFP-PLK4. Values in parentheses indicate the intensity ratio of the larger band to the normal band.

Western blot analysis of HeLa lysates transfected with the EGFP-tagged PLK4 expression plasmids was performed using an anti-GFP antibody (Figure 3c). An ~ 136 kDa band was detected for each construct consistent with the calculated molecular weight of the EGFP-tagged PLK4. In addition to the 136 kDa band, higher molecular weight bands of ~ 145 kDa were also detectable with WT and the p.(M148V) variant, although the intensity of these bands was remarkably reduced for the p.(C779Y) variant. These higher molecular weight bands are likely to originate from the post-translation modification of the PLK4 protein. The ratio of the band intensity of the ~ 145 kDa to the 136 kDa p.(M148V) products was twofold lower than that of the WT proteins (Figure 3c). Although the origin of this

band shift has not been identified, this result indicates that the p.(M148V) variant is not functionally equivalent to WT PLK4. Because the intensity of the higher molecular weight band is considerably weaker for the p.(C779Y) PLK4, which lacks centriole duplication ability, we speculate that the p.(M148V) variant may also have an effect on the centriole function of PLK4, and these two variants may thus coordinately produce the microcephaly phenotype of our study patient.

DISCUSSION

In our present study, we have identified novel compound heterozygous missense *PLK4* variants in a patient with microcephaly,

microphthalmos and persistent hyperplastic primary vitreous. Autosomal recessive MCCR1 is characterized by delayed psychomotor development and visual impairment, often accompanied by short stature. To date, three responsible genes have been described. MCCR1 is caused by homozygous or compound heterozygous variants in the *TUBGCP6* gene,¹ MCCR2 [MIM616171] is caused by homozygous truncating variant in the *PLK4* gene,¹ and MCCR3 is caused by compound heterozygous variants in the *TUBGCP4* gene.⁸ The features of the visual impairment in MCCR patients are variable, but are typically characterized by punched-out retinal lesions and occasional retinal folds leading to retinal detachment.⁸ A persistent hyperplastic primary vitreous is included in the chorioretinopathy caused by the mutations in *KIF11*.⁹ The clinical features of our current patient accorded with those of MCCR.

PLK4 is one of the key regulators of centriole duplication.^{6,10} *PLK4* variants thus possibly produce the MCCR phenotype in a similar way to MCPH and Seckel syndrome caused by variants in genes encoding centrosomal proteins.¹¹ The prevailing hypothesis is that the variants in the centrosome genes impair centriole duplication and reduce mitosis efficiency, thereby inducing cell death or reduced cellular proliferation during early embryogenesis and leading to dwarfism. In support of this possibility, neurogenic cells with impaired regulation of centriole duplication are predisposed to mitotic delay or chromosomal aneuploidy leading to a microcephaly and/or retinal phenotype in the patient.¹² Indeed, a mouse model of centrosome amplification manifests microcephaly.¹³

PLK4 has a kinase domain at its amino terminal and three PB domains mediating centriole localization and homodimerization at its carboxyl terminal.¹⁴ PLK4 autophosphorylation regulates its activity,^{15,16} which is strictly controlled in terms of timing and location during the cell cycle.¹⁷ We have shown from our current analyses that the p.(C779Y) PLK4 variant lacks the normal function in centriole duplication. It is thus probable that the p.(C779Y) variant in the PB2 domain impedes the homodimerization of PLK4 and consequently the loss of normal protein function due to the prevalence of the monomeric form.¹⁶ On the other hand, the p.(M148V) variant in the kinase domain of PLK4 could amplify the number of centrioles at WT levels when overexpressed in HeLa cells. It is therefore possible that the overexpressed p.(M148V) variant does not reduce the overall kinase activity levels of PLK4 in the presence of the WT protein even if it lacks kinase activity itself.¹⁸ Western blot analysis of overexpressed PLK4 suggests that the p.(M148V) variant has slightly less activity than WT. Although the exact function of the M148 residue has not yet been characterized, the strong evolutionary conservation of this residue suggests that it has functional importance.

Finally, previous studies of *Plk4* mutant mice have revealed that a homozygous knockout or mutation in the kinase domain is embryonic lethal whilst a haploinsufficiency of *PLK4* appears to produce no phenotype other than cancer susceptibility.^{19–21} Hence, our current study patient likely survived due to the residual marginal activity of PLK4. We speculate that the reduced activity of the p.(M148V) variant rather than a loss-of-function prevented embryonic lethality. The

variants we have here described provide a better understanding of the clinical and biological relevance of PLK4 to centriole duplication.

CONFLICT OF INTEREST

The authors declare no conflict of interest.

ACKNOWLEDGEMENTS

We thank E. Hosoba for technical assistance. This study was supported in part by a grant for Research on Applying Health Technology from the Ministry of Health, Labour and Welfare of Japan to F.M., N.O., M.K., M.Y., Y.K., K.K. and S.S.

- Martin CA, Ahmad I, Klingseisen A *et al*: Mutations in PLK4, encoding a master regulator of centriole biogenesis, cause microcephaly, growth failure and retinopathy. *Nat Genet* 2014; **46**: 1283–1292.
- Shaheen R, Al Tala S, Almoisheer A, Alkuraya FS: Mutation in PLK4, encoding a master regulator of centriole formation, defines a novel locus for primordial dwarfism. *J Med Genet* 2014; **51**: 814–816.
- Yokoi S, Ishihara N, Miya F *et al*: TUBA1A mutation can cause a hydranencephaly-like severe form of cortical dysgenesis. *Sci Rep* 2015; **5**: 15165.
- Tsutsumi M, Kogo H, Kowa-Sugiyama H *et al*: Characterization of a novel mouse gene encoding an SYCP3-like protein that relocalizes from the XY body to the nucleolus during prophase of male meiosis I. *Biol Reprod* 2011; **85**: 165–171.
- Marchler-Bauer A, Derbyshire MK, Gonzales NR *et al*: CDD: NCBI's conserved domain database. *Nucleic Acids Res* 2015; **43**: D222–D226.
- Habedanck R, Stierhof YD, Wilkinson CJ, Nigg EA: The Polo kinase Plk4 functions in centriole duplication. *Nat Cell Biol* 2005; **7**: 1140–1146.
- Kleylein-Sohn J, Westendorf J, Le Clech M, Habedanck R, Stierhof YD, Nigg EA: Plk4-induced centriole biogenesis in human cells. *Dev Cell* 2007; **13**: 190–202.
- Scheidecker S, Etard C, Haren L *et al*: Mutations in TUBGCP4 alter microtubule organization via the γ -tubulin ring complex in autosomal-recessive microcephaly with chorioretinopathy. *Am J Hum Genet* 2015; **96**: 666–674.
- Jones GE, Ostergaard P, Moore AT *et al*: Microcephaly with or without chorioretinopathy, lymphoedema, or mental retardation (MCLMR): review of phenotype associated with KIF11 mutations. *Eur J Hum Genet* 2014; **22**: 881–887.
- Bettencourt-Dias M, Rodrigues-Martins A, Carpenter L *et al*: SAK/PLK4 is required for centriole duplication and flagella development. *Curr Biol* 2005; **15**: 2199–2207.
- Verloes A, Drunat S, Gressens P, Passemard S: Primary autosomal recessive microcephalies and seckel syndrome spectrum disorders. In: Pagon RA *et al* (eds): *Gene Reviews*. Seattle, WA, USA: University of Washington, 1993.
- Chavali PL, Pütz M, Gergely F: Small organelle, big responsibility: the role of centrosomes in development and disease. *Philos Trans R Soc Lond B Biol Sci* 2014; **369**: pii: 20130468.
- Marthiens V, Rujano MA, Penetier C, Tessier S, Paul-Gilloteaux P, Basto R: Centrosome amplification causes microcephaly. *Nat Cell Biol* 2013; **15**: 731–740.
- Slevin LK, Nye J, Pinkerton DC, Buster DW, Rogers GC, Slep KC: The structure of the plk4 cryptic polo box reveals two tandem polo boxes required for centriole duplication. *Structure* 2012; **20**: 1905–1917.
- Cunha-Ferreira I, Bento I, Pimenta-Marques A *et al*: Regulation of autophosphorylation controls PLK4 self-destruction and centriole number. *Curr Biol* 2013; **23**: 2245–2254.
- Klebba JE, Buster DW, McLamarrah TA, Rusan NM, Rogers GC: Autoinhibition and relief mechanism for Polo-like kinase 4. *Proc Natl Acad Sci USA* 2015; **112**: E657–E666.
- Sillibourne JE, Bornens M: Polo-like kinase 4: the odd one out of the family. *Cell Div* 2010; **5**: 25.
- Guderian G, Westendorf J, Uldschmid A, Nigg EA: Plk4 trans-autophosphorylation regulates centriole number by controlling betaTrCP-mediated degradation. *J Cell Sci* 2010; **123**: 2163–2169.
- Hudson JW, Kozarova A, Cheung P *et al*: Late mitotic failure in mice lacking Sak, a polo-like kinase. *Curr Biol* 2001; **11**: 441–446.
- Ko MA, Rosario CO, Hudson JW *et al*: Plk4 haploinsufficiency causes mitotic infidelity and carcinogenesis. *Nat Genet* 2005; **37**: 883–888.
- Harris RM, Weiss J, Jameson JL: Male hypogonadism and germ cell loss caused by a mutation in Polo-like kinase 4. *Endocrinology* 2011; **152**: 3975–3995.

Supplementary Information accompanies this paper on *European Journal of Human Genetics* website (<http://www.nature.com/ejhg>)

Complex X-Chromosomal Rearrangements in Two Women with Ovarian Dysfunction: Implications of Chromothripsis/Chromoanasythesis-Dependent and -Independent Origins of Complex Genomic Alterations

Erina Suzuki^a Hirohito Shima^a Machiko Toki^b Kunihiko Hanew^c
Keiko Matsubara^a Hiroki Kurahashi^d Satoshi Narumi^a Tsutomu Ogata^{a,e}
Tsutomu Kamimaki^{b,f} Maki Fukami^a

^aDepartment of Molecular Endocrinology, National Research Institute for Child Health and Development, Tokyo, ^bDepartment of Pediatrics, Hiratsuka City Hospital, Hiratsuka, ^cHanew Endocrine Clinic, Sendai, ^dDivision of Molecular Genetics, Institute for Comprehensive Medical Science, Fujita Health University, Toyoake, ^eDepartment of Pediatrics, Hamamatsu University School of Medicine, Hamamatsu, and ^fDepartment of Pediatrics, Shizuoka City Shimizu Hospital, Shizuoka, Japan

Keywords

Chromothripsis · Genomic rearrangement · Isochromosome · Turner syndrome · X inactivation

Abstract

Our current understanding of the phenotypic consequences and the molecular basis of germline complex chromosomal rearrangements remains fragmentary. Here, we report the clinical and molecular characteristics of 2 women with germline complex X-chromosomal rearrangements. Patient 1 presented with nonsyndromic ovarian dysfunction and hyperthyroidism; patient 2 exhibited various Turner syndrome-associated symptoms including ovarian dysfunction, short stature, and autoimmune hypothyroidism. The genomic abnormalities of the patients were characterized by array-based comparative genomic hybridization, high-resolution karyotyping, microsatellite genotyping, X-inactivation anal-

ysis, and bisulfite sequencing. Patient 1 carried a rearrangement of unknown parental origin with a 46,X,der(X)(pter→p22.1::p11.23→q24::q21.3→q24::p11.4→pter) karyotype, indicative of a catastrophic chromosomal reconstruction due to chromothripsis/chromoanasythesis. Patient 2 had a paternally derived isochromosome with a 46,X,der(X)(pter→p22.31::q22.1→q10::q10→q22.1::p22.31→pter) karyotype, which likely resulted from 2 independent, sequential events. Both patients showed completely skewed X inactivation. CpG sites at Xp22.3 were hypermethylated in patient 2. The results indicate that germline complex X-chromosomal rearrangements underlie nonsyndromic ovarian dysfunction and Turner syndrome. Disease-causative mechanisms of these rearrangements likely include aberrant DNA methylation, in addition to X-chromosomal mispairing and haplo-

E.S., H.S., and M.T. contributed equally to this study.

insufficiency of genes escaping X inactivation. Notably, our data imply that germline complex X-chromosomal rearrangements are created through both chromothripsis/chromoanasythesis-dependent and -independent processes.

© 2017 S. Karger AG, Basel

Complex chromosomal rearrangements are common in cancer genomes and can also appear in the germline [Liu et al., 2011; Kloosterman and Cuppen, 2013]. To date, germline complex rearrangements have been identified in a small number of individuals [Liu et al., 2011; Ochalski et al., 2011; Auger et al., 2013; Kloosterman and Cuppen, 2013; Plaisancié et al., 2014]. Of these, complex autosomal rearrangements were often associated with congenital malformations and mental retardation, which probably reflect dysfunction or dysregulation of multiple genes on the affected chromosome [Liu et al., 2011; Kloosterman and Cuppen, 2013; Plaisancié et al., 2014]. In contrast, complex X-chromosomal rearrangements were detected primarily in women with nonsyndromic ovarian dysfunction and were occasionally associated with other clinical features such as short stature, muscular hypotonia, and an unmasked X-linked recessive disorder [Ochalski et al., 2011; Auger et al., 2013]. The lack of severe developmental defects in women with complex X-chromosomal rearrangements is consistent with prior observations that structurally abnormal X chromosomes, except for X;autosome translocations, frequently undergo selective X inactivation [Heard et al., 1997]. The clinical features of these women, such as ovarian dysfunction and short stature, are ascribable to X-chromosomal mispairing and haploinsufficiency of genes that escape X inactivation [Zhong and Layman, 2012]. Mutations in *BMP15* at Xp11.22, *POF1B* at Xq21.1, *DIAPH2* at Xq21.33, or *PGRMC1* at Xq24 have been shown to lead to ovarian dysfunction, while mutations in *SHOX* at Xp22.33 impair skeletal growth [Bione et al., 1998; Bione and Toniolo, 2000; Mansouri et al., 2008; Zhong and Layman, 2012]. However, considering the limited number of reported cases, further studies are necessary to clarify the phenotypic characteristics of germline complex X-chromosomal rearrangements. Furthermore, it remains uncertain whether such rearrangements perturb DNA methylation of the affected X chromosomes.

Recent studies revealed that complex genomic rearrangements are caused by catastrophic cellular events referred to as chromothripsis and chromoanasythesis [Liu et al., 2011; Pellestor, 2014; Leibowitz et al., 2015; Zhang et al., 2015]. Chromothripsis is characterized by massive

DNA breaks in a single or a few chromosomes followed by random reassembly of the DNA fragments [Liu et al., 2011; Pellestor, 2014; Zhang et al., 2015]. Chromothripsis is predicted to arise from micronucleus-mediated DNA breakage of mis-segregated chromosomes, although several other mechanisms such as telomere erosion, p53 inactivation, and abortive apoptosis have also been implicated [Liu et al., 2011; Pellestor, 2014; Zhang et al., 2015]. Chromothripsis typically results in copy-number-neutral translocations/inversions or rearrangements with copy number loss; however, in some cases, genomic rearrangements with copy number gain have also been linked to chromothripsis [Liu et al., 2011; Pellestor, 2014]. Copy number gains in these cases are ascribed to replication-based errors during chromosomal reassembly [Liu et al., 2011]. Chromoanasythesis is proposed to arise from serial template switching during DNA replication [Leibowitz et al., 2015]. Chromoanasythesis has been reported as a cause of complex rearrangements with duplications and triplications [Leibowitz et al., 2015]. To date, the clinical significance of germline chromothripsis/chromoanasythesis has not been fully determined. In particular, it remains unknown whether these catastrophic events account for all cases of complex rearrangements in the germline. Here, we report the clinical and molecular characteristics of 2 women with complex X-chromosomal rearrangements.

Patients and Methods

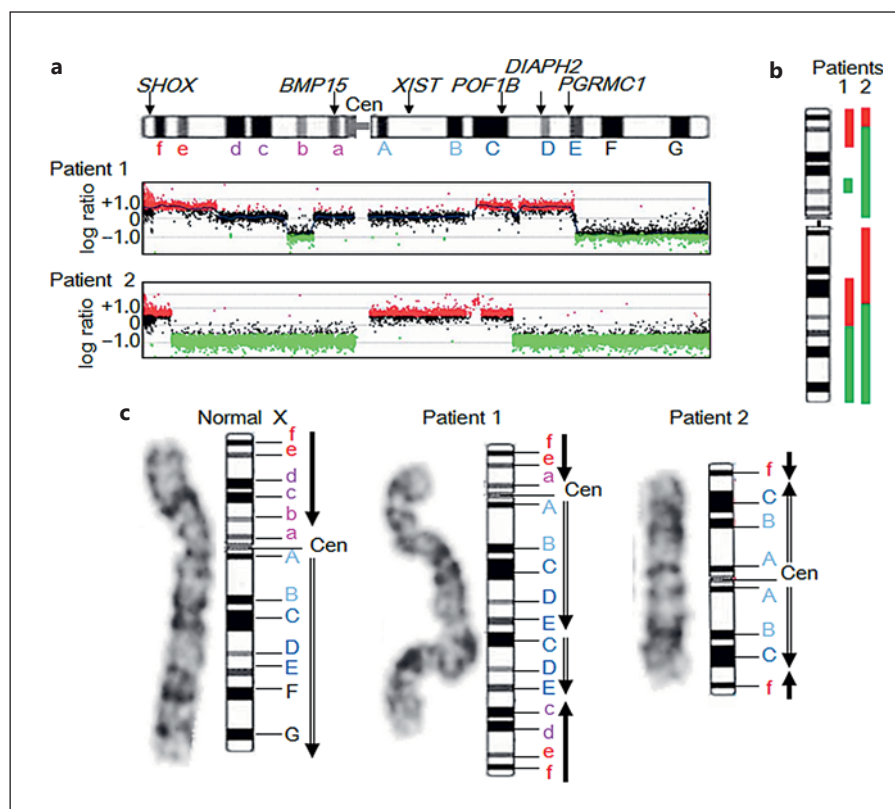
Patients

Patients 1 and 2 were unrelated Japanese women. Patient 1 was hitherto unreported, while patient 2 was previously reported as a female with Turner syndrome [Uehara et al., 2001]. Both patients underwent G-banding analysis in endocrine clinics and were found to have X-chromosomal rearrangements. Thus, they were referred to our institute for further investigation.

Molecular Analysis

Copy number alterations in the genomes were analyzed by comparative genomic hybridization using catalog human arrays (2x400K or 4x180K formats; Agilent Technologies, Palo Alto, CA, USA). We referred to the Database of Genomic Variants (<http://dgv.tcag.ca/dgv/app/home>) to exclude benign copy number polymorphisms. Then, we genotyped 15 microsatellite loci on the X chromosome. Each locus was PCR-amplified using fluorescently labeled forward primers and unlabeled reverse primers. Primer sequences are available from the authors upon request. We also examined the X inactivation status by performing methylation analysis of CpG sites and microsatellite assays of a polymorphic CAG repeat tract in the androgen receptor (*AR*) gene. The methods were described previously [Muroya et al., 1999]. Furthermore, to clarify whether the genomic rearrangements in the patients affect the

Fig. 1. a Array-based comparative genomic hybridization of the patients' X chromosomes. The black, red, and green dots denote normal, increased (log ratio higher than +0.4), and decreased (log ratio lower than -0.8) copy numbers, respectively. The upper panel shows the structure of the X chromosome and the positions of *SHOX*, *BMP15*, *XIST*, *POF1B*, *DIAPH2*, and *PGRMC1*. Cen, centromere. **b** Summary of copy number alterations in patients 1 and 2. The red and green lines depict duplicated and deleted regions, respectively. **c** High-resolution banding of a normal and the rearranged X chromosomes. The black and double-line arrows indicate the orientation of the X chromosome segments (from pter to the centromere and from the centromere to qter, respectively).



DNA methylation of X-chromosomal genes, we performed bisulfite sequencing for CpG sites in the upstream region of *SHOX*. In this experiment, genomic DNA samples were treated with bisulfite using the EZ DNA Methylation Kit (Zymo Research, Irvine, CA, USA). A DNA fragment (chrX:580,597–580,771, hg19, build 37) containing 12 *SHOX*-flanking CpG sites was PCR-amplified using a primer set that hybridizes with both the methylated and unmethylated clones. The PCR products were subcloned with the TOPO TA Cloning Kit (Life Technologies, Carlsbad, CA, USA) and subjected to direct sequencing.

Results

Clinical Manifestations of Patients 1 and 2

Patient 1 was born to phenotypically normal nonconsanguineous parents. This patient showed normal growth during childhood. At 12 years of age, she developed goiter. She was diagnosed with hyperthyroidism and was treated with propylthiouracil for 13 years. This patient exhibited age-appropriate sexual development and experienced menarche at 12 years of age (mean menarcheal age in the Japanese population: 12.3 years). However, her menstrual cycles were irregular and ceased at 15 years of age. Blood examinations at 26 years of age revealed mark-

edly increased gonadotropin levels. She received estrogen and progesterone supplementation and had periodic withdrawal bleeding. She was otherwise healthy and had no Turner stigmata. Her mental development was normal. Her adult height was within the normal range (151.0 cm, -1.3 SD).

Patient 2 was previously reported as a female with Turner syndrome [Uehara et al., 2001]. At 16 years of age, she presented with short neck, shield chest, and cubitus valgus. She also exhibited hypertension, diabetes mellitus, and autoimmune hypothyroidism. In addition, she showed severe short stature (138 cm, -3.8 SD) despite being treated with growth hormone from 8 years of age. She lacked spontaneous pubertal development and was diagnosed with hypogonadism. Her mental development was normal.

Characterization of Genomic Rearrangements

Patient 1 had a 46,X,der(X)(pter→p22.1::p11.23→q24::q21.3→q24::p11.4→pter) karyotype (Fig. 1). The rearranged X chromosome involved at least 5 breakpoints and showed copy number gain of ~20-Mb and ~27-Mb regions at Xp and Xq, respectively, and copy number loss of ~7-Mb and ~36-Mb regions at Xp and Xq, respective-

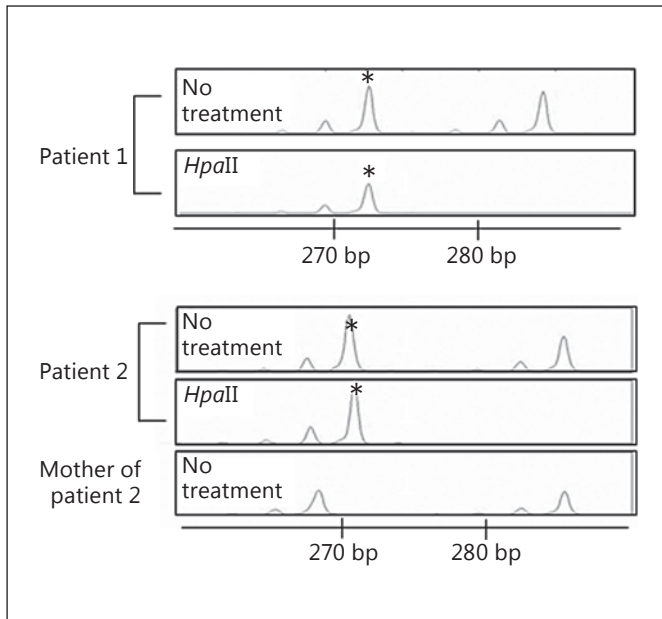


Fig. 2. X-inactivation analysis of *AR*. Microsatellite analysis was performed for polymorphic dinucleotide repeats before and after digestion with the methylation-sensitive enzyme *HpaII*. In patient 1, the 274-bp peak (indicated by an asterisk) represents the PCR products amplified from the inactive X chromosome, while the 283-bp peak indicates the products amplified from the active X chromosome. In patient 2, the 271-bp peak (asterisk) represents the PCR products amplified from the inactive rearranged X chromosome, while the 286-bp peak depicts the products amplified from the maternally transmitted normal X chromosome. These data suggest that the rearranged X chromosome of patient 2 was of paternal origin.

Table 1. Representative results of the microsatellite analysis in patient 2 and her mother

Locus	Chromosomal position ^a	Copy number in the genome of patient 2	PCR products, bp	
			patient 2	mother
<i>SHOX</i> (CA)	Xp22.33	3	142/150	132/142
DXYS233	Xp22.33	3	277	277
DXYS85	Xp22.33	3	200/204	204
DXS1449	Xp22.33	3	116	116
DXS85	Xp22.2	3	174/232	174/232
DXS8025	Xp11.4	1	186	180/186
DXS1069	Xp11.4	1	256	256
DXS1068	Xp11.4	1	254	250/254
<i>ALAS2</i>	Xp11.21	1	155	155/157
<i>AR</i>	Xq12	3	271/286	268/286
DXS8020	Xq22.1	3	194/196	194/196
<i>HPRT1</i>	Xq26.2–26.3	1	290	282/290
DXS8377	Xq28	1	233	229/233
DXS7423	Xq28	1	187	183/187
DXS15	Xq28	1	148	146/148

^a Based on Ensembl Genome Browser (<http://www.ensembl.org>).

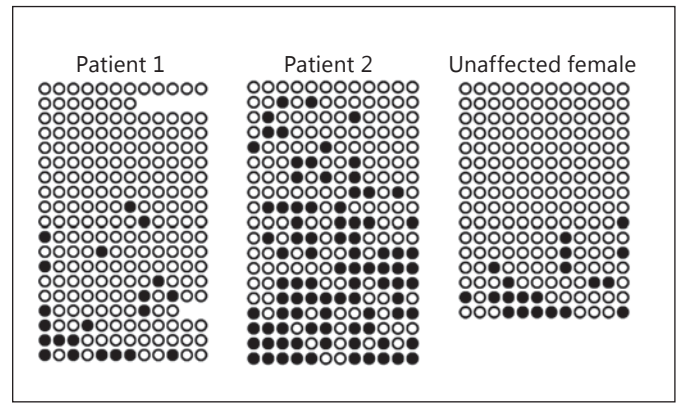


Fig. 3. Methylation analysis of *SHOX*-flanking CpG sites. Each horizontal line indicates the results of 1 clone. Filled and open circles indicate methylated and unmethylated cytosines in the CpG dinucleotides, respectively.

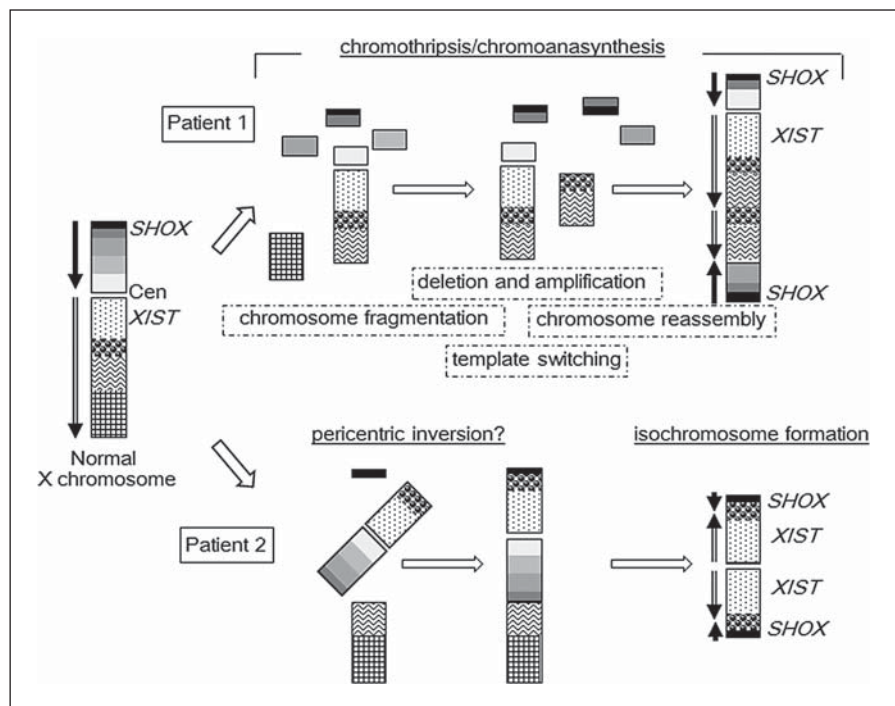
ly. This rearrangement caused overdosage of *SHOX*, *POF1B*, *DIAPH2*, and *PGRMC1* but did not affect the copy number of *BMP15* or *XIST* (X inactive specific transcript). X-inactivation analysis confirmed completely skewed inactivation (Fig. 2). *SHOX*-flanking CpG sites were barely methylated both in patient 1 and in an unaffected control individual (Fig. 3).

Patient 2 had a 46,X,der(X)(pter→p22.31::q22.1→q10::q10→q22.1::p22.31→pter) karyotype (Fig. 1). The rearranged X chromosome comprised at least 3 breakpoints and showed copy number gain of an ~8-Mb region at Xp and an ~40-Mb region at Xq and copy number loss of an ~53-Mb region at Xp and an ~54-Mb region at Xq. *SHOX*, *XIST*, and *POF1B* were duplicated, while *BMP15*, *DIAPH2*, and *PGRMC1* were deleted. There were no copy-number-neutral regions on this X chromosome. Microsatellite analysis suggested that this chromosome consisted of 2 identical arms (“isochromosome”) of paternal origin (Table 1). The rearranged X chromosome was selectively inactivated (Fig. 2). *SHOX*-flanking CpG islands in patient 2 were hypermethylated (Fig. 3).

Discussion

We characterized complex germline X-chromosomal rearrangements in 2 patients. The clinical manifestations of the patients are consistent with the genomic structure. First, both patients manifested ovarian dysfunction. This feature is attributable to X-chromosomal mispairing, as suggested in cases of Turner syndrome due to X mono-

Fig. 4. Predicted mechanisms of the chromosomal rearrangements. The black and double-line arrows indicate the orientation of X chromosome segments (from pter to the centromere and from the centromere to qter, respectively). The rearranged X in patient 1 is consistent with a catastrophic reconstruction due to chromothripsis/chromoanasythesis, while that in patient 2 likely results from 2 independent sequential events. It remains to be clarified whether the father of patient 2 carries a pericentric inversion.



somy [Ogata and Matsuo, 1995]. Furthermore, patient 2 lacked *BMP15*, *DIAPH2*, and *PGRMC1*, which have been implicated in ovarian function [Bione et al., 1998; Bione and Toniolo, 2000; Mansouri et al., 2008]. Copy number changes of other genes might also have contributed to the ovarian dysfunction in patients 1 and 2, because multiple X-chromosomal loci have been linked to this phenotype [Zhong and Layman, 2012]. Second, Turner stigmata such as short neck, shield chest, and cubitus valgus were observed in patient 2 but not in patient 1. These results support the previously proposed notion that a lymphogenic gene responsible for Turner stigmata resides at Xp11.2 [Ogata et al., 2001a], a genomic region deleted in patient 2 and preserved in patient 1. Third, both patients manifested thyroid disorders. Notably, isochromosome Xq is known to be associated with a high risk of autoimmune thyroid disorders [Elsheikh et al., 2001]. Indeed, the hypothyroidism of patient 2 may have resulted from copy number gain of *GPR174* at Xq21.1, because increased expression of *GPR174* has been linked to the risk of an autoimmune thyroid disorder [Chu et al., 2013]. However, the copy number of *GPR174* remained intact in patient 1. Thus, the genomic interval at Xq21.32q22.1>Xq21.32-q22.1, duplicated in both patients, may contain a hitherto uncharacterized gene associated with autoimmune thyroid disorders. Lastly, patient 1 had a normal

stature, and patient 2 showed severe short stature, although both patients carried 3 copies of *SHOX*. This is inconsistent with previous findings that trisomy of the Xp22.3 region encompassing *SHOX* leads to tall stature [Ogata et al., 2001b]. In patients 1 and 2, positive effects of *SHOX* overdosage on skeletal growth may be balanced by negative effects of X-chromosomal mispairing and copy number alterations of minor growth genes on the X chromosome. Furthermore, short stature in patient 2 may be associated with *SHOX* dysregulation, because *SHOX*-flanking CpG islands were hypermethylated in this individual. These sites were barely methylated in the control individual, which is in agreement with the fact that *SHOX* escapes X inactivation [Rao et al., 1997]. It has been shown that in patients with X;autosome translocations, aberrant DNA methylation can spread to regions larger than 1 Mb of the autosomal segments [Cotton et al., 2014]. Hypermethylation of the *SHOX*-flanking CpG sites in patient 2 may reflect decreased physical distance between *SHOX* and *XIST* and/or copy number gain of *XIST*.

The genomic rearrangements in patients 1 and 2 appear to have been formed through different mechanisms (Fig. 4). The rearrangement in patient 1 is consistent with catastrophic reconstruction due to chromothripsis/chromoanasythesis [Liu et al., 2011; Leibowitz et al., 2015].

This case provides further evidence that X-chromosomal chromothripsis/chromoanasythesis accounts for a small portion of cases with nonsyndromic ovarian dysfunction. In contrast, the rearrangement in patient 2 is inconsistent with the “all-at-once” nature of chromothripsis/chromoanasythesis [Liu et al., 2011; Hatch and Hetzer, 2015]. The rearranged chromosome of this patient had 2 identical arms consisting of Xp and Xq material, indicating that this chromosome arose by 2 independent sequential events, namely, a fusion between the Xp22.31 and Xq22.1 segments followed by isochromosome formation. Notably, the rearrangement occurred in the paternally inherited X chromosome. Thus, although the Xp22.31;Xq22.1 translocation is the simplest explanation of this rearrangement, it is implausible in this case, because X;X translocation rarely occurs during male meiosis. The results of patient 2 can be explained by assuming that the phenotypically normal father carried a pericentric inversion, inv(X)(p22.31q22.1), which was subjected to meiotic or postzygotic isochromosome formation (Fig. 4). However, since a paternal DNA sample was not available for genetic testing, we cannot exclude the possibility that this rearrangement was formed via other rare processes.

In conclusion, the results indicate that complex X-chromosomal rearrangements in the germline lead to ovarian dysfunction with and without other Turner syndrome-associated features. Clinical outcomes of such re-

arrangements likely reflect X-chromosomal mispairing, haploinsufficiency of genes escaping X inactivation, and/or perturbed DNA methylation. Most importantly, our findings imply that germline complex X-chromosomal rearrangements are created through both chromothripsis/chromoanasythesis-dependent and -independent processes.

Acknowledgements

This study was supported by the Grants-in-Aid from the Japan Society for the Promotion of Science; and by the Grants from the Ministry of Health, Labor and Welfare, the Japan Agency for Medical Research and Development, the National Center for Child Health and Development, and the Takeda Foundation.

Statement of Ethics

This study was approved by the Institutional Review Board Committee at the National Center for Child Health and Development and performed after obtaining written informed consent.

Disclosure Statement

The authors have no competing interests to declare.

References

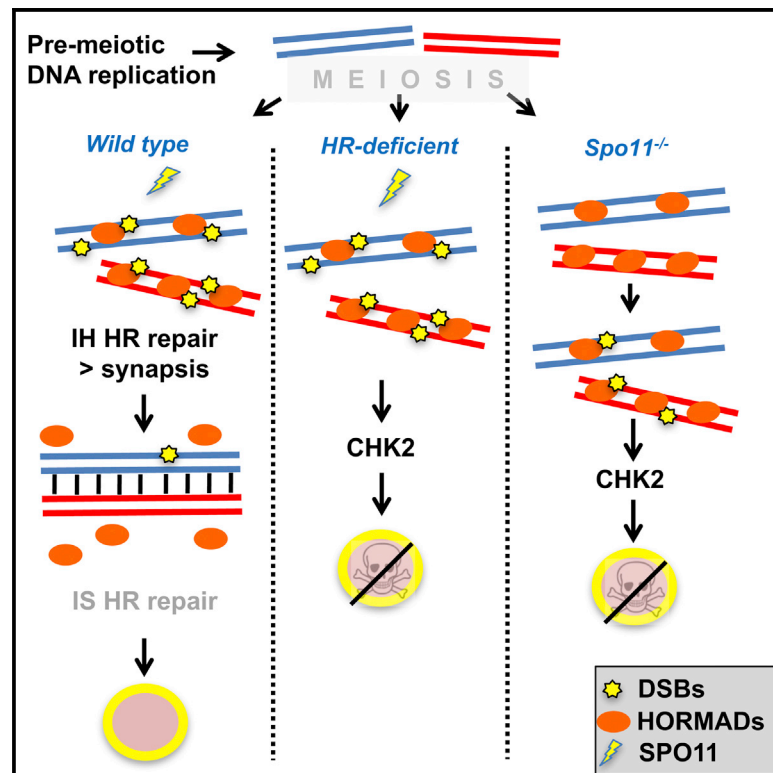
- Auger J, Bonnet C, Valduga M, Philippe C, Bertolo-Houriez E, et al: De novo complex X chromosome rearrangement unmasking maternally inherited *CSF2RA* deletion in a girl with pulmonary alveolar proteinosis. *Am J Med Genet A* 161A:2594–2599 (2013).
- Bione S, Toniolo D: X chromosome genes and premature ovarian failure. *Semin Reprod Med* 18:51–57 (2000).
- Bione S, Sala C, Manzini C, Arrigo G, Zuffardi O, et al: A human homologue of the *Drosophila melanogaster diaphanous* gene is disrupted in a patient with premature ovarian failure: evidence for conserved function in oogenesis and implications for human sterility. *Am J Hum Genet* 62:533–541 (1998).
- Chu X, Shen M, Xie F, Miao XJ, Shou WH, et al: An X chromosome-wide association analysis identifies variants in *GPR174* as a risk factor for Graves' disease. *J Med Genet* 50:479–485 (2013).
- Cotton AM, Chen CY, Lam LL, Wasserman WW, Kobor MS, Brown CJ: Spread of X-chromosome inactivation into autosomal sequences: role for DNA elements, chromatin features and chromosomal domains. *Hum Mol Genet* 23:1211–1223 (2014).
- Elsheikh M, Wass JA, Conway GS: Autoimmune thyroid syndrome in women with Turner's syndrome – the association with karyotype. *Clin Endocrinol (Oxf)* 55:223–226 (2001).
- Hatch EM, Hetzer MW: Chromothripsis. *Curr Biol* 25:R397–399 (2015).
- Heard E, Clerc P, Avner P: X-chromosome inactivation in mammals. *Annu Rev Genet* 31:571–610 (1997).
- Kloosterman WP, Cuppen E: Chromothripsis in congenital disorders and cancer: similarities and differences. *Curr Opin Cell Biol* 25:341–348 (2013).
- Leibowitz ML, Zhang CZ, Pellman D: Chromothripsis: A new mechanism for rapid karyotype evolution. *Annu Rev Genet* 49:183–211 (2015).
- Liu P, Erez A, Nagamani SC, Dhar SU, Kołodziejaska KE, et al: Chromosome catastrophes involve replication mechanisms generating complex genomic rearrangements. *Cell* 146:889–903 (2011).
- Mansouri MR, Schuster J, Badhai J, Stattin EL, Lösel R, et al: Alterations in the expression, structure and function of progesterone receptor membrane component-1 (*PGRMC1*) in premature ovarian failure. *Hum Mol Genet* 17:3776–3783 (2008).
- Muroya K, Kosho T, Ogata T, Matsuo M: Female carriers of Xp22.3 deletion including MRX locus. *Am J Med Genet* 84:384–385 (1999).
- Ochalski ME, Engle N, Wakim A, Ravnan BJ, Hoffner L, et al: Complex X chromosome rearrangement delineated by array comparative genome hybridization in a woman with premature ovarian insufficiency. *Fertil Steril* 95:2433.e9–e15 (2011).

- Ogata T, Matsuo N: Turner syndrome and female sex chromosome aberrations: deduction of the principal factors involved in the development of clinical features. *Hum Genet* 95:607–629 (1995).
- Ogata T, Muroya K, Matsuo N, Shinohara O, Yorifuji T, et al: Turner syndrome and Xp deletions: clinical and molecular studies in 47 patients. *J Clin Endocrinol Metab* 86:5498–508 (2001a).
- Ogata T, Matsuo N, Nishimura G: *SHOX* haploinsufficiency and overdosage: impact of gonadal function status. *J Med Genet* 38:1–6 (2001b).
- Pellestor F: Chromothripsis: how does such a catastrophic event impact human reproduction? *Hum Reprod* 29:388–393 (2014).
- Plaisancié J, Kleinfinger P, Cances C, Bazin A, Julia S, et al: Constitutional chromoanagenesis: description of a rare chromosomal event in a patient. *Eur J Med Genet* 57:567–570 (2014).
- Rao E, Weiss B, Fukami M, Rump A, Niesler B, et al: Pseudoautosomal deletions encompassing a novel homeobox gene cause growth failure in idiopathic short stature and Turner syndrome. *Nat Genet* 16:54–63 (1997).
- Uehara S, Hanew K, Harada N, Yamamori S, Nata M, et al: Isochromosome consisting of terminal short arm and proximal long arm X in a girl with short stature. *Am J Med Genet* 99:196–199 (2001).
- Zhang CZ, Spektor A, Cornils H, Francis JM, Jackson EK, et al: Chromothripsis from DNA damage in micronuclei. *Nature* 522:179–184 (2015).
- Zhong Q, Layman LC: Genetic considerations in the patient with Turner syndrome – 45,X with or without mosaicism. *Fertil Steril* 98:775–779 (2012).

Molecular Cell

The DNA Damage Checkpoint Eliminates Mouse Oocytes with Chromosome Synapsis Failure

Graphical Abstract



Authors

Vera D. Rinaldi, Ewelina Bolcun-Filas, Hiroshi Kogo, Hiroki Kurahashi, John C. Schimenti

Correspondence

jcs92@cornell.edu

In Brief

Proper chromosome segregation during meiosis requires recombination repair of programmed DNA breaks to drive homolog pairing. Gametes with potentially devastating unsynapsed chromosomes or unrepaired breaks are killed. Surprisingly, Rinaldi et al. find that the CHK2 DNA damage checkpoint is important for eliminating mutant oocytes with either type of defect.

Highlights

- Late meiosis I oocytes bearing more than 10 DSBs are killed by the DNA damage checkpoint
- CHK2 is responsible for eliminating many asynaptic, SPO11-deficient mouse oocytes
- *Spo11^{-/-}* oocytes acquire spontaneous DSBs that often exceed the 10-DSB threshold
- HORMAD2 on pachytene chromosomes prevents DSB repair via intersister recombination



The DNA Damage Checkpoint Eliminates Mouse Oocytes with Chromosome Synapsis Failure

Vera D. Rinaldi,¹ Ewelina Bolcun-Filas,^{1,2} Hiroshi Kogo,⁴ Hiroki Kurahashi,³ and John C. Schimenti^{1,5,*}

¹Cornell University, Departments of Biomedical Sciences and Molecular Biology and Genetics, Ithaca, NY 14850, USA

²The Jackson Laboratory, Bar Harbor, ME 14850, USA

³Fujita Health University, Institute of Comprehensive Molecular Science, Toyoake, Aichi 470-1192, Japan

⁴Gunma University, Department of Anatomy and Cell Biology, Maebashi, Gunma 371-8511, Japan

⁵Lead Contact

*Correspondence: jcs92@cornell.edu

<http://dx.doi.org/10.1016/j.molcel.2017.07.027>

SUMMARY

Pairing and synapsis of homologous chromosomes during meiosis is crucial for producing genetically normal gametes and is dependent upon repair of SPO11-induced double-strand breaks (DSBs) by homologous recombination. To prevent transmission of genetic defects, diverse organisms have evolved mechanisms to eliminate meocytes containing unrepaired DSBs or unsynapsed chromosomes. Here we show that the CHK2 (CHEK2)-dependent DNA damage checkpoint culls not only recombination-defective mouse oocytes but also SPO11-deficient oocytes that are severely defective in homolog synapsis. The checkpoint is triggered in oocytes that accumulate a threshold level of spontaneous DSBs (~10) in late prophase I, the repair of which is inhibited by the presence of HORMAD1/2 on unsynapsed chromosome axes. Furthermore, *Hormad2* deletion rescued the fertility of oocytes containing a synapsis-proficient, DSB repair-defective mutation in a gene (*Trip13*) required for removal of HORMADs from synapsed chromosomes, suggesting that many meiotic DSBs are normally repaired by intersister recombination in mice.

INTRODUCTION

Genome maintenance in germ cells is critical for fertility, prevention of birth defects, and the genetic stability of species. Throughout mammalian germline development, from primordial germ cells (PGCs) through completion of meiosis, there are mechanisms that prevent the transmission of gametes with genetic defects. Indeed, mutation rates in germ cells are far lower than in somatic cells (Conrad et al., 2011; Murphey et al., 2013; Stambrook and Tichy, 2010). This is reflected by the exquisite sensitivity of PGCs to mutations in certain DNA repair genes (Agoulnik et al., 2002; Luo et al., 2014; Nadler and Braun, 2000) (Watanabe et al., 2013), sensitivity of resting oocytes to clastogens such as radiation and chemotherapeutics (Maltaris

et al., 2007; Perez et al., 1997; Suh et al., 2006), and sensitivity of developing prophase I meocytes to genetic anomalies, including a modicum of DNA damage (Meirow and Nugent, 2001; Suh et al., 2006) or the presence of a single asynapsed chromosome or even a chromosomal subregion (Burgoyne and Baker, 1985; Homolka et al., 2012).

Genetic and developmental analyses of mouse mutants have suggested that there are at least two distinct checkpoints during meiotic prophase I in oocytes, one that monitors double-strand break (DSB) repair and another that monitors synapsis. Oocytes defective for either synapsis or DSB repair are eliminated with different dynamics and severity. Females with mutations causing pervasive asynapsis alone (e.g., *Spo11*^{-/-}) are born with a grossly reduced oocyte pool. The surviving oocytes undergo folliculogenesis but are reproductively inviable, becoming exhausted within a few weeks by atresia and ovulation (Di Giacomo et al., 2005). Oocytes defective in DSB repair alone (*Trip13*^{Gt/Gt}) or defective in both synapsis and meiotic DSB repair (e.g., *Dmc1*^{-/-}; *Msh5*^{-/-}) are virtually completely eliminated between late gestation and wean age by the action of a DNA damage checkpoint (Di Giacomo et al., 2005; Li and Schimenti, 2007). Furthermore, genetic ablation of meiotic DSB formation confers a *Spo11*^{-/-}-like phenotype to such DSB repair mutants, consistent with the existence of separate DNA damage and synapsis checkpoints (Di Giacomo et al., 2005; Finsterbusch et al., 2016; Li and Schimenti, 2007; Reinholdt and Schimenti, 2005). For DSB repair, CHK2 (checkpoint kinase 2) signaling to TRP53/TAp63 is crucial for eliminating *Trip13*^{Gt/Gt} mutant oocytes that exhibit full chromosome synapsis but have unrepaired SPO11-induced DSBs (Bolcun-Filas et al., 2014). Interestingly, *Chk2* deficiency imparted a *Spo11* null-like phenotype upon *Dmc1*^{-/-} ovaries, consistent with separate, sequentially acting checkpoints (Bolcun-Filas et al., 2014). Genetic evidence for a distinct synapsis checkpoint came from studies of mice lacking HORMAD1 or HORMAD2, proteins that load onto axes of meiotic chromosomes throughout early prophase I but are removed upon synapsis (Wojtasz et al., 2009). Ablation of either in mice prevented loss of SPO11-deficient oocytes, resulting in the persistence of a nonfertile primordial follicle reserve in adults (Daniel et al., 2011; Kogo et al., 2012a; Wojtasz et al., 2012). These data suggest that the HORMADs are components of a synapsis checkpoint pathway. Another mechanism for elimination of oocytes is related to the phenomenon of MSUC (meiotic

silencing of unsynapsed chromatin). Although not formally a checkpoint, the transcriptional inactivation of a chromosome containing genes essential for oocyte survival and development can block progression past diplotene (Cloutier et al., 2015).

Although these lines of evidence support the existence of separate checkpoints monitoring DNA damage and synapsis, studies in non-mammalian organisms indicate that the “pachytene checkpoint”—a term referring to delayed progression of meiosis or death of meiocytes triggered by genetic aberrations present in late pachynema—is more complex, consisting of both distinct and overlapping signaling pathways that also affect DNA repair modalities such as choice of recombination partner for the repair of meiotic DSBs (e.g., sister chromatid versus homolog) (Joshi et al., 2015; MacQueen and Hochwagen, 2011; Roeder and Bailis, 2000; Subramanian and Hochwagen, 2014). Here we report the results of a series of experiments designed to discriminate whether the pachytene checkpoint in mouse oocytes indeed consists of distinct pathways responding to different signals or whether the responses are integrated into a single checkpoint pathway. Using a variety of mouse mutants, we show that most oocytes that are highly defective for chromosome synapsis accumulate spontaneous DSBs at a level that can trigger the CHK2-dependent DNA damage signaling pathway, leading to their elimination. Additionally, we present evidence that the reason why asynaptic *Spo11*^{-/-} oocytes can be rescued by *HORMAD1/2* deficiency is that their absence disrupts the so-called barrier to sister chromatid recombination (BSCR), enabling intersister (IS) repair of those spontaneous DSBs. Taken together, we propose that the pachytene checkpoint consists primarily of a canonical DNA damage signaling pathway and that extensive asynapsis leads to oocyte loss by inhibiting homologous recombination (HR) repair rather than triggering a distinct “synapsis checkpoint.”

RESULTS

CHK2 Is Involved in the Elimination of *Spo11*^{-/-} Oocytes

To investigate potential overlap of the meiotic DSB repair and synapsis checkpoint pathways in mice, we tested whether CHK2, a well-defined DSB signal transducer, contributes to the elimination of *Spo11*^{-/-} oocytes that are asynaptic because of lack of programmed meiotic DSBs needed for recombination-driven homolog pairing. Consistent with prior reports (Baudat et al., 2000; Di Giacomo et al., 2005), we observed a greatly reduced number of total follicles in 3-week-postpartum (pp) *Spo11*^{-/-} ovaries compared with the WT, and, in particular, the oocyte reserve (the pool of primordial resting follicles) was almost completely exhausted by 8 weeks of age (Figure 1). Surprisingly, *Chk2* deletion rescued the oocyte reserve (Figures 1A and 1B), albeit not to WT levels. The rescued follicles in double-mutant females persisted robustly at least until 6 months pp (in one case, 554 total in a single ovary).

HORMAD2 Deficiency Prevents Elimination of *Trip13* Mutant Oocytes that Have Complete Synapsis but Unrepaired Meiotic DSBs, Restoring Female Fertility

Taken alone, the rescue of *Spo11*^{-/-} oocytes by *Chk2* deletion suggests that severe asynapsis leads to CHK2 activation and

signaling to mediate oocyte elimination. This led us to postulate that either CHK2 is a common component of otherwise distinct synapsis and DNA damage checkpoints or that there is a single linear checkpoint pathway that responds to both asynapsis and DNA damage and that DNA damage activates the checkpoint pathway more robustly or sooner in prophase I (thus accounting for the different patterns of oocyte elimination in asynaptic versus DSB repair-deficient oocytes mentioned above; Di Giacomo et al., 2005).

We reasoned that if there is a single linear checkpoint pathway, then putative synapsis checkpoint genes required to eliminate *Spo11*^{-/-} oocytes would also be required to eliminate *Trip13*^{Gt/Gt} oocytes. *Trip13*^{Gt/Gt} meiocytes have synapsed chromosomes and persistent SPO11-dependent DSBs, which leads to neonatal depletion of follicles in a *CHK2* > *TRP53/TAP63* pathway-dependent manner (Figure 2A; Bolcun-Filas et al., 2014; Li and Schimenti, 2007). To test this, we determined whether deficiency of *HORMAD2*, a putative synapsis checkpoint protein, could rescue *Trip13*^{Gt/Gt} oocytes. *HORMAD2* and its paralog *HORMAD1* are *HORMA* (Hop1, Rev7, and Mad2) domain-containing proteins orthologous to the *Saccharomyces cerevisiae* synaptonemal complex (SC) axial element protein Hop1p, and deletion of either prevents elimination of *Spo11*^{-/-} oocytes (Daniel et al., 2011; Kogo et al., 2012a; Wojtasz et al., 2012). We used a mutant of *Hormad2* rather than *Hormad1* because deletion of the latter disrupts recombination and homolog synapsis (Daniel et al., 2011; Kogo et al., 2012b; Shin et al., 2010). Remarkably, not only did ovaries of 2-month-old *Trip13*^{Gt/Gt} *Hormad2*^{-/-} mice retain a substantial primordial follicle pool (Figures 2A and 2B), but these females were also fertile (Figure 2C). The rescued fertility of these oocytes suggests either that these DSBs were compatible with further oocyte maturation or that they were eventually repaired, as in the case of *Trip13*^{Gt/Gt} females, whose fertility was restored by *Chk2* ablation (Bolcun-Filas et al., 2014). The dynamics of DSB repair are addressed below.

Because *TRIP13* is required for removal of the *HORMADs* from chromosome axes upon synapsis (Wojtasz et al., 2009), and persistence of *HORMADs* on unsynapsed chromosomes correlates with *MSUC*-mediated silencing of essential genes (Cloutier et al., 2015; Wojtasz et al., 2012), the question arises of whether *Trip13*^{Gt/Gt} oocytes are eliminated not because of unrepaired DSBs but, rather, by transcriptional silencing. However, this is unlikely for the following reasons. First, *Trip13*^{Gt/Gt} oocytes are depleted with a temporal pattern and degree consistent with mutants defective in DSB repair, not asynapsis (Di Giacomo et al., 2005; Li and Schimenti, 2007). Second, *Spo11* is epistatic to *Trip13* in that *Trip13*^{Gt/Gt} *Spo11*^{-/-} ovaries resemble *Spo11* single mutants in their pattern of oocyte elimination (Li and Schimenti, 2007), demonstrating that unrepaired meiotic DSBs drive early culling of *Trip13* mutant oocytes. Third, *HORMAD* persistence on synapsed *Trip13*^{Gt/Gt} or unsynapsed *Spo11*^{-/-} meiotic chromosome axes is not affected by *Chk2* deletion (Figure S1), which might be predicted if CHK2 was rescuing either mutant class by disrupting the ability of *HORMADs* to signal asynapsis. The latter is further supported by the fact that CHK2 depletion does not interfere with *MSCI* (meiotic sex chromosome inactivation), which is mechanistically similar or identical to *MSUC*, in

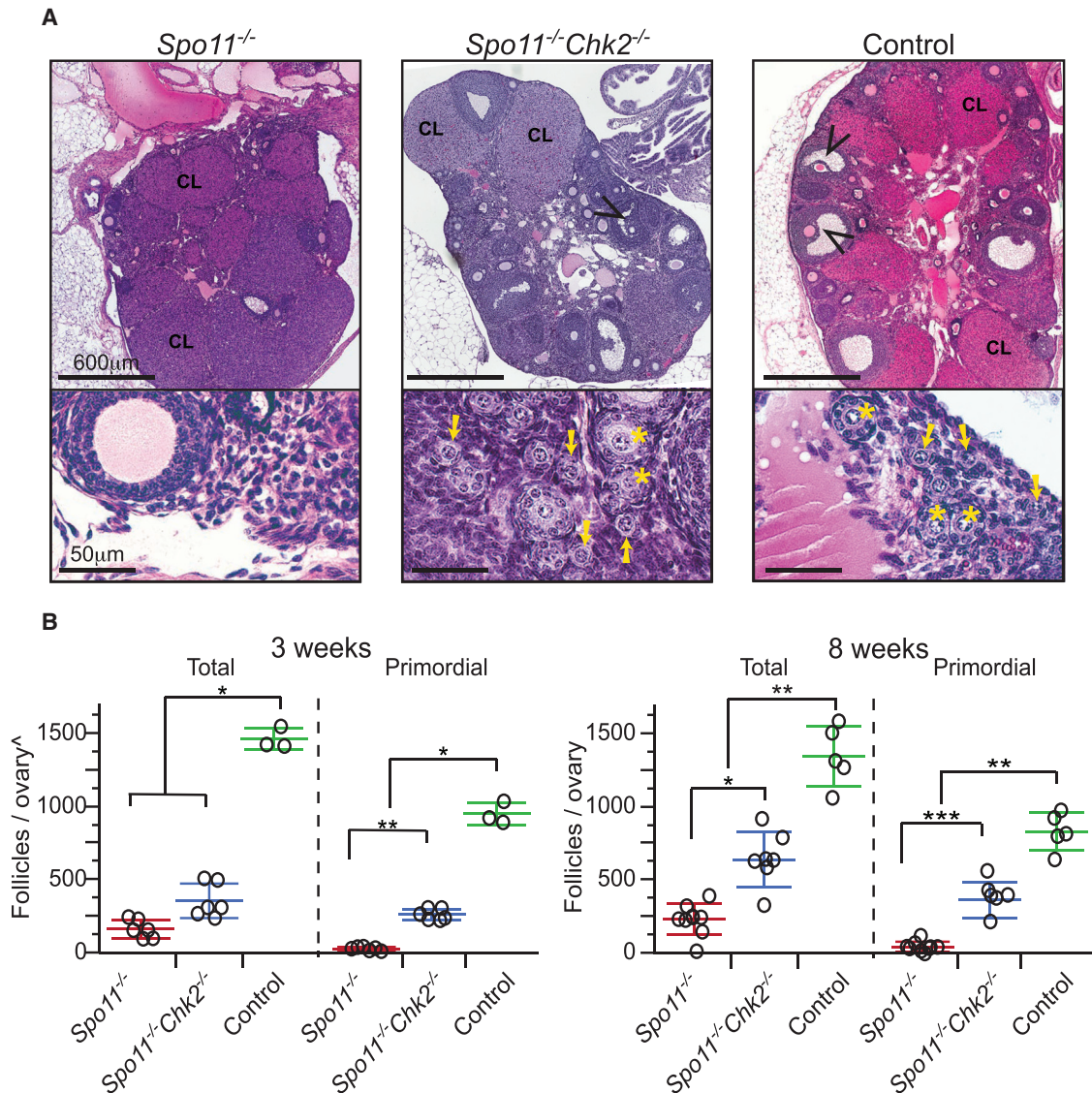


Figure 1. CHK2 Is Required for Efficient Elimination of Asynaptic *Spo11*^{-/-} Mouse Oocytes

(A) H&E-stained histological sections of 8-week-old ovaries. Black arrowheads indicate antral follicles. The presence of corpora lutea (CL) is indicative of prior rounds of ovulation. Shown at the bottom are higher-magnification images of an ovarian cortical region, where primordial follicles reside. Yellow arrows and asterisks indicate primordial and primary follicles, respectively.

(B) Follicle counts from ovaries of the indicated genotypes at 3 and 8 weeks pp, respectively. Each data point is from a single ovary, each from a different animal. Total, all follicle types. Horizontal hashes denote mean and SD. Littermate controls included animals with the following genotypes: *Spo11*^{+/+}*Chk2*^{+/+}, *Spo11*^{+/+}*Chk2*^{+/-}, and *Spo11*^{+/+}*Chk2*^{-/-}. ^, the values obtained for the 3-week follicles/ovaries counts are not comparable with the 8-week ones (see STAR Methods). *p = 0.005–0.05, **p = 0.001–0.005 and ***p ≤ 0.001 derived from a non-parametric, one-way ANOVA test (Kruskal-Wallis).

males (Pacheco et al., 2015) and that *Chk2*^{-/-} mice are fertile, unlike *Hormad1*^{-/-} animals (Daniel et al., 2011; Kogo et al., 2012b; Shin et al., 2013).

HORMAD2 Inhibits DSB Repair in Prophase I Oocytes

That HORMAD2 deficiency could rescue both *Trip13*^{Gt/Gt} and *Spo11*^{-/-} oocytes is consistent with a single checkpoint capable of detecting both damaged DNA and asynapsed chromosomes. If there is indeed a single checkpoint pathway, then combined deficiency for CHK2 and HORMAD2 should rescue asynaptic

and DSB repair-defective *Dmc1*^{-/-} oocytes to the same degree as deficiency for either one alone. However, *Dmc1*^{-/-} *Chk2*^{-/-} *Hormad2*^{-/-} females had ≥3-fold increase in primordial and total follicles compared with *Dmc1*^{-/-} *Hormad2*^{-/-} or *Dmc1*^{-/-} *Chk2*^{-/-} ovaries (Figures 3A and 3B; Figure S2). This lack of epistasis indicates that HORMAD2 and CHK2 are not functioning solely as members of a single linear checkpoint pathway sensing either or both asynapsis and DNA damage.

We therefore considered two alternative explanations for why *Hormad2* deficiency rescues *Trip13*^{Gt/Gt} oocytes: it reduces the

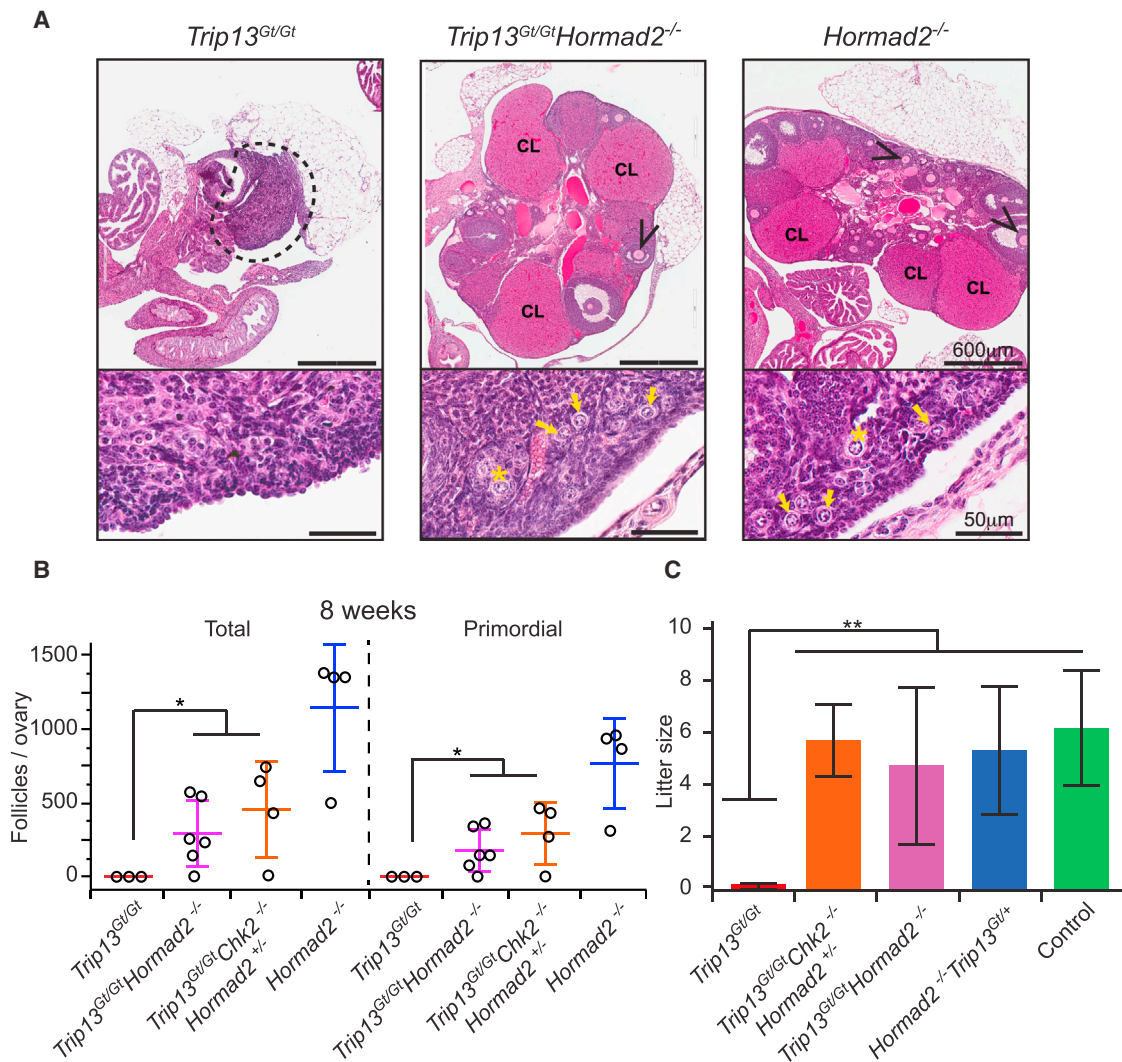


Figure 2. Synapsis-Competent *Trip13^{Gt/Gt}* Oocytes Are Eliminated in a HORMAD2-Dependent Manner

(A) H&E-stained histological sections of 8-week-old ovaries of the indicated genotypes. Black arrowheads indicate antral follicles. Shown at the bottom are higher-magnification images of cortical regions of ovaries. Yellow arrows and asterisks indicate primordial and primary follicles, respectively.

(B) Follicle quantification of 8-week-old ovaries. Each data point is from a single ovary, each from a different animal. Total, all follicle types. Horizontal hashes denote mean and SD. The statistic used was a Kruskal-Wallis test. * $p = 0.002$.

(C) Graphed are mean litter sizes. $n \geq 3$ females tested for fertility per genotypic group. Control matings were between mice with the genotypes *Trip13^{Gt/+}* and *Trip13^{Gt/+} Hormad2^{+/-}*. Error bars represent SD, and ** $p \leq 0.005$, derived from the Kruskal-Wallis test.

number of SPO11-induced DSBs to a level sufficient for synapsis but below the threshold for checkpoint activation, and/or it facilitates DSB repair. Studies of related proteins support both explanations. Absence of the budding yeast ortholog Hop1p not only decreases meiotic DSB formation but also increases use of the sister chromatid as a template for HR repair (Carballo et al., 2008; Lam and Keeney, 2014; Latypov et al., 2010; Mao-Draayer et al., 1996; Niu et al., 2005; Schwacha and Kleckner, 1997). Mouse HORMAD1 is required for loading HORMAD2 onto unsynapsed axes, proper SC formation (Daniel et al., 2011), and normal levels of meiotic DSBs (Daniel et al., 2011; Stanzione et al., 2016). Although *Dmc1^{-/-} Hormad1^{-/-}* or irradiated *Hormad1^{-/-}* oocytes exhibit fewer DSB markers than oocytes

containing HORMAD1 (Daniel et al., 2011; Shin et al., 2010), this can be attributable largely to enhanced repair (Shin et al., 2013). IS HR repair of DSBs in *S. cerevisiae* is substantial, and it increases in *hop1* mutants (Goldfarb and Lichten, 2010). Moreover, disruption of SC axes in mice (deletion of *Sycp2* or *Sycp3*) appears to alter recombination partner choice in favor of the sister chromatid, decreasing persistent DSBs in *Trip13^{Gt/Gt}* oocytes to a degree that diminishes their elimination in a RAD54-dependent manner (Li et al., 2011). These data led us to hypothesize that the rescue of *Trip13* mutant oocytes by *Hormad2* deficiency was due to increased DSB repair, possibly by diminishing the BSCR.

To test this, we quantified the levels and rates of meiotic DSB repair in various genotypes of prophase I oocytes. Although the

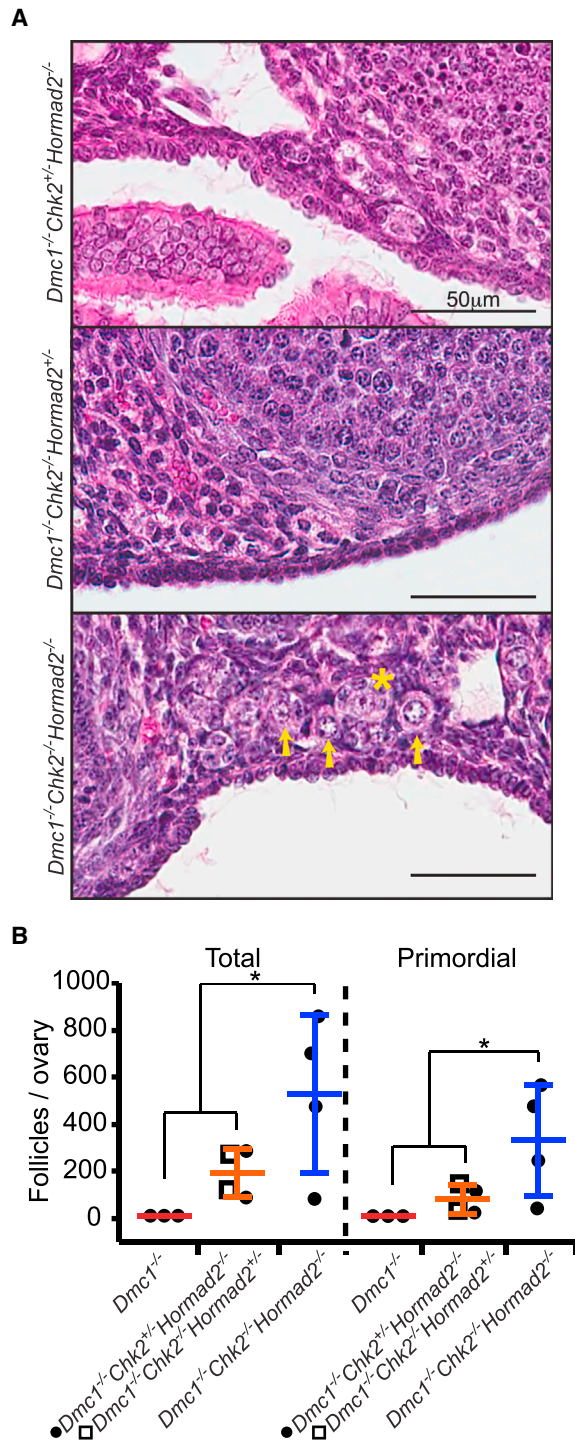


Figure 3. HORMAD2 and CHK2 Are Not in the Same Checkpoint Pathway

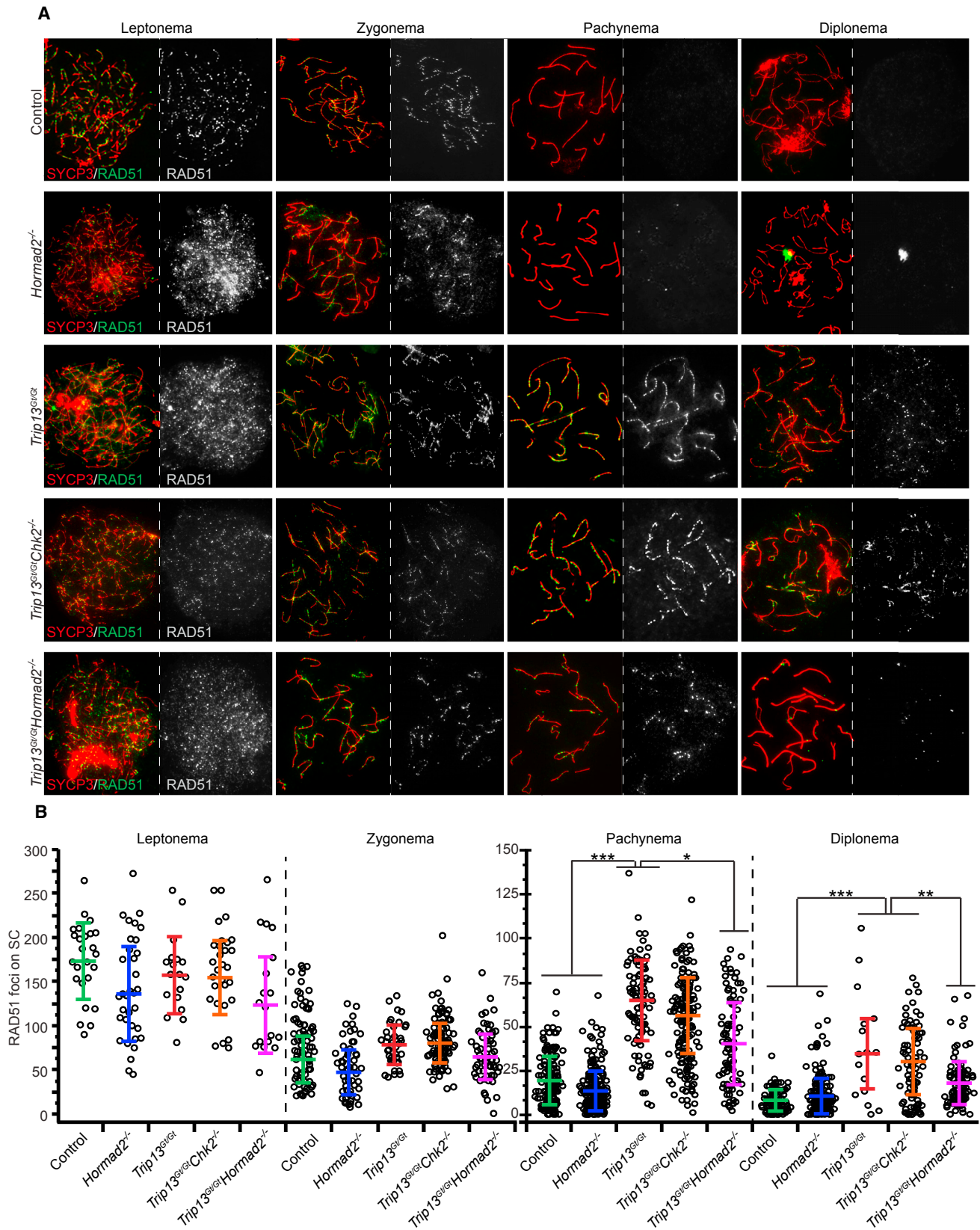
(A) H&E-stained histological sections of cortical regions of 8-week-old mutant mouse ovaries, where primordial follicles are concentrated. Histologies of whole ovaries of these genotypes are presented in Figure S2. Primordial follicles, which constitute the oocyte reserve, are indicated by yellow arrows, and a primary follicle by an asterisk. Residual *Dmc1^{-/-}* ovaries are not represented because they are completely devoid of oocytes (Pittman et al., 1998).

number of leptotene- and zygotene-stage RAD51 foci was not significantly different in *Trip13^{Gt/Gt} Hormad2^{-/-}* oocytes compared with *Trip13^{Gt/Gt}* or other control and mutant genotypes (Figures 4A and 4B; Table S1), there were significantly fewer compared with *Trip13^{Gt/Gt}* by pachynema and diplonema ($p = 0.02$ and 0.03 , respectively, using Tukey honest significant difference (HSD) in a mixed model). RAD51 levels in *Trip13^{Gt/Gt}* and *Trip13^{Gt/Gt} Chk2^{-/-}* newborn oocytes remained high in diplonema compared with all other genotypes (Figures 4A and 4B; Table S1), presumably reflecting a relative deficiency in DSB repair. Furthermore, we found that RAD51 foci induced by 2 Gy of ionizing radiation (IR) disappeared more rapidly in *Spo11^{-/-} Hormad2^{-/-}* oocytes than in either *Spo11^{-/-}* or *Spo11^{-/-} Chk2^{-/-}* oocytes, as assessed 8 hr after treatment (Figure 5; Table S2). Overall, the data suggest that HORMAD2 on the axes of either asynapsed (*Spo11^{-/-}*) or synapsed (*Trip13^{Gt/Gt}*) (Wojtasz et al., 2009) meiotic chromosomes inhibits IS recombination-mediated DSB repair.

Evidence that CHK2-Mediated Elimination of Asynaptic Oocytes Is Driven by Accumulation of SPO11-Independent DSBs

If indeed *Hormad2* deletion rescues DSB-containing oocytes by weakening or eliminating the BSCR, then this raises the question of why HORMAD2 deficiency rescues *Spo11^{-/-}* oocytes that do not make meiotic DSBs. A clue comes from the surprising observation that *Spo11^{-/-}* oocytes sustain DSBs of unknown origin (but possibly from LINE-1 retrotransposon activation) during early pachynema (Malki et al., 2014; Carofiglio et al., 2013). We hypothesized that these DSBs occur at levels sufficient to trigger the CHK2-dependent checkpoint in *Spo11^{-/-}* oocytes but that, in the absence of SC axis-bound HORMAD2, there is sufficient DSB repair to prevent checkpoint activation. To test this, we determined the threshold number of DSBs that kills WT and *Chk2^{-/-}* oocytes by exposing explanted newborn ovaries to a range of IR. RAD51 foci on chromosome axes accumulated roughly linearly in oocytes exposed to 0.5–9 Gy (Figure 6A; Figure S5), and *Chk2^{-/-}* oocytes withstood up to 7 Gy (Figure 6B), a dosage that induces 73.3 RAD51 foci (Figure 6A). In contrast, as little as 0.3 Gy (10.3 foci by linear regression) abolished the entire primordial follicle pool of wild-type (WT) ovaries. Consistent with our hypothesis that HORMAD2 prevents DSB repair, the SC axes of *Spo11^{-/-}* zygotene/pachytene-like chromosomes in newborn oocytes contained far more discrete RAD51 foci (raw average of 39.8; likely an underestimate; see Figure S3) than in *Spo11^{-/-} Hormad2^{-/-}* oocytes (average of 7.3 foci), the latter being almost identical to WT or *Chk2^{-/-}* oocytes (7.5 and 7.3, respectively; Figure 6C; Table S3), in which HORMAD2 has been removed from synapsed chromosomes. These data indicate that the majority of *Spo11^{-/-}* oocytes (60.8%) bear a level of DSBs (>10.3 foci) sufficient to trigger their elimination by the CHK2-dependent DNA damage checkpoint, whereas most WT oocytes (71%) are below this threshold (Table S3).

(B) Follicle counts from ovaries of the indicated genotypes at 8 weeks of age. Total, all types of follicles. Data points represent follicle counts derived from one ovary, each ovary originating from a different animal. * $p \leq 0.05$ (Kruskal-Wallis test).



(legend on next page)

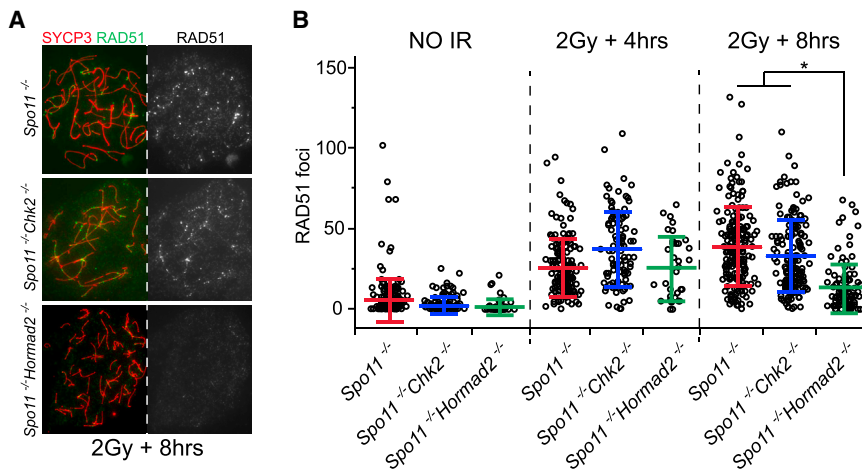


Figure 5. Depletion of HORMAD2 Accelerates Repair of Induced DSBs in Oocytes

(A) Immunolabeling of surface-spread chromosomes from oocytes after exposure to ionizing radiation (IR). Fetal ovaries were collected at 15.5 DPC, cultured for 24 hr, exposed to 2 Gy of IR, and then cultured for an additional 4–8 hr. Shown are those recovered 8 hr after IR. See Figure S4 for single *Hormad2*^{-/-} single-mutant results.

(B) Quantification of RAD51 foci. Each data point represents one oocyte. The graphs include mean and SD and are color-coded according to genotypic group. The 4- and 8-hr unirradiated samples were combined. Data were derived from at least two different animals per condition. See Table S2 for associated raw data and statistical calculations.

DISCUSSION

Meiocytes have genetic quality control mechanisms that respond to their unique developmental circumstances, chromosome biology, and cell cycle. For example, the pachytene/prophase I checkpoint is active only at a point in prophase I at which DSBs have normally been repaired but not during the time between programmed DSB formation and HR repair. Although the oocyte pachytene checkpoint is distinct with respect to its cell cycle timing and its ability to monitor an event (chromosome synapsis) unique to meiosis, our current and prior (Bolcun-Filas et al., 2014) work indicate that, for circumstances involving extensive asynapsis and DNA damage, this checkpoint in oocytes involves a DNA damage response (DDR) common to somatic cells. Our surprising finding that the DDR is involved in culling of *Spo11*^{-/-} oocytes raises the question of how SPO11-independent DSBs, first reported by Carofiglio et al. (2013) and confirmed here, arise on unsynapsed chromosomes. One possible source is LINE-1 retrotransposon activation, which has been correlated with natural oocyte attrition (Malki et al., 2014). However, transposon expression normally occurs only transiently at the onset of meiosis before epigenetic silencing (van der Heijden and Bortvin, 2009). It is possible that the extensive asynapsis in *Spo11*^{-/-} oocytes per se or disruption of the meiotic program, including the normal course of DSB induction and repair, interferes with transposon silencing. Another possibility is that unsynapsed chromosomes are more susceptible to spontaneous breakage. These outcomes could be exacerbated by extended retention of HORMADs on unsynapsed axes, inhibiting repair of these breaks. An intriguing question is

whether the production of these SPO11-independent DSBs, whatever their origin, evolved as a contributory mechanism for genetic quality control. It is also conceivable that the extended presence of HORMADs themselves contributes to spontaneous DSB formation, possibly as a “last ditch” mechanism to drive pairing or synapsis in chromosomes devoid of sufficient interhomolog recombination events.

The late appearance and highly variable number (Figure 6C) of SPO11-independent DSBs in *Spo11*^{-/-} oocytes may explain the differences in timing and extent of oocyte elimination in exclusively asynaptic versus DSB repair-deficient (e.g., *Dmc1*, *Trip13*) mutants. As reported by Di Giacomo et al. (2005), although *Dmc1*^{-/-} oocytes were completely eliminated before dictyate arrest and follicle formation, *Spo11*^{-/-} ovaries contained ~15%–20% of the WT number of follicles (including 27-fold fewer primordial follicles by 4 days pp); this reduced oocyte reserve was depleted by 2–3 months of age by subsequent cycles of recruitment and maturation. Additionally, *Dmc1*^{-/-} oocytes degenerate before *Spo11*^{-/-} oocytes, suggesting that an earlier-acting mechanism was triggering *Dmc1*^{-/-} oocyte death. These distinctions, in conjunction with epistasis analysis of mutants doubly deficient for *Spo11* and DSB repair mutations, led to the conclusion that there are DSB-dependent and -independent mechanisms to eliminate defective oocytes. We suggest that the difference in timing of oocyte elimination, at least in part, may be related to the DSB load. The abundant SPO11 DSBs formed early in prophase I may trigger the checkpoint sooner and more uniformly in recombination mutants that fail to reduce DSB levels in a timely manner. According to this scenario, spontaneous DSBs that do

Figure 4. Depletion of HORMAD2 Accelerates DSB Repair during Early Stages of Meiotic Prophase I

(A) Representative images of meiotic chromosome spreads from oocytes at different substages of meiotic prophase I, probed with antibodies for SYCP3 (SC axis protein) and the DSB marker RAD51. Oocytes were isolated from female embryos ranging from 15.5 DPC to newborns. See Figure S1 for HORMAD2 localization in meiotic mutants.

(B) Numbers of RAD51 foci in the specified meiotic prophase I substage of the indicated mutants. Only RAD51 foci present on SYCP3-stained axes were scored. Each data point represents one cell. In each genotypic group, at each stage, the counts are derived from at least three animals. Horizontal hashes in summary statistic plots denote mean and SD. Values of the mixed-model calculation can be found in Table S1. Colors correspond to genotypes. Asterisks indicate statistical significant differences between groups in terms of the least square means of RAD51 foci: ****p* ≤ 0.001, ***p* ≤ 0.005, **p* ≤ 0.05 (Tukey HSD). See Table S1 for associated raw data and statistical calculations.

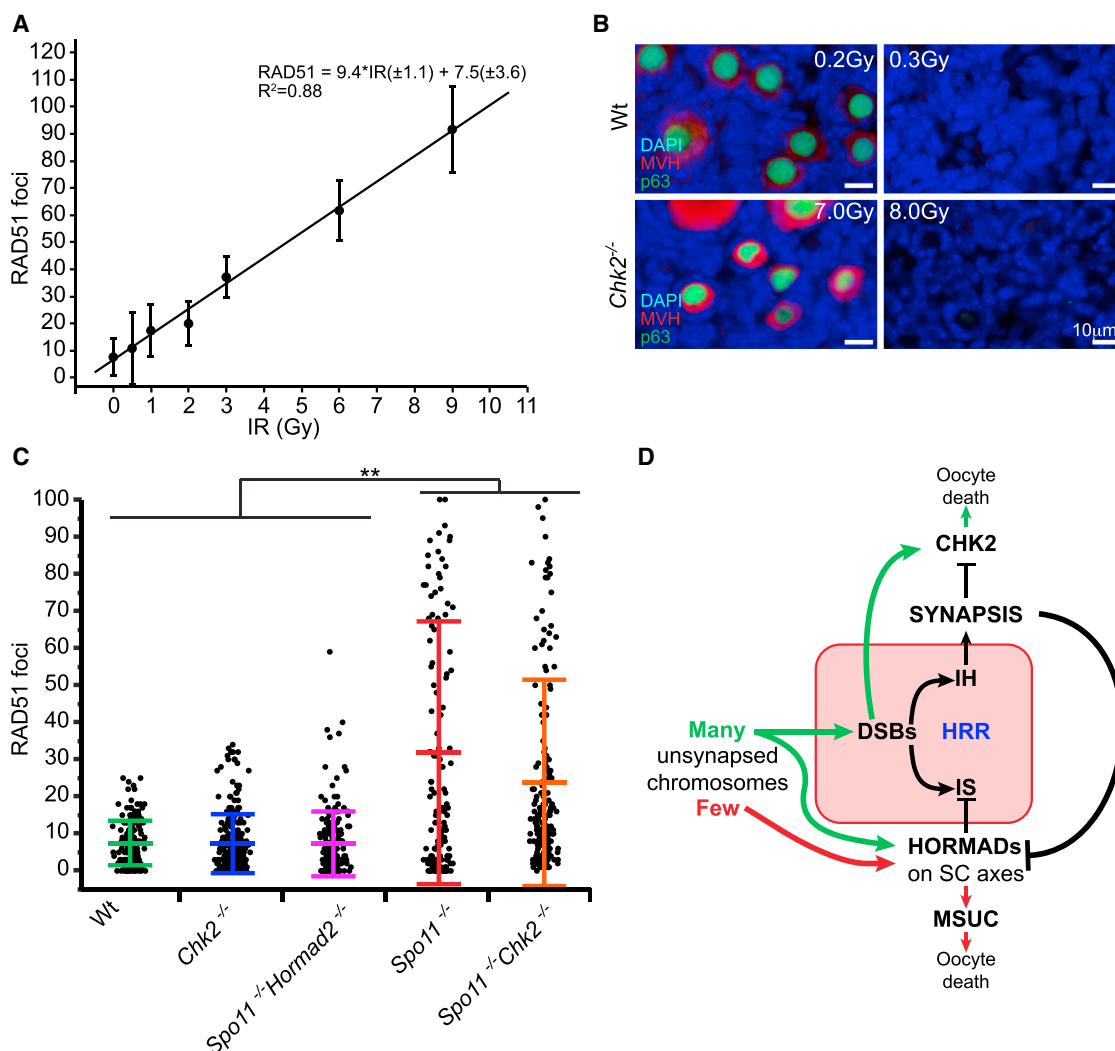


Figure 6. DNA Damage Threshold Required to Trigger Oocyte Death and Evidence for HORMAD-Mediated Inhibition of IS Repair

(A) Linear regression for conversion of radiation dosages to RAD51 focus counts. Meiotic surface spreads were made from WT neonatal ovaries 2.5 hr after IR. Plotted are means with SD. Each IR dose has focus counts from ~25 pachytene oocytes derived from a total of 18 animals. See Figure S5 for single-cell focus counts and numerical values.

(B) *Chk2*^{-/-} oocytes are highly IR-resistant. Shown are immunofluorescence images of ovarian sections labeled with nuclear and cytoplasmic germ cell markers (p63 and MVH, respectively).

(C) RAD51 focus counts from newborn oocyte spreads. Only oocytes with discrete patterns of RAD51 foci were scored, as defined in Figure S3. Data points represent individual oocytes, derived from at least five different animals from each genotypic group. Horizontal hashes denote means and SD calculated using a mixed model (see STAR Methods). Asterisks indicate statistically significant differences between groups: ***p ≤ 0.001, **p ≤ 0.005, *p ≤ 0.05 (Tukey HSD). See Table S3 for raw data and statistical calculations.

(D) Model for pachytene checkpoint activation in mouse oocytes. Oocytes with many unsynapsed chromosomes (green) ultimately accumulate DSBs, which cannot be repaired because of block to IS recombination imposed by HORMADs on asynapsed axes. Failure of DSB repair leads to activation of CHK2 and downstream effector proteins (p53/TAp63) that trigger apoptosis. Few asynapsed chromosomes (red) lead to inactivation of essential genes by MSUC, thereby causing oocyte death.

not arise until latter stages of prophase I in *Spo11*^{-/-} oocytes would trigger the DNA damage checkpoint at a later point. Based on our data (Figure 6A; Figure S5), we suggest that oocytes with below-threshold DSB levels escape the DNA damage checkpoint and are either eliminated by other mechanisms (see below) or survive to constitute the reduced follicular reserve in *Spo11* mutants.

Although the CHK2-dependent checkpoint is of central importance to genetic quality control in oocytes, our observations that *Chk2* deletion does not fully restore oocyte numbers to WT levels in mutants indicates that it is not absolutely required for eliminating all oocytes with unrepaired DSBs. Rather, the fraction of oocytes rescued is inversely related to the burden of unrepaired meiotic DSBs. For example, although *Chk2* deficiency rescued

nearly one-third of *Trip13^{Gt/Gt}* oocytes (which are partially proficient for DSB repair and harbor 35 ± 4 and 63 ± 4.7 persistent RAD51 foci in diplonema and pachynema, respectively; Figure 4B), it rescued only a small fraction (~5%) of profoundly recombination-deficient *Dmc1^{-/-}* oocytes (harboring an average of ~150 RAD51 foci; Li et al., 2011). We posit that the oocytes that fail to be rescued in these mutants are eliminated either by a separate or a complementary checkpoint pathway (for example, ATR-CHK1; Smith et al., 2010) or succumb to catastrophic levels of DNA damage. It is informative that deletion of *Hormad1*, but not *Hormad2*, rescues *Dmc1^{-/-}* oocytes to a greater extent than *Chk2* deletion. As discussed earlier, the rescued *Dmc1^{-/-} Hormad1^{-/-}* oocytes had a marked reduction in DSBs (Bolcun-Filas et al., 2014; Shin et al., 2013; Wojtasz et al., 2012). Because HORMAD1 is needed to load HORMAD2 onto unsynapsed chromosome axes (not vice versa), the effect of *Hormad1* deletion upon IS recombination constitutes the combined roles of both HORMAD proteins. However, when *Hormad2* alone is deleted, the continued presence of chromosomally bound HORMAD1 may provide a less effective but still substantive BSCR. The lower level of residual DSBs in *Spo11* and *Trip13* mutant oocytes (compared with *Dmc1^{-/-}*) may render them responsive to a weaker BSCR, such as when *Hormad2* is deleted. We postulate that, because of its involvement in stimulating SPO11 activity (Daniel et al., 2011), *Hormad1* deletion is very effective in rescuing a DSB repair mutant like *Dmc1* because not only are fewer DSBs formed, but IS recombination is also more active.

Our results add to increasing evidence that IS recombination is important in mammalian meiosis. As discussed in the text, the HORMADs and SC axial element structure appear to inhibit IS repair of meiotic DSBs preferentially, thus allowing interhomolog (IH) recombination to drive homolog pairing and synapsis. However, as synapsis progresses and the SC is formed, the HORMADs are removed and, presumably, both IS and IH recombination can occur readily, as in yeast (Subramanian et al., 2016). Because not all RAD51 foci disappear by pachynema when synapsis is complete (for example, see Figure 4B), it is possible that a substantial fraction of these DSBs is normally repaired by IS recombination. We speculate that the persistent unrepaired DSBs on synapsed chromosomes of *Trip13* mutants, which retain HORMADs on their SCs, may actually constitute a substantial fraction of SPO11-induced DSBs (an average of ~65/oocyte nucleus of the 200–300 induced; Figure 4) that would normally be repaired by IS recombination. However, we cannot rule out the possibility that the “persistent” DSBs on synapsed *Trip13^{Gt/Gt}* chromosomes actually arise from continued SPO11 cleavage signaled by continued presence of SC-bound HORMADs (Kauppi et al., 2013).

When trying to decipher the quality control mechanisms functioning during meiosis, it is important to recognize that experimental studies such as those performed here employ mutants with pervasive, non-physiological levels of defects. Meioocytes in WT individuals would have less extreme genetic defects. In oocytes bearing a small number (1–3) of unsynapsed chromosomes, the unsynapsed chromosomes undergo transcriptional silencing (MSUC) during pachynema, causing elimination at the diplotene stage (Cloutier et al., 2015; Kouznetsova et al., 2009)

from lack of essential gene products encoded by these chromosomes (Cloutier et al., 2015). However, oocytes with more than 2–3 unsynapsed chromosomes impair MSUC, presumably because of a limiting amount of BRCA1 (Kouznetsova et al., 2009). Nevertheless, *Spo11^{-/-}* meioocytes typically exhibit “pseudo sex bodies,” named as such because they resemble the XY (sex) body involving a small number of asynapsed autosomes (Bellani et al., 2005). Formation of pseudo sex bodies in *Spo11^{-/-}* oocytes is dependent on HORMADs (Daniel et al., 2011; Kogo et al., 2012b), leading to the proposal that these are responsible for oocyte elimination (Kogo et al., 2012a). This may be the case in a subset of oocytes where the pseudo sex body affects either a chromosomal region containing haploinsufficient loci or both alleles of a locus needed for meiotic progression or oocyte survival. Because CHK2 deficiency can rescue *Spo11^{-/-}* oocytes while not abolishing HORMAD localization (Figure S1) or pseudo sex body formation (data not shown) but does not rescue all *Spo11* oocytes, it is likely that neither MSUC nor CHK2 alone is entirely responsible for elimination of all oocytes with pervasive asynapsis. Finally, because MSUC involves many components of the DNA damage response (Fernandez-Capetillo et al., 2003; Ichijima et al., 2011; Turner et al., 2004), it is conceivable that asynapsis leading to MSUC would activate effector elements of the DNA damage checkpoint pathway, including CHK2. However, this does not appear to be the case because silenced supernumerary chromosomes do not eliminate oocytes (Cloutier et al., 2015), MSCI does not kill spermatocytes, and asynaptic oocytes are not eliminated in a pattern typical of DNA repair mutants.

The pachytene checkpoint has commonly been thought to consist of separate DNA damage and synapsis checkpoints in multiple organisms. However, the finding that MSUC can cause the death of oocytes led to the suggestion that there is only 1 formal cell cycle checkpoint in mouse oocytes, the DNA damage checkpoint (Cloutier et al., 2015), - and our data provide mechanistic evidence consistent with this idea. Current information supports a model (Figure 6D) for two major mechanisms by which oocytes with synapsis defects are eliminated: 1) MSUC, for oocytes with a small number of asynapsed chromosomes that do not accumulate unrepaired DSBs above a threshold and in which both homologs bear essential genes for meiotic progression are silenced (Cloutier et al., 2015), and the DNA damage checkpoint, for oocytes with multiple asynapsed chromosomes that accumulate a sufficient number of DSBs to trigger the DNA damage checkpoint (Figure 6D). These disparate mechanisms may have distinct purposes. Because oocytes with only 1 or 2 unsynapsed chromosomes may not efficiently trigger the spindle assembly checkpoint (SAC) (LeMaire-Adkins et al., 1997), the MSUC pathway would safeguard against aneuploidy. Superficially, it would seem that, because oocytes with extensive asynapsis would effectively trigger the SAC, the DNA damage checkpoint mechanism is redundant. However, it is likely advantageous reproductively to eliminate such defective oocytes before they enter dictyate as constituents of the ovarian reserve, otherwise the fraction of unproductive ovulations (those terminated by the SAC) would increase, compromising fecundity.

STAR★METHODS

Detailed methods are provided in the online version of this paper and include the following:

- KEY RESOURCES TABLE
- CONTACT FOR REAGENT AND RESOURCE SHARING
- EXPERIMENTAL MODEL AND SUBJECT DETAILS
- METHOD DETAILS
 - Organ Culture and Irradiation
 - Histology and Immunostaining
 - Immunofluorescence of meiotic chromosome surface spreads
 - Focus Quantification
 - Fertility Test
- QUANTIFICATION AND STATISTICAL ANALYSIS
 - Statistical analysis
- DATA AND SOFTWARE AVAILABILITY

SUPPLEMENTAL INFORMATION

Supplemental Information includes five figures and three tables and can be found with this article online at <http://dx.doi.org/10.1016/j.molcel.2017.07.027>.

AUTHOR CONTRIBUTIONS

V.D.R. and E.B.F. performed the experiments and contributed to the writing of the paper. H Kogo and H. Kurahashi provided the *Hormad2* mutant ESCs and provided feedback on the manuscript. J.C.S. supervised the work and wrote most of the paper.

ACKNOWLEDGMENTS

This work was supported by a grant from the NIH (R01 GM45415 to J.C.S.) and contract CO29155 from the New York State Stem Cell Program (NYSTEM). The authors would like to thank R. Munroe and C. Abratte for generating chimeric mice, Stephen Parry from the Cornell Statistical Consulting Unit for help with statistical analysis, Dr. Attila Toth for the *HORMAD2* antibody, and M.A. Handel for feedback on the manuscript.

Received: April 3, 2017

Revised: June 14, 2017

Accepted: July 28, 2017

Published: August 24, 2017

REFERENCES

- Agoulnik, A.I., Lu, B., Zhu, Q., Truong, C., Ty, M.T., Arango, N., Chada, K.K., and Bishop, C.E. (2002). A novel gene, *Pog*, is necessary for primordial germ cell proliferation in the mouse and underlies the germ cell deficient mutation, *gcd*. *Hum. Mol. Genet.* *11*, 3047–3053.
- Baudat, F., Manova, K., Yuen, J.P., Jasin, M., and Keeney, S. (2000). Chromosome synapsis defects and sexually dimorphic meiotic progression in mice lacking *Spo11*. *Mol. Cell* *6*, 989–998.
- Bellani, M.A., Romanienko, P.J., Cairatti, D.A., and Camerini-Otero, R.D. (2005). SPO11 is required for sex-body formation, and *Spo11* heterozygosity rescues the prophase arrest of *Atm*^{-/-} spermatocytes. *J. Cell Sci.* *118*, 3233–3245.
- Bolcun-Filas, E., Rinaldi, V.D., White, M.E., and Schimenti, J.C. (2014). Reversal of female infertility by Chk2 ablation reveals the oocyte DNA damage checkpoint pathway. *Science* *343*, 533–536.
- Burgoyne, P.S., and Baker, T.G. (1985). Perinatal oocyte loss in XO mice and its implications for the aetiology of gonadal dysgenesis in XO women. *J. Reprod. Fertil.* *75*, 633–645.
- Carballo, J.A., Johnson, A.L., Sedgwick, S.G., and Cha, R.S. (2008). Phosphorylation of the axial element protein Hop1 by Mec1/Tel1 ensures meiotic interhomolog recombination. *Cell* *132*, 758–770.
- Carofiglio, F., Inagaki, A., de Vries, S., Wassenaar, E., Schoenmakers, S., Vermeulen, C., van Cappellen, W.A., Sleddens-Linkels, E., Grootegoed, J.A., Te Riele, H.P., et al. (2013). SPO11-independent DNA repair foci and their role in meiotic silencing. *PLoS Genet.* *9*, e1003538.
- Cloutier, J.M., Mahadevaiah, S.K., Ellnati, E., Nussenzweig, A., Tóth, A., and Turner, J.M. (2015). Histone H2AFX links meiotic chromosome asynapsis to prophase I oocyte loss in mammals. *PLoS Genet.* *11*, e1005462.
- Conrad, D.F., Keebler, J.E., DePristo, M.A., Lindsay, S.J., Zhang, Y., Casals, F., Idaghdour, Y., Hartl, C.L., Torroja, C., Garimella, K.V., et al.; 1000 Genomes Project (2011). Variation in genome-wide mutation rates within and between human families. *Nat. Genet.* *43*, 712–714.
- Daniel, K., Lange, J., Hached, K., Fu, J., Anastassiadis, K., Roig, I., Cooke, H.J., Stewart, A.F., Wassmann, K., Jasin, M., et al. (2011). Meiotic homologue alignment and its quality surveillance are controlled by mouse *HORMAD1*. *Nat. Cell Biol.* *13*, 599–610.
- Di Giacomo, M., Barchi, M., Baudat, F., Edelmann, W., Keeney, S., and Jasin, M. (2005). Distinct DNA-damage-dependent and -independent responses drive the loss of oocytes in recombination-defective mouse mutants. *Proc. Natl. Acad. Sci. USA* *102*, 737–742.
- Fernandez-Capetillo, O., Celeste, A., and Nussenzweig, A. (2003). Focusing on foci: H2AX and the recruitment of DNA-damage response factors. *Cell Cycle* *2*, 426–427.
- Finsterbusch, F., Ravindranathan, R., Dereli, I., Stanzione, M., Tränkner, D., and Tóth, A. (2016). Alignment of homologous chromosomes and effective repair of programmed DNA double-strand breaks during mouse meiosis require the minichromosome maintenance domain containing 2 (MCMDC2) protein. *PLoS Genet.* *12*, e1006393.
- Goldfarb, T., and Lichten, M. (2010). Frequent and efficient use of the sister chromatid for DNA double-strand break repair during budding yeast meiosis. *PLoS Biol.* *8*, e1000520.
- Gray, S., and Cohen, P.E. (2016). Control of meiotic crossovers: from double-strand break formation to designation. *Annu. Rev. Genet.* *50*, 175–210.
- Hirao, A., Cheung, A., Duncan, G., Girard, P.M., Elia, A.J., Wakeham, A., Okada, H., Sarkissian, T., Wong, J.A., Sakai, T., et al. (2002). Chk2 is a tumor suppressor that regulates apoptosis in both an ataxia telangiectasia mutated (ATM)-dependent and an ATM-independent manner. *Mol. Cell. Biol.* *22*, 6521–6532.
- Homolka, D., Jansa, P., and Forejt, J. (2012). Genetically enhanced asynapsis of autosomal chromatin promotes transcriptional dysregulation and meiotic failure. *Chromosoma* *121*, 91–104.
- Ichijima, Y., Ichijima, M., Lou, Z., Nussenzweig, A., Camerini-Otero, R.D., Chen, J., Andreassen, P.R., and Namekawa, S.H. (2011). MDC1 directs chromosome-wide silencing of the sex chromosomes in male germ cells. *Genes Dev.* *25*, 959–971.
- Joshi, N., Brown, M.S., Bishop, D.K., and Börner, G.V. (2015). Gradual implementation of the meiotic recombination program via checkpoint pathways controlled by global DSB levels. *Mol. Cell* *57*, 797–811.
- Kauppi, L., Barchi, M., Lange, J., Baudat, F., Jasin, M., and Keeney, S. (2013). Numerical constraints and feedback control of double-strand breaks in mouse meiosis. *Genes Dev.* *27*, 873–886.
- Kogo, H., Tsutsumi, M., Inagaki, H., Ohye, T., Kiyonari, H., and Kurahashi, H. (2012a). *HORMAD2* is essential for synapsis surveillance during meiotic prophase via the recruitment of ATR activity. *Genes Cells* *17*, 897–912.
- Kogo, H., Tsutsumi, M., Ohye, T., Inagaki, H., Abe, T., and Kurahashi, H. (2012b). *HORMAD1*-dependent checkpoint/surveillance mechanism eliminates asynaptic oocytes. *Genes Cells* *17*, 439–454.

- Kouznetsova, A., Wang, H., Bellani, M., Camerini-Otero, R.D., Jessberger, R., and Höög, C. (2009). BRCA1-mediated chromatin silencing is limited to oocytes with a small number of asynapsed chromosomes. *J. Cell Sci.* *122*, 2446–2452.
- Lam, I., and Keeney, S. (2014). Mechanism and regulation of meiotic recombination initiation. *Cold Spring Harb. Perspect. Biol.* *7*, a016634.
- Latypov, V., Rothenberg, M., Lorenz, A., Octubre, G., Csutak, O., Lehmann, E., Loidl, J., and Kohli, J. (2010). Roles of Hop1 and Mek1 in meiotic chromosome pairing and recombination partner choice in *Schizosaccharomyces pombe*. *Mol. Cell. Biol.* *30*, 1570–1581.
- LeMaire-Adkins, R., Radke, K., and Hunt, P.A. (1997). Lack of checkpoint control at the metaphase/anaphase transition: a mechanism of meiotic nondisjunction in mammalian females. *J. Cell Biol.* *139*, 1611–1619.
- Li, X.C., and Schimenti, J.C. (2007). Mouse pachytene checkpoint 2 (*trip13*) is required for completing meiotic recombination but not synapsis. *PLoS Genet.* *3*, e130.
- Li, X.C., Bolcun-Filas, E., and Schimenti, J.C. (2011). Genetic evidence that synaptonemal complex axial elements govern recombination pathway choice in mice. *Genetics* *189*, 71–82.
- Luo, Y., Hartford, S.A., Zeng, R., Southard, T.L., Shima, N., and Schimenti, J.C. (2014). Hypersensitivity of primordial germ cells to compromised replication-associated DNA repair involves ATM-p53-p21 signaling. *PLoS Genet.* *10*, e1004471.
- MacQueen, A.J., and Hochwagen, A. (2011). Checkpoint mechanisms: the puppet masters of meiotic prophase. *Trends Cell Biol.* *21*, 393–400.
- Malki, S., van der Heijden, G.W., O'Donnell, K.A., Martin, S.L., and Bortvin, A. (2014). A role for retrotransposon LINE-1 in fetal oocyte attrition in mice. *Dev. Cell* *29*, 521–533.
- Maltaris, T., Seufert, R., Fischl, F., Schaffrath, M., Pollow, K., Koelbl, H., and Dittrich, R. (2007). The effect of cancer treatment on female fertility and strategies for preserving fertility. *Eur. J. Obstet. Gynecol. Reprod. Biol.* *130*, 148–155.
- Mao-Draayer, Y., Galbraith, A.M., Pittman, D.L., Cool, M., and Malone, R.E. (1996). Analysis of meiotic recombination pathways in the yeast *Saccharomyces cerevisiae*. *Genetics* *144*, 71–86.
- Meirow, D., and Nugent, D. (2001). The effects of radiotherapy and chemotherapy on female reproduction. *Hum. Reprod. Update* *7*, 535–543.
- Murphey, P., McLean, D.J., McMahan, C.A., Walter, C.A., and McCarrey, J.R. (2013). Enhanced genetic integrity in mouse germ cells. *Biol. Reprod.* *88*, 6.
- Nadler, J.J., and Braun, R.E. (2000). Fanconi anemia complementation group C is required for proliferation of murine primordial germ cells. *Genesis* *27*, 117–123.
- Niu, H., Wan, L., Baumgartner, B., Schaefer, D., Loidl, J., and Hollingsworth, N.M. (2005). Partner choice during meiosis is regulated by Hop1-promoted dimerization of Mek1. *Mol. Biol. Cell* *16*, 5804–5818.
- Pacheco, S., Marcet-Ortega, M., Lange, J., Jasin, M., Keeney, S., and Roig, I. (2015). The ATM signaling cascade promotes recombination-dependent pachytene arrest in mouse spermatocytes. *PLoS Genet.* *11*, e1005017.
- Perez, G.I., Knudson, C.M., Leykin, L., Korsmeyer, S.J., and Tilly, J.L. (1997). Apoptosis-associated signaling pathways are required for chemotherapy-mediated female germ cell destruction. *Nat. Med.* *3*, 1228–1232.
- Peters, A.H., Plug, A.W., van Vugt, M.J., and de Boer, P. (1997). A drying-down technique for the spreading of mammalian meiocytes from the male and female germline. *Chromosome Res.* *5*, 66–68.
- Pittman, D.L., Cobb, J., Schimenti, K.J., Wilson, L.A., Cooper, D.M., Brignull, E., Handel, M.A., and Schimenti, J.C. (1998). Meiotic prophase arrest with failure of chromosome synapsis in mice deficient for Dmc1, a germline-specific RecA homolog. *Mol. Cell* *1*, 697–705.
- Reinholdt, L.G., and Schimenti, J.C. (2005). *Mei1* is epistatic to *Dmc1* during mouse meiosis. *Chromosoma* *114*, 127–134.
- Reinholdt, L., Ashley, T., Schimenti, J., and Shima, N. (2004). Forward genetic screens for meiotic and mitotic recombination-defective mutants in mice. *Methods Mol. Biol.* *262*, 87–107.
- Rinaldi, V.D., Hsieh, K., Munroe, R., Bolcun-Filas, E.M., and Schimenti, J.C. (2017). Pharmacological inhibition of the DNA damage checkpoint prevents radiation-induced oocyte death. *Genetics*. Published online June 2, 2017. <http://dx.doi.org/10.1534/genetics.117.203455>.
- Roeder, G.S., and Bailis, J.M. (2000). The pachytene checkpoint. *Trends Genet.* *16*, 395–403.
- Schindelin, J., Arganda-Carreras, I., Frise, E., Kaynig, V., Longair, M., Pietzsch, T., Preibisch, S., Rueden, C., Saalfeld, S., Schmid, B., et al. (2012). Fiji: an open-source platform for biological-image analysis. *Nat. Methods* *9*, 676–682.
- Schwacha, A., and Kleckner, N. (1997). Interhomolog bias during meiotic recombination: meiotic functions promote a highly differentiated interhomolog-only pathway. *Cell* *90*, 1123–1135.
- Shin, Y.H., Choi, Y., Erdin, S.U., Yatsenko, S.A., Kloc, M., Yang, F., Wang, P.J., Meistrich, M.L., and Rajkovic, A. (2010). *Hormad1* mutation disrupts synaptonemal complex formation, recombination, and chromosome segregation in mammalian meiosis. *PLoS Genet.* *6*, e1001190.
- Shin, Y.H., McGuire, M.M., and Rajkovic, A. (2013). Mouse HORMAD1 is a meiosis I checkpoint protein that modulates DNA double-strand break repair during female meiosis. *Biol. Reprod.* *89*, 29.
- Smith, J., Tho, L.M., Xu, N., and Gillespie, D.A. (2010). The ATM-Chk2 and ATR-Chk1 pathways in DNA damage signaling and cancer. *Adv. Cancer Res.* *108*, 73–112.
- Stambook, P.J., and Tichy, E.D. (2010). Preservation of genomic integrity in mouse embryonic stem cells. *Adv. Exp. Med. Biol.* *695*, 59–75.
- Stanzione, M., Baumann, M., Papanikos, F., Dereli, I., Lange, J., Ramlal, A., Tränkner, D., Shibuya, H., de Massy, B., Watanabe, Y., et al. (2016). Meiotic DNA break formation requires the unsynapsed chromosome axis-binding protein IHO1 (CCDC36) in mice. *Nat. Cell Biol.* *18*, 1208–1220.
- Subramanian, V.V., and Hochwagen, A. (2014). The meiotic checkpoint network: step-by-step through meiotic prophase. *Cold Spring Harb. Perspect. Biol.* *6*, a016675.
- Subramanian, V.V., MacQueen, A.J., Vader, G., Shinohara, M., Sanchez, A., Borde, V., Shinohara, A., and Hochwagen, A. (2016). Chromosome synapsis alleviates Mek1-dependent suppression of meiotic DNA repair. *PLoS Biol.* *14*, e1002369.
- Suh, E.K., Yang, A., Kettenbach, A., Bamberger, C., Michaelis, A.H., Zhu, Z., Elvin, J.A., Bronson, R.T., Crum, C.P., and McKeon, F. (2006). p63 protects the female germ line during meiotic arrest. *Nature* *444*, 624–628.
- Turner, J.M., Aprelikova, O., Xu, X., Wang, R., Kim, S., Chandramouli, G.V., Barrett, J.C., Burgoyne, P.S., and Deng, C.X. (2004). BRCA1, histone H2AX phosphorylation, and male meiotic sex chromosome inactivation. *Curr. Biol.* *14*, 2135–2142.
- van der Heijden, G.W., and Bortvin, A. (2009). Transient relaxation of transposon silencing at the onset of mammalian meiosis. *Epigenetics* *4*, 76–79.
- Watanabe, N., Mii, S., Asai, N., Asai, M., Niimi, K., Ushida, K., Kato, T., Enomoto, A., Ishii, H., Takahashi, M., and Murakumo, Y. (2013). The REV7 subunit of DNA polymerase ζ is essential for primordial germ cell maintenance in the mouse. *J. Biol. Chem.* *288*, 10459–10471.
- Wojtasz, L., Daniel, K., Roig, I., Bolcun-Filas, E., Xu, H., Boonsanay, V., Eckmann, C.R., Cooke, H.J., Jasin, M., Keeney, S., et al. (2009). Mouse HORMAD1 and HORMAD2, two conserved meiotic chromosomal proteins, are depleted from synapsed chromosome axes with the help of TRIP13 AAA-ATPase. *PLoS Genet.* *5*, e1000702.
- Wojtasz, L., Cloutier, J.M., Baumann, M., Daniel, K., Varga, J., Fu, J., Anastassiadis, K., Stewart, A.F., Reményi, A., Turner, J.M., and Tóth, A. (2012). Meiotic DNA double-strand breaks and chromosome asynapsis in mice are monitored by distinct HORMAD2-independent and -dependent mechanisms. *Genes Dev.* *26*, 958–973.

STAR★METHODS

KEY RESOURCES TABLE

REAGENT or RESOURCE	SOURCE	IDENTIFIER
Antibodies		
mouse anti-p63	Novus Biologicals	Novus Cat# NB 100-691; RRID: AB_525968
rabbit anti-MVH	Abcam	Abcam Cat# ab13840; RRID: AB_443012
rabbit anti-RAD51 Chip-Grade	Abcam	Abcam Cat# ab176458; RRID: AB_2665405
mouse anti-SYCP3	Abcam	Abcam Cat# ab97672; RRID: AB_10678841
guinea pig anti-HORMAD2	Wojtasz et al., 2012	gift from Dr. Attila Toth
Deposited Data		
Raw images	This paper; Mendeley Data	http://dx.doi.org/10.17632/3n2yfpk4vh.1
Experimental Models: Organisms/Strains		
Mouse: <i>Trip13^{Gt/Gt}; Trip13^{Gt(RRB047)Byg}</i>	Li and Schimenti, 2007	RRID:MGI:372059
Mouse: <i>Dmc1^{-/-}; Dmc1^{tm1Jcs}</i>	Pittman et al., 1998	RRID:MGI:3768914
Mouse: <i>Chk2^{-/-}; Chk2^{tm1Mak}</i>	Tak Mak; Hirao et al., 2002	RRID:MGI:2662578
Mouse: <i>Spo11^{-/-}; Spo11^{tm1Mjn}</i>	Maria Jasin; Baudat et al., 2000	RRID:MGI:4358251
Mouse: <i>Hormad2^{-/-}; Hormad2</i>	Kogo et al., 2012a	RRID:MGI:5466572
Software and Algorithms		
JMP Pro12 software v.12.0.1	SAS Inc., Cary, NC-USA	RRID:SCR_014242
Fiji-ImageJ	Schindelin et al., 2012	RRID:SCR_002285

CONTACT FOR REAGENT AND RESOURCE SHARING

Further information and requests for reagents may be directed to and will be fulfilled by the Lead Contact, John Schimenti (jcs92@cornell.edu).

EXPERIMENTAL MODEL AND SUBJECT DETAILS

Experiments were performed on female mice, and of course male mice were used for matings to produce desired genotypes. Samples for histological analysis were from eight week old animals. The alleles used have been previously described and were the following: *Trip13^{Gt(RRB047)Byg}* (referred to as *Trip13^{Gt}* in the manuscript) (Li and Schimenti, 2007); *Dmc1^{tm1Jcs}* (Pittman et al., 1998); *Chk2^{tm1Mak}* (Hirao et al., 2002); *Spo11^{tm1Mjn}* (Baudat et al., 2000); and *Hormad2* (Kogo et al., 2012a). All mice were in a mixed genetic background of strains C57BL/6J and C3H/HeJ. The Cornell's Animal Care and Use Committee approved all animal usage, under protocol 2004-0038 to JCS.

The embryonic age of pre-term animals was counted using the morning in which copulation plug was detected as being the 0.5 days post coitus (dpc).

METHOD DETAILS

Organ Culture and Irradiation

Embryonic and pp explanted ovaries were cultured under conditions as we previously detailed (Rinaldi et al., 2017). Ovaries were irradiated in a ¹³⁷cesium irradiator with a rotating turntable. Immediately after irradiation, the media was replaced, and ovaries were cultured for indicated periods of time prior to tissue processing.

Histology and Immunostaining

Ovaries were dissected and incubated in Bouin's fixative overnight at room temperature. Afterward, tissues were washed in 70% ethanol prior to being embedded in paraffin for serial sectioning at 6 μm thickness. Ovaries were stained with Harris Hematoxylin and Eosin (H&E) and follicles counted in every fifth section except for the three-week counts reported in Figure 1B, in which every 12th section was counted. There was no correction factor applied to the values reported. Only one ovary per animal was used.

Cultured ovaries, used for histological sections followed by immunostaining, were fixed in 4% paraformaldehyde/PBS over night at 4°C. After 70% ethanol washes, ovaries were embedded in paraffin and serially sectioned at 5 μm. These ovaries were immunostained using standard methods. Briefly, slides were deparaffinized and re-hydrated prior to antigen retrieval using sodium citrate buffer. Slides were blocked with 5% goat serum (PBS/Tween 20) and incubated at 4°C overnight with primary antibodies: mouse anti-p63 (1:500, 4A4, Novus Biologicals); and rabbit anti-MVH (1:1000, Abcam). Afterward, sections were incubated with Alexa Fluor® secondary antibodies for one hour and Hoechst dye for 5 min. Slides were mounted with ProLong Anti-fade (Thermo-Fisher) and imaged.

Histological images were obtained from slides digitized using a Leica Scanscope CS2.

Immunofluorescence of meiotic chromosome surface spreads

Meiotic surface spreads of prophase I female meiocytes were prepared using an adaptation (Reinholdt et al., 2004) of a drying-down technique (Peters et al., 1997) that was described in great detail in the former reference. Meiotic stages (leptonema-diakinesis) were determined based on SYCP3 staining patterns (Gray and Cohen, 2016). Slides were stored at –80°C until immunostained. For staining, slides were brought to room temperature (RT) and washed once with PBS+0.1% Tween-20 (PBS-T). Slides were blocked for 40 min at RT with PBS-T containing 5% normal goat serum (5%GS-PBS-T). Primary antibodies were diluted into 5%GS-PBS-T and incubated overnight at RT in a humidified chamber. Antibodies and dilutions used included: rabbit anti-RAD51 (1:250 Abcam 176458), mouse anti-SYCP3 (1:600 Abcam) and guinea pig anti-HORMAD2 antibody (1:1000, kind gift from Attila Toth). Secondary antibodies used were diluted 1:1000 in 5%GS-PBS-T and included goat anti-rabbit Alexa 488/594, goat anti-mouse Alexa 488/594 and goat anti-guinea pig Alexa 488/594. Images were taken using an Olympus microscope with 40X lens or 100X immersion oil lens and CCD camera.

Focus Quantification

Foci were quantified both manually, through the visualization and annotation of individual foci, and also semi-automatically using Fiji-ImageJ (Schindelin et al., 2012). Semi-automated counts were performed using binary images obtained from the RAD51-labeled channel, with the threshold set above background level. The count was obtained after performing “Watershed,” by the “Analyze Particles” functionality with size set for 1.5 to infinity. Cell counts that displayed discrepancy of more than 20% between manual and semi-automated counts were discarded.

Fertility Test

To test if HORMAD2 deficiency was able to rescue the *Trip13^{Gt/Gt}* sterility phenotype, three double mutant females were mated to WT C3H/HeJ males proven to be fertile through previous matings. Each female provided more than 4 consecutive litters up to the time of preparation of this manuscript. All three females originated from different litters. *Trip13^{Gt/Gt}* littermates were housed with fertile males and used as negative controls.

QUANTIFICATION AND STATISTICAL ANALYSIS

Statistical analysis

Comparisons between compound mutants and controls were done using littermates or related animals. Unless otherwise noted, all experiments used at least three mice per experimental group. All statistical analyses were done using JMP Pro12 software (SAS Inc., Cary, NC-USA, version 12.0.1). Comparisons of fertility and follicle counts between genotypic groups were tested using both the Tukey honest significance different (HSD) and the non-parametric, one-way ANOVA test (Kruskal -Wallis). Both tests provided concordant results. RAD51 focus counts were analyzed using a mixed model with animal ID as random effect and genotype as fixed effect. Least square means (LSMeans) differences were tested using Tukey HSD. The residuals from the mixed model were normally distributed.

DATA AND SOFTWARE AVAILABILITY

Raw data of RAD51 foci counts are in supplementary tables (Table S1, Table S2, and Table S3). The raw image files can be downloaded at Mendeley data: <http://dx.doi.org/10.17632/3n2yfpk4vh.1>.

Genomic Characterization of Chromosomal Insertions: Insights into the Mechanisms Underlying Chromothripsis

Takema Kato^a Yuya Ouchi^{a,b} Hidehito Inagaki^{a,b} Yoshio Makita^g
Seiji Mizuno^c Mitsuharu Kajita^d Toshiro Ikeda^e Kazuhiro Takeuchi^f
Hiroki Kurahashi^{a,b}

^aDivision of Molecular Genetics, Institute for Comprehensive Medical Science (ICMS), and ^bGenome and Transcriptome Analysis Center, Fujita Health University, Toyoake, ^cDepartment of Pediatrics, Central Hospital, Aichi Human Service Center, Kasugai, ^dDepartment of Pediatrics, Toyota Kosei Hospital, Toyota, ^eDepartment of Obstetrics and Gynecology, Faculty of Medicine, Kagoshima University, and ^fTakeuchi Ladies Clinic/Infertility Center, Kagoshima, and ^gEducation Center, Asahikawa Medical University, Hokkaido, Japan

Keywords

Chromothripsis · Insertion · Trisomy rescue

Abstract

Chromosomal insertions are rare structural rearrangements, and the molecular mechanisms underlying their origin are unknown. In this study, we used whole genome sequencing to analyze breakpoints and junction sequences in 4 patients with chromosomal insertions. Our analysis revealed that none of the 4 cases involved a simple insertion mediated by a 3-chromosomal breakage and rejoining events. The inserted fragments consisted of multiple pieces derived from a localized genomic region, which were shuffled and rejoined in a disorderly fashion with variable copy number alterations. The junctions were blunt ended or with short microhomologies or short microinsertions, suggesting the involvement of nonhomologous end-joining. In one case, analysis of the parental origin of the chromosomes using nucleotide varia-

tions within the insertion revealed that maternal chromosomal segments were inserted into the paternal chromosome. This patient also carried both maternal alleles, suggesting the presence of zygotic trisomy. These data indicate that chromosomal shattering may occur in association with trisomy rescue in the early postzygotic stage.

© 2017 S. Karger AG, Basel

Chromosomal structural rearrangements (CSRs), also known as gross chromosomal rearrangements, are generated by 2 double-strand DNA breaks (DSBs) followed by aberrant DNA repair [Shaffer and Lupski, 2000; Kurahashi et al., 2009]. The DSBs are generally processed by an error-free pathway, called homologous recombination, and repaired properly. However, recurrent CSRs are

T.K. and Y.O. contributed equally to this work.

caused by genomic instability induced by 2 specific sequences that exist as DSB hotspots [Kato et al., 2012]. Alternatively, DSBs at the segmental duplications are often repaired aberrantly by nonallelic homologous recombination (NAHR), leading to recurrent CSRs [Ou et al., 2011; Hermetz et al., 2012]. In contrast, DSBs that arise randomly are often repaired by an error-prone pathway, nonhomologous end-joining (NHEJ), which leads to nonrecurrent CSRs [Gu et al., 2008]

Recent advances in genomic analysis have provided detailed information on the breakpoints and junction sequences of CSRs and have helped us to understand their origin and mechanism. We now know that replication-based pathways such as fork-stalling and template-switching as well as microhomology-mediated break-induced replication are the major pathways leading to CSRs [Zhang et al., 2009]. The products of these pathways occasionally manifest complex junction structures that include duplication or triplication of the breakpoint proximity. In addition, recent high-resolution microarray and next-generation sequencing studies have found that large numbers of complex chromosomal rearrangements occur in one or a few chromosomes [Holland and Cleveland, 2012]. This catastrophic rearrangement is called chromothripsis. Unfortunately, the precise mechanism that induces the chromosome shattering is still unknown [Kloosterman et al., 2011; Stephens et al., 2011].

Chromosomal insertion, also called insertional translocation, is one of several gross interchromosomal structural rearrangements [Van Hemel and Eussen, 2000]. Insertions involve a translocation of a segment from one chromosome and its insertion as an interstitial region into another nonhomologous chromosome [Weckselblatt and Rudd, 2015]. Balanced carriers are healthy but occasionally have reproductive problems such as infertility, recurrent pregnancy loss, or offspring with multiple congenital anomalies due to an unbalanced insertion. Unbalanced insertions also arise *de novo*. They are relatively rare CSRs, with an estimated incidence of about 1:80,000 according to conventional cytogenetic techniques [Van Hemel and Eussen, 2000]. However, 3 recent cohort studies using high-resolution aCGH in conjunction with FISH found a higher incidence than previously estimated [Kang et al., 2010; Neill et al., 2011; Nowakowska et al., 2012].

Little is known about the mechanism of the insertion. It requires at least 3 breaks followed by aberrant repair, but information on the breakpoints and junctions is scarce. One previous study using microarray analysis showed that a small subset of insertions may involve the

NAHR pathway, but the etiology of most nonrecurrent insertions is unclear [Neill et al., 2011]. A recent large-scale study using next-generation sequencing of 6 cases with an insertion identified the underlying mechanism leading to the insertion to be a chromothripsis-like replication-related pathway [Gu et al., 2016]. In the present study, we characterized 4 insertion cases via a combination of cytogenetic and genomic techniques such as whole genome sequencing and mate-pair sequencing for the detection of rearrangement breakpoints. We subsequently genotyped the polymorphisms on the relevant chromosomes and determined their parental origin, thereby shedding light on the mechanisms underlying the origin of the insertion.

Case Reports and Results

Case 1

This patient was referred to our facility because of developmental delay. Initial G-banding revealed a 46,XX,add(14)(q32.1) karyotype. We performed cytogenetic microarray analysis and detected a duplication in chromosome 4q and a deletion in 14q. Detailed copy number analysis revealed complex chromosomal rearrangements that included duplications encompassing a 13.1-Mb region at 4q32.1q32.3 and a 0.3-Mb region in 4q35.2, some parts of which appeared to be triplicated, while a 2.7-Mb deletion was found in 14q32.33 (Fig. 1a). Subsequently, using FISH, we found that these copy number variations were due to a chromosomal insertion of 4q32.1q32.3 into 14q32.33 (Fig. 1b). This insertion was not identified in either of the parents and was found to have occurred *de novo* in the index case.

Next, we performed whole genome sequencing to determine the breakpoints and junctions. LUMPY, a probabilistic structural variant caller, revealed the presence of 6 discordant reads, possibly including the junctions of the rearrangements. To characterize breakpoints at a nucleotide resolution, breakpoint-spanning PCR followed by Sanger sequencing was performed. According to the sequence information of the 6 junctions, the original fragments were shuffled and rejoined in a disorderly manner (Fig. 1c). Some regions were lost, while some appeared twice among the inserted fragments, resulting in triplication. Of the junction sequences identified, 1 involved simple end-joining (junction 1), 2 had microhomology of a few nucleotides (junctions 3 and 6), and 1 had a 4-nucleotide microinsertion (junction 1). The remaining 2 junctions carried insertions consisting of small pieces of a segment derived from the vicinity of the breakpoint region in chromosome 4 (Fig. 1d; junctions 4 and 5). The likely structure is shown in Figure 1d, e.

To determine the parental origin of the chromosomal insertion, we genotyped common SNPs in the related regions of chromosomes 4 and 14 using DNA from the proband and his parents. When we compared the SNP data of the 14q32.33 region deleted in the proband, the proband carried only the maternal allele, supposedly reflecting the normal homolog of chromosome 14. This suggests that the original chromosome 14 of *der*(14) with the insertion was of paternal origin (Fig. 1f). Following, we genotyped

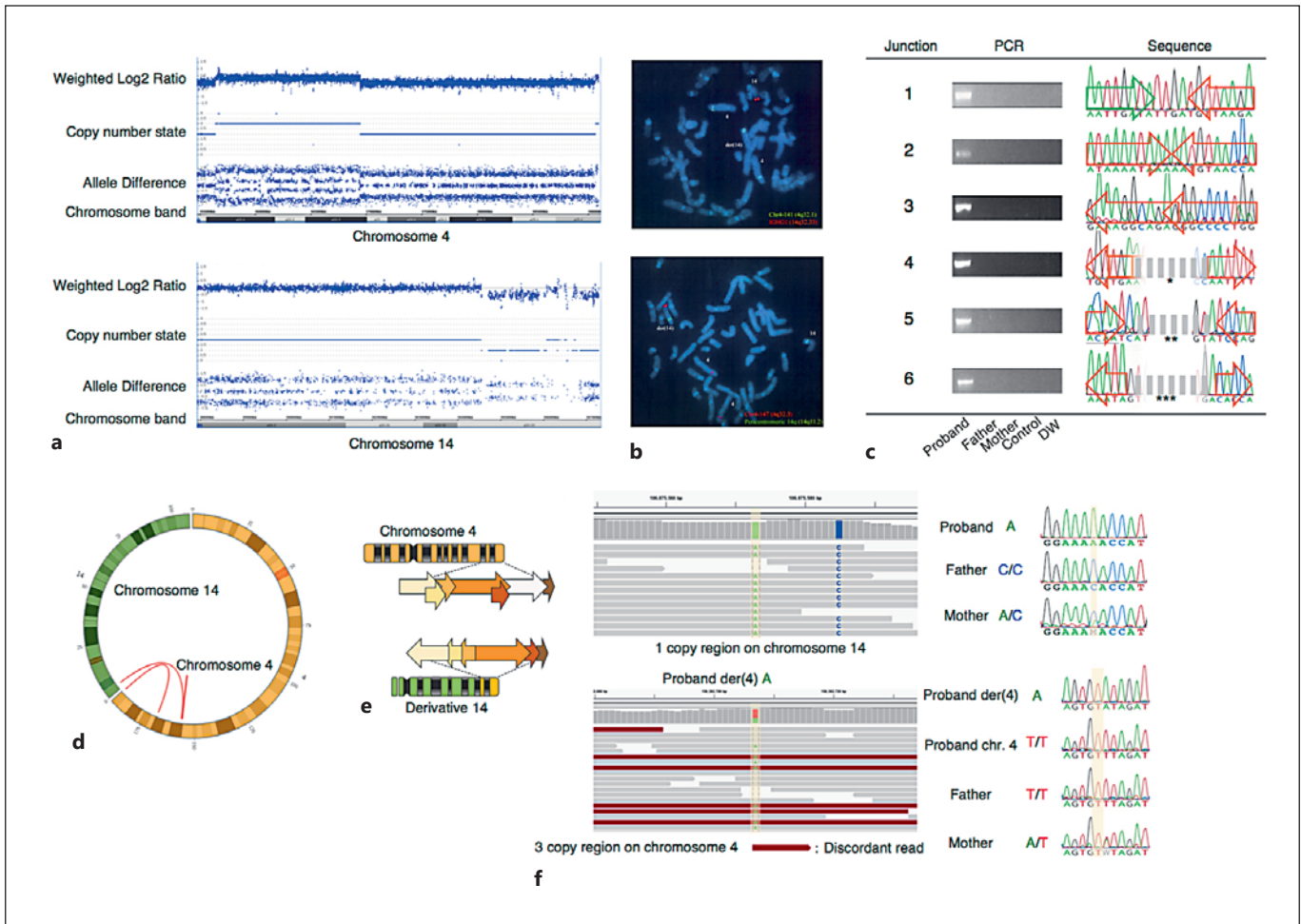


Fig. 1. Analysis of the chromosomal insertion in case 1. **a** Chromosome Analysis Suite (ChAS) graphic results for chromosomes 4 and 14 showing copy number gain and loss, respectively. The results are designated as $\text{arr}[\text{hg}19] \ 4\text{q}32.1\text{q}32.3(156,376,846-169,441,822) \times 3 \sim 4, 4\text{q}35.2(190,659,209-190,957,473) \times 3, 14\text{q}32.33(104,549,511-107,285,437) \times 1$. Although ChAS showed a normal copy number region within the deletion in chromosome 14, FISH analysis did not identify it as a diploid region (data not shown). **b** FISH confirming the deletion in 14q32.33 (red) shown at the top and the insertion of 4q32.3 (red) into the long arm of chromosome 14 (green) shown at the bottom. **c** Breakpoint-specific PCR and its sequence. Green and orange arrows indicate chromosomes 14 and 4, respectively. The distance between the arrows correlates with microhomology or microinsertion. Asterisks indicate the insertion of a few dozen nucleotides. * The gray-dashed line encompasses a 35-nt sequence at position

156,671,582–156,671,616 in chromosome 4 and a 37-nt sequence of unknown origin. ** The gray-dashed line encompasses a 24-nt sequence of unknown origin, a 21-nt sequence at position 156,711,369–156,711,389 in chromosome 4 with inverted orientation, and a 34-nt sequence of unknown origin. *** The gray-dashed line encompasses a 25-nt sequence of unknown origin. **d** The detected chromosomal rearrangements are visualized by a Circos plot using ClicO FS. **e** Multiple segments in chromosome 4 were shuffled and inserted into chromosome 14. Some of the segments were missing or duplicated during the rearrangements. **f** An example of a parent-of-origin analysis. The top shows the vicinity of the breakpoint, and the bottom shows a deleted region in chromosome 14. Discordant reads (dark red) and SNPs (light green and blue) are visualized by different colors. SNP genotyping was conducted by Sanger sequencing. SNPs are superimposed on the yellow background.

the SNPs within the insertional region in chromosome 4. The inserted segments were found to originate from the maternal chromosome. This indicates a postzygotic origin of the insertion. Furthermore, the proband was found to have 2 normal chromosomes 4, one paternal and the other maternal, and this normal maternal chromosome 4 was revealed to be a different allele from

the inserted segments of maternal origin. Thus, it is suggested that 2 normal chromosomes 4 were transmitted from the mother and one from the father and that one of the maternal chromosomes 4 was then shattered and integrated into the paternal chromosome 14 in the early postzygotic stage in the trisomic zygote (Fig. 5a).

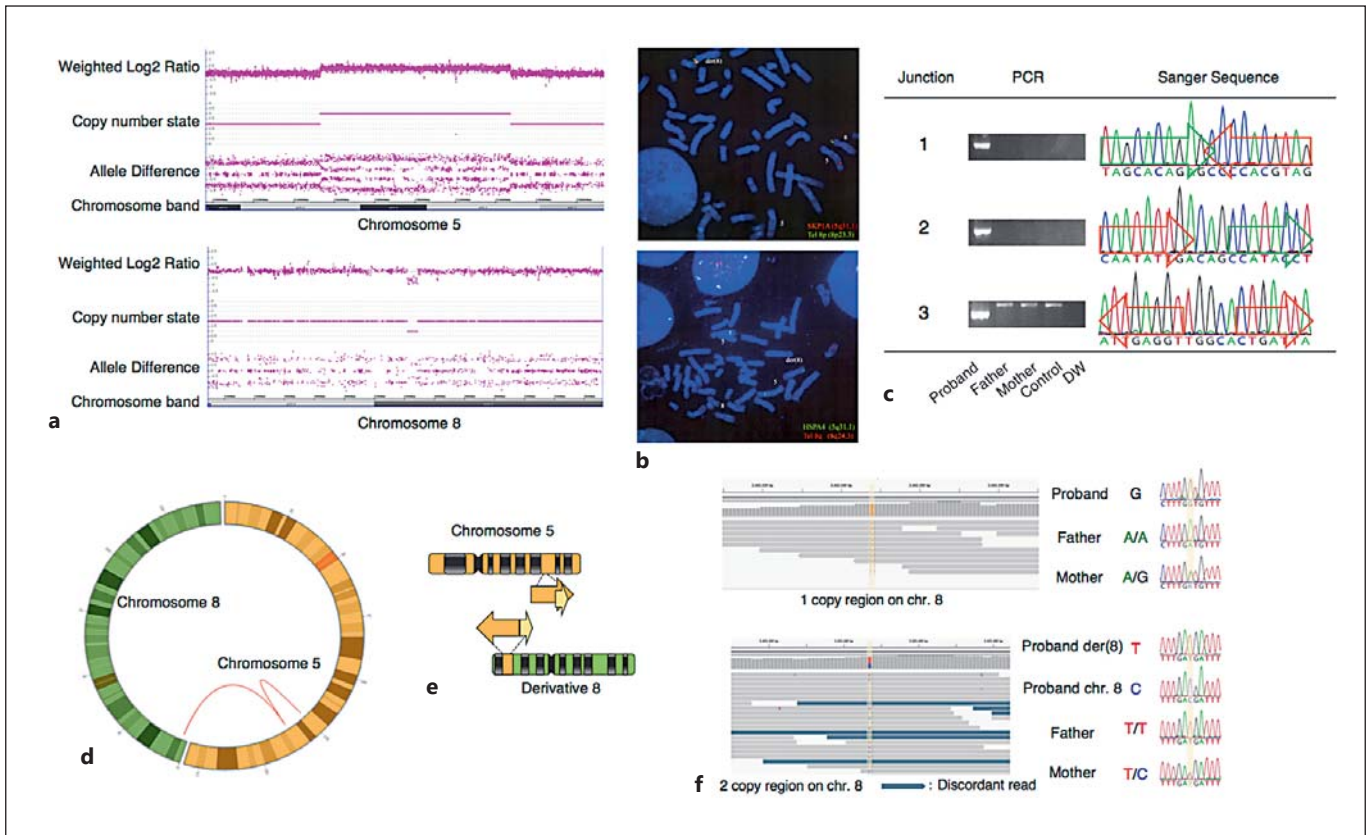


Fig. 2. Analysis of the chromosomal insertion in case 2. **a** Copy number abnormalities in chromosomes 5 and 8 are graphically displayed using ChAS. Positional information on the copy number change is designated as $\text{arr}[\text{hg}19] \ 5\text{q}23.2\text{q}31.1(125,311,267\text{--}134,731,795)\times 3,8\text{p}23.2(2,421,059\text{--}2,488,315)\times 1$. **b** FISH analysis confirming the insertion of 5q31.1 (red) into the vicinity of 8p23.3. **c** Breakpoint-specific PCR and its sequence. The analysis was performed as described in Figure 1. Orange and green arrows indicate chromosomes 5 and 8, respectively. The distance between the arrows corresponds to microhomology or microinsertion. **d** The de-

tected chromosomal rearrangements are visualized by a Circos plot using ClicO FS. **e** Two segments in chromosome 5 were shuffled and translocated into chromosome 8. One segment completely overlaps another segment. **f** SNP-based parental origin determination. The top shows the 1-copy region in chromosome 8, whereas the bottom shows the 2-copy region in chromosome 8. The details are the same as those provided in Figure 1. Discordant reads are shown in dark blue. SNPs used for analysis are presented on a yellow background.

Case 2

This case was referred to our facility for the examination of postnatal short stature. Initial G-banding revealed a 46,XX,add(8)(p22) karyotype. Cytogenetic microarray data showed that the patient had both a duplication at 5q23.2q31.1 and a deletion in chromosome 8p23.2 (Fig. 2a). FISH analysis showed that the interstitial chromosome 8p23.2 deletion was due to an insertion at chromosome 5q23.2q31.1 (Fig. 2b). This insertion was not identified in either of the parents and was thus determined to have occurred de novo in the index case.

To identify the deletion and insertion breakpoints, we applied LUMPY to the whole genome sequencing data. Three breakpoints were found and validated by PCR and Sanger sequencing. One breakpoint was between the 5q regions, while the others were re-joined between chromosomes 5 and 8 but with different orientations. The inserted 5q chromosome comprised 2 segments in chromosome 5, one large segment spanning from 125,317,703 to

134,732,368 and the other spanning from 134,730,551 to 134,731,048. This suggests that smaller 497-bp fragments were triplicated and inserted adjacent to the larger insertion in an inverted orientation. Similar to case 1, one junction had a 2-nucleotide microhomology (junction 1), whereas 2 junctions had microinsertions of an unknown origin (Fig. 2c; junctions 2 and 3). The likely structure is shown in Figure 2d, e.

SNP genotyping of the deleted region in chromosome 8 showed that the paternal chromosome 8p23.2 was deleted and that the normal chromosome 8 was of maternal origin. In addition, the inserted 5q segments originated from the paternal chromosome, suggesting that the paternal fragment from chromosome 5 was integrated into the paternal chromosome 8 (Fig. 2f). However, the inserted 5q segments were different from the normal paternal homologue chromosome, indicating the presence of 2 paternal 5q chromosomes. This suggests that one of the paternal chromosomes 5 was shattered and integrated into the paternal chromo-

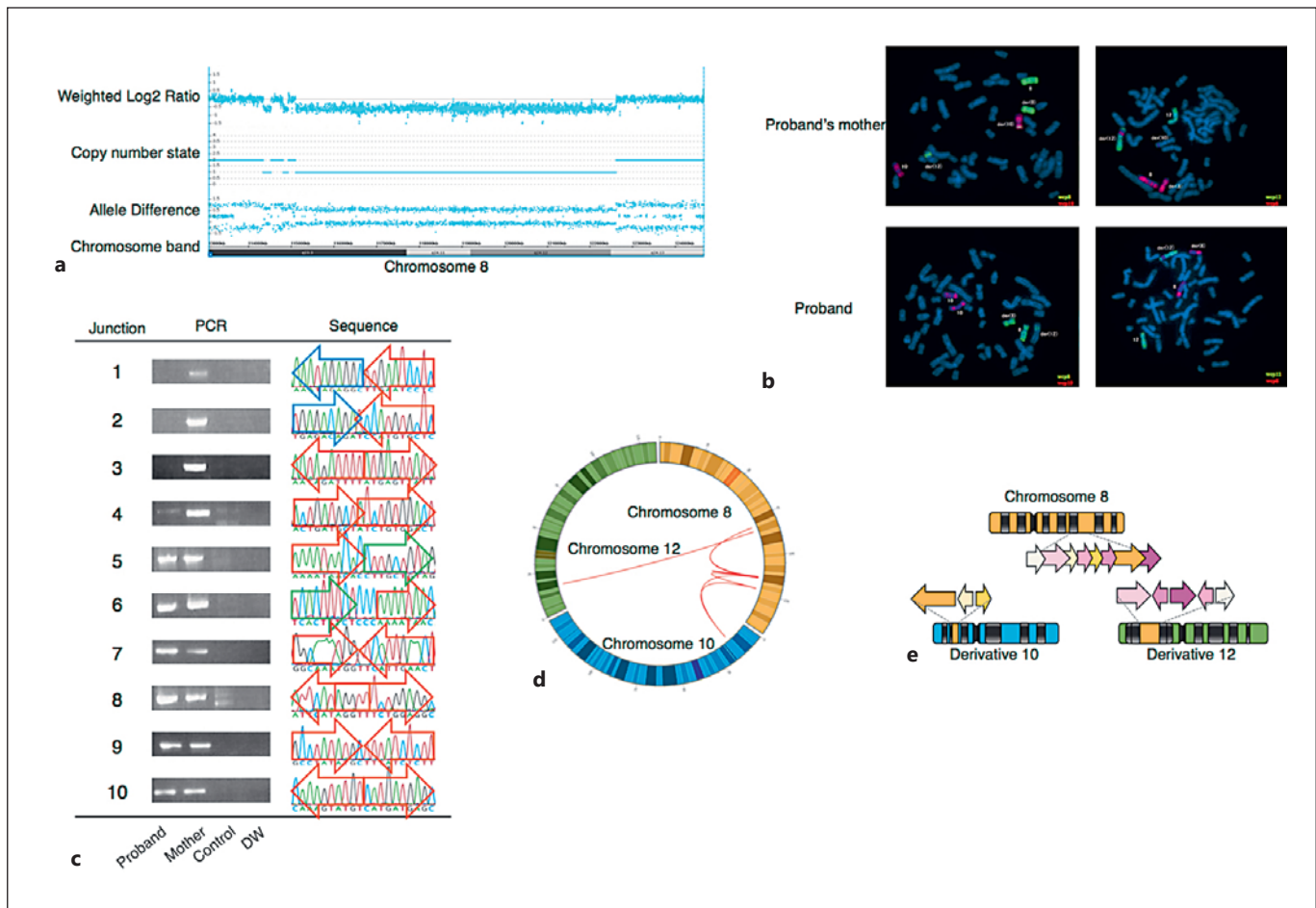


Fig. 3. Analysis of the chromosomal insertion in case 3. **a** Analysis of copy number state using ChAS software revealed that the proband had 3 distinct deletions in chromosome 10. The copy number change was designated as $\text{arr}[\text{hg19}] \ 8\text{q}23.3(114,340,065\text{--}114,527,620)\times 1$, $\text{arr}[\text{hg19}] \ 8\text{q}23.3(114,806,300\text{--}114,925,879)\times 1$, $\text{arr}[\text{hg19}] \ 8\text{q}23.3\text{q}24.13(115,101,169\text{--}122,616,401)\times 1$. **b** FISH analysis of the proband's mother with whole chromosome painting of chromosomes 8, 10, and 12 confirms the insertion of chromosome 8 into chromosomes 10 and 12. FISH analysis of the proband confirming the insertion of chromosome 8 into chromosome

12. **c** PCR validation of a discordant read. The details are the same as those provided in Figure 1. Orange arrows show chromosome 8, blue arrows show chromosome 10, and green arrows show chromosome 12. The distance between the arrows corresponds to microhomology or microinsertion. **d** The detected chromosomal rearrangements are visualized by a Circos plot using ClicO FS. **e** A number of segments in chromosome 8 were shuffled and translocated into chromosomes 10 and 12. There may be uncharacterized breakpoints in the region of chromosome 8 of the derivative chromosome 12.

some 8p in the premeiotic stage, during MII, or in the postzygotic stage in the trisomic zygote (Fig. 5b).

Case 3

This patient was referred to our facility for the diagnosis of Langer-Giedion syndrome. Initial G-banding revealed a $46,\text{XY},\text{der}(12)\text{ins}(12;8)(\text{p}12;\text{q}21\text{q}23)$ karyotype. CytoScan HD array analysis showed that the proband had a deletion at chromosome $8\text{q}23.3\text{q}24.13$ (Fig. 3a). The mother of the proband was $46,\text{XX}$ (data not shown). FISH with whole chromosome painting probe analysis revealed that she had a balanced insertion that involved chromosomes 8, 10, and 12. The long arm of chromosome 8 was found to be inserted into chromosomes 10 and 12. The pro-

band inherited only $\text{der}(8)$ and $\text{der}(12)$, not $\text{der}(10)$, resulting in the deletion of chromosome bands $8\text{q}23.3\text{q}24.13$ and causing Langer-Giedion syndrome (Fig. 3b).

Breakpoint analysis of the chromosomal rearrangements allowed us to identify 10 discordant reads. Of these, 6 junctions were detected in both proband and maternal DNA (junctions 5–10), whereas the remaining 4 were not detected in the proband (junctions 1–4), suggesting that 6 junctions are in $\text{der}(8)$ and $\text{der}(12)$, and 4 are in $\text{der}(10)$ (Fig. 3c). The inserted chromosome 8 regions consisted of pieces of segments, which were shuffled, rejoined in direct or inverted orientation, and inserted into either chromosome 10 or 12. Six junctions of rearrangements involved simple end-joining (junctions 1, 3, 5, 7, 9, and 10), and the remaining 4

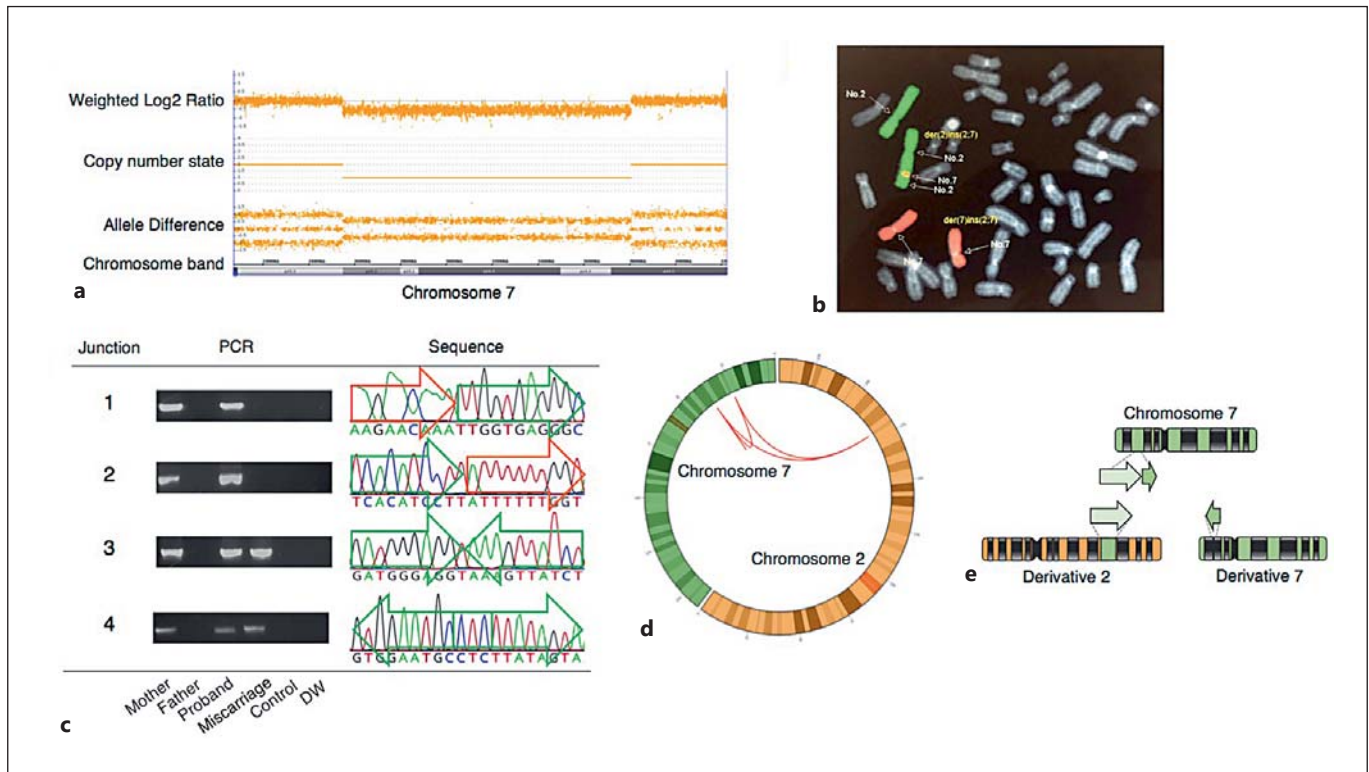


Fig. 4. Analysis of the chromosomal insertion in case 4. **a** The fetus has a copy number loss in chromosome 7. The genomic position of the copy number change is arr[hg19] 7p15.3p14.1 (25,471,046–38,067,611)×1. **b** Whole chromosome painting of chromosomes 2 (green) and 7 (red) showing the insertion from chromosome 7 into band 2q. **c** PCR confirmation of a discordant

read. The details are the same as those provided in Figure 1. Orange and green arrows indicate chromosomes 2 and 7, respectively. The distance between the arrows corresponds to microhomology or microinsertion. **d** The detected chromosomal rearrangements are visualized by a Circos plot using ClicO FS. **e** Two pieces of segments in chromosome 7 were inserted into chromosomes 2 and 7.

junctions had either microhomology (junctions 2 and 4) or microinsertion (junction 6). The likely structure is shown in Figure 3d, e.

Because we did not obtain the parental sample of the mother, who was a carrier of a balanced insertion, we could not analyze the origin of the insertion.

Case 4

This patient was referred to our facility because of recurrent pregnancy loss. The initial G-banded karyotype was 46,XY,ins(2;7)(q31;p11.2p13). We confirmed the balanced insertion of the proband by whole chromosome painting (Fig. 4b). Cytogenetic microarray analysis revealed that the aborted fetus of the proband had a deletion at 7p15.3p14.1 (Fig. 4a).

Breakpoint analysis of chromosomal rearrangements allowed us to identify discordant reads. Four discordant reads were discovered by LUMPY and validated by junction-specific PCR and Sanger sequencing. Two junctions formed by rejoining between chromosomes 2q and 7p were identified only in the proband, not in the fetus (junctions 1 and 2), whereas the remaining 2 junctions composed of 7p rejoining in an inverted orientation were identified in both the proband and fetus (Fig. 4c; junctions 3 and 4). These results suggest that the fragments of 7p were divided into 2 pieces, one in-

serted into 2q and the other inserted into the same 7p region but in the opposite direction (Fig. 4d). Three were blunt-end rejoined junctions (junctions 1–3) and 1 had a 3-nucleotide microhomology (junction 4). The likely structure is shown in Figure 4d, e.

Junction-spanning PCR showed that the proband's mother also had a balanced insertion. Because we did not obtain samples from the grandparents, we could not analyze the origin of the insertion.

Materials and Methods

We obtained blood from the patients and their family members. Genomic DNA was extracted using standard procedures. We analyzed 4 patients with an unbalanced chromosomal insertion and their relatives in this study.

Cytogenetic Analyses of Chromosomal Insertions

Individuals with a chromosomal insertion were identified by FISH and SNP array analysis. FISH analysis was performed on metaphase spreads or interphase nuclei from the patients and their

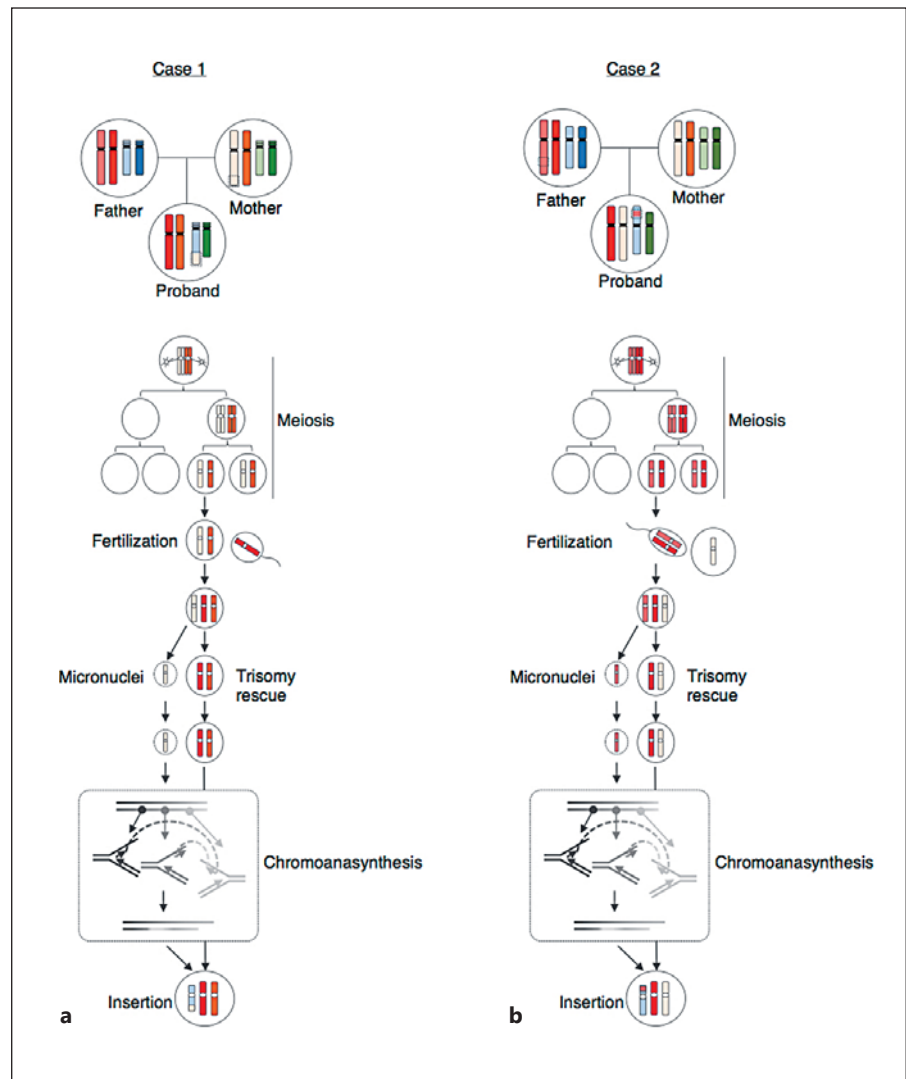


Fig. 5. The parental origin of chromosomal rearrangements reveals the mechanism of chromosomal insertion. Parent-of-origin analysis diagrams are shown at the top. Each chromosome is shown in a different color. A trisomic chromosome resulting from malsegregation in meiosis was corrected by subsequent anaphase lagging during an early embryonic stage.

parents, obtained by standard protocols using appropriate region-specific probes and whole chromosome painting probes. SNP array was performed using a CytoScan HD Array Kit (Affymetrix, Santa Clara, CA, USA) for high-resolution analysis of copy number variations and determination of the genotypes of derivative chromosomes. The genome coordinates were based on hg19 in this manuscript.

Breakpoint Characteristics of Chromosomal Insertions by Next-Generation Sequencing

Mate-pair or paired-end whole genome sequencing was performed to detect the breakpoints of chromosomal rearrangements. Libraries were prepared using a Nextera Mate Pair Library Preparation Kit or TruSeq DNA PCR-Free Library Preparation Kit (Illumina, San Diego, CA, USA) according to the manufacturer's protocol. For preparation of the mate-pair library, fragments of 9 kb in length were extracted. Libraries for next-generation sequencing analysis were then subjected to 2×100 -bp paired-end sequencing on a HiSeq 1500 platform (Illumina). Se-

quence data were demultiplexed using bcl2fastq-1.8.4 (Illumina). In the mate-pair sequence case, duplex reads were trimmed using NxTrim [O'Connell et al., 2015]. Sequence reads were then mapped onto the human reference hg19 using BWA 0.7.10 [Li and Durbin, 2010]. Sorting and recalibration of the mapped reads were done using SAMtools 0.1.19 and GATK 3.3-0 [Li et al., 2009; McKenna et al., 2010]. LUMPY was used to identify putative breakpoints of chromosomal rearrangements [Layer et al., 2014]. We focused on discordant reads in the vicinity of the breakpoint junction from FISH and SNP array information. All putative breakpoints were confirmed by visual inspection using the Integrative Genomics Viewer and breakpoint-spanning PCR [Thorvaldsdóttir et al., 2013]. The detected structural variants were visualized by a Circos plot using Ciclo FS [Cheong et al., 2015]. PCR was performed with appropriate primer sets and conditions using TaKaRa Ex Taq DNA polymerase (Takara Bio, Otsu, Japan). Sanger sequencing of breakpoint-spanning PCR fragments was carried out using an ABI3130xl sequencer (Life Technologies, Foster City, CA, USA).

SNP-Based Parental Origin Determination

To determine the parental origin of the chromosomal rearrangement, genotype information from derivative chromosome-specific PCR, SNP array, or whole genome sequencing was compared with that of the parental genotype.

Discussion

In this study, we analyzed chromosomal insertions in 4 individuals. We found that the chromosomal insertions in all 4 cases were not generated by simple inaccurate repair of 3 DSBs, but showed structural complexity. Many pieces of genomic fragments derived from a highly localized chromosomal region were reconstructed in a disorderly array associated with copy number alterations. A recent study of 6 insertion cases also showed similar results [Gu et al., 2016]. The insertion of similar highly shuffled chromosomal segments was also documented in another subset of CSRs, namely, unbalanced translocations [Weckselblatt et al., 2015]. Thus, CSRs, even when observed as a simple rearrangement in conventional karyotyping, are actually more complex than we thought.

Such localized complex CSRs have been termed chromoanagenesis [Holland and Cleveland, 2012; Zhang et al., 2013]. Chromoanagenesis includes 2 different concepts, chromothripsis and chromoanasythesis. Chromothripsis is a local chromosome shattering and restitching by NHEJ, whereas chromoanasythesis is a replication-based complex rearrangement that involves fork-stalling and template-switching as well as microhomology-mediated break-induced replication [Zhang et al., 2009; Kloosterman et al., 2011; Stephens et al., 2011]. Our data show that chromosomal insertions include regions of more than 4 copies in diploid cells, which is not compatible with the definition of chromothripsis (an alteration of 2 copy number states), but rather implies the involvement of a replication-mediated complex rearrangement mechanism. On the other hand, junction analysis showed that the junctions were blunt ended or with short microhomologies or short microinsertions in junction sequences. This conversely implicates the involvement of NHEJ, which is a characteristic of chromothripsis. Given that micronucleus-related chromosome shattering is a mechanism for the origin of chromothripsis, chromosome replication in the micronucleus is not synchronous with that in the nucleus, suggesting that a variable copy number is acceptable in chromothripsis [Crasta et al., 2012; Ly et al., 2017]. Thus, this micronucleus-related chromothripsis pathway may possibly be the mechanism that leads to chromosomal insertion.

Determination of the parental origin of a de novo insertion can shed light on the timing and mechanisms of its formation. In general, de novo constitutional structural rearrangements are predominantly of paternal origin [Thomas et al., 2010]. However, we showed compound paternal and maternal rearrangements in case 1, suggesting a postzygotic origin of the insertion. Such postzygotic CSRs of both parental chromosomes are also observed in de novo unbalanced translocations [Robberecht et al., 2013]. Furthermore, surprisingly, case 1 may have undergone trisomy rescue in the postzygotic stage as evidenced by the presence of 2 maternal and 1 paternal chromosomes. Even in case 2, the presence of 2 paternal chromosomes suggested that the insertion may have arisen in the premeiotic stage or, possibly, in the postzygotic stage in the trisomic zygote. These data imply that the trisomic fertilization may precede the chromothripsis event and be followed by trisomy rescue in the early postzygotic stage, resulting in insertion. [Conlin et al., 2010; Taylor et al., 2014]. Micronuclei formed from anaphase-lagging chromosomes may predispose a pulverized insertion due to low stringency at the spindle checkpoint in this embryonic stage [Mertzanidou et al., 2013]. To conclude, further studies involving higher sample numbers may elucidate a more precise understanding of the mechanisms underlying the etiology of chromosomal insertions.

Acknowledgments

We thank the patients and their families who participated in this study. We also thank Drs. Kazuhiro Matsuda and Masanobu Ito for providing samples as well as Ms. Makiko Tsutsumi, Naoko Fujita, and Asami Kuno for technical assistance. This study was supported by a Grant-in-Aid for Scientific Research from the Ministry of Education, Culture, Sports, Science, and Technology of Japan (15K19042 to T.K., 15H04710 and 24390085 to H.K.) and from the Ministry of Health, Welfare and Labor (16ek0109067h0003 to H.K.).

Statement of Ethics

This study was approved by the Ethical Review Board for Human Genome Studies at the Fujita Health University. Written informed consent was obtained from the patients. All experiments were carried out in accordance with the relevant guidelines and regulations.

Disclosure Statement

The authors have no conflicts of interest to declare.

References

- Cheong WH, Tan YC, Yap SJ, Ng KP: ClicO FS: an interactive web-based service of Circos. *Bioinformatics* 31:3685–3687 (2015).
- Conlin LK, Thiel BD, Bonnemann CG, Medne L, Ernst LM, et al: Mechanisms of mosaicism, chimerism and uniparental disomy identified by single nucleotide polymorphism array analysis. *Hum Mol Genet* 19:1263–1275 (2010).
- Crasta K, Ganem NJ, Dagher R, Lantermann AB, Ivanova EV, et al: DNA breaks and chromosome pulverization from errors in mitosis. *Nature* 482:53–58 (2012).
- Gu S, Szafranski P, Akdemir ZC, Yuan B, Cooper ML, et al: Mechanisms for complex chromosomal insertions. *PLoS Genet* 12:e1006446 (2016).
- Gu W, Zhang F, Lupski JR: Mechanisms for human genomic rearrangements. *Pathogenetics* 1:4 (2008).
- Hermetz KE, Surti U, Cody JD, Rudd MK: A recurrent translocation is mediated by homologous recombination between HERV-H elements. *Mol Cytogenet* 5:6 (2012).
- Holland AJ, Cleveland DW: Chromoanagenesis and cancer: mechanisms and consequences of localized, complex chromosomal rearrangements. *Nat Med* 18:1630–1638 (2012).
- Kang SH, Shaw C, Ou Z, Eng PA, Cooper ML, et al: Insertional translocation detected using FISH confirmation of array-comparative genomic hybridization (aCGH) results. *Am J Med Genet A* 152A:1111–1126 (2010).
- Kato T, Kurahashi H, Emanuel BS: Chromosomal translocations and palindromic AT-rich repeats. *Curr Opin Genet Dev* 22:221–228 (2012).
- Kloosterman WP, Guryev V, van Roosmalen M, Duran KJ, de Bruijn E, et al: Chromothripsis as a mechanism driving complex de novo structural rearrangements in the germline. *Hum Mol Genet* 20:1916–1924 (2011).
- Kurahashi H, Bolor H, Kato T, Kogo H, Tsutsumi M, et al: Recent advance in our understanding of the molecular nature of chromosomal abnormalities. *J Hum Genet* 54:253–260 (2009).
- Layer RM, Chiang C, Quinlan AR, Hall IM: LUMPY: a probabilistic framework for structural variant discovery. *Genome Biol* 15:R84 (2014).
- Li H, Durbin R: Fast and accurate long-read alignment with Burrows-Wheeler transform. *Bioinformatics* 26:589–595 (2010).
- Li H, Handsaker B, Wysoker A, Fennell T, Ruan J, et al: The sequence alignment/map format and SAMtools. *Bioinformatics* 25:2078–2079 (2009).
- Ly P, Teitz LS, Kim DH, Shoshani O, Skaletsky H, et al: Selective Y centromere inactivation triggers chromosome shattering in micronuclei and repair by non-homologous end joining. *Nat Cell Biol* 19:68–75 (2017).
- McKenna A, Hanna M, Banks E, Sivachenko A, Cibulskis K, et al: The Genome Analysis Toolkit: a MapReduce framework for analyzing next-generation DNA sequencing data. *Genome Res* 20:1297–1303 (2010).
- Mertzaniadou A, Spits C, Nguyen HT, Van de Velde H, Sermon K: Evolution of aneuploidy up to Day 4 of human preimplantation development. *Hum Reprod* 28:1716–1724 (2013).
- Neill NJ, Ballif BC, Lamb AN, Parikh S, Ravnani JB, et al: Recurrence, submicroscopic complexity, and potential clinical relevance of copy gains detected by array CGH that are shown to be unbalanced insertions by FISH. *Genome Res* 21:535–544 (2011).
- Nowakowska BA, de Leeuw N, Ruivenkamp CA, Sikkema-Raddatz B, Crolla JA, et al: Parental insertional balanced translocations are an important cause of apparently de novo CNVs in patients with developmental anomalies. *Eur J Hum Genet* 20:166–170 (2012).
- O’Connell J, Schulz-Trieglaff O, Carlson E, Hims MM, Gormley NA, Cox AJ: NxTrim: optimized trimming of Illumina mate pair reads. *Bioinformatics* 31:2035–2037 (2015).
- Ou Z, Stankiewicz P, Xia Z, Breman AM, Dawson B, et al: Observation and prediction of recurrent human translocations mediated by NAHR between nonhomologous chromosomes. *Genome Res* 21:33–46 (2011).
- Robberecht C, Voet T, Zamani Esteki M, Nowakowska BA, Vermeesch JR: Nonallelic homologous recombination between retrotransposable elements is a driver of de novo unbalanced translocations. *Genome Res* 23:411–418 (2013).
- Shaffer LG, Lupski JR: Molecular mechanisms for constitutional chromosomal rearrangements in humans. *Annu Rev Genet* 34:297–329 (2000).
- Stephens PJ, Greenman CD, Fu B, Yang F, Bignell GR, et al: Massive genomic rearrangement acquired in a single catastrophic event during cancer development. *Cell* 144:27–40 (2011).
- Taylor TH, Gitlin SA, Patrick JL, Crain JL, Wilson JM, Griffin DK: The origin, mechanisms, incidence and clinical consequences of chromosomal mosaicism in humans. *Hum Reprod Update* 20:571–581 (2014).
- Thomas NS, Morris JK, Baptista J, Ng BL, Crolla JA, Jacobs PA: De novo apparently balanced translocations in man are predominantly paternal in origin and associated with a significant increase in paternal age. *J Med Genet* 47:112–115 (2010).
- Thorvaldsdóttir H, Robinson JT, Mesirov JP: Integrative Genomics Viewer (IGV): high-performance genomics data visualization and exploration. *Brief Bioinform* 14:178–192 (2013).
- Van Hemel JO, Eussen HJ: Interchromosomal insertions. *Hum Genet* 107:415–432 (2000).
- Weckselblatt B, Rudd MK: Human structural variation: mechanisms of chromosome rearrangements. *Trends Genet* 31:587–599 (2015).
- Weckselblatt B, Hermetz KE, Rudd MK: Unbalanced translocations arise from diverse mutational mechanisms including chromothripsis. *Genome Res* 25:937–947 (2015).
- Zhang CZ, Leibowitz ML, Pellman D: Chromothripsis and beyond: rapid genome evolution from complex chromosomal rearrangements. *Genes Dev* 27:2513–2530 (2013).
- Zhang F, Carvalho CMB, Lupski JR: Complex human chromosomal and genomic rearrangements. *Trends Genet* 25:298–307 (2009).

Intragenic *DOK7* deletion detected by whole-genome sequencing in congenital myasthenic syndromes

OPEN

Yoshiteru Azuma, MD,
PhD
Ana Töpf, PhD
Teresinha Evangelista,
MD
Paulo José Lorenzoni,
MD, PhD
Andreas Roos, PhD
Pedro Viana, MD
Hidehito Inagaki, PhD
Hiroki Kurahashi, MD,
PhD
Hanns Lochmüller, MD

Correspondence to
Dr. Lochmüller:
hanns.lochmuller@newcastle.ac.
uk

ABSTRACT

Objective: To identify the genetic cause in a patient affected by ptosis and exercise-induced muscle weakness and diagnosed with congenital myasthenic syndromes (CMS) using whole-genome sequencing (WGS).

Methods: Candidate gene screening and WGS analysis were performed in the case. Allele-specific PCR was subsequently performed to confirm the copy number variation (CNV) that was suspected from the WGS results.

Results: In addition to the previously reported frameshift mutation c.1124_1127dup, an intragenic 6,261 bp deletion spanning from the 5' untranslated region to intron 2 of the *DOK7* gene was identified by WGS in the patient with CMS. The heterozygous deletion was suspected based on reduced coverage on WGS and confirmed by allele-specific PCR. The breakpoints had microhomology and an inverted repeat, which may have led to the development of the deletion during DNA replication.

Conclusions: We report a CMS case with identification of the breakpoints of the intragenic *DOK7* deletion using WGS analysis. This case illustrates that CNVs undetected by Sanger sequencing may be identified by WGS and highlights their relevance in the molecular diagnosis of a treatable neurologic condition such as CMS. *Neurol Genet* 2017;3:e152; doi: 10.1212/NXG.000000000000152

GLOSSARY

aCGH = array comparative genomic hybridization; **AChE** = acetylcholinesterase; **CMS** = congenital myasthenic syndromes; **CNV** = copy number variation; **MLPA** = multiplex ligation-dependent probe amplification; **MuSK** = muscle-specific tyrosine kinase; **NMJ** = neuromuscular junction; **WES** = whole-exome sequencing; **WGS** = whole-genome sequencing.

Congenital myasthenic syndromes (CMS) are inherited disorders characterized by fatigable muscle weakness with or without other associated signs or symptoms.¹ They are caused by mutations in genes expressed at the neuromuscular junction (NMJ). *DOK7* is one of the components of the NMJ and an activator of the muscle-specific tyrosine kinase (MuSK).² Recessive mutations in *DOK7* cause approximately 10% of the genetically diagnosed CMS cases.¹

CMS are heterogeneous diseases, and to date, more than 25 genes have been reported to be causative. Consecutive single-gene screening has been routinely used as a diagnostic tool; however, next-generation sequencing allows the analysis of all these genes simultaneously to identify the causative variant and obtain a genetic diagnosis. The efficacy of whole-exome sequencing (WES) for the diagnosis of CMS cases has been reported,^{3,4} as well as its ability to identify new causal genes.^{5,6} However, the limitation is that WES is designed to detect only protein-coding regions and exon-intron boundaries of the genome.

Supplemental data
at Neurology.org/ng

From the Institute of Genetic Medicine (Y.A., A.T., T.E., P.J.L., A.R., H.L.), Newcastle University, UK; Division of Neurology (P.J.L.), Federal University of Parana, Brazil; Leibniz-Institut für Analytische Wissenschaften ISAS e.V. (A.R.), Germany; Department of Neurosciences and Mental Health (P.V.), University of Lisbon, Portugal; and Division of Molecular Genetics (H.I., H.K.), Fujita Health University, Japan.

Funding information and disclosures are provided at the end of the article. Go to Neurology.org/ng for full disclosure forms. The Article Processing Charge was funded by the Medical Research Council.

This is an open access article distributed under the terms of the Creative Commons Attribution License 4.0 (CC BY), which permits unrestricted use, distribution, and reproduction in any medium, provided the original work is properly cited.

On the other hand, whole-genome sequencing (WGS) allows the analysis of deep intronic, intergenic, and other noncoding regions. Furthermore, WGS allows to detect copy number variations (CNVs), as coverage is more homogeneous than that of WES.⁷

We present a CMS case in which a large intragenic *DOK7* deletion was identified by WGS compound heterozygous to a known exonic mutation.

METHODS *DOK7* screening. DNA from the patient was extracted from whole blood by standard methods. Screening of hot-spot mutations was performed by Sanger sequencing, encompassing a region of ~600 bp covering the previously reported European founder mutation c.1124_1127dup.² Subsequently, full screening of coding regions and exon-intron boundaries of the *DOK7* gene was performed. Primer sequences are listed in table e-1 at Neurology.org/ng. Annotation of the human *DOK7* cDNA is according to the GenBank accession number NM_173660.

Mutation analysis by WGS. WGS was performed by the TruSeq PCR-free library preparation kit and HiSeqX v2 SBS kit (Illumina, San Diego, CA) for 30× mean coverage on a HiSeqX sequencer. Reads were mapped against hg19 reference genome using the Burrows-Wheeler transform,⁸ and duplicates were removed using Picard tools.⁹

Sequence variants were called using the Genome Analysis Toolkit.¹⁰ WGS data were then analyzed using deCODE's platform (Clinical Sequence Miner; WuXi NextCODE, Cambridge, MA). Rare variants were filtered by threshold of coverage (≥8), variant call (≥2), and ratio of variant (≥0.2) and allele frequency of 1% in 1000 Genomes database.¹¹

Sanger sequencing of large deletion. We amplified DNA samples to identify the suspected intragenic deletion with primers 5'-CCCAGATGGTGCGCTTGCTCC-3' and 5'-GCCACCCCTCACGCTCAG-3'. The PCR protocol comprised 35 cycles and annealing temperature of 68°C using HotStarTaq DNA polymerase with Q-Solution for the GC rich region (QIAGEN, Düsseldorf, Germany).

Standard protocol approvals, registrations, and patient consents. All human studies including genetic analysis were approved by institutional review boards, and appropriate written informed consent was obtained from all the patients and family members.

RESULTS *Clinical findings.* The patient is a 39-year-old Portuguese man who presented with bilateral ptosis and exercise-induced muscle weakness. He had no family history of muscle disease, and his motor milestones in childhood were normal. He showed mild ptosis from infancy and noticed mild lower limb weakness at 13 years of age. He was admitted to hospital for a month because of sudden severe generalized muscle weakness and worsening ptosis at 15 years of age. He has bilateral facial weakness and winged scapula, and the clinical diagnosis of a neuromuscular transmission defect was confirmed by neurophysiologic studies. EMG showed myopathic

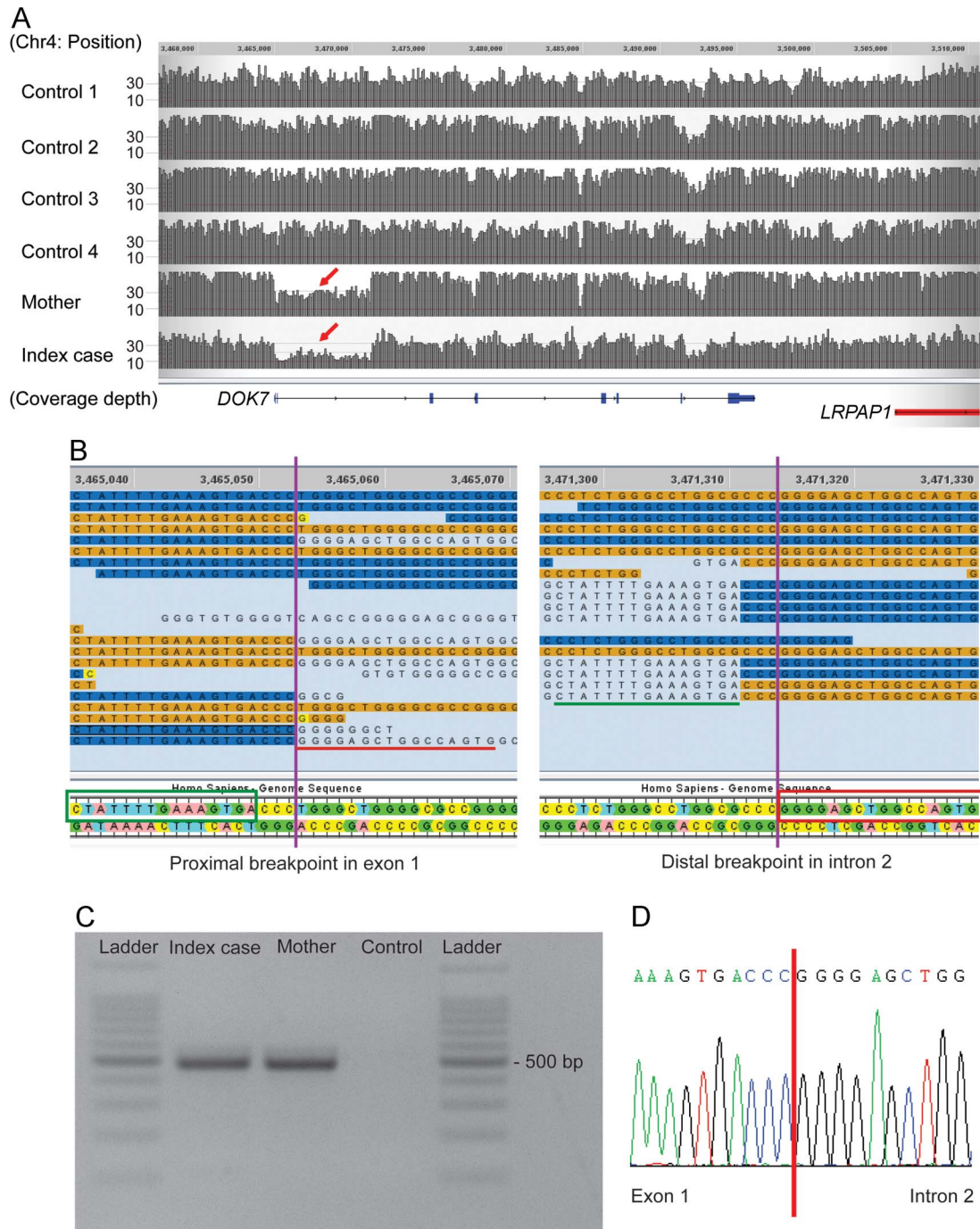
changes on facial muscles. Repetitive nerve stimulation showed a remarkable decremental response of 76% in proximal muscles. Both antiacetylcholine-receptor and anti-MuSK antibodies were negative, and immunosuppressive treatment was unsuccessful. Acetylcholinesterase (AChE) inhibitor of pyridostigmine up to 360 mg/d for 10 years had little effect and was discontinued without clinical deterioration after the trial of oral administration of salbutamol which effected significantly. He has not experienced severe muscle weakness for 5 years since salbutamol was started.

***DOK7* screening.** Based on the limb-girdle clinical presentation of the patient, a hot-spot region of *DOK7* was investigated as a first screening step. Sanger sequencing revealed that the patient carried the heterozygous c.1124_1127dup reported as a founder mutation in European CMS patients.² This mutation was not present in the mother (DNA from the father was unavailable). However, this single heterozygous mutation does not explain *DOK7*-CMS, which invariably shows autosomal recessive inheritance. To identify a second heteroallelic *DOK7* variant, the whole coding region and exon-intron boundaries of the *DOK7* gene were Sanger sequenced, but no potentially pathogenic exonic or splice site variants were found. The sample was therefore subjected to WGS to try to identify other mutations within the *DOK7* gene or elsewhere in the genome.

WGS analysis. As expected, applying a standard pipeline for variant filtering (minor allele frequency 1% in coding region), the heterozygous c.1124_1127dup in *DOK7* was detected in the WGS data. This filtering did not identify any other coding variants in known CMS causal genes.

However, visual inspection of the sequencing reads of the *DOK7* gene for this patient revealed that the read depth for exons 1 and 2 was lower than that of neighboring regions and other control samples (figure 1A). Furthermore, there were no heterozygous variants within this region, indicating a run of homozygosity or hemizyosity suggesting a single copy region. Close inspection of the boundaries of this region showed that in some instances, sections of the sequencing reads did not match the reference sequence. These reads were considered chimeric or split reads, as the unmatched sequences did align to a different region of the genome. Split reads are indicative of structural variation. In fact, the 3' section of the split reads of the proximal boundary aligns to the 3' end of the distal boundary, and vice versa (figure 1B, red underline and red box). The proximal and distal breakpoints lie approximately 6 kb away. These findings suggested that this patient

Figure 1 Whole-genome sequencing analysis and allele-specific PCR



(A) Both index case and his mother show reduced read depth (coverage) from exon 1 to deep intron 2 of the *DOK7* gene (red arrow). Controls 1-4 correspond to samples sequenced and analyzed through the same pipeline and without the diagnosis of congenital myasthenic syndromes. (B) Split reads were observed at both presumed breakpoints. Nucleotides matching the reference sequence of *DOK7* are highlighted in orange/blue. Single unmatched nucleotides are highlighted in yellow, and further unmatched sequences are not highlighted. The unmatched sequence (indicated with red/green underline) of the split reads of the proximal breakpoint aligns to the reference sequence (indicated in green/red boxes) at the distal breakpoint, and vice versa. (C) The expected products amplified by allele-specific PCR were identified in the index case and the mother. (D) The junction of the breakpoint in the allele with the intragenic deletion was confirmed by Sanger sequencing of the PCR product. Coverage and reads were drawn by the graphical user interface of Sequence Miner 5.21.1 (WuXi NextCODE).

has a heterozygous 6-kb deletion in *DOK7* encompassing exons 1 and 2.

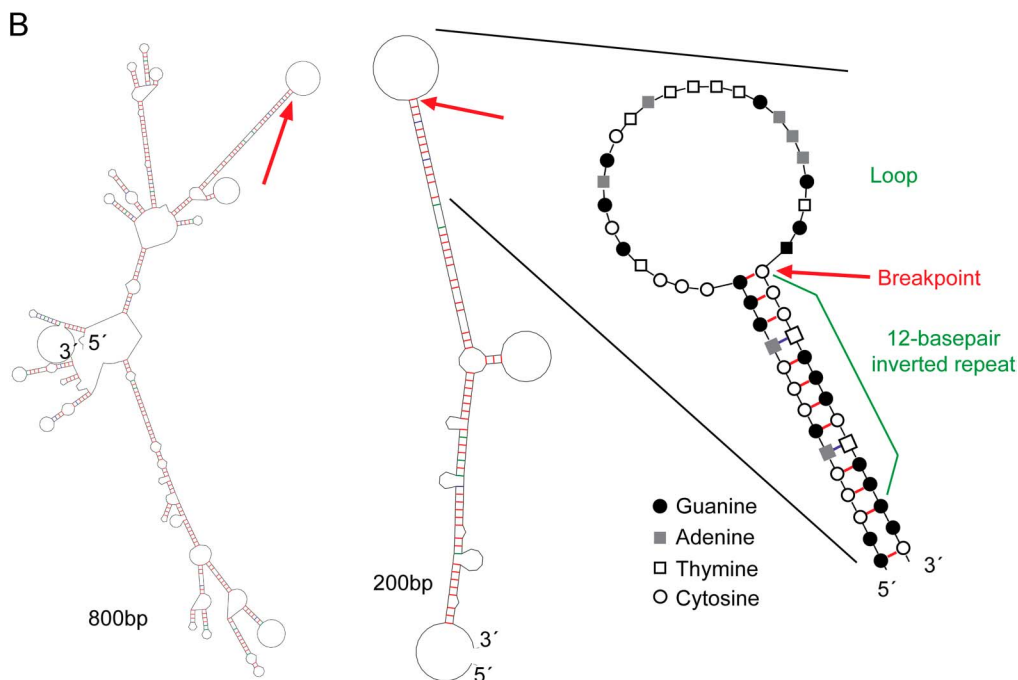
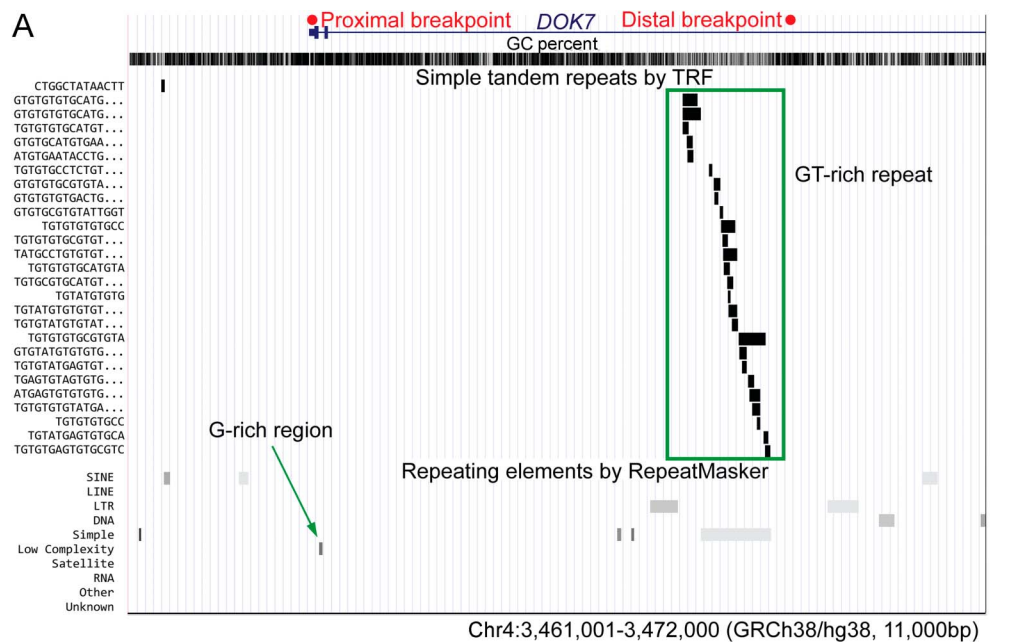
Identification and analysis of the intragenic *DOK7* deletion. We performed PCR using a pair of primers

designed around 250 bp away from the presumed breakpoints of the deletion, between the 5' untranslated region and intron 2. The expected product of 488 bp was amplified in the DNA samples of the patient, but not in control DNA

(figure 1C). The junction of the 2 breakpoints was identified by Sanger sequencing of the PCR product (figure 1D). The exact size of the deletion is 6,261 bp. The deletion was also detected by PCR

in the mother, who did not carry the c.1124_1127dup mutation. We therefore concluded that the CMS in the patient is caused by the compound heterozygous mutations in *DOK7*.

Figure 2 Analysis of the breakpoints of the intragenic 6-kb deletion



(A) University of California Santa Cruz genome browser (genome.ucsc.edu/) view of the deleted region showing the Simple Tandem Repeats track (based on Tandem Repeats Finder, TRF²⁸) and the Repeating Elements track (based on RepeatMasker¹⁹). GT-rich repeat regions (green box) are seen around the distal breakpoint, and a G-rich region (green arrow) is located near the proximal breakpoint. (B) The secondary DNA structure with the lowest delta G value was predicted by the mfold tool (unafold.rna.albany.edu/?q=mfold) for the 800 and 200 bp regions around the proximal breakpoint. An enlarged view of the breakpoint area highlighting the complementary nucleotides is also shown. The proximal breakpoint (indicated by the red arrows) is at the boundary of a loop and a 12-bp inverted repeat that may cause stalling of DNA replication. It is possible that deletion/duplication can occur if stalled replication resumes using an alternate location on the same chromosome. Red/blue/green bars represent hydrogen bonds between G-C/T-A/G-T.

The 2 breakpoints of the deletion have a C-triplet homology region, and the deleted region contains a G-rich region and GT-rich repeat region (figure 2A). In silico secondary structure analysis using the prediction program mfold¹² showed that the proximal breakpoint is at the boundary of a loop and a 12-bp inverted repeat (figure 2B). This may cause stalling of DNA replication and subsequently result in chromosomal structural changes including deletions, if replication resumes using an alternate chromosomal location.

Screening of the intragenic deletion in a CMS cohort. To identify carriers of single heterozygous mutations in *DOK7* (i.e., without a second rare variant within coding regions and exon-intron boundaries), we interrogated our database of clinically diagnosed CMS cases referred to us in the years 1996–2015. The total number of patients with CMS was 577, of which 7 genetically unsolved cases had single frameshift mutations in *DOK7* (c.1124_1127dup in 6 cases and c.1378dup in 1 case). These samples were amplified using the deletion-specific pair of primers used to detect the 6-kb deletion of the index family. All 7 samples were negative using this PCR method. This does not exclude that they carry CNVs in *DOK7* different from the one described in this study.

DISCUSSION We identified an intragenic *DOK7* deletion in a patient with clinically diagnosed CMS. Patients lacking a second heteroallelic mutation in *DOK7* were reported in a previous study.² Moreover, multiexon genomic deletions of *RAPSN*¹³ and *COLQ*¹⁴ have also been identified as causative of CMS. It is therefore conceivable that CNVs in *DOK7* may explain a proportion of cases assessed as negative or inconclusive by conventional sequencing analysis.

Our study shows the advantage of WGS analysis and detailed interrogation for detecting CNVs, using coverage and visual analysis of split reads. Traditionally, multiplex ligation-dependent probe amplification (MLPA) is considered the method of choice to detect previously described CNVs, where kits are available commercially. To identify new CNVs, however, specific MLPA primers for each gene need to be designed, rendering it expensive and time consuming for testing a genetically heterogeneous syndrome such as CMS. Array comparative genomic hybridization (aCGH) is also a valuable method for CNVs analysis; nevertheless, deletions/duplications are not detectable by aCGH if they are shorter than the spacing of the hybridization probes. In addition, neither MLPA nor aCGH can detect single nucleotide variants. Despite WES being widely used for clinical sequencing, the library preparation step results in uneven coverage, which makes the estimation

of CNVs by read depth less reliable. This can be overcome by the homogenous coverage of WGS, allowing both the detection of single nucleotide as well as CNV.

WGS analysis is still more expensive than WES and Sanger sequencing. In addition, computational tools need further improvement in sensitivity and specificity to detect CNVs exhaustively.¹⁵ Taken together, we believe that WGS is advantageous and will become the method of choice for genetic diagnosis in rare, heterogeneous conditions such as CMS. We suggest that previously unsolved cases or the carriers of a single mutation in a causal gene are especially suitable cases of CMS for WGS analysis. The 6-kb deletion was not identified in other cases tested by PCR, although it is inherited from the mother, suggesting this is likely a private mutation. However, it is possible that other CNVs in *DOK7* underlie in CMS cases.

We also determined the breakpoints of the 6-kb deletion, and analysis of the sequence and secondary structure suggested that long inverted repeats might cause the development of the deletion due to a stall of replication, and microhomology might have played a role in the repair process.¹⁶ Further documentation of breakpoints and sequences would help understand the mechanism for the development of CNVs.

Obtaining genetic diagnosis of CMS is very important because the therapy varies depending on the affected gene. Poor response to AChE inhibitors is often observed in patients affected by limb-girdle CMS due to *DOK7* mutations. Salbutamol therapy has now been started for the patient described in this study, which has been reported of good response in *DOK7*-CMS.¹⁷

AUTHOR CONTRIBUTIONS

Yoshiteru Azuma: drafting the manuscript, acquisition of data, and analysis and interpretation. Ana Töpf: analysis and interpretation and critical revision of the manuscript. Teresinha Evangelista and Paulo José Lorenzoni: acquisition of data. Andreas Roos: analysis and interpretation and study supervision. Pedro Viana: acquisition of data. Hidehito Inagaki and Hiroki Kurahashi: analysis and interpretation. Hanns Lochmüller: study concept and design and study supervision.

STUDY FUNDING

Study funded by European Commission's Seventh Framework Programme (FP7/2007-2013) under grant agreement no. 2012-305121 (NEUROMICS). Hanns Lochmüller—funding from the Medical Research Council as part of the MRC Centre for Neuromuscular Diseases (reference G1002274, grant ID 98482) and by the European Union Seventh Framework Programme (FP7/2007-2013) under grant agreement no. 305444 (RD-Connect).

DISCLOSURE

Yoshiteru Azuma, Ana Töpf, and Teresinha Evangelista report no disclosures. Paulo José Lorenzoni has received research support from CNPq (Brazil). Andreas Roos, Pedro Viana, Hidehito Inagaki, and Hiroki Kurahashi report no disclosures. Hanns Lochmüller has served on the scientific advisory boards of German Duchenne parents project, IRDiRC Interdisciplinary Scientific Committee, German Muscular Dystrophy

Network, Myotubular Trust Patient Registry, Action Duchenne Patient Registry, German Patient Registries on DMD, and SMA; has received travel funding/speaker honoraria from PTC Therapeutics Inc. and Ultragenyx Pharmaceuticals Inc.; serves on the editorial boards of the *Journal of Neuromuscular Diseases* and the *Journal of Neurology*; has been a consultant for Roche Pharmaceuticals, ASD Therapeutics Partners LLC, IOS Press, Alexion Pharmaceuticals Inc., Ultragenyx Pharmaceutical Inc., and Fondazione Cariplo (funding from each paid to Newcastle University); and has received research support from Marigold Foundation Ltd., Ultragenyx Pharmaceutical Inc., PTC Therapeutics Inc., Eli Lilly and Co., Action Benni & Co., GSK (GlaxoSmithKline), Trophos SA, European Commission (RD-Connect), European Commission (OPTIMISTIC), European Commission (NeurOmics), Medical Research Council (MRC), National Institute for Health Research (NIHR), Action Duchenne, Association Française Contre les Myopathies, British Heart Foundation, Muscular Dystrophy UK, National Cancer Institute, Spinal Muscular Atrophy Support UK, Wellcome Trust, Jennifer Trust, and Duchenne Parent Project. Go to Neurology.org/ng for full disclosure forms.

Received January 19, 2017. Accepted in final form March 14, 2017.

REFERENCES


- Engel AG, Shen XM, Selcen D, Sine SM. Congenital myasthenic syndromes: pathogenesis, diagnosis, and treatment. *Lancet Neurol* 2015;14:420–434.
- Beeson D, Higuchi O, Palace J, et al. Dok-7 mutations underlie a neuromuscular junction synaptopathy. *Science* 2006;313:1975–1978.
- Das AS, Agamanolis DP, Cohen BH. Use of next-generation sequencing as a diagnostic tool for congenital myasthenic syndrome. *Pediatr Neurol* 2014;51:717–720.
- Garg N, Yiannikas C, Hardy TA, et al. Late presentations of congenital myasthenic syndromes: how many do we miss? *Muscle Nerve* 2016;54:721–727.
- Bauche S, O'Regan S, Azuma Y, et al. Impaired presynaptic high-affinity choline transporter causes a congenital myasthenic syndrome with episodic apnea. *Am J Hum Genet* 2016;99:753–761.
- O'Connor E, Topf A, Muller JS, et al. Identification of mutations in the MYO9A gene in patients with congenital myasthenic syndrome. *Brain* 2016;139:2143–2153.
- Lelieveld SH, Spielmann M, Mundlos S, Veltman JA, Gilissen C. Comparison of exome and genome sequencing technologies for the complete capture of protein-coding regions. *Hum Mutat* 2015;36:815–822.
- Li H, Durbin R. Fast and accurate long-read alignment with Burrows-Wheeler transform. *Bioinformatics* 2010;26:589–595.
- Picard. Available at: broadinstitute.github.io/picard/. Accessed March 23, 2017.
- McKenna A, Hanna M, Banks E, et al. The Genome Analysis Toolkit: a MapReduce framework for analyzing next-generation DNA sequencing data. *Genome Res* 2010;20:1297–1303.
- Auton A, Brooks LD, Durbin RM, et al. A global reference for human genetic variation. *Nature* 2015;526:68–74.
- Zuker M. Mfold web server for nucleic acid folding and hybridization prediction. *Nucleic Acids Res* 2003;31:3406–3415.
- Gaudon K, Penisson-Besnier I, Chabrol B, et al. Multiexon deletions account for 15% of congenital myasthenic syndromes with RAPSN mutations after negative DNA sequencing. *J Med Genet* 2010;47:795–796.
- Wang W, Wu Y, Wang C, Jiao J, Klein CJ. Copy number analysis reveals a novel multiexon deletion of the *COLQ* gene in congenital myasthenia. *Neurol Genet* 2016;2:e117. doi: 10.1212/NXG.0000000000000117.
- Pirooznia M, Goes FS, Zandi PP. Whole-genome CNV analysis: advances in computational approaches. *Front Genet* 2015;6:138.
- Hastings PJ, Ira G, Lupski JR. A microhomology-mediated break-induced replication model for the origin of human copy number variation. *PLoS Genet* 2009;5:e1000327.
- Lorenzoni PJ, Scola RH, Kay CS, et al. Salbutamol therapy in congenital myasthenic syndrome due to DOK7 mutation. *J Neurol Sci* 2013;331:155–157.
- Benson G. Tandem repeats finder: a program to analyze DNA sequences. *Nucleic Acids Res* 1999;27:573–580.
- Smit A, Hubley R, Green P. RepeatMasker Open-3.0. 1996–2010. Available at: repeatmasker.org. Accessed March 23, 2017.

CASE REPORT

Open Access



A case with concurrent duplication, triplication, and uniparental isodisomy at 1q42.12-qter supporting microhomology-mediated break-induced replication model for replicative rearrangements

Tomohiro Kohmoto^{1†}, Nana Okamoto^{2†}, Takuya Naruto¹, Chie Murata¹, Yuya Ouchi³, Naoko Fujita³, Hidehito Inagaki³, Shigeko Satomura⁴, Nobuhiko Okamoto⁵, Masako Saito¹, Kiyoshi Masuda¹, Hiroki Kurahashi³ and Issei Imoto^{1*} 

Abstract

Background: Complex genomic rearrangements (CGRs) consisting of interstitial triplications in conjunction with uniparental isodisomy (isoUPD) have rarely been reported in patients with multiple congenital anomalies (MCA)/intellectual disability (ID). One-ended DNA break repair coupled with microhomology-mediated break-induced replication (MMBIR) has been recently proposed as a possible mechanism giving rise to interstitial copy number gains and distal isoUPD, although only a few cases providing supportive evidence in human congenital diseases with MCA have been documented.

Case presentation: Here, we report on the chromosomal microarray (CMA)-based identification of the first known case with concurrent interstitial duplication at 1q42.12-q42.2 and triplication at 1q42.2-q43 followed by isoUPD for the remainder of chromosome 1q (at 1q43-qter). In distal 1q duplication/triplication overlapping with 1q42.12-q43, variable clinical features have been reported, and our 25-year-old patient with MCA/ID presented with some of these frequently described features. Further analyses including the precise mapping of breakpoint junctions within the CGR in a sequence level suggested that the CGR found in association with isoUPD in our case is a triplication with flanking duplications, characterized as a triplication with a particularly long duplication-inverted triplication-duplication (DUP-TRP/INV-DUP) structure. Because microhomology was observed in both junctions between the triplicated region and the flanking duplicated regions, our case provides supportive evidence for recently proposed replication-based mechanisms, such as MMBIR, underlying the formation of CGRs + isoUPD implicated in chromosomal disorders.

Conclusions: To the best of our knowledge, this is the first case of CGRs + isoUPD observed in 1q and having DUP-TRP/INV-DUP structure with a long proximal duplication, which supports MMBIR-based model for genomic rearrangements. Molecular cytogenetic analyses using CMA containing single-nucleotide polymorphism probes with further analyses of the breakpoint junctions are recommended in cases suspected of having complex chromosomal abnormalities based on discrepancies between clinical and conventional cytogenetic findings.

Keywords: 1q, Complex genomic rearrangement, Uniparental isodisomy, DUP-TRP/INV-DUP structure, Microhomology-mediated break-induced replication model, Template switching, Chromosomal microarray, Breakpoint junction sequence

* Correspondence: issehgen@tokushima-u.ac.jp

†Equal contributors

¹Department of Human Genetics, Graduate School of Biomedical Sciences, Tokushima University, 3-18-15 Kuramoto-cho, Tokushima 770-8503, Japan
Full list of author information is available at the end of the article

Background

Complex genomic rearrangements (CGRs) consisting of two or more breakpoint junctions have been frequently observed during the characterization of nonrecurrent microduplications associated with genomic disorders [1, 2]. The occurrence of CGRs, such as partial tetrasomy induced by an interstitial triplication, contiguous distally with an extended segment uniparental isodisomy (isoUPD), has recently been reported as a rare event [3–7]. The recent establishment of high-resolution chromosomal microarray (CMA) using probes designed to detect copy number variations (CNVs) and genotype single-nucleotide polymorphism (SNP) simultaneously in a genome-wide manner has accelerated the identification of cases with such CGRs + isoUPD observations [8]. Although the cause, mechanism, and phenotypic effect of such CGR + isoUPD remain unclear, Carvalho et al. [5] provided evidence that CGRs generated post-zygotically through microhomology-mediated break-induced replication (MMBIR) can lead to regional isoUPD. In this replication-based mechanism model, a triplicated segment inserted in an inverted orientation between two copies of the duplicated segments (duplication-inverted triplication-duplication, DUP-TRP/INV-DUP) followed by regional isoUPD is generated via template switches between homologs and sister chromatids using MMBIR [5].

Here, we report on a patient with the co-occurrence of interstitial trisomy at 1q42.12-q42.2 and tetrasomy at 1q42.2-q43, followed by a segmental isoUPD for 1q43-qter, as additional evidence for an MMBIR-based model generating DUP-TRP/INV-DUP rearrangement followed by isoUPD. Detailed molecular genetic analyses at the sequence level revealed the presence of microhomology at two breakpoint junctions of the CGR, probably underlying the formation of the complicated genomic alteration (CGR + isoUPD). Notably, this is the first case of CGR + isoUPD detected in the long arm of chromosome 1. In addition, the pattern of flanking duplications experimentally documented in the present case, namely, a long duplicated segment with a size on the order of megabases at the centromeric junction observed by CMA with a short duplication at the telomeric junction only identified by sequencing of the breakpoint, has not been reported previously.

Case presentation

The 25-year-old Japanese male reported on here was the first child of a non-consanguineous healthy mother (G0P0, 24 years of age) and father (details are unclear due to a divorce) with no notable family disease history. After an uncomplicated pregnancy, he had been born at 38 weeks of gestation by a normal delivery. His birth weight was 1958 g (−2.52 SD) and he was introduced into a neonatal incubator to treat intrauterine growth

retardation (IUGR) and poor sucking by tube feeding for 20 days, although detailed medical records of his physique are not available. Physical examination at the age of 1 month showed height 46 cm (−3.4 SD), weight 2715 g (−2.6 SD), and head circumference 29.8 cm (−4.6 SD). The abilities to hold up his head, eat solid food, imitate the behaviors of others, and walk alone were recognized at 6 months, 18 months, 2 years and 6 months, and 3 years of age, respectively. The patient had never been able to speak until now, and his comprehension was limited to simple signs, but he recognized various sounds. At 3 years of age, he was diagnosed with the congenital heart defect of tetralogy of Fallot (TOF) but was not treated surgically, although he showed frequent squatting and cyanotic attacks. On physical examination at 24 years and 6 months of age, he showed growth retardation with height 136 cm (−6 SD), weight 28.1 kg (−3.3 SD), and severe mental retardation with a developmental quotient of 5. At 25 years of age, he had TOF, bilateral congenital inguinal hernia, bilateral cryptorchidism, club feet, scoliosis, Chilaiditi's syndrome, and several facial anomalies, such as thinning of the hair, strabismus, widely spaced eyes, a down-slanted palpebral fissure, low-set ears, a prominent forehead, and a coarse face. He has some missing teeth due to having suffered from periodontal disease. Serial complete blood counts showed thrombocytopenia, and magnetic resonance imaging showed cerebral atrophy especially of the frontal lobe, with enlargement of the ventricles. His karyotype at birth was reported to be normal, but repeatedly performed karyotyping revealed 46,XY,dup(1)(q32.1q42.1),inv(9)(p12q13).

Molecular cytogenetic studies

This research protocol for this study was approved by the local ethics committee of Tokushima University. Written informed consent for the participation of the patient in this study was obtained from the patient's mother DNA was extracted from a peripheral blood sample.

A high-resolution CMA using the CytoScan HD array (Affymetrix, Santa Clara, CA) with Chromosome Analysis Suite software (ChAS, Affymetrix) to process the raw data detected a 9.2-Mb trisomy at 1q42.12-q42.2, a 6.7-Mb tetrasomy consisting of the duplication of two haplotypes, each of which probably derives from either the father or the mother, at 1q42.2-q43, and a 8.2-Mb segment with the absence of heterozygosity at 1q43-qter consistent with isoUPD (arr[hg19]1q42.12q42.2(225,101,799_234,324,222)x3,1q42.2q43(234,330,738_240,992,219)x4,1q43qter(240,993,835_249,224,684)x2 hmz, Fig. 1a). Trisomic, tetrasomic, and iUPD regions contain 88, 38, and 94 Refseq genes, and 49, 21, and 24 OMIM genes, respectively. Neither copy number abnormalities nor iUPD around 1q42.2-qter was detected in the DNA of the patient's mother (data not shown). Since the genotyping

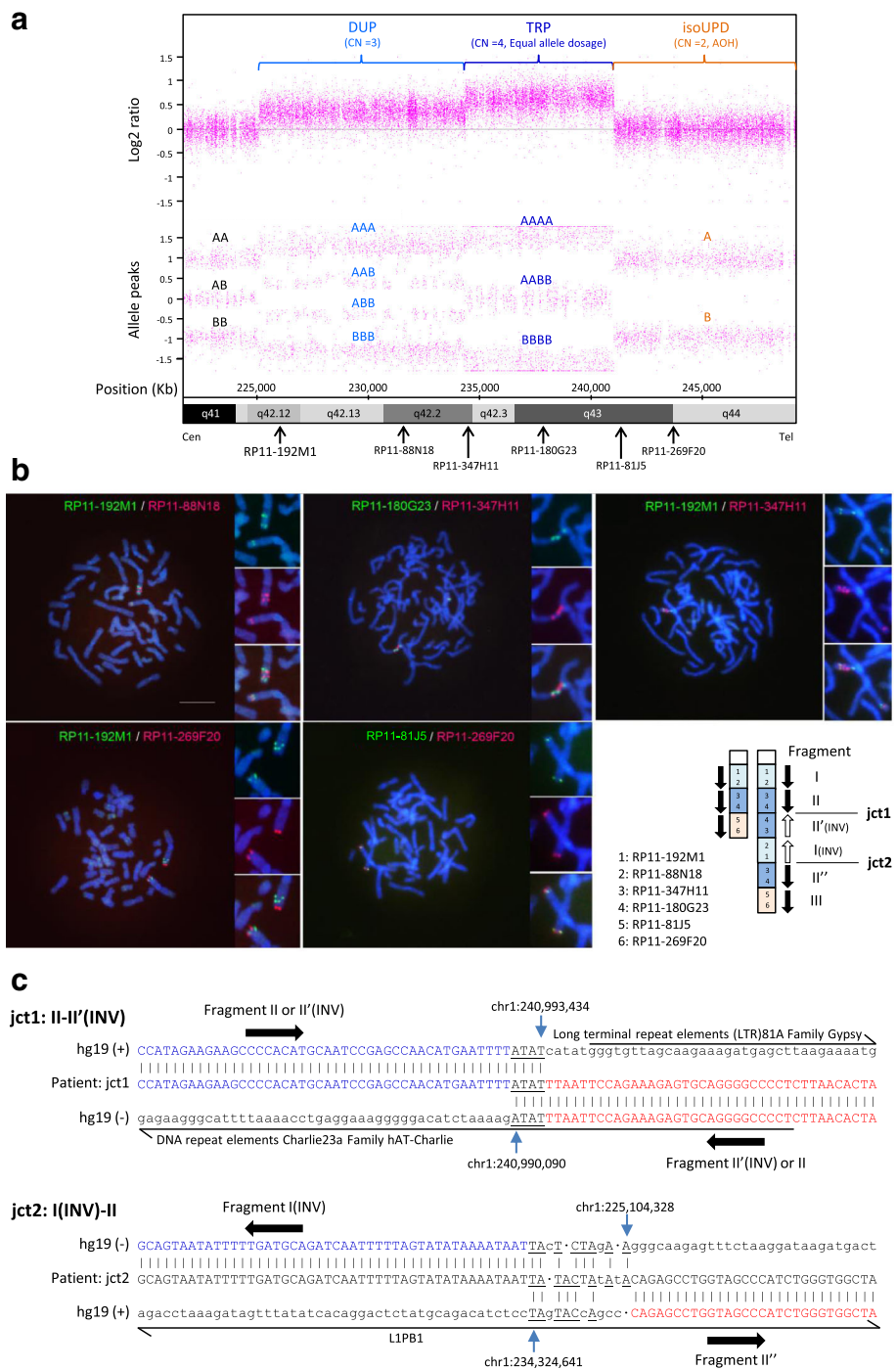


Fig. 1 (See legend on next page.)

(See figure on previous page.)

Fig. 1 a Chromosome Analysis Suite (ChAS) graphic results of Affymetrix CytoScan HD analysis for the 1q region that presented duplication (DUP), triplication (TRP), or isoUPD in the patient. Detection of CGR and isoUPD were performed using an Affymetrix CytoScan HD CMA platform (Affymetrix), which provides 906,600 polymorphic (SNP) and 946,000 non-polymorphic (CNV) markers, according to the manufacturer's recommendations. In addition, we used Chromosome Analysis Suite software (ChAS, Affymetrix) to process the raw data, and the output data were interpreted with the UCSC Genome Browser (<http://genome.ucsc.edu>; GRCh37/hg19 assembly). *Top*, copy number log₂ ratio; *bottom*, allele peaks. CN, copy number. Possible genotype calls based on the allele dosage normalization algorithm are shown using A and B. The location of each BAC used for FISH analysis is shown. **b** Images of two-color FISH mapping using six BAC clones and the scheme of distal 1q CGR based on FISH data. Metaphase FISH images with high-magnification images of the distal 1q. BAC clones labeled with either FITC (*green*) or rhodamine (*red*) were hybridized to 4',6-diamidino-2-phenylindole (DAPI)-stained chromosomes of the patient. The location and detailed information of each BAC are shown in Fig. 1a and Additional file 1: Table S1, respectively. In the scheme, arrows indicate the direction of chromosomal fragments I, II (II', II''), and III, which presented duplication, triplication, and isoUPD, respectively, in CMA. Two junctions (jct 1 and jct2) between fragments II and II' and between I and II'' are also shown. **c** Color-matched sequence alignment of breakpoint junctions in rearrangements. *Top*, jct1 (breakpoint junction 1 between segments II and II'); *bottom*, jct2 (breakpoint junction 2 between segments I and II'') (see Fig. 1b). Microhomology at the junctions is represented by underlined letters. Frequent mismatch sequences were only observed near jct2 within long-range PCR products (data not shown). Thick arrows indicate the possible orientation of chromosomal fragments. Various types of repeat elements observed around junctions are shown

results using SNP typing probe within the iUPD region of the patient matched at least one of the maternal alleles, the iUPD segment is likely to have been inherited from his mother (data not shown), although genomic DNA of his father was not available to confirm the inheritance of this region. On the other hand, genotyping results within the trisomic region suggest that the duplicated segment is unlikely to have been inherited from his mother (data not shown). In the tetrasomic region (the triplicated segment), three allele peaks (AA, AB, and BB) with unusually large spaces between them were observed (Fig. 1a), suggesting the presence of AA/AA, AA/BB, and BB/BB tracks, which is only possible if each parent contributed equally with two alleles (either AA or BB).

Next, the location and orientation of each segment within this structurally altered region were determined by a series of dual-color fluorescence *in situ* hybridization (FISH) studies using bacterial artificial chromosome (BAC) clones located around the region (Fig. 1a and b, Additional file 1: Table S1) performed as described elsewhere [9]. Two signals (duplication) with a direct-inverted orientation and three signals (triplication) with a direct-inverted-direct orientation were detected by probes on the trisomic and tetrasomic regions, respectively. The triplicated segment in an inverted orientation was observed between the proximal triplicated segment in a direct orientation (junction 1, jct1) and the distal duplicated segment in an inverse orientation. The distal triplicated segment in a direct orientation is joined with the inversely oriented distal duplicated segment (junction 2, jct2). The isoUPD segment is then joined with this triplicated segment and terminates the abnormal chromosome 1. Taking these findings together, the final karyotype was interpreted as 46,XY,der(1)dup trp(pter → q43::q43 → q42.12::q42.2 → qter).

Genomic investigation

For the precise mapping of breakpoint junctions in the CGR (jct 1 and 2), we first performed mate pair next-

generation sequencing using the Nextera Mate Pair Sample Preparation Kit and Illumina HiSeq 1500 with 100 paired-end cycles according to the manufacturer instructions (Illumina, San Diego, CA). Reads were aligned to the human genome sequence using the Burrows-Wheeler Alignment tool 0.7.12. (<http://bio-bwa.sourceforge.net>). Two recurrent structural variations within 1q42.12-1qter were identified from the discordant read pairs around the estimated boundary areas by the expected number of reads per region and visual inspection using the Integrative Genomics Viewer. Long-range polymerase chain reaction (PCR) using primers designed around the estimated boundaries (Additional file 2: Table S2) and Takara LA Taq (Takara Bio, Otsu, Japan) with the two step protocol according to the manufacturer instructions. The direct sequencing of PCR products defined sequences around two breakpoint junctions, jct1 and jct2 (Fig. 1c). Based on these results, the duplication and the triplication start around chr1:225,104,328 and 234,324,641, respectively, and the triplication stops around 240,990,090. Interestingly, the small telomeric duplication, namely, of approximately 3 Kb, which evaded CMA detection, is located between 240,990,090 and 240,993,434, and isoUPD starts around 240,993,434, although the copy number of the distal flanking duplication was not experimentally validated. Therefore, the CGR observed in our case seems to involve triplication with flanking duplications, which has been characterized as a type II triplication proposed by Liu et al. [10] with a particular DUP-TRP/INV-DUP structure, and isoUPD was also reported to be associated with this type of CGR [5]. Notably, all reported cases with triplication with flanking duplications followed by isoUPD have small flanking duplications (<0.258 Mb and <0.004 Mb in proximal and distal duplications, respectively) [5], indicating that our case is the first with a large proximal duplication (approximately 9.2 Mb) in this type of CGR. Microhomology (ATAT) was observed at the jct1 breakpoint interval, whereas a microhomologous sequence with some mismatch sequences including insertions, deletion,

and point mutations was observed at the jct2 breakpoint interval (Fig. 1c). Mismatch sequences only near jct2 of CGR, which might occur during the same event as the *de novo* CGR/isoUPD formation, have previously been reported [5]. These mismatch sequences near to the breakpoint junctions of CGR are proposed to be one of the potential signature features of highly error prone replication-based mechanisms using DNA polymerase(s) of low fidelity or a replisome with reduced fidelity [2], although it remains unclear why mismatch sequences have been observed only in jct2 of CGR/isoUPD cases.

Within the isoUPD region, three genes were associated with four autosomal recessive diseases, as determined by a search of the Online Mendelian Inheritance in Man database (OMIM, <http://www.omim.org>, accessed 1 December, 2016; Additional file 3: Table S3). No phenotypes matching these four diseases were observed in the patient described here, and no pathogenic mutation was found in the three genes by Sanger sequencing. In addition, databases of imprinted genes, such as Geneimprint (<http://www.geneimprint.com/site/genes-by-species>, accessed 1 December, 2016) and the Catalogue of Parent of Origin Effects (<http://igc.otago.ac.nz/home.html>, accessed 1 December, 2016), indicated that there are no known imprinting genes within this isoUPD region.

Discussion

In the case presented here, our comprehensive analyses of all of the cytogenetic, microarray, and sequencing data suggest that the MMBIR-based template-switching model (Fig. 2a) recently proposed by Carvalho et al. [5] is one of the most plausible mechanisms underlying the gain of interstitial copy number followed by distal isoUPD to the telomere, which has not previously been described in the long arm of chromosome 1. In this model, two-step template switches triggered by stalled or collapsed replication forks might have occurred. The first template switch is supposed to use a sister chromatid to resume replication. Microhomology at the annealing site (jct1, Fig. 1c) in the complementary strand close to breakpoint is used to prime DNA synthesis, although it is difficult to determine whether this template switching occurred between c and d_c or d and c_c in our sequencing method. Then, unidirectional replication resumes in an inverted orientation and forms an inverted partially duplicated segment. A new event of fork stalling or collapsing might occur and release a free 3' end, which can be resolved by a second template switch to the homologous chromosome using microhomology again, resulting in the formation of a jct2 (Figs. 1c and 2a). This second compensating inversion might contribute to result in a viable cell. A target annealing site was selected between alleles B and C in the present case, and the derivative chromosome results in a DUP-TRP/INV-DUP structure

with a unique long proximal duplicated region (b and b_c , Fig. 2b). Because BIR cannot account for the observations of microhomology identified in both jct1 and jct2 (Fig. 1c), MMBIR is probably involved in resolving both the first and the second breaks. In our case and some previously reported cases [5], however, various mismatch sequences including insertions, deletions, and/or point mutations around breakpoint junction sequences were observed only in jct2 of CGR and the size of the proximal duplicated region containing jct2 was commonly larger than that of the distal duplicated region containing jct1. Therefore, the accomplishment of the resolution of the second break might need additional mechanisms. It also remains unknown whether those two events occurred either all at once in a post-zygotic mitotic cell or in two steps: the first step occurring in a pre-meiotic cell was resolved by the second step occurring in a post-zygotic cell. These alternatives cannot be distinguished using the current data. In addition, it is also difficult to rule out tissue-specific mosaicism as a post-fertilization mitotic event in this case, although no finding of mosaicism was observed in all data obtained from the peripheral leukocytes/lymphocytes of the patient.

Recently, several cases along with our own with concurrent triplication (tetrasomy) and isoUPD, which may be explained by the MMBIR-based mechanism, detected by CMA containing SNP probes, have been reported [4–7]. However, detailed analyses of centromeric and telomeric junctions of triplicated regions in a tiling array or at the sequence level have only been performed on the cases reported by Carvalho et al. [5] and the present case. In most of those cases with detailed junctional analyses, relatively short flanking duplications were observed. These findings suggest that the small size of flanking duplications might have led to the evasion of array-based detection in three reported cases without detailed junction analyses [4, 6, 7]. Indeed, the concurrent triplication (tetrasomy) and isoUPD were detected by Affymetrix arrays including SNP probes in all cases, but a flanking duplication was observed in this analysis only at the centromeric junction in the present case. In addition, microhomology was observed in breakpoint junctions in most of the cases with the DUP-TRP/INV-DUP rearrangement followed by isoUPD reported by Carvalho et al. [5] and the present case, suggesting that an MMBIR-based mechanism might underline the formation of at least this type of genomic alteration implicated in constitutional disorders. Detailed junction analyses of additional cases showing CGRs + isoUPD will be needed to provide support for an MMBIR-based mechanism inducing complex copy number gains and segmental isoUPD in tandem in subjects with multiple congenital anomalies.

Because partial 1q trisomy is a rare disorder and unbalanced chromosomal translocations are often observed

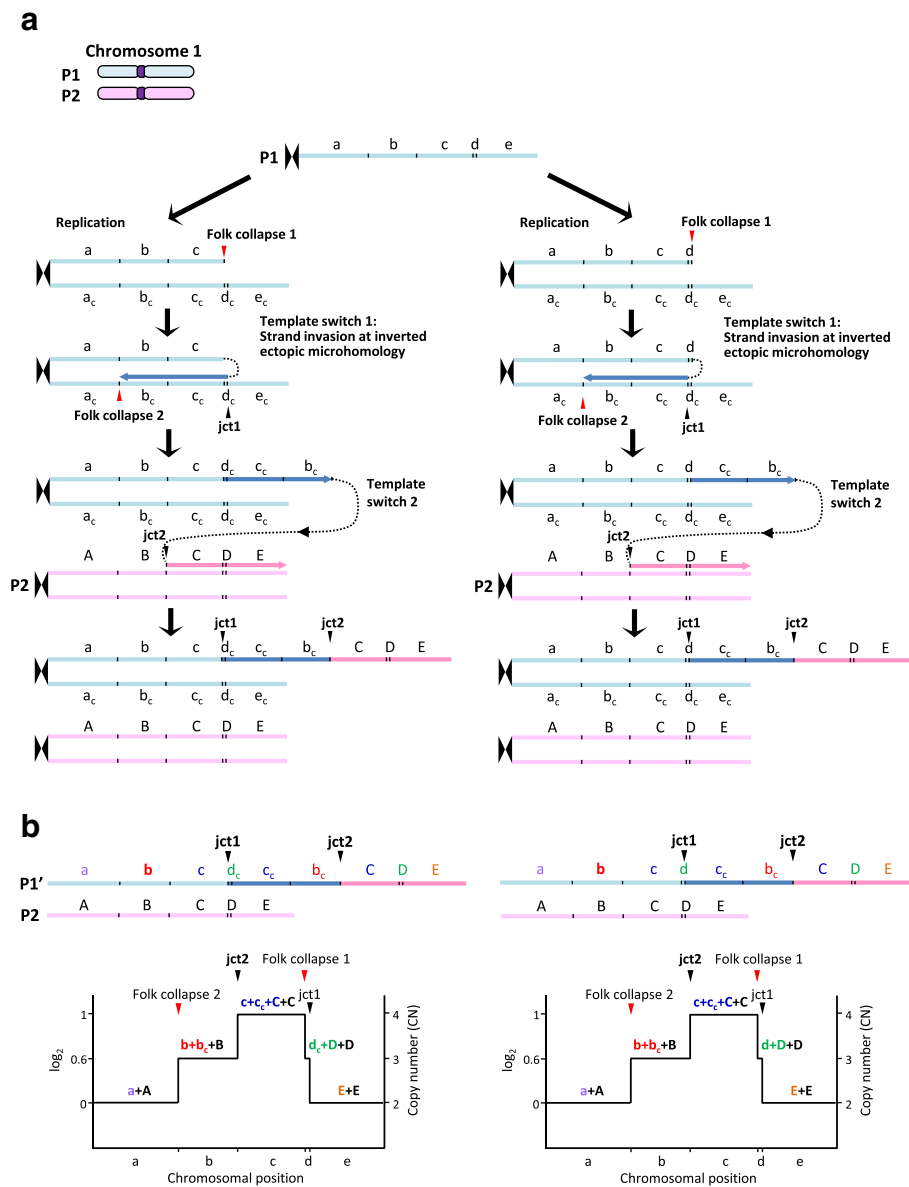


Fig. 2 Replication-based mechanism model for the generation of DUP-TRP/INV-DUP rearrangement followed by isoUPD detected in the present case. **a** The event probably occurred involving parental homolog chromosomes, P1 and P2. The first template switch (template switch 1) have been triggered by a stalled or collapsed replication fork (fork collapse 1), and used a complementary strand to resume replication through using microhomology in the complementary strand at the annealing site (jct1, Fig. 1c) to prime DNA synthesis, resulting in the production of a segment with the inverse orientation compared with the reference genome. Two putative jct1 sites, jct1 between c and d_c (left) and jct1 between d and d_c (right) are predicted, because the same sequence result can be obtained in both cases (see Fig. 1c). Then, a new fork stalling or collapsing event (fork collapse 2) have released a free 3' end that can be resolved by the second template switching (template switch 2) through using the microhomology in the homologous chromosome at the annealing site (jct2, Fig. 1c) to prime and resume DNA synthesis, resulting in the generation of jct2 as well as isoUPD. a–d, representative chromosome alleles in P1 chromosome; a_c–e_c, complementary chromosome alleles in P1 chromosome; A–E: corresponding homologous chromosome alleles in the P2 chromosome. **b** *Top*: different genomic structures are predicted to be generated depending on the location of the selected annealing site (jct1) to prime DNA synthesis in the first template switch event. isoUPD will result if the unidirectional replication fork continues until the telomere. *Bottom*: predicted segmental CNV in a simulated CMA. Note that the small size of the telomeric duplication between fork collapse 1 and jct1 led to the evasion of CMA detection (Fig. 1a), because the region was too small to be detected by Affymetrix Cytoscan HD array

with this alteration [11–16], it is difficult to evaluate the contribution of 1q trisomy to the phenotype in cases involving another chromosome. Patients with pure

partial distal trisomy 1q are known to demonstrate a wide range of manifestations of variable severity. However, distal 1q duplication syndrome is characterized by the

signs present in many of the previously reported cases [15, 16]. The present case showed some of the symptoms characteristic of distal 1q duplication syndrome, such as psychomotor developmental delay, cardiac defect, widely spaced eyes, a down-slanted palpebral fissure, low-set ear, a prominent forehead, club feet, and scoliosis, although psychomotor developmental delay and cardiac defect were very severe compared with those in previously reported cases and some features commonly found elsewhere were not observed [15, 16]. Because the present patient is the first known case of pure distal partial 1q tetrasomy and trisomy, it is possible that the copy number increase in some of the genes located between 1q42.12 and the middle of 1q43 (approximately 180 RefSeq genes) contributes to these symptoms, although no causal regions responsible for each symptom of distal trisomy/tetrasomy 1 syndrome have been clarified. In addition, the influence of isoUPD on the clinical features of the present case remains unknown because of a lack of reported cases with distal 1q UPD.

Conclusions

We report the first case with concurrent CGR (duplications and triplication) + isoUPD in 1q42.12-qter, from an initial diagnosis of interstitial trisomy 1q by conventional karyotyping. Comprehensive cytogenetic and molecular analyses provide additional evidence that DUP-TRP/INV-DUP rearrangement having a unique long proximal DUP structure followed by isoUPD may be generated by an MMBIR-based mechanism. Because it is almost impossible to quantify precise chromosomal copy numbers and detect UPD by conventional karyotyping, molecular cytogenetic analyses using CMA containing SNP probes with additional detailed analyses of the breakpoint junctions in a sequence level are recommended in cases suspected of having complex chromosomal abnormalities based on clinical and cytogenetic findings.

Additional files

Additional file 1: Table S1. BAC clones used in FISH experiments. (DOCX 14 kb)

Additional file 2: Table S2. List of primer sets used in PCR and sequencing for junctions of the CGR. (DOCX 14 kb)

Additional file 3: Table S3. Autosomal recessive diseases and causative genes around the isoUPD region. (DOCX 14 kb)

Abbreviations

BAC: Bacterial artificial chromosome; CGR: Complex genomic rearrangements; CMA: Chromosomal microarray; CNV: Copy number variation; DUP-TRP/INV-DUP: Duplication-inverted triplication-duplication; FISH: Fluorescence *in situ* hybridization; isoUPD: Uniparental isodisomy; IUGR: Intrauterine growth retardation; MCA: Multiple congenital anomalies; MMBIR: Microhomology-mediated break-induced replication; PCR: Polymerase chain reaction; SNP: Single-nucleotide polymorphism; TOF: Tetralogy of Fallot

Acknowledgements

We thank the patient and his mother for their participation in this study and the Support Center for Advanced Medical Sciences, Graduate School of Biomedical Sciences, Tokushima University for technical assistances. This work was partly performed in the Cooperative Research Project Program of the Medical Institute of Bioregulation, Kyushu University.

Funding

This study was supported by JSPS KAKENHI Grant Numbers 26293304, 16K15618, and 15K19620 from the Ministry of Education, Culture, Sports, Science and Technology, Japan, and there is no role for funding agent in this study.

Availability of data and materials

The datasets supporting the conclusions of this article are included within the article and its additional file. More details are available on request.

Authors' contributions

TK, NO, and TN performed the genetic analysis and drafted the paper. CM performed the FISH experiments. YO, NF, and HI performed the genetic analysis. SS and NO collected the data of the patient. MS, KM, and HK contributed in writing the manuscript. II performed CMA, contributed in writing the manuscript, and supervised the study. All the authors have read and approved the final manuscript.

Competing interests

The authors declare that they have no competing interests.

Consent for publication

Mother of the patient has given her informed written consent for publication of the present case report.

Ethics approval and consent to participate

The research protocol for this study was approved by the local ethics committee of Tokushima University. Written informed consent for the participation of the patient in this study was obtained from the patient's mother.

Publisher's Note

Springer Nature remains neutral with regard to jurisdictional claims in published maps and institutional affiliations.

Author details

¹Department of Human Genetics, Graduate School of Biomedical Sciences, Tokushima University, 3-18-15 Kuramoto-cho, Tokushima 770-8503, Japan. ²Department of Oral and Maxillofacial Surgery, Kobe University Graduate School of Medicine, 7-5-1 Kusunoki-cho, Chuo-ku, Kobe, Hyogo 650-0017, Japan. ³Division of Molecular Genetics, Institute for Comprehensive Medical Science, Fujita Health University, 1-98 Dengakugakubo Kutsukake-cho, Toyoake, Aichi 470-1192, Japan. ⁴Japanese Red Cross Tokushima Hinomine Rehabilitation Center for People with Disabilities, 4-1 Shinkai Chuden-cho, Komatsushima, Tokushima 773-0015, Japan. ⁵Department of Medical Genetics, Osaka Medical Center and Research Institute for Maternal and Child Health, 840 Murodo-cho, Izumi, Osaka 594-1101, Japan.

Received: 15 March 2017 Accepted: 21 April 2017

Published online: 28 April 2017

References

- Zhang F, Carvalho CM, Lupski JR. Complex human chromosomal and genomic rearrangements. *Trends Genet.* 2009;25:298–307.
- Carvalho CM, Pehlivan D, Ramocki MB, Fang P, Alleva B, Franco LM, et al. Replicative mechanisms for CNV formation are error prone. *Nat Genet.* 2013;45:1319–26.
- Beneteau C, Landais E, Doco-Fenzy M, Gavazzi C, Philippe C, Béri-Dexheimer M, et al. Microtriplication of 11q24.1: a highly recognisable phenotype with short stature, distinctive facial features, keratoconus, overweight, and intellectual disability. *J Med Genet.* 2011;48:635–9.
- Fujita A, Suzumura H, Nakashima M, Tsurusaki Y, Saito H, Harada N, et al. A unique case of de novo 5q33.3-q34 triplication with uniparental isodisomy of 5q34-qter. *Am J Med Genet A.* 2013;161A:1904–9.

5. Carvalho CM, Pfundt R, King DA, Lindsay SJ, Zuccherato LW, Macville MV, et al. Absence of heterozygosity due to template switching during replicative rearrangements. *Am J Hum Genet.* 2015;96:555–64.
6. Sahoo T, Wang JC, Elnaggar MM, Sanchez-Lara P, Ross LP, Mahon LW, et al. Concurrent triplication and uniparental isodisomy: evidence for microhomology-mediated break-induced replication model for genomic rearrangements. *Eur J Hum Genet.* 2015;23:61–6.
7. Xiao B, Xu H, Ye H, Hu Q, Chen Y, Qiu W. De novo 11q13.4q14.3 tetrasomy with uniparental isodisomy for 11q14.3qter. *Am J Med Genet A.* 2015;167A:2327–33.
8. Wiszniewska J, Bi W, Shaw C, Stankiewicz P, Kang SH, Pursley AN, et al. Combined array CGH plus SNP genome analyses in a single assay for optimized clinical testing. *Eur J Hum Genet.* 2014;22:79–87.
9. Murata C, Kuroki Y, Imoto I, Tsukahara M, Ikejiri N, Kuroiwa A. Initiation of recombination suppression and PAR formation during the early stages of neo-sex chromosome differentiation in the Okinawa spiny rat, *Tokudaia muenninki*. *BMC Evol Biol.* 2015;15:234.
10. Liu P, Carvalho CM, Hastings PJ, Lupski JR. Mechanisms for recurrent and complex human genomic rearrangements. *Curr Opin Genet Dev.* 2012;22:211–20.
11. Nowaczyk MJ, Bayani J, Freeman V, Watts J, Squire J, Xu J. De novo 1q32q44 duplication and distal 1q trisomy syndrome. *Am J Med Genet A.* 2003;120A:229–33.
12. Coccé MC, Villa O, Obregon MG, Salido M, Barreiro C, Solé F, Gallego MS. Duplication dup(1)(q41q44) defined by fluorescence in situ hybridization: delineation of the 'trisomy 1q42- > qter syndrome'. *Cytogenet Genome Res.* 2007;118:84–6.
13. Kulikowski LD, Bellucco FT, Nogueira SI, Christofolini DM, Smith Mde A, de Mello CB, et al. Pure duplication 1q41-qter: further delineation of trisomy 1q syndromes. *Am J Med Genet A.* 2008;146A:2663–7.
14. Balasubramanian M, Barber JC, Collinson MN, Huang S, Maloney VK, Bunyan D, Foulds N. Inverted duplication of 1q32.1 to 1q44 characterized by array CGH and review of distal 1q partial trisomy. *Am J Med Genet A.* 2009;149A:793–7.
15. Watanabe S, Shimizu K, Ohashi H, Kosaki R, Okamoto N, Shimojima K, et al. Detailed analysis of 26 cases of 1q partial duplication/triplication syndrome. *Am J Med Genet A.* 2016;170A:908–17.
16. Morris ML, Baroneza JE, Teixeira P, Medina CT, Cordoba MS, Versiani BR, Roese LL, Freitas EL, Fonseca AC, Dos Santos MC, Pic-Taylor A, Rosenberg C, Oliveira SF, Ferrari I, Mazzeu JF. Partial 1q duplications and associated phenotype. *Mol Syndromol.* 2016;6:297–303.

Submit your next manuscript to BioMed Central and we will help you at every step:

- We accept pre-submission inquiries
- Our selector tool helps you to find the most relevant journal
- We provide round the clock customer support
- Convenient online submission
- Thorough peer review
- Inclusion in PubMed and all major indexing services
- Maximum visibility for your research

Submit your manuscript at
www.biomedcentral.com/submit



1 Disruption of the Responsible Gene 2 in a Phosphoglucomutase 1 Deficiency Patient 3 by Homozygous Chromosomal Inversion

4 Katsuyuki Yokoi · Yoko Nakajima · Tamae Ohye ·
5 Hidehito Inagaki · Yoshinao Wada · Tokiko Fukuda ·
6 Hideo Sugie · Isao Yuasa · Tetsuya Ito ·
7 Hiroki Kurahashi

Received: 13 February 2018 / Revised: 06 April 2018 / Accepted: 10 April 2018
8 © Society for the Study of Inborn Errors of Metabolism (SSIEM) 2018

9 **Abstract** Phosphoglucomutase 1 (PGM1) deficiency is a
10 recently defined disease characterized by glycogenosis and
11 a congenital glycosylation disorder caused by recessive
12 mutations in the *PGM1* gene. We report a case of a 12-year-
13 old boy with first-cousin parents who was diagnosed with a
14 PGM1 deficiency due to significantly decreased PGM1
15 activity in his muscle. However, Sanger sequencing

revealed no pathogenic mutation in the *PGM1* gene in this 16
patient. As this case presented with a cleft palate in addition 17
to hypoglycemia and elevated transaminases and creatine 18
kinase, karyotyping was performed and identified homozy- 19
gous *inv(1)(p31.1p32.3)*. Based on the chromosomal 20
location of the *PGM1* gene at 1p31, we analyzed the 21
breakpoint of the inversion. Fluorescence in situ hybrid- 22
ization (FISH) combined with long PCR analysis revealed 23
that the inversion disrupts the *PGM1* gene within intron 1. 24
Since the initiation codon in the *PGM1* gene is located 25
within exon 1, we speculated that this inversion inactivates 26
the *PGM1* gene and was therefore responsible for the 27
patient's phenotype. When standard molecular testing fails 28
to reveal a mutation despite a positive clinical and 29
biochemical diagnosis, the presence of a gross structural 30
variant that requires karyotypic examination must be 31
considered. 32

Communicated by: Eva Morava, MD PhD

K. Yokoi · Y. Nakajima · T. Ito
Department of Pediatrics, Fujita Health University School of
Medicine, Toyoake, Japan

K. Yokoi · T. Ohye · H. Inagaki · H. Kurahashi (✉)
Division of Molecular Genetics, Institute for Comprehensive Medical
Science, Fujita Health University, Toyoake, Japan
e-mail: kura@fujita-hu.ac.jp

Y. Wada
Department of Obstetric Medicine, Osaka Women's and Children's
Hospital, Osaka, Japan

T. Fukuda
Department of Pediatrics, Hamamatsu University School of Medicine,
Hamamatsu, Japan

H. Sugie
Faculty of Health and Medical Sciences, Tokoha University,
Hamamatsu, Japan

I. Yuasa
Division of Legal Medicine, Tottori University Faculty of Medicine,
Yonago, Japan

H. Kurahashi
Genome and Transcriptome Analysis Center, Fujita Health University,
Toyoake, Japan

H. Kurahashi
Center for Collaboration in Research and Education, Fujita Health
University, Toyoake, Japan

Introduction 34

Phosphoglucomutase 1 (PGM1) deficiency is a recently 35 [AU2](#)
defined disease, characterized by glycogenosis and a 36
congenital disorder of glycosylation (CDG) (Tagtmeyer 37
et al. 2014). ζ PGM1 deficiency is rare with only 38
patients from 29 families with different ethnic backgrounds 39
described in the literature so far (Perez et al. 2013; 40
Ondruskova et al. 2014; Tagtmeyer et al. 2014; Loewenthal 41
et al. 2015; Zeevaert et al. 2016; Wong et al. 2016; Preisler 42
et al. 2017; Nolting et al. 2017; Voermans et al. 2017). 43
PGM1 is an essential enzyme in carbohydrate biosynthesis 44
and metabolism and functions both in glycogen synthesis 45
and breakdown through a reversible conversion of glucose 46

47 1-phosphate to glucose 6-phosphate (Morava 2014). Since
48 glucose 1-phosphate is a precursor of the nucleotide sugars
49 used for glycan biosynthesis, PGM1 activity is also
50 required for protein *N*-glycosylation (Beamer 2015). Hence,
51 PGM1 deficiency has considerably diverse phenotypes.
52 Most of the affected patients develop a congenital anomaly
53 syndrome showing a bifid uvula, cleft palate, and Pierre
54 Robin sequence as clinical manifestations from the time of
55 birth. Hepatopathy, dilated cardiomyopathy (DCM), hypo-
56 glycemia, muscle weakness, exercise intolerance, growth
57 retardation, and endocrine abnormalities emerge in these
58 cases over time (Scott et al. 2014). Many of these
59 manifestations can be linked to the role of PGM1 in
60 glucose metabolism and glycosylation (Beamer 2015).

61 PGM1 deficiency is caused by homozygous or com-
62 pound heterozygous nucleotide alterations in the *PGM1*
63 gene (Herbich et al. 1985). Several types of mutations have
64 been reported to date including missense mutations, frame-
65 shifts, and splicing mutations (Tagtmeyer et al. 2014; Lee
66 et al. 2014; Perez et al. 2013; Timal et al. 2012; Stojkovic
67 et al. 2009; Ondruskova et al. 2014). In our current report,
68 we describe a case of PGM1 deficiency caused by a
69 homozygous chromosomal inversion that disrupts the
70 *PGM1* gene at chromosome 1p31.

71 Materials and Methods

72 Cytogenetic Analysis

73 Fluorescence in situ hybridization (FISH) analysis of the
74 patient and his parents was performed using standard
75 methods to detect the breakpoint region at the chromosome
76 level. Briefly, phytohemagglutinin-stimulated lymphocytes
77 or Epstein-Barr virus-transformed lymphoblastoid cell lines
78 derived from the subjects were arrested by exposure to
79 colcemid. Metaphase preparations were then obtained by
80 hypotonic treatment with 0.075 M KCl followed by
81 methanol/acetate fixation. A bacterial artificial clone
82 (BAC) containing 1p31.1, RP4-534K7 (chr1:63,525,021-
83 63,677,603), was used as the test probe, and a chromosome
84 1 centromere probe (CEN1 SpectrumOrange Probe; Abbott
85 Laboratories, Abbott Park, IL) was used as a reference. The
86 probes were labeled by nick translation with digoxigenin-
87 11-dUTP. After hybridization, the probes were detected
88 with DyLight 488 Anti-Digoxigenin/Digoxin. Chromo-
89 somes were visualized by counterstaining with 4;6-
90 diamino-2-phenylindole.

91 Sequence Analysis

92 To isolate the breakpoint, long-range PCR with several sets
93 of primers for the *PGM1* gene was performed using LA Taq
94 (TaKaRa, Shiga, Japan) (Fig. 3c). The PCR conditions were

35 cycles of 10 s at 98°C and 15 min at 60°C. PCR primers 95
were designed using sequence data from the human 96
genome database. PCR products were separated on 0.8% 97
(w/v) agarose gels and visualized with ethidium bromide. 98
The homology between the obtained sequence around the 99
breakpoint within the *PGM1* gene and the 1p32.3 sequence 100
obtained from the database was examined using the BLAT 101
in UCSC genome browser (<http://genome-asia.ucsc.edu/human GRCh38/hg38>). 102
103

Patient 104

The current study patient was a 12-year-old boy from 105
consanguineous parents who are first cousins without a 106
family history of congenital metabolic disease (Fig. 1). The 107
patient's height was 137 cm (*z*-score -2.3), and he had a 108
normal body weight of 39 kg (*z*-score -0.6). He was born 109
at term with a normal body weight and length. A cleft 110
palate was noted at birth and closure surgery was performed 111
at 12 months. Persistently elevated transaminases (AST 112
50–400 U/L [normal value <33 U/L] and ALT 113
40–300 U/L [normal value <30 U/L]) had been observed 114
since that surgery. In addition, mild hypoglycemia 115
after overnight fasting and an occasionally elevated serum 116
creatinine kinase (100–2,600 U/L [normal value <287 U/L]) 117
were evident from 2 years of age. The echocardiogram and 118
electrocardiogram readings showed no abnormalities, and 119
his psychomotor development was normal. Oral adminis- 120
tration of uncooked corn starch prior to bedtime was 121
commenced to prevent morning hypoglycemia. 122

At 2 years of age, the patient was referred to our 123
department for further examination. Intravenous glucose 124
loading at 2 g/kg led to an elevated lactate level (from 7 to 125
37 mg/dL at 120 min) with a normal lactate/pyruvate ratio. 126
Intramuscular glucagon loading at 0.03 mg/kg caused no 127
increase of blood sugar either during fasting or at 2 h after a 128
meal, indicating a deficiency in the generation of hepatic 129
glucose from glycogen. However, the activity of the 130
debrancher enzyme responsible for glycogen storage dis- 131
ease (GSD) type III, phosphorylase involved in GSD type 132
VI, and phosphorylase kinase enzyme associated with GSD 133
type IX in the peripheral blood was normal. A forearm 134
nonischemic exercise test was performed when the patient 135
was 8 years old. No increase in venous lactate with a large 136
elevation in his ammonia levels (297 μ g/dL) was observed, 137
suggesting inadequate glycogen utilization in the muscle. A 138
muscle biopsy was therefore performed, and a significant 139
decrease in PGM activity was identified (62.1 nmol/min/mg 140
[controls 351.1 ± 81.1]). Isoelectric focusing (IEF) of 141
serum transferrin was performed as previously described 142
(Okanishi et al. 2008) and revealed a mixed type I and 143
type II pattern, typical features of CDG-I and CDG-II 144
(Fig. 2) (Tagtmeyer et al. 2014). 145

AU3

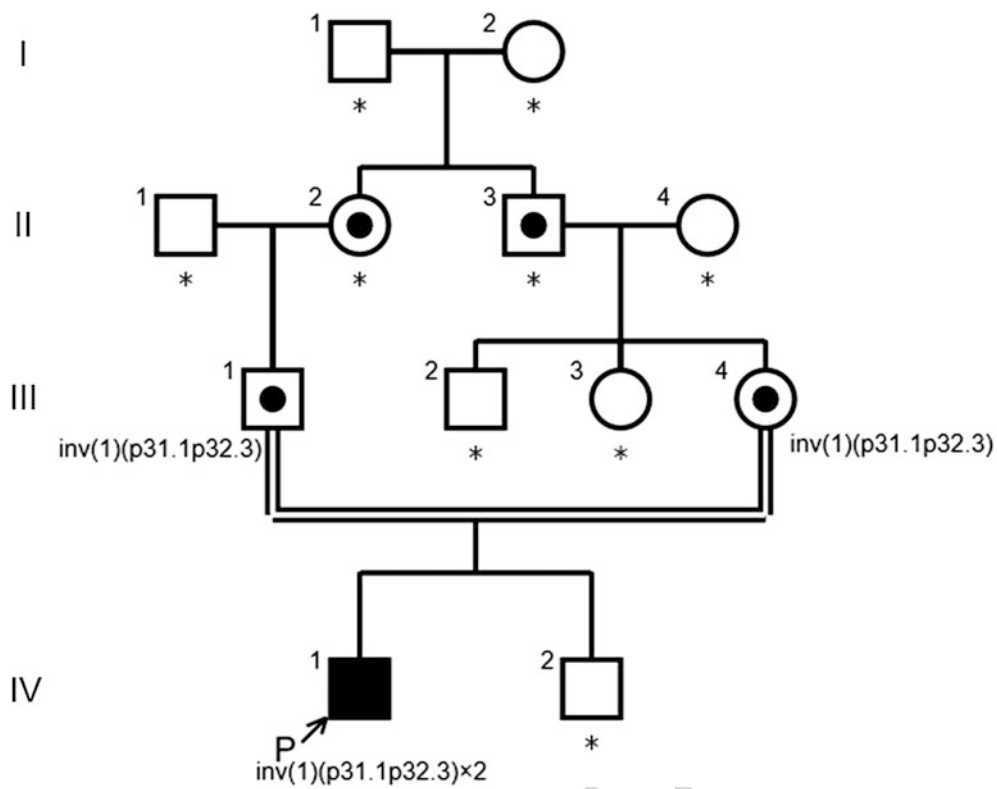


Fig. 1 Pedigree of the family. Arrow indicates proband. Carriers are represented by a dot in the middle of circles or squares. Asterisks indicate the family members who have not been tested

AU4

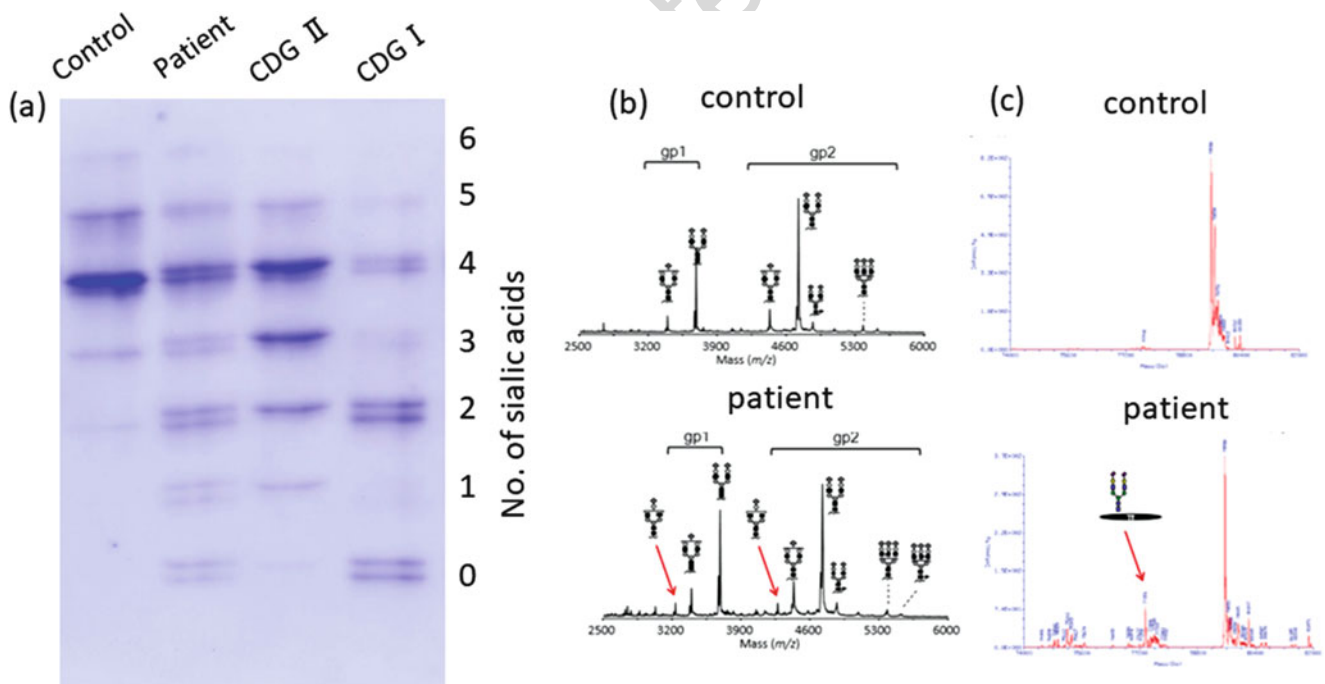


Fig. 2 Serum transferrin isoelectric focusing (IEF) and mass spectrometry (MS) of serum glycoproteins. **(a)** IEF patterns of serum transferrin. The number of negatively charged sialic acids of transferrin is indicated on the right. Reduced glycosylation of transferrin including an unusual mixture of CDG-I and CDG-II patterns (increased tri-, di-, mono-, and asialotransferrin) is shown.

(b) Matrix-assisted laser desorption/ionization (MALDI) mass spectrum of (glycol) tryptic peptides of transferrin. A biantennary glycan lacking galactose and sialic acid are observed in patient's transferrin (arrows). **(c)** Electrospray ionization (ESI) mass spectrum of transferrin. An abnormal transferrin isoform having a single glycan is present in the patient (arrow)

146 Mass spectrometry to characterize the molecular abnormality of transferrin was performed as previously described
 147 (Wada 2016) and further revealed the presence of a variety
 148 of transferrin glycoforms, including forms lacking one or
 149 both glycans as well as forms with truncated glycan
 150 (Fig. 2). These findings were consistent with a *PGM1*
 151 deficiency (Tagtmeyer et al. 2014), and genetic analysis
 152 was performed to confirm this. Sanger sequencing revealed
 153 only c.1258T>C, a common polymorphism in the database.
 154 The karyotype of the patient was determined to be 46,XY,
 155 inv(1)(p31.1p32.3)x2, of which inv(1) was homozygous
 156 (Fig. 3a). Since the *PGM1* gene is localized at 1p31, we
 157 hypothesized that the inversion disrupts this gene in our
 158 patient, and we thus analyzed its distal breakpoint.

160 Results

161 FISH signals for the BAC RP4-534K7 probe that incorpo-
 162 rates the entire *PGM1* gene are observed on the short arm

of chromosome 1 in an individual with a normal karyotype. 163
 In our current study patient however, two distinct signals 164
 were detected on the short arm of both chromosome 1 165
 homologues (Fig. 3b). This result indicated that the 166
 inversion breakpoint in the patient had disrupted the 167
PGM1 genomic region. Karyotype analysis of both parents 168
 showed 46,XY,inv(1)(p31.1p32.3). Both parents carried the 169
 inv(1) in a heterozygous state, suggesting that the two 170
 inv(1) homologues of the patient had been transmitted from 171
 each parent, respectively (data not shown). 172

Long PCR revealed that one of the PCR primer pairs 173
 (4F-4R) within intron 1 failed to amplify the products in the 174
 patient DNA, indicating that the breakpoint of the inversion 175
 was located in intron 1 (Fig. 3d). To analyze the breakpoint 176
 region in more detail, we performed additional long PCR. 177
 The 4F4-4R but not the 4F3-4R primer pair successfully 178
 yielded a PCR product. This indicated that the breakpoint 179
 was located between primer 4F3 and 4F4. We did not 180
 obtain the sequence of the other breakpoint region at 181

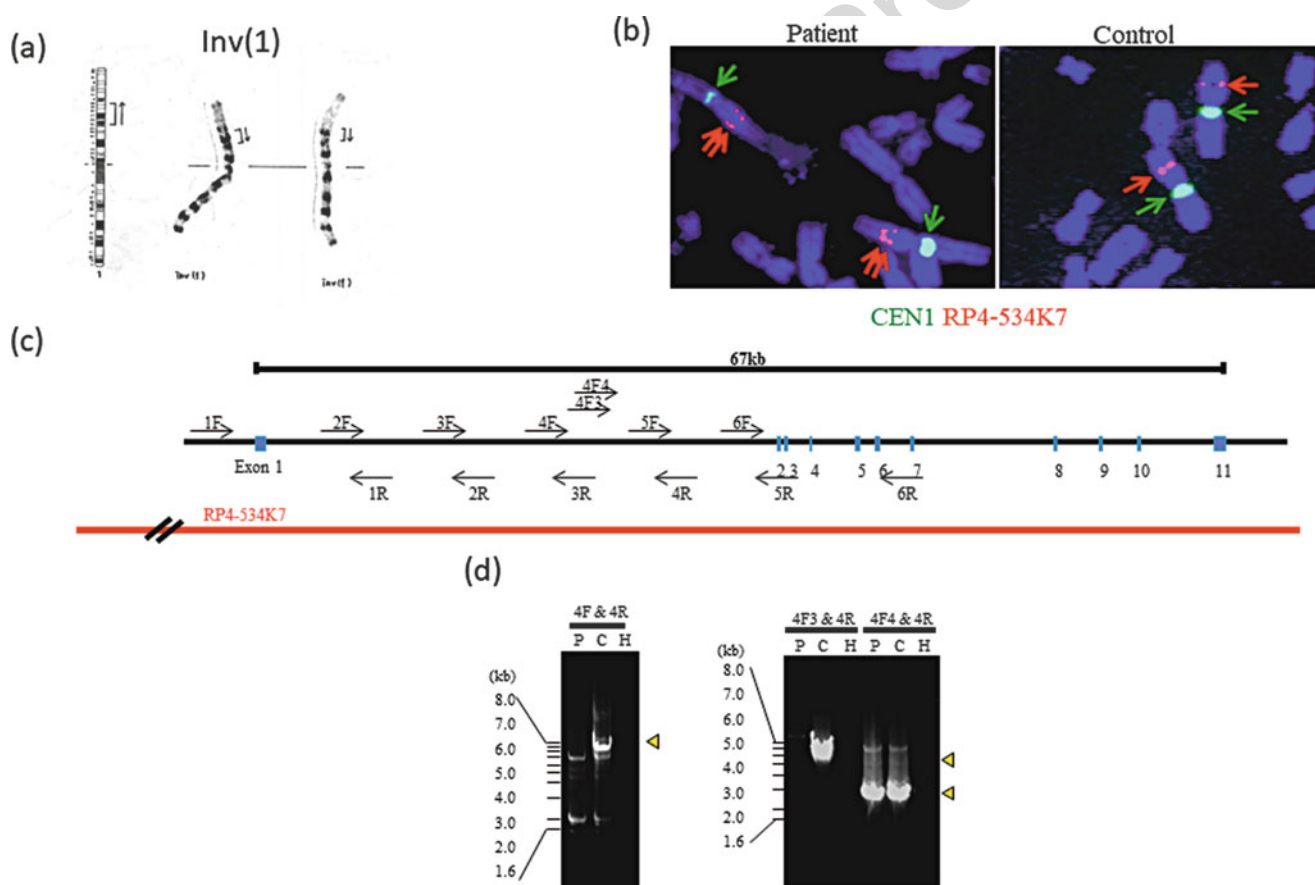


Fig. 3 Disruption of the *PGM1* gene in the study patient by a chromosomal inversion. (a) G-banding of the patient's karyotype which was determined to be 46,XY,inv(1)(p31.1p32.3)x2, in which inv(1) was homozygous. (b) FISH signals for *PGM1* (red arrow) are typically observed on the short arm of chromosome 1 in a normal karyotype. In contrast, the two distinctive signals were detected on the

chromosome 1 arm in the study patient. (c) Schematic representation of the *PGM1* gene structure. The blue boxes denote exons. The positions of the PCR primers are indicated by arrows. The position of the BAC probe is also indicated. (d) Agarose gel electrophoresis of long PCR products. 4F-4R and 4F3-4R primer pairs failed to amplify the PCR products in the study patient. *P* patient, *C* control, *H* H₂O

182 1p32.3. To ascertain the mechanism leading to the
183 inversion, we obtained the sequence information of the
184 1p32.3 from the database and analyzed the homology with
185 the 4F3-4F4 sequence. However, we did not find any
186 sequence similarity between the 4F3-4F4 sequence and the
187 genomic sequence at 1p32.3.

188 Discussion

189 PGM1 deficiency is a newly identified metabolic disorder
190 which manifests features of both CDG and glycogenosis
191 (Tagtmeyer et al. 2014). Our present case report describes a
192 young male patient with PGM1 deficiency caused by a
193 homozygous *inv(1)* inherited from his first-cousin parents
194 that disrupts each of the two *PGM1* alleles. To date, 38
195 PGM1 deficiency patients have been reported, and patho-
196 genic mutations in the *PGM1* gene were identified and
197 genetically confirmed in most of these cases (Perez et al.
198 2013; Ondruskova et al. 2014; Tagtmeyer et al. 2014;
199 Loewenthal et al. 2015; Zeevaert et al. 2016; Wong et al.
200 2016; Preisler et al. 2017; Nolting et al. 2017; Voermans
201 et al. 2017). However, a small subset of patients exists
202 without mutations in the *PGM1* gene. In our present case,
203 Sanger sequencing did not identify any pathogenic muta-
204 tion in the *PGM1* gene initially. However, subsequent
205 chromosome karyotyping of our patient detected the
206 presence of multiple congenital malformations and led to
207 the identification of the aforementioned chromosomal
208 inversion as the responsible mutation for his condition.
209 Hence, when standard molecular testing does not reveal any
210 abnormalities in patients who have been clinically and
211 biochemically diagnosed with a known congenital disorder,
212 chromosome testing may be a fruitful approach for
213 identifying the responsible mutation in the candidate gene.

214 In mutational screening for single-gene disorders involv-
215 ing an autosomal recessive inheritance of a known
216 causative gene, it is often the case that only one of the
217 recessive mutations is identified. If standard PCR and
218 Sanger methods fail to identify two pathogenic mutations
219 within the exons or flanking intronic regions of the
220 responsible gene, a subsequent approach can be MLPA
221 (multiplex ligation-dependent probe amplification) analysis
222 of structural variant copy number variations or repeat PCR/
223 Sanger analysis to identify possible mutations in noncoding
224 regions such as the promoter or enhancer. In addition to
225 these methods, standard chromosomal karyotyping is
226 important for identifying large-scale chromosomal abnor-
227 malities that may disrupt the causative gene.

228 A possible mechanism of inversion formation is inter-
229 spersed repeat sequences that may induce chromosomal
230 aberrations. Direct repeats can induce deletions or duplications

via recombination between them, whereas inverted repeats
231 sometimes cause pericentric or paracentric inversion (Lakich
232 et al. 1993). In our present case, we didn't find any specific
233 segmental duplication sequences at the breakpoint region
234 within the intron of the *PGM1* gene. Likewise, there was no
235 evidence of segmental duplication sequences that were
236 common to the proximal and distal breakpoint regions. Our
237 patient harbored a rare homozygous pericentric inversion of
238 chromosome 1 inherited from first-cousin parents. We assume
239 therefore that the inversion chromosome in this patient is rare
240 in the general population and is not a recurrent type variation.

242 Since the initiation codon in the *PGM1* gene is located
243 within exon 1, the inversion in our patient that disrupts
244 intron 1 produces a truncated protein containing only the
245 amino acids encoded by exon 1 or no protein product at all
246 due to nonsense-mediated mRNA decay. The crystal
247 structure of human PGM1 has not been characterized, but
248 the structure of the analogous PGM from rabbit has been
249 described (Liu et al. 1997). Because of the high amino acid
250 sequence identity (97%) between these two proteins, the
251 rabbit PGM structure provides a highly accurate model for
252 the human enzyme. PGM1 is a monomeric protein of 562
253 amino acids and 4 structural domains (Beamer 2015). The
254 active site is located in a large, centrally located cleft and
255 can be segregated into four highly conserved regions which
256 are located behind exon 2. In our present case therefore,
257 even if a truncated protein was produced, it would have no
258 active site, and PGM1 deficiency would still arise. Further,
259 we performed RT-PCR using the patient's peripheral blood.
260 The exon 1 transcript was found to be present, but we did
261 not find any transcripts distal to the exon 2 (data not
262 shown). Some residual enzymatic activity might be possi-
263 bly due to other members of phosphoglucomutase family,
264 PGM2 and PGM3, that could compensate the PGM1
265 activity (Maliekal et al. 2007; Wong et al. 2016).

266 In conclusion, we have identified and analyzed an
267 inverted chromosome from a PGM1 deficiency patient.
268 Our present report also emphasizes the potential benefits of
269 karyotype analysis in congenital cases in which molecular
270 genetic testing fails to identify the responsible mutations.

271 **Acknowledgments** We thank the patient and his family for their
272 participation in this study. We also thank past and present members of
273 our laboratory. This research was partly supported by the intramural
274 research grant (29-4) for Neurological and Psychiatric Disorders of
275 NCNP (H. Sugie).
276

277 Synopsis Sentence

278 Karyotypic examination must be considered when standard
279 molecular testing fails to reveal a mutation despite a
280 positive clinical and biochemical diagnosis.

281 **Conflict of Interest**

282 Katsuyuki Yokoi, Yoko Nakajima, Ohye Tamae, Hidehito
283 Inagaki, Yoshinao Wada, Tokiko Fukuda, Hideo Sugie, Isao
284 Yuasa, Tetsuya Ito, and Hiroki Kurahashi declare that they
285 have no conflict of interest.

286 **Informed Consent**

287 All procedures followed were in accordance with the ethical
288 standards of the responsible committee on human experi-
289 mentation (institutional and national) and with the Helsinki
290 Declaration of 1975, as revised in 2005(5). Informed
291 consent was obtained from all patients for inclusion in the
292 study.

293 **Author Contributions**

294 Katsuyuki Yokoi retrieved the data and drafted and revised
295 the manuscript.

296 Yoko Nakajima and Tetsuya Ito discovered the patients
297 and provided many data.

298 Tamae Ohye did cytogenetic analysis and sequence
299 analysis.

300 Hidehito Inagaki supported and supervised experiments.

301 Yoshinao Wada did mass spectrometry.

302 Tokiko Fukuda and Hideo Sugie estimated enzyme
303 activity.

304 Isao Yuasa did IEF of serum transferrin.

305 Hiroki Kurahashi: conception and design, analysis and
306 interpretation, and revising the article critically for impor-
307 tant intellectual content.

308 All authors contributed to and reviewed the manuscript.

309 **References**

- 310 Beamer LJ (2015) Mutations in hereditary phosphoglucomutase 1
311 deficiency map to key regions of enzyme structure and function.
312 *J Inherit Metab Dis* 38:243–256
- 313 Herbich J, Szilvassy J, Schnedl W (1985) Gene localisation of the
314 PGM1 enzyme system and the Duffy blood groups on chromo-
315 some no. 1 by means of a new fragile site at 1p31. *Hum Genet*
316 70:178–180
- 317 Lakich D, Kazazian HH Jr, Antonarakis SE, Gitschier J (1993)
318 Inversions disrupting the factor VII gene are a common cause of
319 severe haemophilia A. *Nat Genet* 5:236–241

- Lee Y, Stiers KM, Kain BN, Beamer LJ (2014) Compromised
catalysis and potential folding defects in in vitro studies of
missense mutants associated with hereditary phosphoglucomu-
tase 1 deficiency. *J Biol Chem* 289:32010–32019
- Liu Y, Ray W, Baranidharan S (1997) Structure of rabbit muscle
phosphoglucomutase refined at 2.4 Å resolution. *Acta Crystallogr*
D 53:392–405
- Loewenthal N, Haim A, Parvari R, HersHKovitz E (2015) Phospho-
glucomutase-1 deficiency: intrafamilial clinical variability and
common secondary adrenal insufficiency. *Am J Med Genet A*
167A:3139–3143
- Maliekal P, Sokolova T, Vertommen D, Veiga-da-Cunha M, Van
Schaftingen E (2007) Molecular identification of mammalian
phosphopentomutase and glucose-1,6-bisphosphate synthase, two
members of the alpha-D-phosphohexomutase family. *J Biol*
Chem 282:31844–31851
- Morava E (2014) Galactose supplementation in phosphoglucomutase-
1 deficiency; review and outlook for a novel treatable CDG. *Mol*
Genet Metab 112:275–279
- Nolting K, Park JH, Tegtmeyer LC et al (2017) Limitations of
galactose therapy in phosphoglucomutase 1 deficiency. *Mol*
Genet Metab Rep 13:33–40
- Okanishi T, Saito Y, Yuasa I et al (2008) Cutis laxa with frontoparietal
cortical malformation: a novel type of congenital disorder of
glycosylation. *Eur J Paediatr Neurol* 12:262–265
- Ondruskova N, Honzik T, Vondrackova A, Tesarova M, Zeman J,
Hanskova H (2014) Glycogen storage disease-like phenotype
with central nervous system involvement in a PGM1-CDG
patient. *Neuro Endocrinol Lett* 35:137–141
- Perez B, Medrano C, Ecay MJ et al (2013) A novel congenital
disorder of glycosylation type without central nervous system
involvement caused by mutations in the phosphoglucomutase 1
gene. *J Inherit Metab Dis* 36:535–542
- Preisler N, Cohen J, Vissing CR et al (2017) Impaired glycogen
breakdown and synthesis in phosphoglucomutase 1 deficiency.
Mol Genet Metab 122:117–121
- Scott K, Gadomski T, Kozicz T, Morava E (2014) Congenital
disorders of glycosylation: new defects and still counting.
J Inherit Metab Dis 37:609–617
- Stojkovic T, Vissing J, Petit F et al (2009) Muscle glycogenesis due to
phosphoglucomutase 1 deficiency. *N Engl J Med* 361:425–427
- Tagtmeyer LC, Rust S, van Scherpenzeel M et al (2014) Multiple
phenotypes in phosphoglucomutase 1 deficiency. *N Engl J Med*
370:533–542
- Timal S, Hoischen A, Lehle L et al (2012) Gene identification in the
congenital disorders of glycosylation type I by whole-exome
sequencing. *Hum Mol Genet* 21:4151–4161
- Voermans NC, Preisler N, Madsen KL et al (2017) PGM1 deficiency:
substrate use during exercise and effect of treatment with
galactose. *Neuromuscul Disord* 27:370–376
- Wada Y (2016) Mass spectrometry of transferrin and apolipoprotein
C-III for diagnosis and screening of congenital disorder of
glycosylation. *Glycoconj J* 33:297–307
- Wong SY, Beamer LJ, Gadomski T et al (2016) Defining the
phenotype and assessing severity in phosphoglucomutase-1
deficiency. *J Pediatr* 175:130–136
- Zeevaert R, Scalais E, Muino Mosquera L et al (2016) PGM1
deficiency diagnosed during an endocrine work-up of low IGF-1
mediated growth failure. *Acta Clin Belg* 71:435–437